

CALCIUM REGULATION IN LONG-TERM CHANGES OF NEURONAL  
EXCITABILITY IN THE HIPPOCAMPAL FORMATION

by

ISTVAN MODY

B.Sc.[Hon.], University of British Columbia

A THESIS SUBMITTED IN PARTIAL FULFILLMENT OF  
THE REQUIREMENT FOR THE DEGREE OF  
DOCTOR OF PHILOSOPHY

in

THE FACULTY OF GRADUATE STUDIES  
(Department of Physiology)

We accept this thesis as conforming  
to the required standard

THE UNIVERSITY OF BRITISH COLUMBIA

October, 1985

© Istvan Mody, 1985

In presenting this thesis in partial fulfilment of the requirements for an advanced degree at the University of British Columbia, I agree that the Library shall make it freely available for reference and study. I further agree that permission for extensive copying of this thesis for scholarly purposes may be granted by the head of my department or by his or her representatives. It is understood that copying or publication of this thesis for financial gain shall not be allowed without my written permission.

Department of Physiology

The University of British Columbia  
1956 Main Mall  
Vancouver, Canada  
V6T 1Y3

Date Oct 21, 1985

## ABSTRACT

The regulation of calcium ( $\text{Ca}^{2+}$ ) was examined during long-term changes of neuronal excitability in the mammalian CNS. The preparations under investigation included the kindling model of epilepsy, a genetic form of epilepsy and long-term potentiation (LTP) of neuronal activity. The study also includes a discussion of the possible roles of a neuron-specific calcium-binding protein (CaBP). The findings are summarized as follows:

1) The distribution of CaBP was determined in cortical areas of the rat using a specific radioimmunoassay. The protein was found to have an unequal distribution in various cortical areas with preponderance in ventral structures.

2) Extending previous studies on the role of CaBP in kindling-induced epilepsy, its decline was correlated to the number of evoked afterdischarges (AD's) during the process of kindling.

3) Marked changes in CaBP levels were also found in the brains of the epileptic strain of mice (El). The hippocampal formation and the dorsal occipital cortex contained significantly lower CaBP than the control (CF-1) strain. The induction of seizures further decreased the levels of CaBP in the El mice. These findings are indicative of a possible genetic impairment of neuronal  $\text{Ca}^{2+}$  homeostasis in the El strain.

4) The levels of total hippocampal  $\text{Ca}^{2+}$  and  $\text{Zn}^{2+}$  were measured by atomic absorption spectrophotometry in control and commissural-kindled animals. While no change was found in the total  $\text{Ca}^{2+}$  content of the region, hippocampal  $\text{Zn}^{2+}$  of kindled preparations was found to be significantly elevated.

5) To measure  $\text{Ca}^{2+}$ -homeostasis, the kinetic analysis of  $^{45}\text{Ca}$  uptake curves was undertaken in the in vitro hippocampus. This technique was found to be a valid method for assessment of  $\text{Ca}^{2+}$ -regulation in the CNS under both physiological and pathophysiological conditions. The effect of various extracellular  $\text{Ca}^{2+}$  concentrations, 2,3-dinitrophenol (DNP), calcitonin, nifedipine and 3-isobutyl-1-methylxanthine (IBMX) on  $^{45}\text{Ca}$  uptake curves was examined in order to identify the two exchangeable  $\text{Ca}^{2+}$  pools derived through kinetic analysis.

6) The kinetic analysis of  $^{45}\text{Ca}$  uptake curves revealed that  $\text{Ca}^{2+}$ -regulation of the hippocampus is impaired following amygdala- and commissural kindling. The changes reflect an enhancement of a  $\text{Ca}^{2+}$  pool that includes free cytosolic  $\text{Ca}^{2+}$  and a concomitant decrease in the amount of buffered calcium probably as a result in the decrease of hippocampal CaBP levels.

7) A novel form of long-term potentiation (LTP) of neuronal activity in the CA1 region of the hippocampus is described. Perfusion of 100  $\mu\text{M}$  of IBMX in the hippocampal slice preparation induced a long lasting increase in the amplitude of the stratum radiatum evoked population spike and EPSP responses with changes in synaptic efficacy as indicated by the altered input/output relationships. Intracellular correlates of IBMX-induced LTP



included lowering of synaptic threshold and enhancement of the rate of rise of the EPSP with no alterations in the passive membrane characteristics of CA1 pyramidal neurons. The fact that IBMX was able to exert its effect even in the presence of the calcium-blocker cation  $\text{Co}^{2+}$ , taken together with the drug's action on hippocampal exchangeable  $\text{Ca}^{2+}$ , raises the possibility that the  $\text{Ca}^{2+}$  necessary for induction of LTP may be derived from an intraneuronal storage site.

These studies indicate the significance of intracellular  $\text{Ca}^{2+}$ -regulatory mechanisms in long-term changes of neuronal excitability which occur in experimental models of epilepsy and long-term potentiation.

## TABLE OF CONTENTS

Abstract.....	ii
Table of Contents.....	v
List of Figures.....	ix
List of Tables.....	xiii
Acknowledgements.....	xiv
 CHAPTER I. Introduction.....	 1
1.1. Calcium and the regulation of cellular function.....	1
1.2. The role of calcium in the CNS.....	6
1.3. Calcium and long-term changes in neuronal excitability; The present study.....	14
 CHAPTER II. Distribution and alterations in calcium-binding protein (CaBP) in the CNS.....	 18
2.1. General introduction.....	18
2.1.1. Calcium-binding proteins of the CNS.....	18
2.1.2. The calcium-binding protein CaBP.....	22
2.1.3. Possible roles of CaBP in the CNS.....	24

2.2. Cortical distribution of CaBP in rats.....	31
2.2.1. Introduction.....	31
2.2.2. Methods.....	32
2.2.2.1. Rat cortical samples.....	32
2.2.2.2. CaBP radioimmunoassay (RIA).....	34
2.2.3. Results.....	35
2.2.4. Discussion.....	44
2.3. Relationship of hippocampal afterdischarges to levels of CaBP during development of commissural kindling.....	46
2.3.1. Introduction.....	46
2.3.2. Methods.....	48
2.3.3. Results.....	50
2.3.4. Discussion.....	56
2.4. Distribution of CaBP in the cortical areas of the epileptic El mouse.....	59
2.4.1. Introduction.....	59
2.4.2. Methods.....	61
2.4.3. Results.....	65
2.4.4. Discussion.....	73
CHAPTER III. Measurement of hippocampal $\text{Ca}^{2+}$ homeostasis.....	77
3.1. Measurement of total hippocampal $\text{Ca}^{2+}$ and $\text{Zn}^{2+}$ using atomic absorption spectrophotometry (AAS).....	79
3.1.1. Introduction.....	79
3.1.2. Methods.....	81
3.1.3. Results.....	82
3.1.4. Discussion.....	84

3.2. Measurement of hippocampal exchangeable calcium using kinetic analysis of $^{45}\text{Ca}$ uptake curves.....	87
3.2.1. Introduction.....	87
3.2.2. Methods.....	89
3.2.2.1. Measurement of $^{45}\text{Ca}$ uptake.....	89
3.2.2.2. Curve fitting.....	94
3.2.2.3. Compartmental analysis.....	99
3.2.3. Results.....	103
3.2.3.1. Effect of extracellular calcium ( $[\text{Ca}^{2+}]_0$ ).....	103
3.2.3.2. Effect of drugs that alter $\text{Ca}^{2+}$ metabolism.....	109
3.2.3.3. Theoretical manipulations of the $\text{S}_3$ pool.....	113
3.2.4. Discussion.....	116
3.3. Measurement of $\text{Ca}^{2+}$ -regulation during kindling using the kinetic analysis of $^{45}\text{Ca}$ uptake curves.....	123
3.3.1. Introduction.....	123
3.3.2. Methods.....	125
3.3.3. Results.....	126
3.3.4. Discussion.....	135
CHAPTER IV. Effect of IBMX on hippocampal excitability.....	143
4.1. Introduction.....	146
4.2. Methods.....	149
4.2.1. Extracellular recording and analysis.....	149
4.2.2. Intracellular recording and data analysis.....	156
4.3. Results.....	159

4.3.1. Effect of drugs on stratum radiatum evoked potentials.....	159
4.3.2. Effect of IBMX on paired-pulse inhibition.....	163
4.3.3. Effect of IBMX on input-output (I/O) curves.....	167
4.3.4. Calcium and IBMX-induced LTP.....	178
4.3.5. Effect of IBMX on bursting induced by low calcium.....	186
4.3.6. Effect of IBMX on passive membrane properties of hippocampal CA1 pyramidal cells.....	187
4.3.7. Long-term effect of IBMX on the rate of rise of intracellularly recorded EPSPs.....	190
4.3.8. Intracellular input/output relationships following perfusion of IBMX.....	193
4.3.9. Effect of IBMX on inhibitory mechanisms of CA1 pyramidal neurons recorded intracellularly.....	196
4.3.9.1. Accommodation.....	196
4.3.9.2. Long-lasting hyperpolarization (LHP)....	199
4.3.9.3. Inhibitory post-synaptic potentials (IPSPs) and paired-pulse inhibition.....	202
4.3.10. Long-term effect of IBMX on stimulus threshold...	203
4.4. Discussion.....	206
CHAPTER V. Conclusions.....	216
REFERENCES.....	221

## LIST OF FIGURES

Figure 2.1. CaBP content of the frontal region of rat cortex..	36
Figure 2.2. Levels of CaBP in parietal cortical areas of the rat.....	38
Figure 2.3. CaBP levels in the caudal third of the rat cortex.....	40
Figure 2.4. Summary of CaBP distribution in rat cortex.....	42
Figure 2.5. Development of afterdischarges during commissural kindling.....	51
Figure 2.6. Relationship between the number of evoked AD's and decline of hippocampal CaBP levels during development of commissural kindling.....	54
Figure 2.7. Cortical areas used for determination of CaBP levels in mice.....	63
Figure 2.8. Levels of CaBP in cortical areas of control and El male mice.....	67
Figure 2.9. Levels of CaBP in cortical areas of control and El female mice.....	69

Figure 3.1. Sequential flow-chart representation of the methods used for kinetic analyses of $^{45}\text{Ca}$ uptake curves..	91
Figure 3.2. Graphical analysis and fitting of the $^{45}\text{Ca}$ uptake curve.....	96
Figure 3.3. Effect of alterations in extracellular $\text{Ca}^{2+}$ concentrations on the hippocampal $^{45}\text{Ca}$ uptake curves and electrical activity.....	105
Figure 3.4. Effects of drugs and hormones on $^{45}\text{Ca}$ uptake and electrophysiological properties of hippocampal slices.....	110
Figure 3.5. Effects of theoretical manipulations of the $\text{S}_3$ (buffered) $\text{Ca}^{2+}$ pool.....	114
Figure 3.6. $^{45}\text{Ca}$ uptake curves in control, commissural- (HPC) and amygdala-kindled (AMY) hippocampal slices.....	129
Figure 3.7. Histograms showing exchangeable calcium pools in hippocampal slices obtained from control, commissural- (HPC) and amygdala-kindled animals.....	133
Figure 3.8. Schematic illustration of alterations observed in calcium exchange kinetics of kindled hippocampi.....	136
Figure 4.1. Measurement of extracellular potentials in the CA1 region of the hippocampal slice preparation.....	152
Figure 4.2. Chemical formulae of the drugs used in the present study.....	154

Figure 4.3. Effect of various drugs on the amplitude of population spikes evoked in the CA1 region of the hippocampal formation.....	160
Figure 4.4. Effect of IBMX on paired-pulse inhibition recorded extracellularly.....	165
Figure 4.5. Potentials recorded in the dendritic and somatic region of area CA1 during input/output curves.....	168
Figure 4.6. I/O curves having stimulus intensity (SI) on the abscissa.....	171
Figure 4.7. I/O curves having fiber volley amplitude (V) on the abscissa.....	174
Figure 4.8. I/O curves having the rate of rise of the EPSP (D) on the abscissa.....	176
Figure 4.9. Effect of $\text{Co}^{2+}$ on IBMX-induced LTP.....	179
Figure 4.10. Effect of a short duration (<30 min) perfusion of 0 mM $\text{Ca}^{2+}$ /9 mM $\text{Mg}^{2+}$ on the action of IBMX in the CA1 region of the hippocampus.....	182
Figure 4.11. Effect of a long duration (60 min) perfusion of 0 mM $\text{Ca}^{2+}$ /9 mM $\text{Mg}^{2+}$ on the action of IBMX in the CA1 region of the hippocampus.....	184
Figure 4.12. Effect of 100 $\mu\text{M}$ IBMX on the passive membrane characteristics of CA1 pyramidal neurons.....	188



Figure 4.13. Effect of IBMX on the rate of rise ( $dV/dt$ ) of intracellularly recorded EPSPs.....	191
Figure 4.14. Intracellular I/O relationship following perfusion of IBMX in a CA1 pyramidal cell.....	194
Figure 4.15. Effect of IBMX on the accommodation of pyramidal cell discharge.....	197
Figure 4.16. Effect of IBMX on inhibitory events acting on CA1 pyramidal neurons.....	200
Figure 4.17. Effect of IBMX on stimulus- and firing threshold of CA1 pyramidal neurons.....	204

## LIST OF TABLES

Table 2.1. Effect of afterdischarges (AD's) on levels of hippocampal and cerebellar CaBP.....	53
Table 2.2. Levels of CaBP in various cortical areas of control and epileptic (El) mice.....	71
Table 2.3. Two-way analysis of variance (ANOVA) of the effects of strain, sex and seizures on the cortical levels of CaBP in control and El mice.....	72
Table 3.1. Calcium and zinc in the hippocampal formation of control and commissural-kindled rats as measured by atomic absorption spectrophotometry.....	83
Table 3.2. Effects of extracellular calcium concentrations on hippocampal $\text{Ca}^{2+}$ exchange.....	107
Table 3.3. Effects of drugs on hippocampal $\text{Ca}^{2+}$ exchange.....	112
Table 3.4. Effect of kindling-induced epilepsy on $\text{Ca}^{2+}$ exchange rates and compartment sizes of hippocampal slices.....	131

## ACKNOWLEDGEMENTS

I would like to express my gratitude to Dr. James J. Miller for providing me the opportunity to pursue my scientific goals in his laboratory. Many sincere thanks to Dr. Kenneth G. Baimbridge for his guidance regarding the CaBP radioimmunoassay and to Michael W. Oliver for his friendship and valuable collaboration in some of the experiments. The helpful discussions and comments of other fellow graduate students were also welcome.

I appreciate the technical assistance of K. Henze, J. Naim and R. Anderson. I would like to thank the members of my advisory committee and Dr. G. G. Somjen, the external examiner, for reviewing the thesis. The receipt of the F. F. Wesbrook Fellowship from the University of British Columbia is also acknowledged.

Finally, I wish to dedicate this thesis to my father who expressed so much interest in my work and to the memory of Kevin J. Pittman whose own thesis could never be completed.

## CHAPTER I.

### INTRODUCTION

#### 1.1. Calcium and the regulation of cellular function

The discovery of calcium dates back to the first decade of the 19<sup>th</sup> century when H. Davy isolated the metal, together with other alkaline earths, and gave its name from the Latin word 'calx' meaning lime. Following its discovery, biologists found that living organisms exist in a milieu that contains  $\text{Ca}^{2+}$ , but it wasn't until 1882-83 when Sidney Ringer through a fortuitous discovery gave the first account of its functional significance. Ringer, examining the effects of various ions on the contractions of frog heart, first dismissed the role of  $\text{Ca}^{2+}$ , but later discovered that the solution he was using had been prepared not from distilled water but regular tap water, naturally containing high amounts of  $\text{Ca}^{2+}$ . Subsequent examinations have proven that the presence of  $\text{Ca}^{2+}$  was necessary for maintenance of normal cardiac contractions. Further evidence for the role of  $\text{Ca}^{2+}$  in excitable tissue was obtained by Locke (1894) who showed that

nerve to nerve and nerve to muscle transmission both required extracellular  $\text{Ca}^{2+}$ . Much of the 20<sup>th</sup> century research in biology, physiology and medicine has focused on the important functions of  $\text{Ca}^{2+}$  in cellular systems and has shown that the cation participates in numerous aspects of the physiology and pathophysiology of living organisms. Calcium has major functions in both excitable and non-excitable cells which include, to enumerate just a few, reproduction and development of cells, cell movement, electrical activity, mineralization of a bony or calcareous skeleton, exo- or endocytosis, photoreception, activation and inactivation of enzymes and proteins, and finally, cell death. For a complete review of calcium's involvement in cellular function the reader is directed to the recent book by Campbell (1983). Only some of the recent developments will be discussed below, focusing mainly on the regulation of intracellular calcium and its second messenger function.

The total calcium content of living cells is usually equal to the calcium concentration of the extracellular fluid, but it is differentially distributed in a bound form into the various intracellular organelles, membranes and proteins leaving only a minute cytoplasmic fraction (<0.1%) in the free ionic form (Borle, 1981a). Nevertheless, most of the cellular calcium is exchangeable, which means that it may be replaced with time by its extracellular counterpart. The organelles involved in the maintenance of intracellular  $\text{Ca}^{2+}$ -homeostasis are primarily the mitochondria and the endoplasmic reticulum. To complement the  $\text{Ca}^{2+}$ -regulatory action of intracellular mechanisms, cells possess

various systems responsible for the extrusion of excess  $\text{Ca}^{2+}$ , which include the  $\text{Na}^{+}\text{-Ca}^{2+}$  exchange, and metabolic  $\text{Ca}^{2+}$ -pumps.

Because of the facility of the preparation, the mitochondrial calcium transport has been extensively studied (for reviews see Lehninger et al., 1977; Akerman and Nicholls, 1983). In summary, accumulation of  $\text{Ca}^{2+}$  in the mitochondrial matrix is compensated by extrusion of  $\text{H}^{+}$  which results from the respiratory chain and hydrolysis of ATP. To maintain the electrochemical potential difference across the mitochondrial membrane, two protons have to be exchanged for one  $\text{Ca}^{2+}$ . This however, in the case of a large  $\text{Ca}^{2+}$  loading, would significantly alter the pH of both the mitochondrial matrix and the cytoplasm. Therefore, a permeant anion, such as phosphate or acetate, must be present that will transport  $\text{H}^{+}$  back into the matrix, and following its dissociation binds  $\text{Ca}^{2+}$  to form a  $\text{Ca}^{2+}$ -salt. Much controversy has surrounded the efflux pathway of  $\text{Ca}^{2+}$  from the mitochondrial matrix, which seems to be dependent on cytoplasmic inorganic phosphate (Akerman and Nicholls, 1983). In addition, since most of the experiments are carried out in isolated mitochondria, it is difficult to speculate about the setpoints for release and uptake of calcium in situ. While there is no doubt that mitochondria contain a reasonable amount of the exchangeable cellular  $\text{Ca}^{2+}$ , their  $\text{Ca}^{2+}$ -buffering role in the physiological range remains questionable (Somlyo et al., 1985).

A more likely candidate for physiological regulation of intracellular calcium and  $\text{Ca}^{2+}$ -buffering seems to be the endoplasmic reticulum (ER), which has both a high affinity and a high

capacity for calcium-binding. A recent study by Somlyo et al. (1985) in which the distribution of  $\text{Ca}^{2+}$  in liver cells in vivo was examined, concluded that the endoplasmic fraction of cellular calcium may be as high as 23-27%, while mitochondria only contain about 5%, the amount necessary for the modulation of  $\text{Ca}^{2+}$ -sensitive mitochondrial enzymes. The functional significance of ER-calcium is not only reflected in its calcium buffering capacity. Its muscle equivalent, the sarcoplasmic reticulum, is involved in the release of  $\text{Ca}^{2+}$  which is indispensable for activation of muscle contraction (Endo, 1977; Martonosi, 1984). The role of calcium-receptor and calcium-binding proteins will be discussed in the context of the nervous system (see Section 2.1.).

While the concentration of free calcium is precisely regulated in the vast majority of cells, transient increases in  $[\text{Ca}^{2+}]_i$  which may result from calcium influx or release of endogenous  $\text{Ca}^{2+}$  would activate certain biochemical events that constitute the basis of the second messenger action of the cation (Kretsinger, 1981). The role of calcium as an intracellular messenger is of major importance because  $\text{Ca}^{2+}$  translates the actions of substances (hormones, neurotransmitters, etc.), which are unable to permeate the cell but have receptors on the outside of the plasma membrane, into specific cellular biochemical reactions. The contribution of calcium as a second messenger to hormone or neurotransmitter action is not a simple and easily detectable process, since it may be masked sometimes by activation of other  $\text{Ca}^{2+}$ -dependent mechanisms. Alternatively,

one may argue about the specificity of first messenger action if there was only one intracellular second messenger. Nevertheless, in most cases  $\text{Ca}^{2+}$  acts synergistically with other messenger systems, such as cyclic nucleotides, or its intracellular concentration is under the control of several concomitantly activated regulatory processes.

The cooperativity between  $\text{Ca}^{2+}$  and other second messenger systems has long been recognized (Rasmussen and Goodman, 1977). In a recent review, Rasmussen and Barret (1984) propose an integrated view of the calcium messenger system, in which cyclic nucleotides play an important role. According to their hypothesis, the initial response, which consists of a transient increase in  $[\text{Ca}^{2+}]_i$ , together with a sustained response due to cAMP activation (e.g., protein phosphorylation) may produce an integrated response which constitutes the observed effect of hormone action. This mechanism would allow for a very sensitive gain control, since  $\text{Ca}^{2+}$  itself is involved in several steps of the cyclic nucleotide metabolism, ranging from the activation or inhibition of the cyclase to the activation of phosphodiesterase.

Cyclic nucleotides are not the only other second messenger system that has been involved in calcium's action. The hydrolysis of a membrane lipid, phosphatidylinositol 4,5-bisphosphate, into diacylglycerol and inositol triphosphate ( $\text{InsP}_3$ ) is under the control of hormone or neurotransmitter action in several preparations (Berridge and Irvine, 1984). Although  $\text{InsP}_3$  may have second messenger actions of its own, its principal function appears to be the release of  $\text{Ca}^{2+}$  from intracellular storage



sites, mainly the endoplasmic reticulum. This release mechanism could serve as an amplification of the cellular signal, since it has been suggested that for every molecule of hydrolyzed phosphatidylinositol 10 or more calcium ions could be liberated.

Finally, considering the toxic effects of elevated  $[Ca^{2+}]_i$  (Schanne et al., 1979) it is quite remarkable how cells are able to maintain its concentration at a reasonably steady level and to use its regulatory properties as a messenger system.

### 1.2. The role of calcium in the CNS

Several of the regulatory functions of  $Ca^{2+}$  mentioned in the previous section also apply to neurons. Moreover, in the case of the CNS, calcium plays a pivotal role in the modulation of processes that stand at the very basis of neuronal excitability (Erulkar and Fine, 1979). The variety of  $Ca^{2+}$ -mediated phenomena is so large that in some cases it is almost impossible to determine, following proof of the cation's involvement, which particular mechanism may be the most important in causing or maintaining the observed event. Careful examination is required to distinguish between its action on neurotransmitter release, regulation of membrane excitability, activation of other ionic channels or even some biochemical events that could be triggered by  $Ca^{2+}$ . In many instances, particularly in the mammalian CNS, direct measurements of  $Ca^{2+}$  involvement are difficult to achieve, thus leaving the researcher to rely on indirect evidence, mainly

originating from invertebrate preparations. Despite all the technical obstacles in  $\text{Ca}^{2+}$  measurement (also see Chapter III), there is now considerable evidence for some of the important functions that this cation plays in the mammalian CNS.

### Calcium channels

It is now clear that there are several types of membrane channels that regulate the influx of  $\text{Ca}^{2+}$  into nerve cells from the extracellular milieu. Most of these channels are sensitive to the voltage across the plasma membrane, but there may also be channels that are regulated through the action of hormones and neurotransmitter substances (Hagiwara and Byerly, 1981; Reuter, 1983; Tsien, 1983a).

The voltage-dependent  $\text{Ca}^{2+}$  channels share some properties that are equally applicable to all the excitable tissues examined. In contrast to the  $\text{Na}^+$  channels, they are insensitive to tetrodotoxin (TTX) but are readily blocked by other polyvalent cations ( $\text{Co}^{2+}$ ,  $\text{La}^{3+}$ ,  $\text{Mn}^{2+}$ ,  $\text{Cd}^{2+}$  and  $\text{Ni}^{2+}$ ) at concentrations approximately equivalent to extracellular  $\text{Ca}^{2+}$ . In addition, organic blockers such as verapamil and D-600 (the methoxy derivative of verapamil), and in some cases dihydropyridines (e.g., nifedipine and nitrendipine) antagonize calcium currents. The channels are not absolutely specific for  $\text{Ca}^{2+}$ , thus barium and strontium ions are able to replace  $\text{Ca}^{2+}$  in permeating through the channel molecule. While inactivation of  $\text{Na}^+$  channels is dependent on membrane voltage and the presence of gating particles, the cause of  $\text{Ca}^{2+}$  current reduction following

prolonged opening of the channel is less evident. The current hypothesis, derived from the study of molluscan nerve cells (Tillotson, 1979; Eckert and Tillotson, 1981), is that  $\text{Ca}^{2+}$  ions accumulate on the inside of the plasma membrane and inactivation occurs when their concentration is sufficiently large to stop additional ions from entering the cell. This mechanism would allow for a longer channel opening time and for a more precise control of  $\text{Ca}^{2+}$  entry into neurons, depending on intraneuronal ionic diffusion and the presence of  $\text{Ca}^{2+}$ -buffering systems. However, voltage-dependent inactivation of  $\text{Ca}^{2+}$  channels has been shown to exist in several systems (Hagiwara and Byerly, 1981; Tsien, 1983a).

The identity and functioning of neurotransmitter-dependent  $\text{Ca}^{2+}$  channels is characterized to a lesser degree (Reuter, 1983). Although some substances, that may well be neurotransmitter candidates, enhance  $\text{Ca}^{2+}$  influx into neurons, it is not known whether their effect is due to changes in voltage across the plasma membrane or to activation of specialized channels. Alternatively, these agents may simply modulate permeation of  $\text{Ca}^{2+}$  through the voltage-sensitive channels, as has been postulated for the mechanism of presynaptic inhibition in CNS neurons (Reuter, 1983).

#### **Neurotransmitter release**

Once  $\text{Ca}^{2+}$  crosses the plasma membrane through the channel and enters the neuronal cytoplasm, it is available for the activation of several regulatory mechanisms that are ultimately

underlying normal functioning of neurons. Induction of neurotransmitter release, analogous to exocytosis in other systems, is of primary importance in achieving chemical communication between elements of the CNS. Much of the evidence for calcium's involvement comes from the study of the neuromuscular junction, where it was recognized 90 years ago that the presence of  $\text{Ca}^{2+}$  in the extracellular medium is a necessary requirement for transmission to occur (Locke, 1894). It took however more than seventy years for the 'calcium hypothesis' of neurotransmission to emerge (Katz and Miledi, 1965; 1967). Later, investigation of the squid giant synapse provided experimental proof for the depolarization-induced calcium entry into presynaptic terminals and the release of neurotransmitters (Llinas, 1977). The steps of activation from calcium entry to the final quantal release process have been subject to several reviews (e.g., Rahamimoff, 1976; Llinas and Heuser, 1977). Although direct evidence for the existence of mechanisms analogous to those found at the squid giant synapse is lacking in the mammalian CNS, it is reasonable to assume that calcium ions contribute in a similar manner to the central release of neurotransmitter molecules. It has been postulated (Llinas, 1977; Llinas and Heuser, 1977) that the delay of about 200 usec between depolarization of the synaptic terminal and actual release through exocytosis can be accounted for by accumulation of  $\text{Ca}^{2+}$  at the inside of the plasma membrane (to levels of about two orders of magnitude higher than resting  $[\text{Ca}^{2+}]_i$ ) and subsequent rapid activation of adjacent transmitter releasing sites.

While the direct involvement of  $\text{Ca}^{2+}$  in the release of neurotransmitters seems to be well established, the exact mechanism of the calcium-dependent activation is still somewhat obscure. Dodge and Rahamimoff (1967) examining the effect of various extracellular  $\text{Ca}^{2+}$  concentrations on the release process, proposed a cooperative action for several calcium ions (probably four) at a hypothetical  $\text{Ca}^{2+}$ -binding site. Equally plausible is the involvement of the intracellular mediator protein calmodulin, as outlined in Section 2.1.1. Furthermore, the possibility that a  $\text{Na}^{+}$ -dependent release of  $\text{Ca}^{2+}$  from intracellular storage sites may be responsible for the event has been suggested in light of the observation that transmitter release also occurs in the absence of  $[\text{Ca}^{2+}]_0$  (Rahamimoff et al. 1980).

#### Activation of other ionic conductances

Entry of calcium through specialized channels is not only important at the level of the presynaptic terminal, but also regulates permeability of the membrane to other ions, such as  $\text{K}^{+}$ . Activation of such a  $\text{K}^{+}$  conductance will tend to hyperpolarize the neuronal membrane since the  $\text{K}^{+}$ -equilibrium potential is more negative than the resting membrane potential in most if not all neurons. A  $\text{Ca}^{2+}$ -activated  $\text{K}^{+}$ -conductance, or  $g_{\text{KCa}}$ , discovered by injection of  $\text{Ca}^{2+}$  into neurons (Krnjevic and Lisiewicz, 1972; Meech, 1972) has been shown to be present in many neuronal systems (for review see Schwartz and Passow, 1983). It is also evident that activation of this conductance is not a simple charge displacement, since  $\text{Ba}^{2+}$  readily crosses the membrane

through  $\text{Ca}^{2+}$  channels, but fails to activate  $\text{gK}_{\text{Ca}}$ , and may even result in its inhibition (Gorman and Hermann, 1979). The importance of  $\text{gK}_{\text{Ca}}$  in the control of neuronal excitability is outlined in Section 2.1.3. It is now recognized that many neuro-modulators exert at least a part of their effects through altering this  $\text{Ca}^{2+}$ -activated conductance. Noradrenaline, histamine and corticotropin releasing factor have all been shown to regulate the excitability of CNS neurons through inhibition of  $\text{gK}_{\text{Ca}}$  (Madison and Nicoll, 1982; Aldenhoff et al., 1983; Haas and Konnerth, 1983), while dopamine may hyperpolarize cells through its activation (Benardo and Prince, 1982). It has also been proposed that the  $\text{gK}_{\text{Ca}}$  system may be under the control of cyclic AMP, although the evidence is highly controversial (Benardo and Prince, 1982; Madison and Nicoll, 1982).

As in the case of neurotransmitter release, the entry of  $\text{Ca}^{2+}$  through specialized channels does not seem to be an absolute requirement for activation of the  $\text{gK}_{\text{Ca}}$ . Endogenous calcium ions released from intracellular storage sites may be just as effective in triggering the  $\text{K}^{+}$ -conductance (Kuba, 1980; Akaike et al., 1983), thus contributing to the overall regulation of neuronal excitability.

In addition to the  $\text{Ca}^{2+}$ -activated  $\text{K}^{+}$ -conductance, a chloride-conductance that seems to be dependent on  $\text{Ca}^{2+}$  has been recently observed in cultured spinal cord neurons (Owen et al., 1984). The presence of this conductance, depending on the equilibrium potential for  $\text{Cl}^{-}$  in different neurons, may complement the inhibitory action of the  $\text{gK}_{\text{Ca}}$  system.

### Regulatory functions of intraneuronal $\text{Ca}^{2+}$

The intraneuronal actions of  $\text{Ca}^{2+}$  are not limited to neurotransmitter release or activation of other ionic fluxes. Several biochemical mechanisms are dependent on the presence of  $\text{Ca}^{2+}$ , and some of them may involve the special second messenger function of the cation as described for other systems (see Section 1.1.). Many of these actions are possibly mediated through intraneuronal  $\text{Ca}^{2+}$ -receptor proteins, of which calmodulin is a prime example. The role of these proteins in the nervous system is described in more detail in Chapter II.

Considering the variety of neuronal  $\text{Ca}^{2+}$ -dependent phenomena and their many functional implications, it is of no surprise that cytosolic free calcium is under strict control in nerve cells and is maintained at less than micromolar levels (e.g., Alvarez-Leefmans et al., 1981). The cellular elements which achieve this rigorous function are no different in neurons than in non-neuronal tissue. The endoplasmic reticulum, calcium-binding proteins and mitochondria together with a low resting permeability of the membrane to  $\text{Ca}^{2+}$ , all contribute to the maintenance of low  $[\text{Ca}^{2+}]_i$ . As in non-neuronal tissue, the share of mitochondria in the regulation of calcium levels within the physiological range is questionable (Blaustein et al., 1978; 1980). In addition to the intraneuronal buffering and sequestering mechanisms, excess  $\text{Ca}^{2+}$  is extruded from the cytosol with the aid of the  $\text{Na}^+$ - $\text{Ca}^{2+}$  exchange and activation of  $\text{Ca}^{2+}$

pumps, possibly linked to the  $\text{Ca}^{2+}\text{-Mg}^{2+}$  ATPase (Erulkar and Fine, 1979).

### Extracellular $\text{Ca}^{2+}$

Despite the many regulatory functions of intraneuronal  $\text{Ca}^{2+}$ , it is not necessary to postulate that all changes in nerve cell excitability have to be a direct consequence of alterations in  $[\text{Ca}^{2+}]_i$ . Extracellular  $\text{Ca}^{2+}$  is a very effective modulator of membrane electrical properties, as shown by the experiments of Frankenhaeuser and Hodgkin (1957) in the squid axon. The cation may neutralize the negative charges on the outer surface of the plasma membrane near the voltage sensitive channels, thus having a charge stabilizing effect. In central neurons, lowering of  $[\text{Ca}^{2+}]_o$  induces spontaneous discharges (Richards and Sercombe, 1970; Jefferys and Haas, 1982), while iontophoresis of  $\text{Ca}^{2+}$  reduces their firing rate (Kato and Somjen, 1969; Wright, 1984). This is probably why the calcium concentration of the cerebrospinal fluid, in a manner similar to the regulation of cytosolic  $\text{Ca}^{2+}$ , is maintained at a reasonably steady value of 1.5-1.8 mM (Campbell, 1983).



### 1.3. Calcium and long-term changes in neuronal excitability;

#### The present study

In view of all the possible sites and mechanisms of  $\text{Ca}^{2+}$  action it is not difficult to envisage how an altered neuronal calcium metabolism may contribute to changes in the functional characteristics of neurons. Some pathophysiological changes may indeed result from the altered ability of nerve cells to cope with a  $\text{Ca}^{2+}$  challenge. For example, Heinemann et al., (1977) detected significant declines in extracellular  $\text{Ca}^{2+}$  activities during epileptiform discharges of cortical neurons. Presumably the loss of  $[\text{Ca}^{2+}]_o$  was paralleled by an increase in the intra-neuronal concentration of the cation, indicating the involvement of calcium in epileptiform events. Similarly it has been shown that regenerative  $\text{Ca}^{2+}$  spikes participate in the bursting activity in the penicillin model of experimental epilepsy (Wong and Prince, 1978; Hotson and Prince, 1981) and neuronal calcium accumulation characterizes the status epilepticus induced by l-allylglycine (Griffiths et al., 1982). All of these data indicate that the one possible mechanism underlying epilepsy may involve an impairment of the neuronal regulation of  $\text{Ca}^{2+}$ .

One of the difficulties with the concept of calcium's involvement in epileptiform phenomena is the lack of substantial evidence for chronic alterations in calcium regulation. Acute changes in  $\text{Ca}^{2+}$  homeostasis in various models of experimental epilepsy cannot possibly account for the sustained alterations in

excitability which is considered to be a general characteristic of epileptic neurons (Ward, 1969). In order to result in a persistent effect on neuronal excitability, calcium has to induce a 'permanent' biochemical change. Alternatively, due to some neurochemical mechanism(s), the regulation of calcium itself has to be offset as long as the neurons maintain their pathophysiological state. The recent findings that a neuron specific calcium-binding protein (CaBP) is gradually lost in the granule cells of the dentate gyrus during and following kindling-induced epilepsy are the first indications of a possible involvement of long-term alterations in  $\text{Ca}^{2+}$ -regulation (Miller and Baimbridge, 1983; Baimbridge and Miller, 1984; Baimbridge et al., 1985).

Since CaBP is also distributed in the cerebral cortex, in neurons prone to epileptiform activity, the purpose of the present study included measurement of cortical CaBP distribution with the aid of a specific radioimmunoassay to detect possible regional differences in its levels. Furthermore, extending previous studies on the kindling model of epilepsy, the present experiments address the question regarding the correlation between electrophysiological alterations during epileptogenesis (the development of afterdischarges) and the decline in CaBP. If neuronal regulation of calcium does indeed play a role in seizure mechanisms, then other models of experimental epilepsy should also be characterized by detectable changes in calcium regulation. To examine this possibility, levels of CaBP were measured in the cortical areas of the genetically epileptic strain of mice 'El'. The results were compared to a control

strain and the effect of seizures on CaBP levels was also studied within the El strain itself.

Alternatively, the decline in the levels of CaBP may not result in an altered calcium homeostasis and the changes in the protein content of brain tissue may be simply coincidental with the observed epileptiform activity. In order to determine whether CaBP plays a role in the regulation of neuronal  $\text{Ca}^{2+}$  the technique of kinetic analysis of  $^{45}\text{Ca}$  uptake curves was employed in hippocampal slices obtained from kindled animals. Since this technique has not been widely applied to neuronal tissue, the validity of the method for the CNS had to be determined. Once this was determined, the method proved to be a valuable tool in determination of brain calcium homeostasis. In addition to measurement of exchangeable  $\text{Ca}^{2+}$  using the radioactive tracer method, the amount of total hippocampal calcium was also determined by atomic absorption spectrophotometry (AAS). The zinc content of the hippocampus was determined alongside the calcium levels to determine changes that may have occurred during the process of kindling.

In contrast to the more deleterious effects of calcium in neurons, such as participation in epileptogenesis, the cation is also involved in long-lasting changes in neuronal functions subserving physiological events. For example, plastic changes in synaptic function occur at molluscan synapses and the underlying process is thought to be a persistent change in the regulation of  $\text{Ca}^{2+}$  channels, or some other calcium-mediated event, such as changes in  $\text{K}^{+}$  conductance. The enhanced synaptic efficacy of the

system may directly determine the learning process (Klein et al., 1980; Kandel, 1981). In addition, calcium is readily involved in yet another long-lasting change of neuronal excitability, namely the phenomenon of long-term potentiation (Swanson et al., 1982; Turner et al., 1982; Eccles, 1983).

Part of the present study was therefore undertaken to examine various aspects of  $\text{Ca}^{2+}$ -regulation under experimental conditions where permanent or quasi-permanent alterations in CNS  $\text{Ca}^{2+}$ -homeostasis are likely to occur. A novel form of long-term potentiation is described, caused by a methylxanthine derivative, that is also caused by altered neuronal  $\text{Ca}^{2+}$  regulation. The possibility that release of calcium from intracellular storage sites, rather than calcium entry per se, may be responsible for the observed electrophysiological changes is also examined with the aid of the  $^{45}\text{Ca}$  uptake method.

In summary, the present study examines the regulation of  $\text{Ca}^{2+}$  in neuronal systems that present long-term alterations in their function. The systems under investigation comprised the kindling model of experimental epilepsy, a genetic form of epilepsy and finally, the phenomenon of long-term potentiation induced by a methylxanthine derivative.

## CHAPTER II.

### DISTRIBUTION AND ALTERATIONS IN CALCIUM-BINDING PROTEIN (CaBP) IN THE CNS

#### 2.1. General introduction

##### 2.1.1. Calcium-binding proteins of the CNS

The regulation of intracellular calcium is achieved by most eukaryotic cells through a variety of factors. Apart from intracellular organelles, such as mitochondria and the endoplasmic reticulum, proteins that bind  $\text{Ca}^{2+}$  with a high affinity ( $10^{-6}$ - $10^{-7}$  M) participate in the overall physiological framework of calcium regulation (Borle, 1981a). Some of these proteins are involved in the modulation of enzymatic events thus being part of the second messenger role of  $\text{Ca}^{2+}$  (Kretsinger, 1981), while others subserve transport mechanisms, or constitute intracellular  $\text{Ca}^{2+}$ -buffers. The important contribution of calcium-binding proteins to cellular regulatory mechanisms is probably best illustrated by their presence in virtually all species and in

every tissue from epithelia to brain. There are close to 100 'different' proteins that have been reported to bind calcium, but it is debatable whether they are all capable of exerting physiologically significant alterations upon binding of calcium ions (Kretsinger, 1976).

Most of the calcium binding proteins of known structure share relatively similar  $\text{Ca}^{2+}$ -binding domains, called the EF-hand regions (Kretsinger, 1976). These regions consist of the subunit where binding of  $\text{Ca}^{2+}$  occurs flanked almost at right angles by two structural units consisting of alpha helices (helix-loop-helix conformation). The multiple EF-hand structures (usually four) of some calcium-binding proteins are thought to have resulted from gene duplication. Although several proteins have not retained this quadruple arrangement, the large family of calcium binding proteins is considered to have evolved from a common ancestral protein (Demaille, 1982). The 'on' and 'off' binding rate constants for the  $\text{Ca}^{2+}$ -domains are remarkably fast, making these proteins ideal for rapid  $\text{Ca}^{2+}$  binding and release, while the conformational changes induced by calcium are of a relatively slower time course (Robertson et al., 1981; Levine and Williams, 1982).

The nature of the conformational changes upon  $\text{Ca}^{2+}$  binding has been investigated using nuclear magnetic resonance (NMR) studies (cf., Dalgarno et al., 1984). Binding of pairs of calcium ions is considered to be a cooperative event. The resultant conformational alteration of the protein produces movement of the 'trigger zone' which in turn, in the case of regulatory proteins,

may be attached to other enzymes or macromolecules. Interference caused by drug binding to these proteins, for example, neuroleptic antagonism of calmodulin (Weiss and Levin, 1978), or modulation of the protein molecule itself through phosphorylation (Dalgrano et al., 1984) may hinder the effectiveness of their calcium-dependent regulatory action. Since the discussion of all calcium binding proteins is beyond the scope of the present study, only a relatively few will be briefly described below, particularly those shown to exist within the central nervous system.

Calmodulin (CaM) is one of the most widely distributed calcium binding proteins found in plants as well as in all species of animals examined. It has been discovered as the  $\text{Ca}^{2+}$ -dependent regulator of brain cyclic nucleotide phosphodiesterase (Cheung, 1970; Kakiuchi and Yamazaki, 1970), and during the seventies many intracellular messenger roles of  $\text{Ca}^{2+}$  have been linked to its action (Cheung, 1980; Means and Dedman, 1980; Klee et al., 1980). Other than its obvious function in regulating cyclic nucleotide metabolism in the brain, CaM has been found to be localized in post-synaptic densities (Lin et al., 1980) as well as to participate through  $\text{Ca}^{2+}$ -dependent protein phosphorylation in the release of neurotransmitters from isolated synaptic vesicles (DeLorenzo et al., 1979). Therefore, the involvement of CaM in synaptic function seems quite well established (DeLorenzo, 1982). The phosphorylation of synaptic proteins (presumably tubulin) by CaM action may result in long term alterations of neurotransmitter functions, which may in turn

subserve plastic changes in the CNS. One of these, the long-term potentiation phenomenon (LTP) in the hippocampus has indeed been shown to be blocked by CaM antagonist drugs (Finn et al., 1980; Mody et al., 1984). Recent studies on CaM suggest that it may also regulate the calcium channels of nerve cells or at least it may be homologous to the calcium binding protein that is involved in channel modulation (cf., Johnson et al., 1983).

Another calcium binding protein, parvalbumin is found primarily in muscle and nerve tissue (Heizmann, 1984). It is a relatively small protein ( $M_r$  of approx. 12,000), and was originally isolated from frog and carp muscles. The present working hypothesis concerning its mechanism of action, at least in muscle, states that it serves as a 'shuttle' for  $Ca^{2+}$  between troponin-C (the  $Ca^{2+}$  binding subunit of troponin) and the sarcoplasmic reticulum. The liberation of  $Ca^{2+}$  from troponin-C would then allow for the next contraction to occur. This may be the reason why parvalbumin is primarily localized within the fastest contracting skeletal muscle fibers (Celio and Heizmann, 1982). Parvalbumin's role in the CNS is less well defined, but immunohistochemical studies have shown its localization in small interneurons of the cortex, basket cells of the hippocampus and cerebellum, Purkinje and stellate cells of the cerebellum and periglomerular cells of the olfactory bulb (Celio and Heizmann, 1981). In general, there seems to be a good correlation between parvalbumin distribution and neurons that use GABA as a neurotransmitter, but the functional significance of these findings is presently under investigation.



The S-100 protein is also a specific calcium-binding protein, localized mainly in astrocytes rather than neurons in the CNS. In astrocytes it may activate their putative contractile apparatus. Although the protein is equipped with the typical EF-hand structures for  $\text{Ca}^{2+}$  binding, some of these domains are modified. A  $\text{K}^{+}$ -modulated  $\text{Ca}^{2+}$  binding site is present, and another one may bind  $\text{Zn}^{2+}$  with a higher than normal affinity. Many of the early functional studies of the S-100 protein have implied a role in memory formation (e.g., Hyden and Lange, 1973), but according to more recent research this may not be the case (Moore, 1982).

#### 2.1.2. The calcium-binding protein CaBP

Calcium-binding protein (CaBP) was first shown to be present in chick intestine and its synthesis to be dependent on vitamin-D (Wasserman and Taylor, 1966). Subsequently the protein has been isolated from the intestines of several species and shown to differ in size and the number of calcium-binding domains. For example, the avian protein has a  $M_r$  of 28,000 with four sites for  $\text{Ca}^{2+}$  binding while the bovine and porcine proteins are of lower molecular weight ( $M_r=8,700-9,000$ ) and have two and one site respectively, all of which bind  $\text{Ca}^{2+}$  with an affinity of approximately  $10^{-6}$  M (Wasserman, 1980). The amino acid sequence and three-dimensional structure of these proteins has now been established (e.g., Szebenyi et al., 1981) and it appears that the

calcium-binding domains generally show the EF-hand conformation proposed by Kretsinger (1976) for proteins of the same class.

Immunologically similar, perhaps identical, proteins to the avian gut CaBP have been found in several tissues that are involved in  $\text{Ca}^{2+}$  transport. Most of these proteins show a strong similarity also with respect to their dependency on vitamin-D (Christakos and Norman, 1980). Because of the common calcium transporting function of the tissues where it is found, CaBP has been proposed to function as an intracellular  $\text{Ca}^{2+}$  carrier (Levine and Williams, 1982; Wasserman and Fullmer, 1983). In the gut for example, following the action of vitamin-D, there is a rapid uptake of calcium by the intestinal cells, but calcium transport from one cellular pole to the other does not occur unless CaBP is present (Wasserman and Fullmer, 1983; Wasserman et al., 1983).

The localization of a calcium-binding protein similar to the CaBP of the avian gut in the brain, a tissue where calcium is directly involved in the control of neuronal excitability, has opened new avenues of research for the functional role of this protein. First, it has been demonstrated by radioimmunoassay procedures that avian, rat and even human brain samples contain significant amounts of CaBP (Taylor, 1974; Christakos et al., 1979; Baimbridge and Parkes, 1980; Baimbridge et al., 1980; 1982). Later, by using immunocytochemical techniques, it has been shown that the protein is not randomly distributed throughout the CNS, but it is rather confined to particular neurons while being absent from others and from glial cells

(Jande et al., 1981; Roth et al., 1981; Baimbridge and Miller, 1982; Garcia-Segura et al., 1984). All of these studies have clearly identified the cerebellar Purkinje cells and some neurons of the cerebral cortex and subcortical structures as containing large amounts of the protein. The conspicuous localization of CaBP in some neurons but not in others is well illustrated in the hippocampal formation, where dentate granule cells and pyramidal cells of the CA1 region show high degree of CaBP-immunoreactivity, while the pyramidal neurons of area CA3 do not (Baimbridge and Miller, 1982).

The question remains open whether CaBP of nerve tissue is sensitive to vitamin-D or not. The early study of Taylor (1974) showed some degree of vitamin-D dependency, but the discrepancy between the distribution of  $1,25(\text{OH})_2\text{-D}_3$  binding sites (Stumpf et al., 1982) and CaBP localization in the brain tends to dismiss this hypothesis. Furthermore, in rats, intracerebroventricular injections of  $1,25(\text{OH})_2\text{-D}_3$  (the active metabolite of vitamin D) did not alter brain CaBP levels (K.G. Baimbridge, unpublished observations), indicating that the regulation of CNS CaBP by vitamin-D is unlikely.

### 2.1.3. Possible roles of CaBP in the central nervous system

One of the first possibilities that arises from the studies on intestinal cells is that CaBP may underlie a similar  $\text{Ca}^{2+}$ -transport function in neurons. However, transport of  $\text{Ca}^{2+}$  across the cell is probably less important in brain than in other

tissues such as intestine, kidney and bone, where absorption and reabsorption of calcium is a significant part of the normal functioning of these structures. Nevertheless, CaBP may still be involved in intraneuronal transport of  $\text{Ca}^{2+}$ , and considering its high affinity for  $\text{Ca}^{2+}$ -binding, it may serve as a temporary storage site for the cation. This mechanism may operate especially under circumstances where the lower affinity mitochondria would be insensitive to changes in  $[\text{Ca}^{2+}]_i$ . According to this hypothesis, following cessation of the  $\text{Ca}^{2+}$  signal, CaBP would 'migrate' to the mitochondria, or other more permanent  $\text{Ca}^{2+}$  storage sites within the neurons, and would release its bound calcium. Because of the different  $\text{Ca}^{2+}$  affinities of the two systems, this mechanism has to involve an active process of  $\text{Ca}^{2+}$  uptake by the mitochondria.

Secondly, the presence of CaBP in certain nerve cells and not in others would make the CaBP-containing neurons less sensitive to the ubiquitously distributed calmodulin (CaM). The relatively similar  $\text{Ca}^{2+}$ -binding constants of the two proteins would enable cells that possess CaBP to bind the  $\text{Ca}^{2+}$  that otherwise could have activated CaM. The net result would be a dampening of CaM-regulated events and enzymatic reactions, including protein phosphorylation. Moreover, if CaM is indeed involved in neurotransmitter release (DeLorenzo, 1982), the presence of CaBP in the presynaptic terminals of some neurons would allow for a more precise and fine tuning of  $\text{Ca}^{2+}$ -CaM regulated exocytosis of synaptic vesicles. In certain neurons where two or possibly more neurotransmitters may be co-localized

in the same synaptic terminal the presence or absence of CaBP may thus permit the selective release of one or the other neurotransmitter molecule, depending on the amount of  $\text{Ca}^{2+}$  entry.

Although neurons tend to maintain their free ionic intracellular calcium at very low levels ( $10^{-8}$ - $10^{-7}$  M), this may rise to 10-100 times its resting value during activity, neurotransmitter action or certain pathological events. Therefore, bearing in mind the high affinity of  $\text{Ca}^{2+}$  binding to CaBP, the protein may serve as an intraneuronal calcium buffering system, especially so when  $[\text{Ca}^{2+}]_i$  is raised to supranormal levels. This hypothesis appears reasonable since it has been estimated that in cerebellar Purkinje cells, which contain the highest CaBP levels in the CNS, the cytosolic concentration of CaBP may be as high as 0.1-0.2 mM (Baimbridge et al., 1982). This would allow for  $\text{Ca}^{2+}$ -buffering up to 0.4-0.8 mmol/litre of cytoplasm since 4 mol of  $\text{Ca}^{2+}$  are bound to each mol of CaBP. Intracellular free  $\text{Ca}^{2+}$  would probably never rise to such levels, indicating that the buffering capacity of CaBP would be able to cope with most, if not all, of physiological and even pathophysiological changes of  $\text{Ca}^{2+}$  inside nerve cells. The neuronal  $\text{Ca}^{2+}$ -buffer function of CaBP seems to be an attractive hypothesis, but raises the question as to how  $\text{Ca}^{2+}$  is buffered in the many neurons that lack the protein? In these cells the only high sensitivity  $\text{Ca}^{2+}$ -sequestering mechanism may be the endoplasmic reticulum (Duce and Keen, 1978), which would make them selectively vulnerable to a supranormal  $\text{Ca}^{2+}$ -challenge.

The calcium-buffering hypothesis would also imply that CaBP could effectively regulate the magnitude of  $\text{Ca}^{2+}$  influx through calcium channels. As shown for molluscan nerve cells calcium channels are not only sensitive to membrane voltage, but are inactivated due to accumulation of  $\text{Ca}^{2+}$  on the inside of the plasma membrane (Tillotson, 1979; Eckert and Tillotson, 1981). There is reason to believe that similar events also occur in the mammalian CNS. If this proves to be the case, then  $\text{Ca}^{2+}$  binding to an intracellular calcium-buffer, such as CaBP in the proximity of the calcium channel would remove free calcium ions which otherwise would hinder further entry of  $\text{Ca}^{2+}$  through the channel as proposed by the kinetic model of Chad et al. (1984). The diminished  $\text{Ca}^{2+}$ -dependent  $\text{Ca}^{2+}$  inactivation would enable the CaBP-containing neurons to have larger  $\text{Ca}^{2+}$ -spikes of longer duration.

While regulating the amount of calcium entry into neurons, CaBP may also be involved, although somewhat indirectly, in the modulation of the  $\text{Ca}^{2+}$ -activated  $\text{K}^+$  conductance ( $g_{\text{KCa}}$ ) of nerve cells. This hyperpolarizing conductance is present in virtually every nerve cell (Schwarz and Passow, 1983) and its activation in CNS neurons stops their bursting or repetitive discharge (Alger and Nicoll, 1980; Hotson and Prince, 1980). Furthermore, since signal encoding in the firing pattern of neurons is an important feature of information transmission in the CNS (Stein, 1967), it is expected that sustained repetitive neuronal discharge is under rigorous control. The underlying regulatory mechanism must be the activation of an outward current (Jack et al., 1975). Both

the late  $K^+$  current ( $I_A$ ) and the  $Ca^{2+}$ -activated  $K^+$  current possess the time course and magnitude required to control the frequency of neuronal firing. In neurons of the mammalian CNS there is evidence that adaptation (or accommodation) of spike discharge during a long depolarizing current pulse is under the control of  $gK_{Ca}$  (Madison and Nicoll, 1982; 1984). The suggestion has been made that calcium entry per se is not the primary factor that controls the magnitude of the  $gK_{Ca}$ . Injection of the  $Ca^{2+}$ -chelator EGTA into CA1 pyramidal cells of the hippocampus, which facilitates  $Ca^{2+}$ -dependent potentials, abolishes  $gK_{Ca}$  conductance resulting in a prolonged and a more rapid (unaccommodated) firing of these neurons (Madison and Nicoll, 1984). More direct evidence that the  $Ca^{2+}$  necessary for  $K^+$  conductance activation originates from the endoplasmic reticulum comes from the work of Kuba (1980) in the sympathetic ganglion or Akaike et al. (1983) in snail neurons. If the calcium necessary for activation of  $gK_{Ca}$  is derived from intracellular storage sites, how could CaBP be involved in the regulation of this conductance?

The hypothesis regarding the release of intraneuronal  $Ca^{2+}$  as activator of the  $K^+$  conductance is based on the role of parvalbumin in rapidly contracting muscle fibers (see Section 2.1.1.). The fibers that contain parvalbumin are able to contract several hundred times a second due to the fast removal of  $Ca^{2+}$  from troponin-C by binding to parvalbumin. If the neuronal  $gK_{Ca}$  is activated by  $Ca^{2+}$  released from intracellular storage sites, possibly the endoplasmic reticulum, then binding of  $Ca^{2+}$  to parvalbumin or CaBP would prevent  $Ca^{2+}$  from reaching

the  $K^+$  channel and thus its activation. Alternatively, the calcium binding proteins, due to their high affinity for the cation, may be able to remove the already bound  $Ca^{2+}$  from the  $K^+$  channel molecule resulting in the inactivation of the  $K^+$  channel. A mechanism of inactivation somewhat similar to this, although involving diffusion of  $Ca^{2+}$  away from the channel, has been proposed by Gorman and Thomas (1980). Further evidence to support this latter alternative comes from the work of Barish and Thomas (1983) in molluscan neurons where mitochondria do not seem to participate in removal of  $Ca^{2+}$  from the activated  $K^+$  channel and therefore the presence of a high affinity buffering system had to be proposed. Baldissera and Parmiggiani (1979) constructed a model of the spinal motoneurone, which includes this form of  $gK_{Ca}$  inactivation. In their model, depending on the duration and magnitude of the inactivation process, the neuron is capable of high rate repetitive firing and changes of discharge frequencies.

It has yet to be determined whether involvement in activation or inactivation of the  $gK_{Ca}$  proves to be the site of action for calcium-binding proteins. In either case,  $Ca^{2+}$ -dependent  $K^+$  channels would stay open for shorter times in neurons which possess parvalbumin and/or CaBP. This in turn would enable neurons that contain any of these proteins to maintain a longer duration repetitive discharge. As mentioned in Section 2.1.1., parvalbumin is localized mainly in interneurons, cells that are capable of firing action potentials at extremely high frequencies for sustained intervals. The Purkinje cells of



the cerebellum which show two types of firing patterns (Llinas and Sugimori, 1980a,b), both at relatively high frequencies, contain both parvalbumin and CaBP in high concentrations.

In general terms, there is quite a good correlation between the ability of neurons to sustain their frequency of discharge and the localization of CaBP within these cells. The two notable exceptions are the granule cells of the dentate gyrus and neurons of the inferior olivary nucleus. In these cells, repetitive discharge may be additionally regulated by specific membrane characteristics which also play a role in determining the firing pattern of neurons (Jack et al., 1975). However, both of these cell types show a depolarizing after-potential (DAP) of a marked amplitude (Llinas and Yarom, 1981a,b; Fricke and Prince, 1984; M.W. Oliver, personal communication) that may be a reflection of the lack of  $gK_{Ca}$  coupled with a concomitant long-lasting  $Ca^{2+}$  entry.

The correlation of CaBP localization in certain neurons together with their electrophysiological investigation will result in the elucidation of the exact function of this protein in the CNS.

## 2.2. Cortical distribution of CaBP in rats

### 2.2.1. Introduction

It has been established that nervous tissue contains a large amount of CaBP which is unequally distributed in various areas of the CNS with little species differences (Christakos et al., 1979; Baimbridge and Parkes, 1980; Baimbridge et al., 1980; 1982). Although the exact function of the protein was not determined, at the time it appeared that it participated in the regulation of neuronal calcium. Further immunohistochemical studies (Jande et al., 1981; Baimbridge and Miller, 1982; Garcia-Segura et al., 1984) have established its confinement to some neurons but not others and demonstrated its presence in elements of the neocortex. Since there are profound changes in extracellular calcium concentrations during cortical epileptogenesis (Heinemann et al., 1977), it is possible that the presence of an intraneuronal  $\text{Ca}^{2+}$ -buffering protein, such as CaBP, may alter the neurons' responsiveness to the calcium challenge.

The present study was therefore undertaken to examine in detail the cortical distribution of CaBP considering the differential sensitivity of various neocortical areas to aberrant forms of activity (Ward, 1969). With the use of a specific radioimmunoassay it was also possible to determine the CaBP content of several cortical areas to complement the available immunohistochemical studies.

## 2.2.2. Methods

### 2.2.2.1. Rat cortical samples

Male rats of the Wistar strain (body weights: 250-300 g) were sacrificed through decapitation and their brains removed. Various cortical areas were dissected free on ice, following removal of the hippocampus, brain stem and subcortical structures including the basal ganglia. The cortical regions were dissected as follows: frontal cortical tissue was obtained by cutting the most rostral 2.0-2.5 mm of the two cerebral hemispheres; the parietal region contained the tissue between this cut and the central sulcus that was identified visually by the artery of the central sulcus running alongside; occipital area included the remaining caudal parts of the cerebral cortex. Once these sections were obtained in a frontal plane, the parietal and occipital parts were further subdivided dorso-ventrally into four equal parts (on both sides). These regions were roughly equivalent to the areas defined by Krieg (1946):

Parietal area I : A. cingularis posterior ventralis;  
A. gigantopyramidalis;  
A. postcentralis oralis.

Parietal area II : A. postcentralis caudalis.

Parietal area III: A. postcentralis caudalis;  
A. insularis dorsalis.

Parietal area IV : A. insularis ventralis;

Cortex pyriformis anterior;

A. amygdala anterior.

Occipital area I : A. retrosplenialis lateralis;

A. occipitalis medialis.

Occipital area II: A. striata;

A. occipitalis lateralis.

Occipital area III: A. auditoria;

A. temporalis;

A. insularis ventralis.

Occipital area IV: A. insularis ventralis;

A. entorhinalis;

Cortex pyriformis;

A. amygdala posterior;

Cortical amygdaloid nucleus.

In addition to the aforementioned regions, the hippocampus was dissected free and divided into two roughly equal parts: the dorsal and the ventral hippocampus.

Two homologous cortical samples originating from one animal were pooled in a test-tube regardless of hemispheric origin (left or right) and were homogenized for 20 sec in 50 volumes of 20 mM Tris-HCl, 5 mM NaCl, 1 mM EGTA (pH 7.4) at 4°C. The homogenates were then centrifuged for 30 min at 30,000 g (at 4°C) and the clear supernatant was used for CaBP radioimmunoassay (RIA) and total soluble protein (TSP) determinations.

For CaBP RIA, 100 µl aliquots of the supernatant were used in 6-10 fold dilutions and assayed in triplicates. The total

soluble protein content of the supernatant was determined in triplicates of 50  $\mu$ l samples using the one step BioRad method and porcine gamma globulin as the protein standard.

#### 2.2.2.2. CaBP radioimmunoassay (RIA)

The RIA for CaBP used antibody raised in rabbits against the purified 28,000 dalton CaBP isolated from human cerebella (Baimbridge et al., 1982) at a final dilution of 1:25,000. The RIA buffer contained 0.03 M Na-barbital, 6 g/L bovine serum albumin and 1 mM EDTA at pH 8.6. Standards for CaBP, containing 1.62-80  $\mu$ g of purified protein were prepared in the buffer, using the technique of serial dilutions. Each RIA tube contained 700  $\mu$ l of buffer, 100  $\mu$ l of antibody, or 100  $\mu$ l of buffer (for non-specific binding tubes) and 100  $\mu$ l standard or samples or buffer (for maximum binding tubes). Tubes were incubated for 6 h at 4°C and  $^{125}$ I-labelled CaBP was added in 100  $\mu$ l RIA buffer (usually 9,000-10,000 cpm per tube) and the incubation was continued for another 20 h. Following the incubation, to precipitate the antibody-bound fraction of the labelled protein, 100  $\mu$ l of 8 mg/ml of porcine gamma globulin and 700  $\mu$ l of 25 w/v polyethylene glycol (Carbowax PEG 6000, Fisher Scientific) was added to each tube. After mechanical agitation of the tubes on a multi-vortexer, precipitation was achieved by centrifugation for 30 min. The supernatant was discarded, the tubes were rinsed off with water and counted in a gamma-counter. The percentage of bound/total was calculated taking in account the corrections

for non-specific binding (usually <5%). A standard curve was constructed from the known CaBP concentrations and the CaBP content of unknown samples was determined using interpolation from this curve between the range of 2.5-30 ng CaBP/tube. Tissue CaBP levels were expressed as ng/mg total soluble protein (TSP). This RIA procedure had a sensitivity of 1-2 ng CaBP and has previously been shown to be specific for rat, mouse, bovine and human CaBP (Baimbridge et al., 1982).

### 2.2.3. Results

The CaBP content of various cortical areas of rats (n=12) is shown on the coronal sections of Figs 2.1.-2.3. The levels of CaBP ranged from about 600-1800 ng/mg TSP which are approximately 1/10<sup>th</sup> the level of cerebellar CaBP content (e.g., Baimbridge et al., 1982). Both the pyriform and entorhinal cortices contain the highest CaBP levels in the cerebral cortex of the rat, and represent about 14% of the total cortical CaBP. The least amount of protein was found in the most dorsal occipital areas accounting only for about 4.5% of the cortical CaBP content.

From the coronal sections, as well as from the histogram representation in Fig. 2.4., it is evident that there is a clear dorso-ventral distribution of CaBP in the cerebral cortex. Dorsal regions contain significantly less protein, while the highest levels in a given coronal plane are localized to the most ventral areas. This observation also applies to phylogenetically older cortical structures, such as the hippocampus, where the ventral

Figure 2.1. CaBP content of the frontal region of rat cortex. The section is taken at 10,550  $\mu\text{m}$  from Konig and Klippel (1963) and corresponds to the A. frontalis (Krieg, 1946). The number represents the average CaBP content expressed in ng/mg total soluble protein of 12 animals.

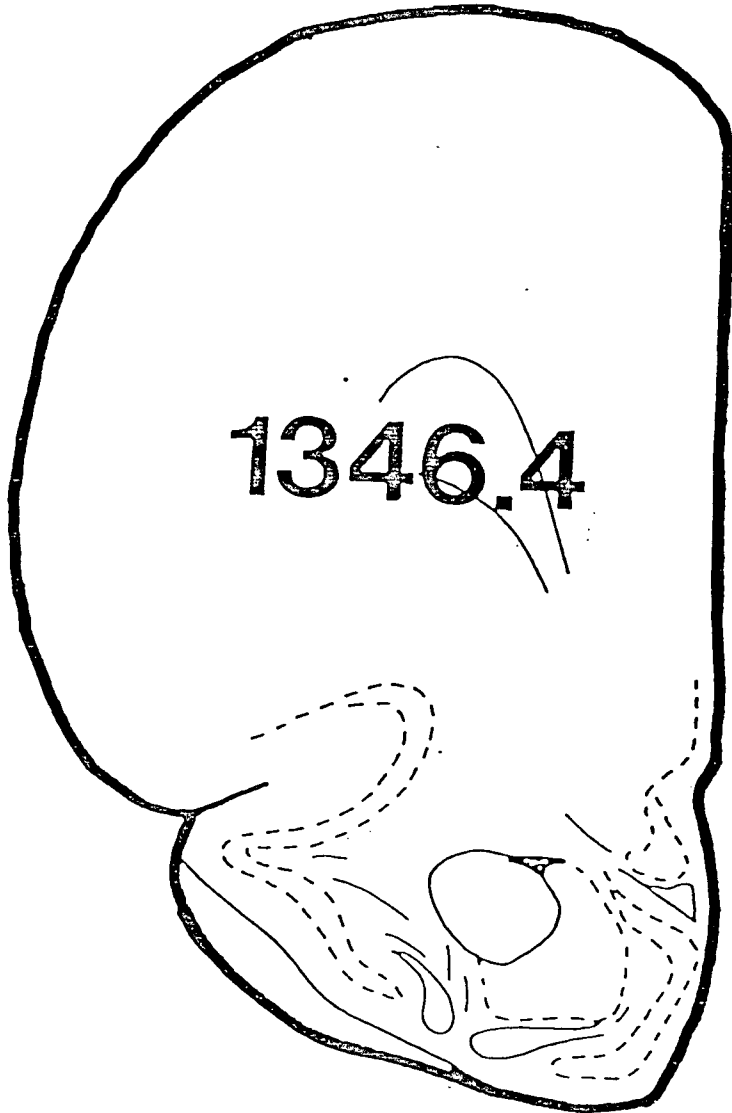




Figure 2.2. Levels of CaBP in parietal cortical areas of the rat. This section was taken from 7020  $\mu\text{m}$  of Konig and Klippel (1963) or 1.2 mm anterior to bregma from Pellegrino et al. (1979). The parietal cortical divisions as described in the text as 'Parietal I-IV' going from dorsal to ventral correspond to areas based on Krieg (1946). The numbers represent average CaBP content in ng/mg TSP (n=12).

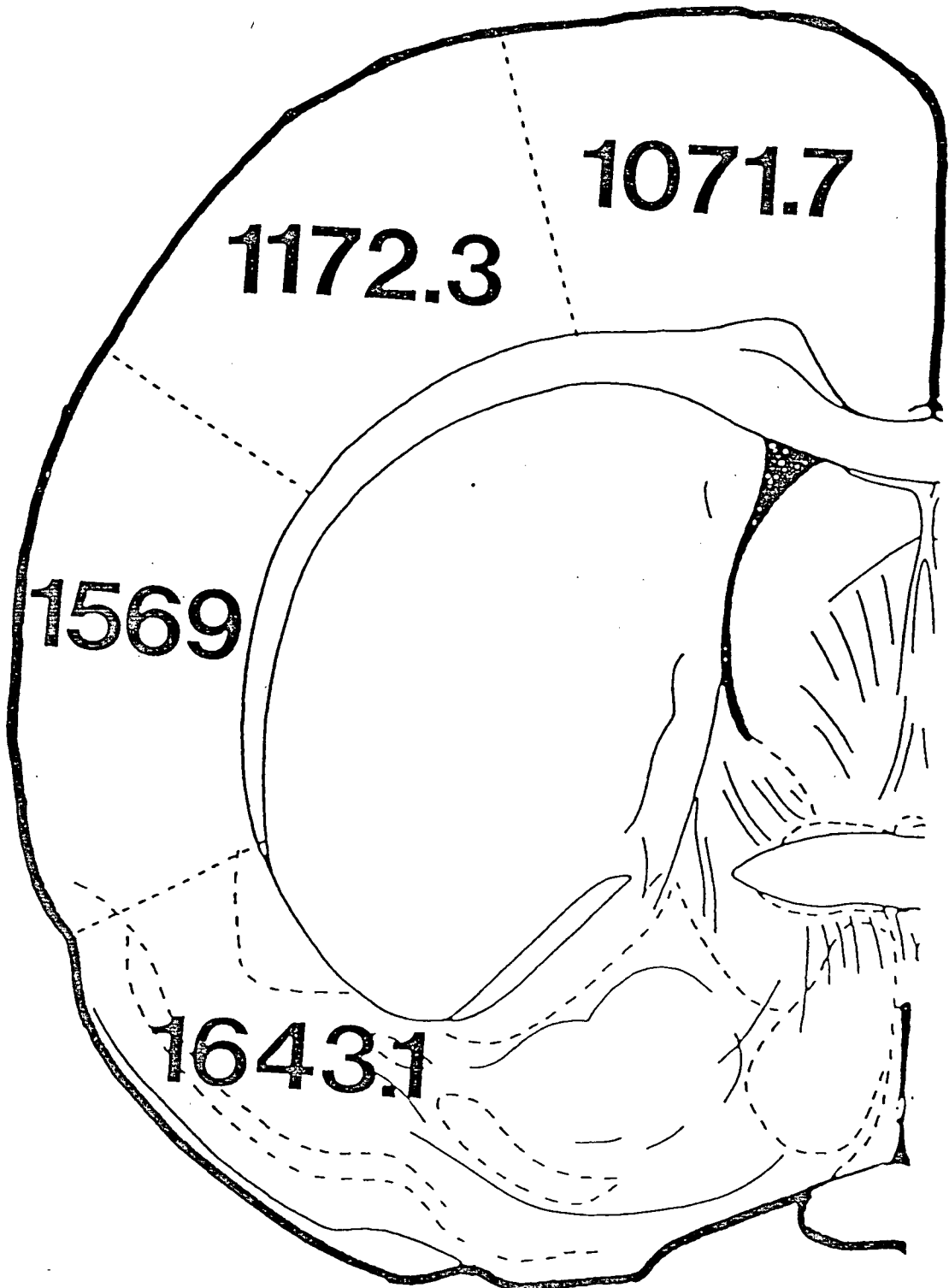


Figure 2.3. CaBP levels in the caudal third of the rat cortex. The section corresponds to 2580  $\mu\text{m}$  of Konig and Klippel (1963) or 3.2 mm posterior to bregma of Pellegrino et al. (1979). The dorso-ventral cortical divisions correspond to 'Occipital areas I.-IV.' indicated in the text. The dorsal and ventral regions of the hippocampal formation are also indicated. The numbers represent averaged CaBP content in ng/mg TSP of 12 animals.

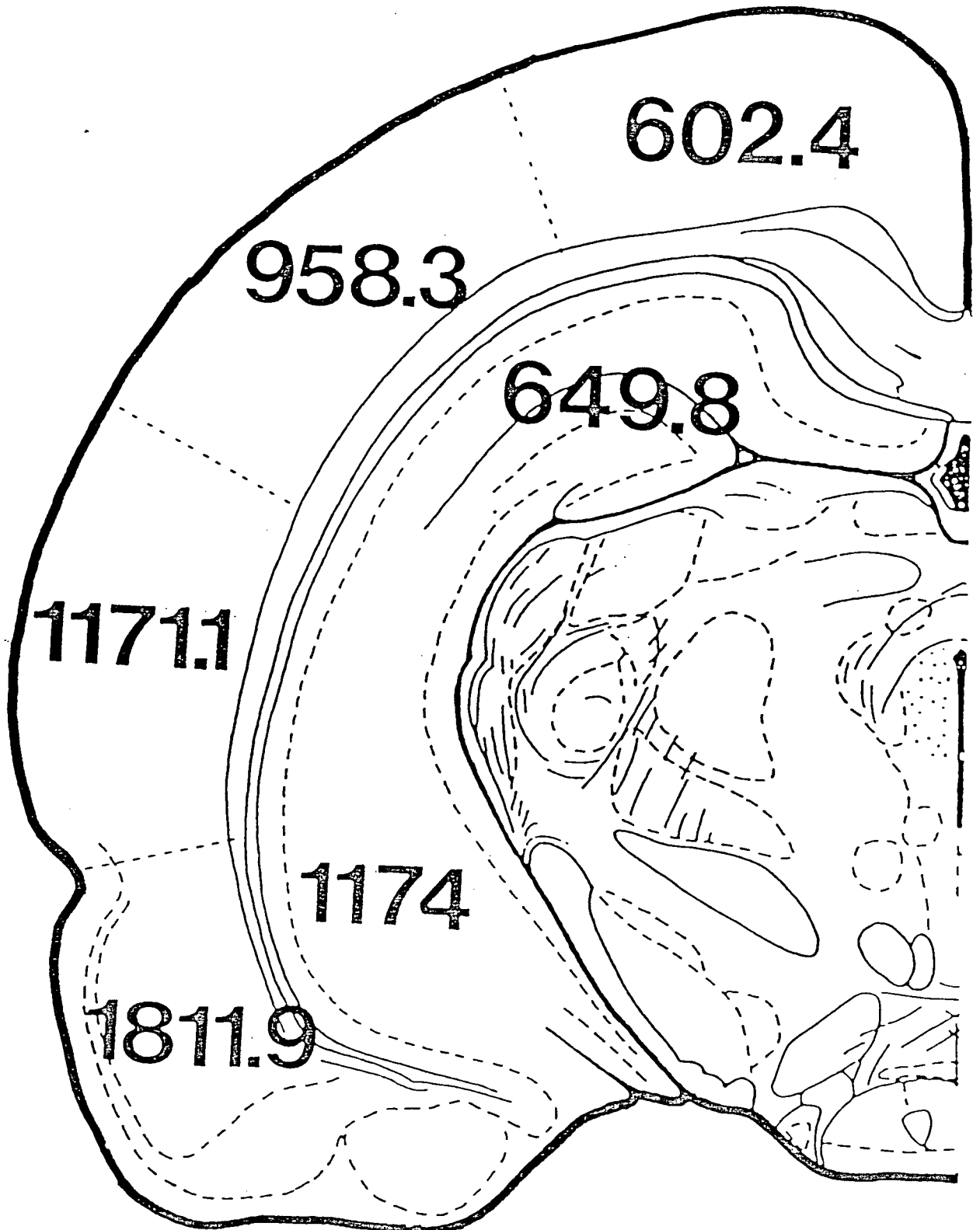
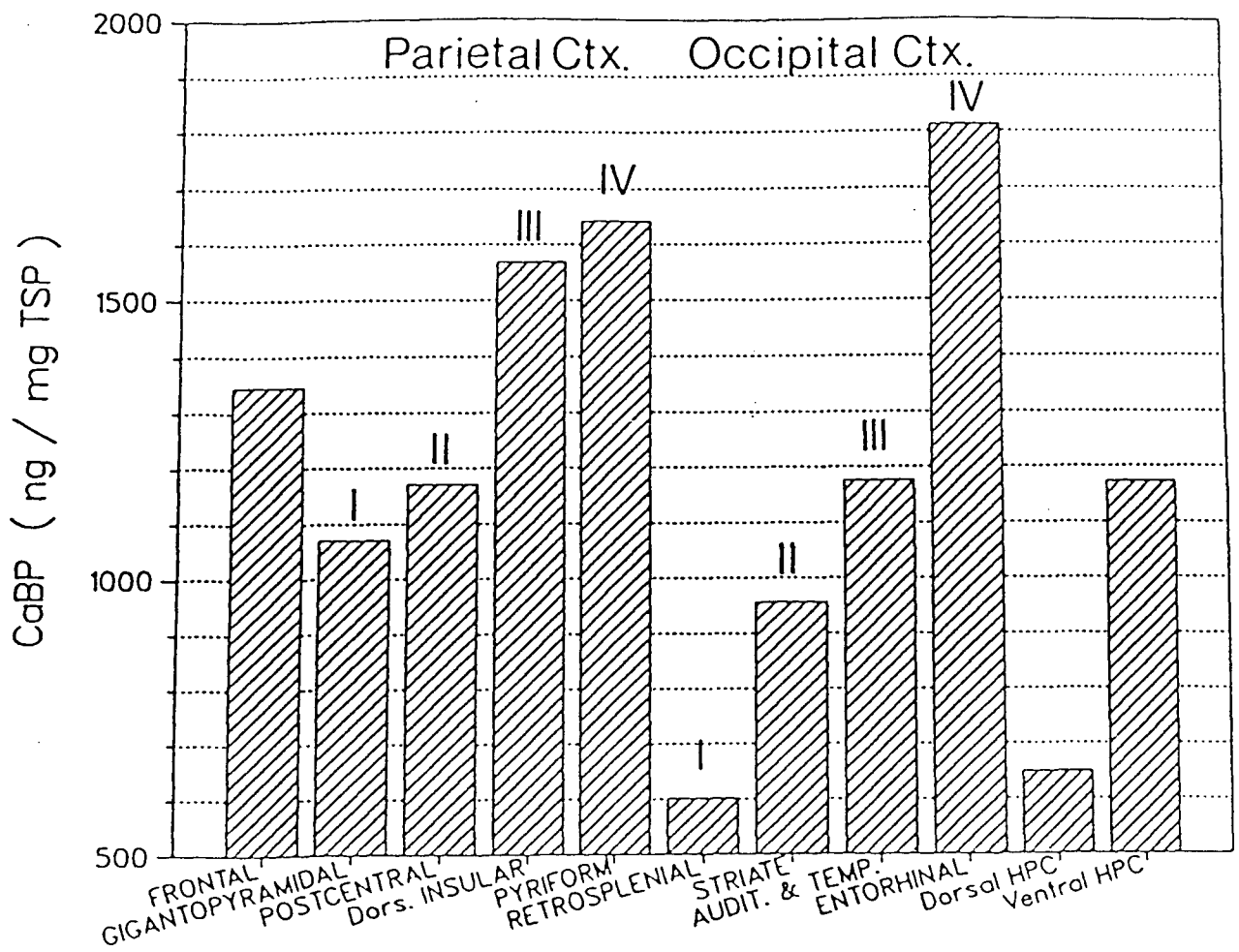


Figure 2.4. Summary of CaBP distribution in rat cortex. The various cortical areas are indicated on the X-axis in terms of their dorso-ventral and rostro-caudal location. 'HPC' stands for hippocampal formation.



hippocampal formation contains about twice the amount of CaBP found in the dorsal part. Immunohistochemical observations (unpublished) indicate that the protein is mainly confined to the neurons of layers II-IV of the cortex while weaker staining is seen in layers I and V.

The amounts of total soluble protein or tissue wet weight did not vary significantly from one cortical area to another. Therefore, the marked differences in levels of CaBP in the various cortical regions are not due to sample variability of TSP or wet weight.

#### 2.2.4. Discussion

The present study extends the findings of Baimbridge et al. (1982) who measured the levels of CaBP in various areas of the rat brain. CaBP content of the cerebral cortex was found to be comparable to the rest of the brain although with significant regional variations. The most consistent finding was the dorsal to ventral distribution of the protein. Some of these findings however, may be biased, at least in part, by preponderance of regions in the ventral sections that contain high levels of CaBP. The hippocampal formation is a good example, since the ventral part has a significantly larger volume/volume contribution from the dentate gyrus, which alone contains about three times more CaBP than the CA1 or CA3 areas (Baimbridge et al., 1982).

In other samples the regional differences may be due to the elevated CaBP content of the cells themselves. For example,

only about 4% of the neurons of the entorhinal cortex have been shown to have immunoreactive CaBP (Garcia-Segura et al., 1984). Since CaBP in this cortical region is approximately 0.2% of the total soluble protein, the absolute amount of CaBP in the neurons that contain it may be as high as 5% of TSP. This would be equivalent to a cytosolic CaBP concentration of about 30-70  $\mu\text{M}$ , and considering 4 mols of  $\text{Ca}^{2+}$  bound per molecule of CaBP, the  $\text{Ca}^{2+}$ -buffering capacity would be 0.1-0.3 mmol/L. This value is about a third of that found in cerebellar Purkinje cells (Baimbridge et al., 1982), but is large enough to make the protein well suited for the possible functional role as an intraneuronal  $\text{Ca}^{2+}$ -buffer in the cerebral cortex. It remains to be determined through the use of combined electrophysiological and immunohistochemical methods, which one of the several likely functions of CaBP as a buffering/sequestering element applies in the case of cortical neurons.



### 2.3. Relationship of hippocampal afterdischarges to levels of CaBP during development of commissural kindling

#### 2.3.1. Introduction

Kindling is one of the most widely used animal models of experimental epilepsy and resembles numerous characteristics of the human disease (Racine, 1978; McNamara et al., 1980). In order to induce this condition low intensity daily electrical stimulations are delivered to any part of the limbic system or other cortical structures and this paradigm ultimately results in a permanent neurophysiological change leading to a convulsive state (Goddard, 1967; Goddard et al., 1969; Racine, 1978). With little exception, the seizures and paroxysms resulting from kindling are usually not spontaneous, but show a typical progression that involves several stages culminating in full motor convulsions classified according to the schema of Racine (1972b) as being 'stage 5'. Although it has been discovered in rodents, the phenomenon is not specific to these animals since it can be induced in all species studied thus far sampled from amphibians to mammals.

While there has been a concerted effort to determine the physiological and biochemical correlates of kindling (Kalichman, 1983; McNamara, 1984), these have for the most part concentrated on alterations which occur in the period following its induction. Thus there is little evidence to suggest whether the observed

changes are due either to motor-seizures or to the process of kindling itself. One notable exception is the loss of hippocampal CaBP, shown earlier to be localized to the granule cells of the dentate gyrus (Miller and Baimbridge, 1983), that precedes the onset of motor seizures, and thus seems likely to be a true neurochemical correlate of kindling-induced epilepsy (Baimbridge and Miller, 1984). This study however, did not examine the possible relationship between changes in hippocampal CaBP levels and known electrophysiological correlates that parallel the development of kindling.

Regardless of the limbic stimulation site, the process of kindling is generally characterized by electrographic events, termed afterdischarges (AD's), that show a typical progression starting with the first stimulation trial (Racine, 1972a; 1978). The form of the AD's (biphasic spike or spike and wave) is rather simple at the early stages and their frequency is quite low (102/sec). Following several stimulations the AD's become more complex and the frequency tends to double or triple. Although the occurrence of AD's precedes the development of characteristic motor activity in the stimulated animals, the changes in afterdischarge frequency and duration is a good correlate of behavioral manifestations during the kindling process. The progressive lengthening of AD's duration is indicative of changes in neuronal functions, suggesting sudden recruitment of additional neuronal circuitry, and occurs in steps paralleling the behavioral changes (Burnham, 1975). Racine (1972b) has classified into five stages these characteristic motor activities

which develop during kindling: 1.- Mouth and facial movements; 2.- Head nodding; 3.- Forelimb clonus; 4.- Rearing; 5.- Rearing and falling, i.e., a full motor seizure.

Since no previous study has correlated the electrophysiological alterations to possible neurochemical changes, the present experiments were undertaken to examine the relationship of evoked AD's to levels of hippocampal CaBP in an attempt to establish a causal link between the change in  $\text{Ca}^{2+}$ -regulation and the development of kindling-induced AD's.

#### 2.3.2. Methods

Male rats of the Wistar strain (200-300g) were anesthetized with Nembutal (30 mg/kg i.p.) and chronically implanted with bipolar stainless steel stimulating and recording electrodes (MS 303/2-Plastic Products Co.) positioned in the hippocampal commissure (AP from bregma: -1.8 mm; L: 0 mm; V: 4.2 mm below the surface of cortex) and hilar region of the dentate gyrus (AP from bregma: -3.3 mm; L: 1.8 mm; V: 3.7 mm below the surface of cortex) respectively. The diameter of the electrodes was 0.2 mm and the stimulating electrodes (placed in the commissure) had a tip separation of 0.1-0.2 mm. The recording electrode of the dentate gyrus had one pole cut 0.5-1.0 mm shorter than the other to enhance the recording of hippocampal EEG activity. All implants were done with the aid of a stereotaxic apparatus. A ground electrode consisting of a stainless steel screw mounted in

the skull and touching the surface of the cortex was also added before the electrode assembly was embedded in dental cement.

Following one week of post-operative recovery, daily kindling stimulation (100 uA, 60 Hz sine-wave, for 1s) was initiated. Each rat was brought directly from its home cage into a wooden stimulation/recording box, the respective leads were connected and the kindling stimulus was delivered following 0.5-1 min of baseline EEG recording. The electrical activity of the hilus was amplified and led to an oscilloscope as well as to a Gould chart-recorder to obtain hard copies of the EEG activity.

The number and duration of AD's were noted and six groups were defined on the basis of the number of AD's that had been evoked, i.e., 0, 5, 10, 15, 20, and 'stage 5' motor-seizure. The control group was implanted but not stimulated. Twenty-four hours following the last stimulation, the rats were sacrificed and the hippocampi and cerebellum were removed. The electrode placements were visually identified in the hippocampi which were then either prepared for in vitro electrophysiological recordings (Oliver and Miller, 1985) or CaBP radioimmunoassay (RIA) according to the procedures described earlier. In all electrophysiological experiments only one hippocampus was utilized from one animal, the other was prepared for RIA. Cerebellar tissue was used as control/reference for the RIA.

In the in vitro preparation the efficacy of synaptic transmission and the contribution of inhibitory processes in the dentate gyrus were assessed using the paired-pulse paradigm

(Oliver and Miller, 1985). The results of these experiments are however, not included in the present study.

### 2.3.3. Results

The first kindling stimuli, delivered to the hippocampal commissures, evoked a brief (approx. 10 s) afterdischarge in forty-one of forty-five animals. Subsequent trials resulted in the progressive lengthening of the AD's (up to 35-40 sec) with the occurrence of characteristic behavioral signs (e.g., grooming, rearing and wet-dog shakes; Racine, 1972b). A typical record of the electrographic development of hilar AD's is shown in Fig. 2.5. (A-D) culminating in the generation of a kindling-induced seizure (Fig. 2.5.E), usually after 25-32 stimulation trials. Following the AD's, a period of low electrical activity was observed which lasted for at least 3 min, and it was usually during this depressed portion of the EEG when wet-dog shakes appeared (Fig. 2.5.C and D). The duration of full motor-seizures was in excess of 1 min in all cases observed.

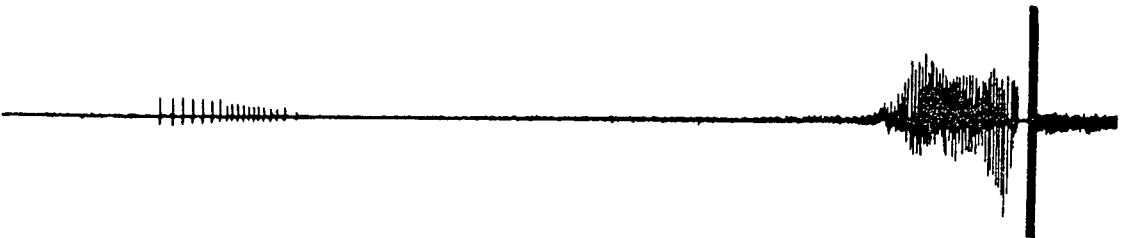
The levels of hippocampal CaBP, as measured by RIA, showed a decline correlated to the number of recorded AD's (Table 2.1.). A significant loss of CaBP (about 18%) was detected in animals following 10 AD's and the decline continued up to 20 AD's when it reached a maximal reduction of 32% (Fig. 2.6.). This change was not further altered by motor-seizures, in fact a slight but not significant increase was noted compared to the 20 AD's group.

Figure 2.5. Development of afterdischarges during commissural kindling. EEG activity recorded in the hilus of the dentate gyrus following a 1 sec kindling stimulus (large artefacts at the beginning of each record) delivered to the hippocampal commissures. A, electrographic response recorded from an animal with no AD's after 23 stimulation trials. The records in B, C, D show the progression of AD's development through the 5<sup>th</sup>, 10<sup>th</sup> and 20<sup>th</sup> stimulation trials respectively. Note the lengthening of the primary AD's (immediately following the stimulus artefact) and the subsequent depression of electrical activity. Wet-dog shakes usually occurred during the second, lower frequency AD's and are indicated by closed arrowheads. E, record of a full motor seizure (during the interval between the open arrows) induced on the 30<sup>th</sup> stimulation trial lasting typically in excess of 1 min. Traces in B, C, D, and E are from the same animal.

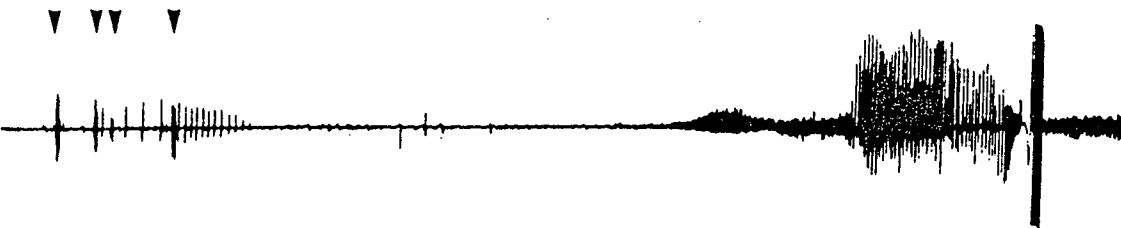
A.



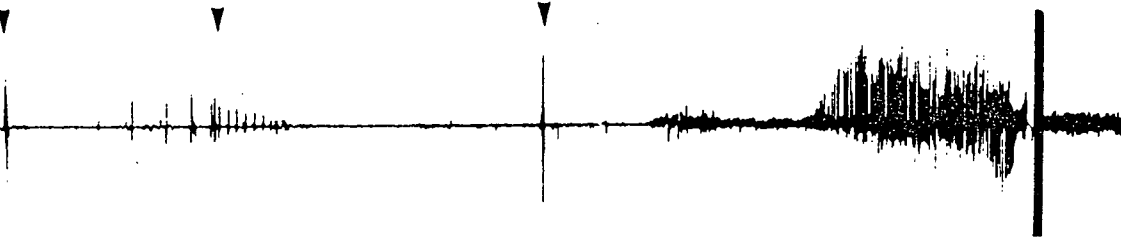
B.



C.



D.



E.

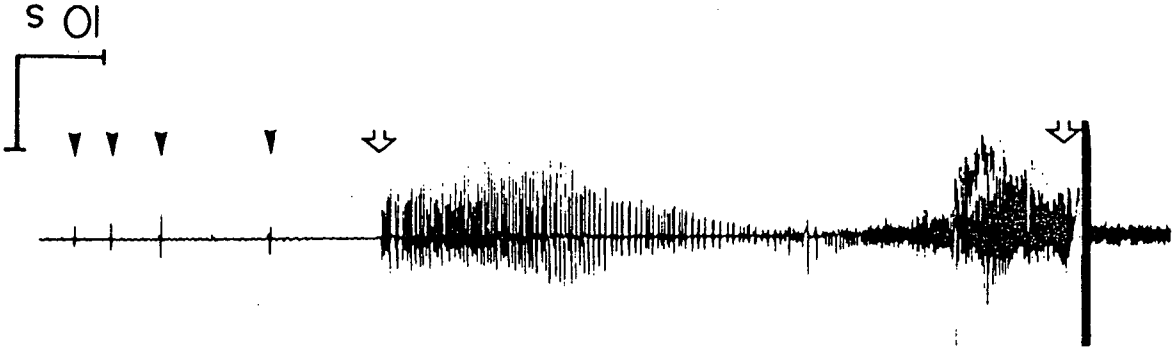


Table 2.1.

Effect of afterdischarges (AD's) on levels of hippocampal and cerebellar CaBP.

Afterdischarges recorded in the hilus of the dentate gyrus were evoked through commissural stimulation as described in the text. The levels of CaBP in brain samples were determined by the use of a specific radioimmunoassay (RIA).

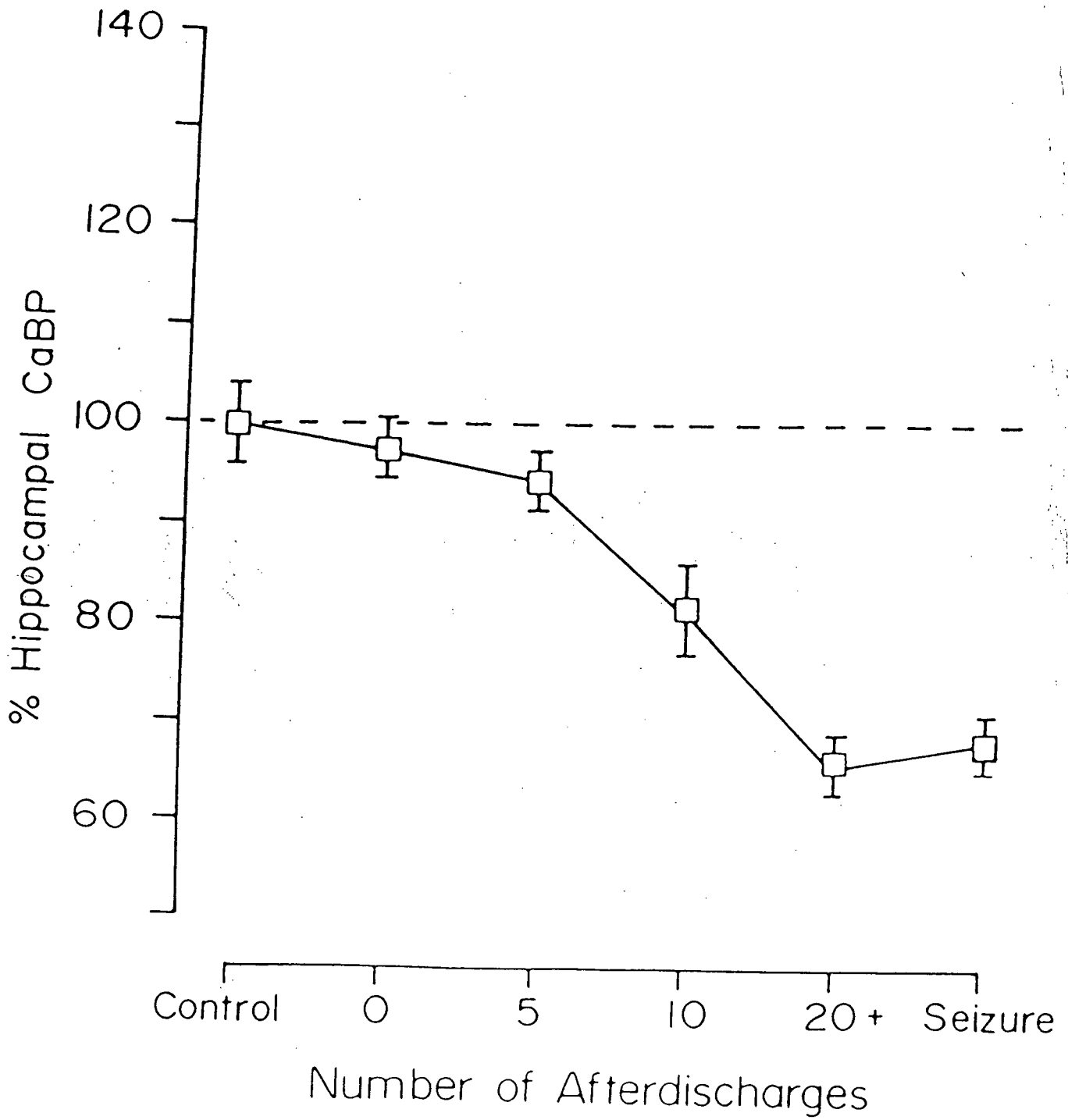
	Control	0 AD's	5 AD's	10 AD's	20 AD's	Seizures
=====						
HIPPOCAMPUS						
TSP (ug/mg wet wt)	34.1 $\pm$ .7	33.3 $\pm$ 1.1	33.5 $\pm$ .7	34.6 $\pm$ .8	35.9 $\pm$ .8	36.2 $\pm$ 1.3
CaBP (ng/mg TSP)	962 $\pm$ 40	936 $\pm$ 36	907 $\pm$ 29	786 $\pm$ 43*	635 $\pm$ 31*	653 $\pm$ 31*
CEREBELLUM						
TSP (ug/mg wet wt)	30.8 $\pm$ 1.6	31.9 $\pm$ 1.1	30.6 $\pm$ 1.3	32.2 $\pm$ 1.8	31.9 $\pm$ .8	30.2 $\pm$ .9
CaBP (ng/mg TSP)	11852 $\pm$ 603	11721 $\pm$ 554	12547 $\pm$ 406	12014 $\pm$ 501	12537 $\pm$ 540	12024 $\pm$ 309
NUMBER OF ANIMALS	6	7	9	8	9	7
=====						

NOTE: numbers represent mean  $\pm$  S.E.M.

\* Denotes significant difference from control group ( $p < 0.001$ ) -- Duncan's multiple range test.



Figure 2.6. Relationship between the number of evoked AD's and decline of hippocampal CaBP levels during development of commissural kindling. "Control" refers to animals implanted with electrodes, but not stimulated, while the "0 afterdischarges" group consists of animals with no detectable afterdischarges after several (5-25) kindling stimuli probably due to their high afterdischarge thresholds. Error bars: S.E.M.; n for each point = 12-18.



Since in this study levels of CaBP were expressed as fraction of total soluble proteins (TSP), it is important to note that TSP levels were unaltered by kindling. In addition, no significant changes were found in either CaBP or TSP levels of the control/reference cerebellar tissue (Table 2.1.).

#### 2.3.4. Discussion

The present study confirms and extends the observations of Baimbridge and Miller (1984) on the progressive decline of hippocampal CaBP during the process of kindling. The findings indicate that alterations in both biochemical and electrophysiological functions occur well before the onset of motor-seizures and further demonstrate that they are dependent on the number of hippocampal afterdischarges. Not only is there a biochemical alteration which precedes the onset of a full motor-seizure there is also an apparent correlation between these changes and the occurrence of AD's.

It has been established that the loss of hippocampal CaBP is confined to the granule cells of the dentate gyrus (Miller and Baimbridge, 1983) and to be independent of the limbic stimulation site (Baimbridge et al., 1985). This reduction in CaBP depends on the number of evoked hippocampal AD's with a half-maximal loss (16%) present by 10 AD's (cf., Baimbridge and Miller, 1984). A slight decline in the levels of CaBP was already detected after 5 AD's, and although this change was not significant (6%), the absolute loss may be greater. It has to be considered that

measurement of CaBP in the whole hippocampus tends to underestimate the changes localized to the dentate gyrus. While other cell types within the hippocampus, most notably the CA1 and CA2 pyramidal neurons, also contain CaBP, their CaBP content is unaffected by kindling (Miller and Baimbridge, 1983). Thus the granule cell specific loss of CaBP even after 5 AD's is probably larger than 12% when the volume to volume ratio of dentate gyrus/CA1+CA2 is taken into account. The maximum loss (32% in whole hippocampus) was reached after 20 AD's confirming the previous studies of Baimbridge and Miller (1984).

Electrophysiological parameters other than afterdischarges are also affected in the process of kindling. It is known for example, that in the dentate gyrus there is an enhancement of paired pulse inhibition following kindling-induced epilepsy (Tuff et al., 1983; Oliver and Miller, 1985) probably reflecting the pronounced interictal inhibition which is known to occur following kindling-induced seizures (Engel and Ackermann, 1982; Fujita et al., 1983). This increase in inhibitory events may serve as a protective mechanism which would retard the development and spread of kindling-induced seizure activity.

It is difficult to ascertain whether any of the changes observed in the present study (i.e., loss of CaBP and prolonged AD's) are causally related, and furthermore, whether the loss of CaBP may be responsible for the augmented inhibitory processes of the dentate gyrus (Tuff et al., 1983, Oliver and Miller, 1985). As described by the many possible functions of CaBP in the CNS (see Section 2.1.3.), a decline in a putative intraneuronal

$\text{Ca}^{2+}$  buffer might alter multiple and perhaps competitive processes leading to both enhanced excitability (AD's development) and increased inhibitory events (paired-pulse). The loss of CaBP during kindling may result in an increased neuronal calcium influx analogous to cortical structures where the bursting characteristic of epileptiform activity is paralleled by a decrease of extracellular  $\text{Ca}^{2+}$  (Heinemann et al., 1977) and seizures induced by l-allylglycine, where the amount of intra-neuronal  $\text{Ca}^{2+}$  becomes elevated (Griffiths et al., 1982). Recent evidence suggests that this may indeed be the case, at least when the kindling stimulus is delivered directly to CA1 neurons (Wadman et al., 1985). Furthermore, the kindling model of epilepsy is also characterized by an altered calcium-homeostasis (see Section 3.3.), although total hippocampal  $\text{Ca}^{2+}$  remains constant (see Section 3.1). With the loss of CaBP, the elevated levels of inhibition may be due to a sustained activation of the  $\text{gK}_{\text{Ca}}$  which would also promote a decrease in firing rate of the neurons to counteract the high frequency kindling stimulation. If the enhancement of inhibitory events of the dentate granule cells during kindling proves to be  $\text{Ca}^{2+}$ -dependent, a link between the loss of a  $\text{Ca}^{2+}$ -buffer (CaBP) and the electrophysiological alterations may be revealed. Alternatively, the fall in CaBP and the change in  $\text{Ca}^{2+}$ -regulation may be coincidental with the enhancement of paired-pulse inhibition. In this case the events could be part of global neurochemical and electrophysiological alterations characteristic of the kindling-induced epilepsy.

## 2.4. Distribution of CaBP in cortical areas of the epileptic

### El mouse

#### 2.4.1. Introduction

It has been acknowledged that genetic factors, if not solely responsible for epileptiform activity, may significantly contribute to the generation of seizures. Particularly in human epilepsy the importance of genetic determinants seems evident, as stressed in a review by Newmark and Penry (1980). In several species including the chicken, mouse, gerbil, rat, dog and baboon at least one genetic model of epilepsy is available and numerous investigators have provided evidence for specific neurochemical changes associated with these models (cf., Jobe and Laird, 1981; Laird et al., 1984). Most of the animals exhibit seizures following presentation, in some cases repeated over several weeks, of one or more environmental factors such as postural, auditory or photic stimuli.

The genetic influences may be directly responsible for the enhanced susceptibility for seizures. Alternatively, they may cause permanent changes in the CNS with resulting effects whereby neuronal tissue will more easily contribute to epileptogenesis when adequately stimulated. In view of the role of  $\text{Ca}^{2+}$  in neuronal excitability it is feasible that some of these permanent, genetically determined alterations may involve some calcium-dependent mechanism(s). This seems to be the case with

the seizure prone strain of mice (DBA/2N) where a deficiency of the  $\text{Ca}^{2+}$ -ATPase enzyme has been demonstrated (Rosenblatt et al., 1976).

The epileptic (El) strain of mice, as opposed to its more widely used audiogenic counterpart (the DBA/2J strain), is characterized by induction of seizures through vestibular stimulation. It has been developed in Japan and reported as the 'ep' mouse (Imaizumi et al., 1959), and later registered as the 'El strain' (Imaizumi et al., 1964). The El mouse has therefore been mainly studied by Japanese investigators who have shown that its induced seizures are true electrographic events (Suzuki, 1976; Suzuki and Nakamoto, 1977). The documented neurochemical findings include a lower than normal level of brain norepinephrine (Hiramatsu et al., 1976), and abnormally elevated acetylcholine, GABA and taurine concentrations (Naruse et al., 1960; Kurokawa et al., 1966; Iwata et al., 1979). In addition, a recent study using the 2-deoxyglucose technique, to detect metabolic alterations, has established the hippocampus as the presumed epileptic focus (Suzuki et al., 1983).

The involvement of the hippocampal formation in the generation of seizures, as it is in the kindling model of epilepsy (see Section 2.3.), could mean that similarities may exist between the two models of experimental epilepsy regarding epileptiform phenomena. Some of these mechanisms may be related to altered regulation of  $\text{Ca}^{2+}$  in certain CNS structures. The cortical distribution of CaBP was therefore examined in the epileptic El strain and in a control, non-seizure prone strain

(Swiss Albino CF-1) to detect possible genetic differences. Furthermore, sex differences in the levels of the protein were analyzed and the effect of seizures on cortical CaBP content was determined using seizing and non-seizing El mice.

#### 2.4.2. Methods

The epileptic El strain was obtained from Dr. J. Suzuki of the Psychiatric Research Institute of Tokyo and generations El-F-75 and El-F-76 were bred at the U.B.C. Department of Physiology's animal care facilities. The animals were housed in plastic boxes covered with a mesh and were cleaned once a week to avoid excessive vestibular stimulation upon moving of the cages. Weight and age matched mice of the Swiss Albino strain (CF-1) were used as controls. The weights of all animals used in the study ranged from 20 to 38 g.

The seizures of the El strain may be induced by vestibular stimulation of various forms. Among the several stimulation paradigms including pendulum type swinging, repeated vertical or horizontal movements, and tossing up of the animal, the most effective method is a 15-20 cm throw in the air, whereafter the mice land on their paws on a soft surface (Kurokawa et al., 1966). In the present study the animals were stimulated mainly through this latter procedure, although vertical swinging was also used and found to be just as effective.

Each stimulation trial consisted in careful removal of the animal from its cage and 30 consecutive throws or vertical



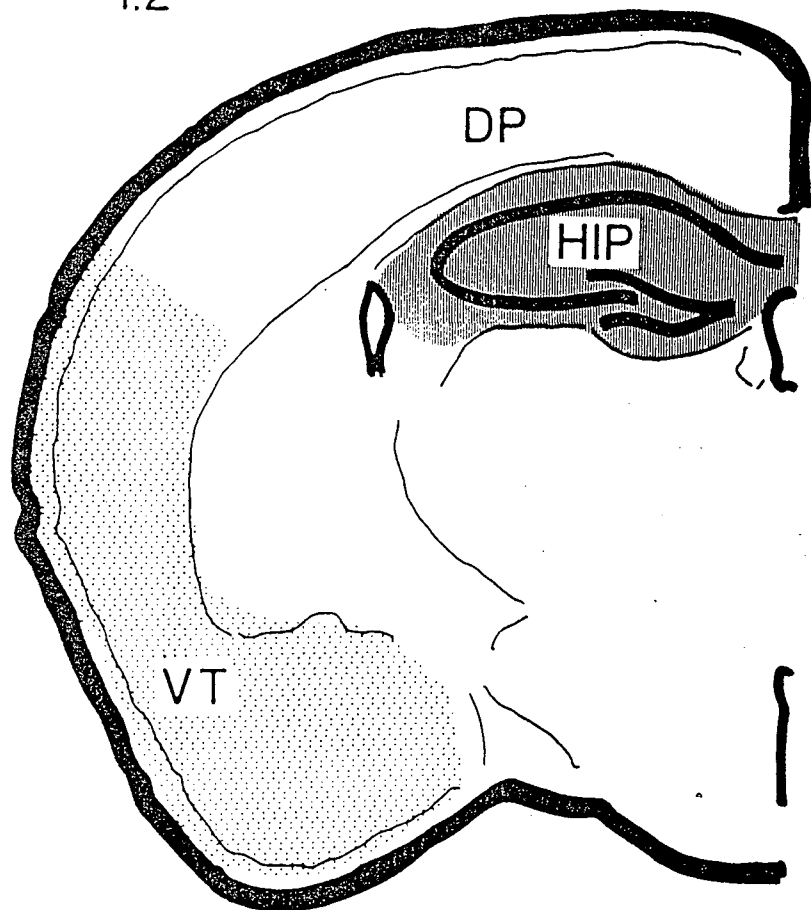
movements. The first stimulation started when the animals reached the age of 3 weeks (Suzuki and Nakamoto, 1977) and continued every 4-5 days until the desired number of seizures was obtained. If the animal had a convulsion, no further stimuli were delivered during the session. Control El mice did not undergo stimulation trials and their handling was minimal to avoid excessive vestibular input.

Animals of both sexes were sacrificed 2-4 days following the last seizure together with non-stimulated counterparts and mice of the control strain. The brains were removed and dissected into the approximate cortical areas of Fig. 2.7. following separation of the cerebellum, hippocampal formation and caudate nucleus. The landmark for distinguishing between parietal and occipital areas was the artery of the central sulcus. The tissue was prepared for radioimmunoassay (RIA) as described in Section 2.1.2.2. with pooling of right and left hemispheric samples. The procedure of RIA for CaBP was similar to that described for rat samples (Section 2.2.2.1.) and the CaBP content was expressed as ng/mg TSP (total soluble protein).

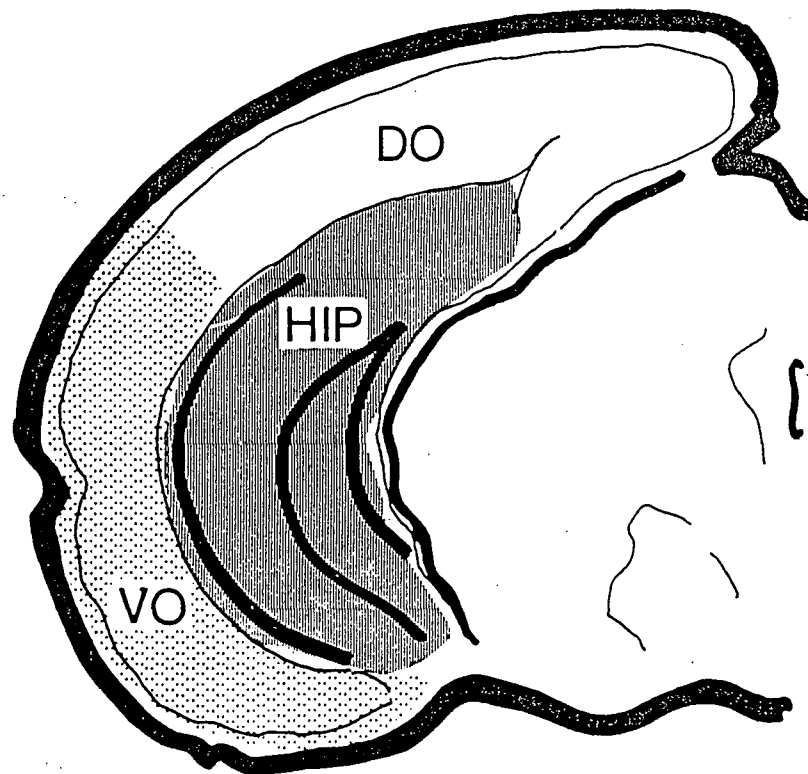
Statistical analysis was done on the pooled data from several experiments and consisted of a two-factor ANOVA. One analysis involved the combined effect of strain and sex on levels of CaBP and compared the control strain to non-seizing El. The other comprized the seizing (animals exhibiting more than 7 full motor seizures) and the non-seizing El group to find possible alterations due to the sex of animals and/or seizures.

Figure 2.7. Cortical areas used for determination of CaBP levels in mice. The drawings are diagrammatic representations from Slotnick and Leonard (1975) with the numbers marked by an asterisk indicating mm from bregma. The abbreviations for the various cortical areas as used in this and subsequent figures (2.8 and 2.9.) are indicated on the lower part of the figure.

-1.2★



-3.2★



HIP- Hippocampus

DP - Dorsal Parietal Cortex

VT - Ventral Temporal Cortex

DO - Dorsal Occipital Cortex

VO - Ventral Occipital Cortex

### 2.4.3. Results

Following repeated vestibular stimulation, mice of the El strain exhibited strong tonic or clonic convulsions mostly preceded by squeaks, as described by Kurokawa et al. (1966). These seizures usually lasted for about 15-30 s and were typically evoked between the 4<sup>th</sup> and the 9<sup>th</sup> stimulation sessions. Although not frequently, some of the previously stimulated animals exhibited spontaneous seizures following their removal from the common housing cage, probably due to the inadvertent mild vestibular stimulation.

Histograms representing the cortical distribution of CaBP in control and El mice are shown in Figs. 2.8. and 2.9., for males and females respectively. As has been shown for the cortical distribution of CaBP in rats (see Section 2.2.3.), there was a clear dorso-ventral distribution of the protein with higher levels confined to ventral cortical regions. The cumulative data and the statistical analysis are summarized in Tables 2.2. and 2.3 respectively.

#### Effect of strain

Certain cortical areas of the El strain were found to contain lower levels of CaBP than the control CF-1 strain. The hippocampi of male El mice have on the average 13% less CaBP than mice of the CF-1 strain while female Els have 8% lower hippocampal CaBP levels than their CF-1 counterparts. The strain

differences are more pronounced in the dorsal occipital cortex where the respective changes are 14% and 15%. In other cortical areas the CaBP levels were quite comparable and no significant differences could be detected with the two-way ANOVA.

#### **Effect of sex**

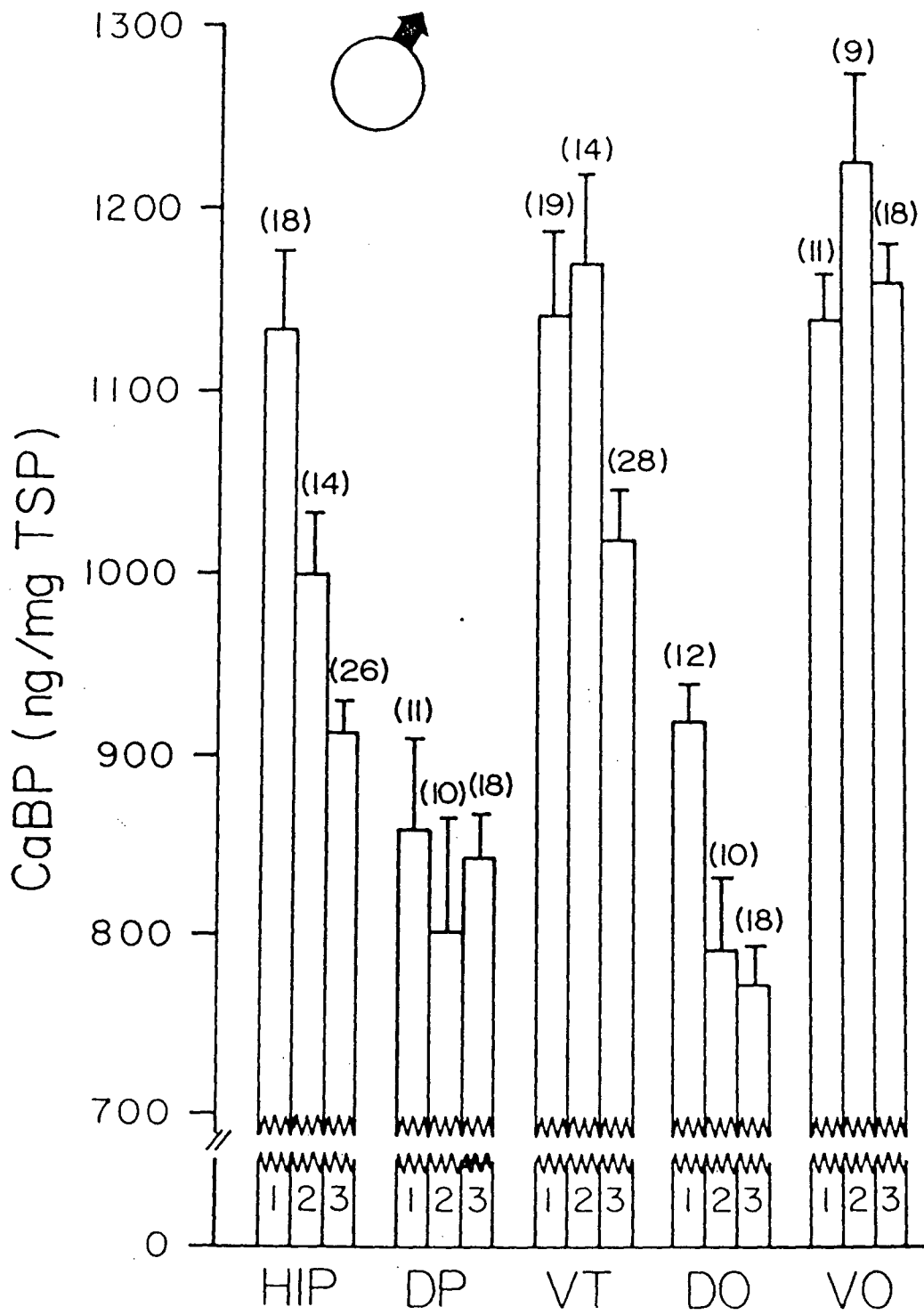
Significantly lower CaBP levels were detected in females of both strains in the hippocampal formation (13% in CF-1 and 8% in El) and the ventral occipital cortical areas (6% in CF-1 and 18% in El). The CaBP content of the dorsal parietal cortex in female mice was found to be elevated compared to males (19% in CF-1 and 17% in El). Differences due to sex appeared to be significant in the El strain even after seizures have been induced. The seizing female El mice retained the characteristic changes of the ventral occipital and dorsal parietal cortices, but hippocampal CaBP levels only showed the effect of seizures.

#### **Effect of seizures in the El strain**

The induction of seizures decreased the levels of CaBP in the El strain, particularly in the hippocampus and the ventral parietal/temporal cortices. The largest change was observed in the ventral temporal cortex of male El mice which contained 12% less CaBP than the corresponding cortical region of their non-stimulated counterparts.

All cortical and cerebellar samples examined had a comparable TSP content and the ratio of TSP/tissue wet weight was found to be constant, indicating that the observed alterations in

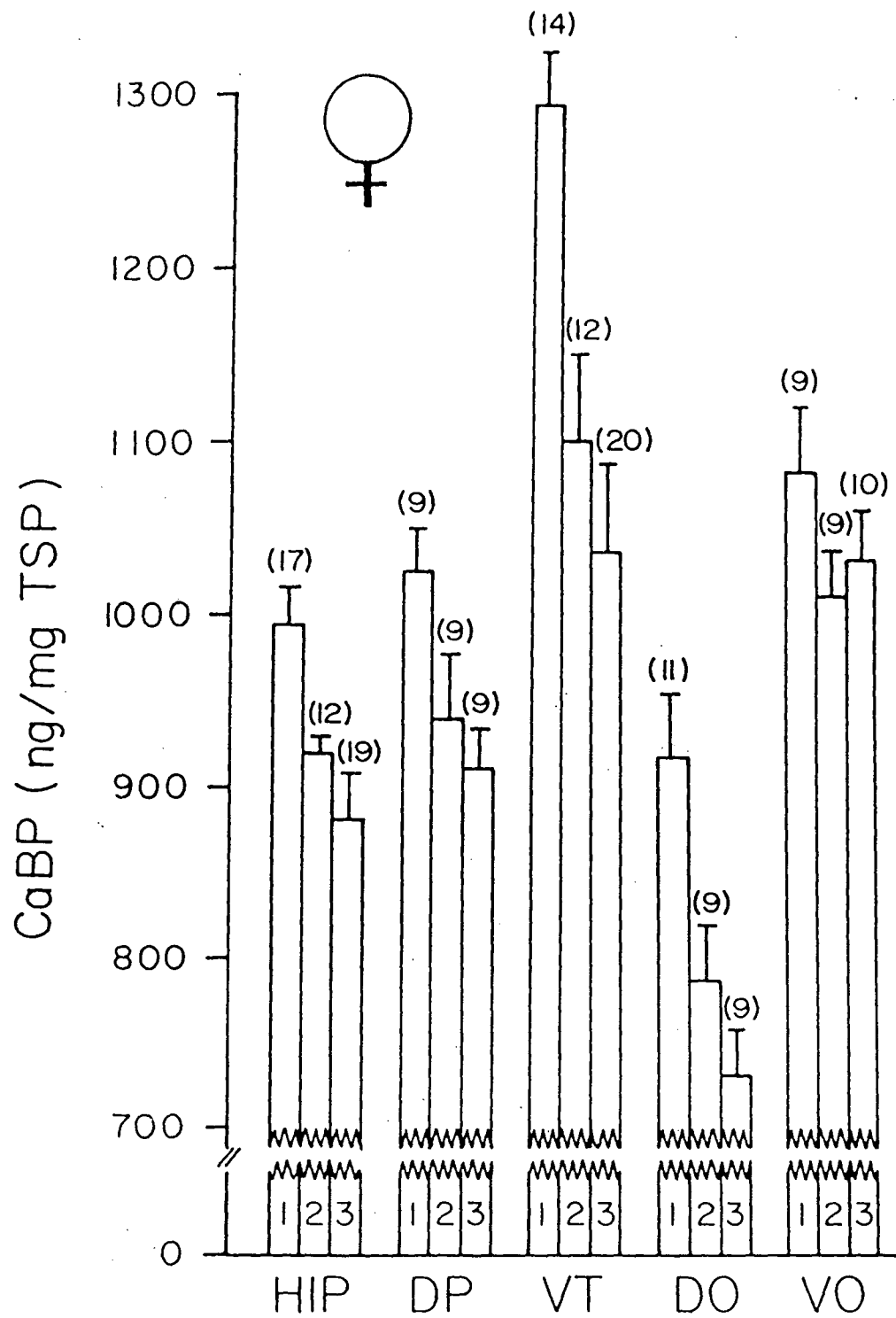
Figure 2.8. Levels of CaBP in cortical areas of control and El male mice. The cortical regions are abbreviated as shown in Fig. 2.7. Error bars indicate S.E.M. while the numbers in parentheses represent the number of samples.



- ① Control strain (Swiss)
- ② EL strain (no seizures)
- ③ Seizing EL (>7 seizures)

Figure 2.9. Levels of CaBP in cortical areas of control and E1 female mice. The cortical regions are abbreviated as shown in Fig. 2.7. Error bars indicate S.E.M. while the numbers in parentheses represent the number of samples.





① Control strain (Swiss)

② EL strain (no seizures)

③ Seizing EL (>7 seizures)

CaBP was measured according to the RIA described in the text. Cortical areas from mice of the control strain CF-1 (Swiss) and the epileptic strain El are shown on Fig. 2.7. The control El group (El<sub>ns</sub>) received no stimulations and exhibited no seizures, whereas the seizing El (El<sub>s</sub>) group had at least 7 full motor seizures each. Number of samples = (n).

Cortical Area	CaBP content (ng/mg TSP)					
	MALES			FEMALES		
	Swiss	El <sub>ns</sub>	El <sub>s</sub>	Swiss	El <sub>ns</sub>	El <sub>s</sub>
<b>CEREBELLUM</b>						
mean	12,506	13,233	13,036	13,322	12,361	12,660
S.D.	1,099	1,290	958	971	1,055	1,220
(n)	(12)	(10)	(18)	(17)	(12)	(20)
<b>HIPPOCAMPUS</b>						
mean	1,134	999	912	993	920	881
S.D.	184	119	83	81	120	110
(n)	(18)	(14)	(26)	(17)	(12)	(19)
<b>DORSAL PARIETAL CTX.</b>						
mean	859	802	843	1,025	939	910
S.D.	156	190	97	68	110	65
(n)	(11)	(10)	(18)	(9)	(9)	(9)
<b>VENTRAL TEMPORAL CTX.</b>						
mean	1,141	1,157	1,018	1,292	1,101	1,035
S.D.	170	161	100	107	165	224
(n)	(19)	(14)	(28)	(14)	(12)	(20)
<b>DORSAL OCCIPITAL CTX.</b>						
mean	918	792	772	917	787	730
S.D.	77	108	77	119	89	78
(n)	(12)	(10)	(18)	(11)	(9)	(9)
<b>VENTRAL OCCIPITAL CTX.</b>						
mean	1,139	1,225	1,160	1,082	1,010	1,032
S.D.	70	153	89	103	78	95
(n)	(11)	(9)	(18)	(9)	(9)	(10)

Table 2.3.

Two-way analysis of variance (ANOVA) of the effects of strain, sex and seizures on the cortical levels of CaBP in control and El mice.

The two-way ANOVA was done on the data presented in Table 2.2. and involved two comparisons: 1.) between the control group (Swiss) and the non-seizing El group (El<sub>ns</sub>) to determine the effects of sex and strain, and 2.) between the seizing (El<sub>s</sub>) and non-seizing El group to examine the effects of gender and seizures on the cortical CaBP levels. The effect was considered to be non-significant (N.S.) if  $p > 0.01$ . The respective cortical areas are represented in Fig. 2.7.

Cortical Area	1. Swiss vs. El <sub>ns</sub>			2. El <sub>ns</sub> vs. El <sub>s</sub>		
	Sex	Strain	Interaction sex--strain	Sex	Seizure	Interaction sex-seizure
CEREBELLUM	N.S.	N.S.	$p < 0.005$	N.S.	N.S.	N.S.
HIPPOCAMPUS	$p < 0.005$	$p < 0.005$	N.S.	N.S.	$p < 0.025$	N.S.
DORSAL PARIETAL CTX	$p < 0.005$	N.S.	N.S.	$p < 0.025$	N.S.	N.S.
VENTRAL TEMPORAL CTX	N.S.	N.S.	$p < 0.025$	N.S.	$p < 0.025$	N.S.
DORSAL OCCIPITAL CTX	N.S.	$p < 0.001$	N.S.	N.S.	N.S.	N.S.
VENTRAL OCCIPITAL CTX	$p < 0.001$	N.S.	$p < 0.001$	$p < 0.001$	N.S.	N.S.

terms of CaBP levels were not due to abnormally elevated cellular soluble proteins. In addition, the slight changes in cerebellar CaBP levels were found not to be significant except for an interaction between sex and strain.

#### 2.3.4. Discussion

Genetic models of epilepsy have significantly contributed to our current understanding of neurochemical and neurotransmitter alterations in seizure disorders (Jobe and Laird, 1981; Laird et al., 1984). The present study confirms the results of numerous Japanese investigators who have demonstrated that the El strain of mice is a reliable model of experimental epilepsy in which seizures may be triggered through vestibular stimulation in a highly reproducible fashion. Since repeated stimuli (4-9) are necessary to evoke full motor seizures, this model may be considered as being related to kindling-induced epilepsy where successive electrical stimuli are applied in order to induce convulsions (Goddard et al., 1969). Therefore, analogous to kindling, some lasting alterations must take place during the time of stimulation that ultimately result in the abnormal functioning of nerve cells. In contrast to kindling which may be induced in any strain of a given species, the El mice should have some additional neuronal determinants that make it prone to aberrant neuronal activity.

It has been reported that whole brain acetylcholine and GABA levels of the El mice are significantly higher than those of

control strains while excitatory amino acids (glutamate and aspartate) are reduced (Kurokawa et al., 1966). This may reflect a genetic factor that is part of a global defence mechanism against, rather than a direct cause of the seizure disorders. This hypothesis is further supported by the elevated levels of taurine in El mice and the fact that taurine injections raised their convulsion threshold (Iwata et al., 1979). However, some lasting neurochemical alteration is probably responsible for the propensity for seizures in the El strain since these mice have a significantly lowered metrazol- and electrical stimulation-induced seizure threshold (Kurokawa et al., 1966).

Albeit no detailed electrophysiological investigation is available concerning the El strain, it may very well be that inhibitory events are enhanced in various cortical areas due to larger than normal GABA levels. By analogy, supranormal inhibitory events, although not necessarily GABA-mediated, have been described in the dentate gyrus following kindling-induced epilepsy (Tuff et al., 1983; Oliver and Miller, 1985) which may be due to the selective loss of CaBP from the granule cells of this structure (Miller and Baimbridge, 1983).

The decreased levels of CaBP, as measured by RIA, in certain cortical structures of the El mice may thus relate to the variety of neurochemical findings in this strain (Naruse et al., 1960; Kurokawa et al., 1966; Hiramatsu and Mori, 1977; Iwata et al., 1979) or alternatively, may reflect an alteration in cortical  $\text{Ca}^{2+}$ -regulation of the El strain. Since no detectable morphological alterations are noted in neurons of the El mice

under light- or electron microscopic investigation (Kurokawa et al., 1966), the loss of CaBP is not likely to be a result of neuronal degeneration processes.

If mechanisms underlying  $\text{Ca}^{2+}$  homeostasis in certain cortical structures of the El mice are disturbed, it is expected that significant changes in neuronal excitability would parallel these alterations. The hippocampal formation is the only cortical area where significant strain and seizure related differences were found in terms of CaBP levels. It is this structure that presumably constitutes the focus of paroxysmal discharges in the epileptic strain as measured by local glucose utilization (Suzuki et al., 1983). In addition to the hippocampus, the ventral parietal/temporal cortex showed a significant decline in levels of CaBP following seizures. This area has previously been associated with the electrographic focus of aberrant discharge patterns (Suzuki, 1976; Suzuki et al., 1977). It is not known what the significant strain related alteration in CaBP content of dorsal occipital cortical areas may be a reflection of. The sex related differences in both control and El strains are also unclear. No study is available with regard to the effect of sex hormones on brain CaBP levels. However, administration of estradiol markedly lowers seizure threshold in male or ovariectomized female rats (Millichap, 1969), indicating that it has a profound effect on seizure generation in neurons. Whether the significantly lower levels of CaBP in the hippocampi and ventral occipital cortices

of female mice represent the effects of sex hormones remains to be determined.

Further immunohistochemical studies are necessary to ascertain the precise anatomical localization and confinement of the CaBP loss observed in the El mice both with or without seizures. In addition, electrophysiological investigations should determine the nature of excitability changes that occur in this valuable model of genetic epilepsy.

## CHAPTER III.

MEASUREMENT OF HIPPOCAMPAL  $\text{Ca}^{2+}$ -HOMEOSTASIS

There are a considerable number of neuropathological conditions where abnormalities in regulation of intracellular  $\text{Ca}^{2+}$  could explain many of the altered functions of nerve cells. Several methods are available for detection of  $\text{Ca}^{2+}$  activities in various tissues (Borle, 1981a; Blinks et al., 1982; Campbell, 1983; Tsien, 1983b). These methods include measurement of total  $\text{Ca}^{2+}$  content usually by atomic absorption spectrophotometry (AAS), chelating agents or colorimetric titration; measurement of free intracellular  $\text{Ca}^{2+}$  by the use of metallochromic or optical indicators; or determination of ionic compartmentalization by kinetic analysis of radioactive tracer fluxes; and more recently, measurement of  $\text{Ca}^{2+}$  ionic activity (either extra- or intracellularly) with the aid of ion-sensitive microelectrodes (ISMs).

Although the large arsenal of methods for detection and measurement of  $\text{Ca}^{2+}$  would suggest that determination of its ionic activities is a relatively easy task, in practice this is rarely the case. Particularly in the mammalian CNS, where one has to deal with aggregates of small, sometimes not easily accessible



nerve cells, there are only a few applicable procedures for assesement of  $\text{Ca}^{2+}$ -homeostasis. So far AAS and precipitative techniques (e.g., oxalate-pyroantimonate) have been proven successful for determination of total  $\text{Ca}^{2+}$  while ionic flux measurements have been directly estimated using  $^{45}\text{Ca}$  or by monitoring  $\text{Ca}^{2+}$ -dependent electrical events. The use of ISMs has generally been restricted to the mere estimation of changes in intracellular  $\text{Ca}^{2+}$  alterations by monitoring extracellular  $\text{Ca}^{2+}$  activities. The present study examines calcium regulation in the hippocampal formation under normal and various experimental and neuropathological conditions using two direct methods of measurement: the AAS procedure for total  $\text{Ca}^{2+}$  determination, and the kinetic analysis of  $^{45}\text{Ca}$  uptake curves for investigation of intracellular  $\text{Ca}^{2+}$  distribution and compartmentalization.

### 3.1. Measurement of total hippocampal $\text{Ca}^{2+}$ and $\text{Zn}^{2+}$ using atomic absorption spectrophotometry (AAS)

#### 3.1.1. Introduction

Atomic absorption spectrophotometry (AAS) is one of the most sensitive and specific methods available for total cell or tissue  $\text{Ca}^{2+}$  estimates. The technique depends on the excitation of electrons in free atoms that are obtained by vaporization of compounds in a high temperature flame. The atoms in the flame are excited by the absorption of light at a certain wavelength (e.g., for  $\text{Ca}^{2+}$  at 422.7 nm) after the sample has been atomized in an air-acetylene flame (2570 K) or in nitrous oxide-acetylene flame (3230 K) (Willis, 1963). The presence of  $\text{Ca}^{2+}$ -binding anions, such as phosphate reduces atomization and therefore decreases the sensitivity of the method for calcium. However, the interference caused by these calcium ligands can be eliminated by the addition of  $\text{La}^{3+}$  which produces a maximum sensitivity for assay of  $\text{Ca}^{2+}$  (Pybus et al., 1970).

Since the preparation of tissues for AAS measurements is usually similar regardless of the nature of the ion involved, tissue content of a variety of other ions may be determined in conjunction with total  $\text{Ca}^{2+}$ . Of particular relevance to the present study was the determination of hippocampal  $\text{Zn}^{2+}$  levels. The presence of zinc in the hippocampal formation and in particular the dentate granule cell -- mossy fiber system has

been demonstrated in a number of histochemical studies (Timm, 1958; Crawford and Connor, 1972; Haug, 1974; Danscher, 1981; Stengaard-Pedersen et al., 1983), but the role of this transition metal in the CNS remains poorly understood (Crawford, 1983). Electrophysiological investigations have shown some alterations in the function of the mossy fiber input to CA3 pyramidal cells using  $H_2S$  chelating techniques (von Euler, 1962), while little change was detected with the  $Zn^{2+}$ -chelator diethyldithiocarbamate (Danscher et al., 1975). More recent studies have suggested that high levels of zinc may be responsible for convulsive behavior in certain experimental models of epilepsy (Chung and Johnson, 1983; Pei et al., 1983), and have found that iontophoresis of  $Zn^{2+}$  enhances the firing rate of cortical neurons (Wright, 1984).

In view of these findings and the fact that significant biochemical alterations take place in the dentate granule cell -- mossy fiber system during kindling-induced epilepsy (Miller and Baimbridge, 1983; Baimbridge and Miller, 1984; Baimbridge et al., 1985; also see Section 2.2.), i.e., the specific loss of a calcium-binding protein (CaBP), the present study was undertaken to investigate possible changes in hippocampal  $Zn^{2+}$  and  $Ca^{2+}$  levels following kindling. Alterations in the total tissue content of these metals could be responsible for some of the aberrant discharge properties of dentate gyrus granule cells during and following kindling-induced epilepsy (see Section 2.2.3.).

### 3.1.2. Methods

Adult male Wistar rats were kindled through the hippocampal commissures according to the procedures described in Section 2.3.2., with the exception that no recording electrodes were implanted to monitor afterdischarge activity. Following recovery from surgery the animals received daily kindling stimuli (100  $\mu$ A, 60 Hz for 1 s) or sham stimulation (controls). Animals were divided into three experimental groups: a) controls (n=4); b) partially kindled, i.e., 20 stimulation trials but no evidence of motor seizures (n=4); c) fully kindled, i.e., 5-10 motor seizures evoked through 30-40 stimulation trials (n=6).

The day following the last stimulation the animals were decapitated, the brains were removed using plastic instruments washed in HCl to avoid ionic contamination and then placed in HCl-rinsed polystyrene vials containing 4% formaldehyde solution (Fjerdingstad et al., 1974; Kemp and Dansher, 1979). Analysis has shown that the formaldehyde solution was devoid ( $<0.01$  part per million (ppm)) of  $\text{Zn}^{2+}$  and  $\text{Ca}^{2+}$  contamination both before and after storage of the brain samples (see also Fjerdingstad et al., 1974). Following a 3-day storage period at  $4^{\circ}\text{C}$  the hippocampi were dissected free and dried overnight at  $110^{\circ}\text{C}$ . The samples were then weighed and dissolved in 1 ml of concentrated  $\text{HNO}_3$  (Baker Analyzed Reagent) upon gradual heating. Further dilutions were made using bidistilled water which contained 10 mmol/l  $\text{LaCl}_3$  and 50 mmol/l HCl (Baker Analyzed Reagent) for samples prepared

for  $\text{Ca}^{2+}$  analysis (Pybus et al., 1970). Standard solutions containing appropriate concentrations of zinc and calcium (Aldrich) were prepared in  $\text{HNO}_3$  diluted to the same extent as the tissue samples, with 10 mM  $\text{LaCl}_3$  and 50 mM  $\text{HCl}$  added to the  $\text{Ca}^{2+}$  standards.

For detection of the metals a Jarrel-Ash 280 atomic absorption spectrophotometer (with air-acetylene flame) was used connected to a Sargent recorder. Readings were done at 422.7 and 213.9 nm, the principal absorption lines for  $\text{Ca}^{2+}$  and  $\text{Zn}^{2+}$  respectively. The standard curves were linear in the range of 0.01-0.3 ppm for  $\text{Zn}^{2+}$  and 0.1-10.0 ppm for  $\text{Ca}^{2+}$ . Each sample was measured three times and the metal concentration was interpolated using linear regression from the standard curve.

Although measurements were made on parts per million/dry weight basis, the values were extrapolated to wet weight, considering dry weight to be 22% of total tissue weight (Chung and Johnson, 1983).

### 3.1.3. Results

Calcium and zinc content in whole hippocampi of control and commissural-kindled rats is presented in Table 3.1. The dry weight of tissue samples was considerably constant in all three experimental groups and was not different from values published in previous reports (e.g., Frederickson et al., 1982). The amount of calcium in control hippocampi (1.81 mmol/kg wet weight - extrapolated) is somewhat lower than found by other investigators

Table 3.1.

Calcium and zinc in the hippocampal formation of control and commissural-kindled rats as measured by atomic absorption spectrophotometry.

	Sham stimulated (n=8)	Commissural-kindled	
		No seizures (n=8)	5-10 Seizures (n=12)
Whole hippocampus dry weight (mg)	12.15 $\pm$ 1.0	12.85 $\pm$ 1.3	12.46 $\pm$ 1.3
Hippocampal Ca, ppm/dry weight	329.80 $\pm$ 39.6	357.70 $\pm$ 32.4	356.70 $\pm$ 72.1
mmol/kg wet weight*	1.81 $\pm$ 0.22	1.96 $\pm$ 0.17	1.96 $\pm$ 0.39
Hippocampal Zn, ppm/dry weight	88.30 $\pm$ 4.6	92.90 $\pm$ 5.9	101.60 $\pm$ 7.1**
umol/kg wet weight*	297.00 $\pm$ 15.5	312.70 $\pm$ 19.9	342.00 $\pm$ 23.9**

NOTE: Numbers represent means  $\pm$  S.D., n = number of hippocampi.

\* Extrapolated from parts per million dry weight using wet weight dry weight = 100/22 (Chung and Johnson, 1983) and the atomic weights: Ca=40.08, Zn=65.37.

\*\* Significantly different from control ( $p < 0.001$ ) and partially kindled group ( $p < 0.05$ ) -- Duncan's multiple range test.

(cf., Borle, 1981a) but is similar to that obtained by Kemp and Danscher (1979) using X-ray emission spectroscopy in tissue fixed with formaldehyde. Commissural kindling tended to elevate total  $\text{Ca}^{2+}$  of the hippocampus, but this 8% change was found not to be significantly different from controls.

The values for basal  $\text{Zn}^{2+}$  content of the hippocampal formation are in good agreement with other studies using various methods of measurement (Kemp and Danscher, 1979; Frederickson et al., 1982; Baraldi et al., 1983; Chung and Johnson, 1983; Sato et al., 1984). In contrast with  $\text{Ca}^{2+}$ , zinc levels in the hippocampi of commissural-kindled rats with more than five motor seizures showed a marked 15.1% increase over basal  $\text{Zn}^{2+}$  concentrations and a 9.4% enhancement compared with partially kindled animals. In view of the fact that hippocampal zinc is mainly confined to the dentate granule cell -- mossy fiber system, which only accounts for a fraction of total hippocampal dry weight, the magnitude of the changes in the principal  $\text{Zn}^{2+}$ -containing elements may be as large as 40-50%.

#### 3.1.4. Discussion

Several studies have summarized neurochemical and neurotransmitter function alterations produced by kindling-induced epilepsy (McNamara et al., 1980; Kalichman, 1982; Peterson and Albertson, 1982; McNamara, 1984). The finding that a neuron-specific CaBP is selectively decreased in the granule cells of the dentate gyrus (Miller and Baimbridge, 1983) points toward

specific changes regarding calcium regulation in these cells. However, measurements of total hippocampal calcium did not reveal any major changes in its tissue content, suggesting that if  $\text{Ca}^{2+}$ -homeostasis is altered at all following kindling-induced epilepsy, this change has to occur via a distinct mechanism involving redistribution of the ion rather than an absolute change in its concentration.

The increase in zinc content may or may not be linked to an altered hippocampal calcium regulation. Enhanced levels of zinc may be epileptogenic (Chung and Johnson, 1983; Pei et al., 1983) but there is no indication about the exact mechanism(s) whereby  $\text{Zn}^{2+}$  may trigger these pathophysiological changes. Recent studies have shown that granule cells of the dentate gyrus take up zinc and release the cation upon stimulation (Assaf and Chung, 1984; Howell et al., 1984). Therefore, it is reasonable to assume that most of the changes presented in this study are confined to the granule cells and their mossy fibers.

Because zinc participates in the regulation of a wide variety of enzymes (Prasad, 1979; Ebadi et al., 1981; Wolf and Schmidt, 1982), it is difficult to speculate how an elevated zinc concentration may influence biochemical events and ultimately synaptic transmission in the hippocampus. For example, chronic zinc deficiency alters the function of the mossy fibers while CA3 pyramidal cells are unaffected (Hesse, 1979). Furthermore, a decrease in brain zinc during experimental hepatic encephalopathy is paralleled by a decrease in GABA-receptors (Baraldi et al., 1983). Whether the converse is true for an increase in zinc



concentration remains to be determined. The synthesis of CaBP itself may in turn be impaired by larger than normal amounts of  $Zn^{2+}$ , at least this seems to be the case in the gastro-intestinal tract where  $Zn^{2+}$  has been shown to inhibit the synthesis of vitamin D-dependent CaBP (Corradino and Fullmer, 1980). The colocalization of zinc with peptide neurotransmitters in the hippocampal formation (Stengaard-Pedersen et al., 1983) may indicate a similar function of the cation to that shown in pancreatic cells, i.e., the presence of  $Zn^{2+}$  protects insulin from proteolytic cleavage (Emdin et al., 1980).

The progressive increase in hippocampal zinc content during commissural kindling, probably due to an enhanced uptake of the cation from the CSF, is a novel correlate of kindling-induced epilepsy. If zinc is released from the mossy fibers following stimulation (Assaf and Chung, 1984), then its elevated levels during kindling may cause abnormal discharges of CA3 pyramidal cells, analogous to the effects seen in cortical neurons (Wright, 1984). On the other hand, out of the several possible actions of this transition metal, the manner in which it may play a role altering the electrophysiology (Tuff et al., 1983; Oliver and Miller, 1985) or the neurochemical parameters (Miller and Baimbridge, 1983) of dentate granule cells during and following kindling, remains yet to be determined.

### 3.2. Measurement of hippocampal exchangeable calcium using kinetic analysis of $^{45}\text{Ca}$ uptake curves

#### 3.2.1. Introduction

In the majority of physiological systems the level of intracellular calcium is maintained within strict limits by an energy dependent membrane pump linked to the  $\text{Ca}^{2+}/\text{Mg}^{2+}$ -ATPase, the  $\text{Na}^{+}/\text{Ca}^{2+}$  exchange system and a variety of intracellular  $\text{Ca}^{2+}$  chelating and buffering mechanisms consisting primarily of mitochondria, endoplasmic reticulum and calcium-binding proteins (Borle, 1981a). Alterations in any one of these processes will have significant effects on the level of intracellular  $\text{Ca}^{2+}$  which in turn may lead to changes in the physiological functioning of the cells. The measurement of intracellular  $\text{Ca}^{2+}$  concentrations has therefore been an important objective of many investigators. Although there are a number of well-documented methods of measurement, the limitations of their applicability to aggregates of small nerve cells, as is the case in the mammalian nervous system, are obvious (cf. Blinks et al., 1982). Calcium-sensitive microelectrodes that impale molluscan neurons with ease have rarely been used to measure intraneuronal  $\text{Ca}^{2+}$  concentrations of mammalian CNS neurons (Morris et al., 1983). In addition, the amount of  $\text{Ca}^{2+}$  distributed into the several sequestering and buffering systems of these nerve cells cannot be determined using this approach.

A relatively simple method that provides some insight into the compartmentalization of  $\text{Ca}^{2+}$  and its buffering is the kinetic analysis of  $^{45}\text{Ca}$  uptake or efflux curves. Provided the system is at a steady state, the tracer is introduced into the extracellular compartment and its distribution is monitored during a period of time in the cellular network under investigation. The uptake curve is fitted by a mathematical function and according to the principles of compartmental analysis (Robertson, 1957; Sheppard, 1962; Jacquez, 1972) the exchange rates of the cation and its intracellular distribution may then be determined.

Kinetic analysis of the  $^{45}\text{Ca}$  uptake curves has been widely used in several non-neuronal preparations, such as kidney, liver and myocardial tissues. (Borle, 1969; 1970; 1975a,b; 1981a; Claret-Berthon et al., 1977; Barritt et al., 1981; Uchikawa and Borle, 1981; Wakabayashi and Goshima, 1981). Its counterpart, the kinetic analysis of  $^{45}\text{Ca}$  efflux patterns, has been successfully applied to similar preparations (Uchikawa and Borle, 1978a,b) and in some cases to heterogeneous tissues, such as slices of the anterior pituitary (Moriarty, 1980) or brain (Rubiales de Barioglio and Orrego, 1982). Measurements of calcium using this approach have usually agreed with the results obtained through other techniques and methods (Borle, 1981a; Blinks et al., 1982). The aim of the present study was therefore to apply the kinetic analysis of  $^{45}\text{Ca}$  uptake curves to the hippocampal slice preparation in view of the variety of calcium-mediated phenomena that have been shown to exist in this CNS structure. The objectives were two-fold: 1) to determine the uptake function for

compartmental analysis and 2) to identify the nature and factors that influence the different  $\text{Ca}^{2+}$  pools and fluxes in this system.

### 3.2.2. Methods

A flow-chart of the methods used is presented in Fig. 3.1. Following incubation of the slices and calculation of calcium uptake, graphical and computerized methods of curve fitting were used to determine the exchange rates and calcium compartments of the tissue. The procedures underlying each step in the kinetic analysis of  $^{45}\text{Ca}$  uptake curves are described below.

#### 3.2.2.1. Measurement of $^{45}\text{Ca}$ uptake

Adult male Wistar rats were sacrificed, their brains quickly removed and the hippocampus dissected free. Slices, 450  $\mu\text{m}$  in thickness, were prepared using a Sorvall tissue chopper. Twenty-four to thirty slices were routinely obtained from both hippocampi and then were randomly distributed into six porous vials and later transferred into the incubation chamber (a Petri dish of 500 ml capacity) containing 300 ml of artificial cerebrospinal fluid (CSF). The chamber was kept in a water bath at a constant temperature of  $35 \pm 0.5^\circ\text{C}$ , while the medium inside the chamber was continuously oxygenated with a 95%  $\text{O}_2$  / 5%  $\text{CO}_2$  gas mixture. The artificial CSF contained in mM : NaCl 124; KCl 3.75;

$\text{KH}_2\text{PO}_4$  1.25;  $\text{CaCl}_2$  and  $\text{MgSO}_4$  1.5;  $\text{NaHCO}_3$  24 and D-glucose 10; at a pH of 7.4.

Before addition of the tracer to the incubation medium, the slices were allowed at least one hour of equilibration. At time zero 1  $\mu\text{Ci}$  of  $^{45}\text{Ca}$  added and individual holding vials (containing 4-5 slices each) were removed at 2.5, 5, 10, 30, 60 and 90 min following introduction of the tracer. In some experiments the uptake was carried out up to 120 min post tracer addition.

The uptake was terminated by placing the slices within the porous holding vials into ice-cold  $\text{LaCl}_3$  buffer (160 mM Tris HCl + 10 mM  $\text{LaCl}_3$ , adjusted to pH 7.4 with NaOH). The slices were then removed from the holding vials, placed in test tubes containing 3.0 ml of  $\text{LaCl}_3$  buffer and washed five times (for 10 min each). Previous studies have demonstrated that this wash procedure effectively removes excess extracellular calcium while leaving intracellular calcium pools unaffected (Baimbridge and Miller, 1981; Hellman, 1978; Hellman et al., 1975; Van Breemen and McNaughton, 1970). Following the La-wash the slices were individually weighed on a precision balance and transferred into separate counting vials containing 500  $\mu\text{l}$  of Protosol [NEN] to allow for digestion of the tissue. Omnifluor [NEN] - 5 ml/vial - was used as a scintillation fluid and radioactivity was measured the following day on a Beckman LS 9800 liquid scintillation counter. Total counts were obtained from 100  $\mu\text{l}$  samples of the incubation medium removed at various time intervals following addition of the tracer.

Figure 3.1. Sequential flow-chart representation of the methods used for kinetic analyses of  $^{45}\text{Ca}$  uptake curves.

INCUBATION OF SLICES FOR 1 HR.  
 $(Ca)_0 = 1.5 \text{ mM}$ ;  $O_2/CO_2: 95/5\%$ ;  $T^0 = 35 \pm 2^\circ \text{C}$



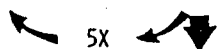
ADDITION OF  $1 \mu\text{Ci } ^{45}\text{Ca}$  AT  $T_0 = 0 \text{ MIN.}$



REMOVAL OF SLICES AT 2.5, 5, 10, 30, 60, AND 90 MIN.



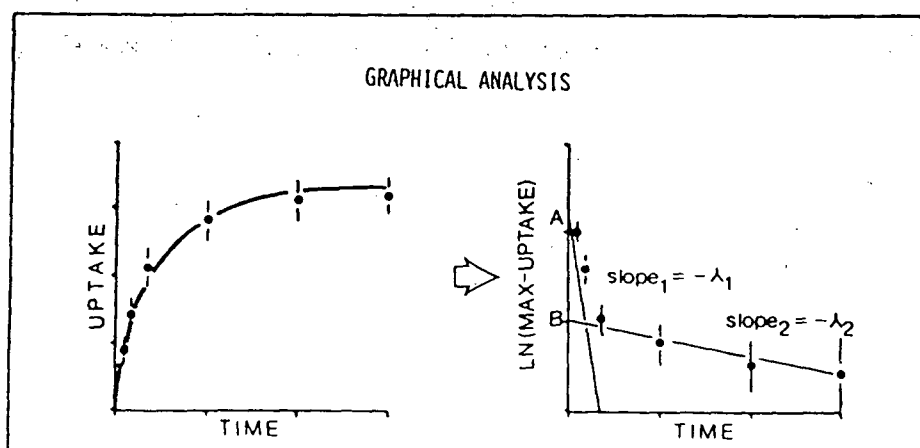
10 MIN WASH IN  $160 \text{ mM TRIS.HCL} + 10 \text{ mM LA}Cl_3$  (PH 7.2) AT  $T^0 = 10^\circ \text{C}$



WEIGHING AND COUNTING



$$\text{UPTAKE} = \frac{\text{TISSUE CPM/MG WET WEIGHT}}{\frac{\text{CPM/100 } \mu\text{L MEDIUM}}{150 \text{ NMOL Ca/100 } \mu\text{L MEDIUM}}} = \frac{\text{NMOL Ca}}{\text{MG WET WEIGHT}}$$



COMPUTER AIDED NON-LINEAR LEAST SQUARE  
 FOR BEST FIT:

$$A[1 - \exp(-\lambda_1 T)] + B[1 - \exp(-\lambda_2 T)]$$



DERIVATION OF POOLS AND FLUXES  
 ACCORDING TO AN OPEN SERIES SYSTEM MODEL  
 CF. UCHIKAWA AND BORLE, 1981

Uptake was calculated according to the formula:

$$\text{UPTAKE} = \frac{\text{Tissue CPM / mg wet weight}}{\text{medium CPM / [Ca] in medium}} = \frac{[\text{Ca}](\text{nmol})}{\text{mg wet weight}}$$

Where CPM represents counts/min.

In experiments where the calcium concentration of the artificial CSF was varied or addition of drugs was necessary, slices were allowed to equilibrate for at least 1 hour to the novel conditions. Drug concentrations used were 100  $\mu\text{M}$  for 3-isobutyl-1-methylxanthine (IBMX) and 2,4-dinitrophenol (DNP) and 1  $\mu\text{M}$  for nifedipine respectively. All drugs were obtained from Sigma Chemical Company. Salmon calcitonin was used in a concentration of 4 U/300 ml (Armour Pharmaceutical Co.).  $^{45}\text{CaCl}_2$  (2 mCi/ml) containing 176  $\mu\text{g}$  Ca/ml was purchased from Amersham Corporation.

To determine the viability of the incubated tissue, some slices were removed after approximately 2 hours and transferred to a superfusion-type electrophysiological recording chamber. Evoked field potentials were recorded in medium similar to the incubation solution. If the characteristic synaptic responses could not be evoked from different cell types of the hippocampal formation, slices for the  $^{45}\text{Ca}$  uptake experiments were discarded. This procedure also allowed for assessment of drug effects on the electrophysiological properties of neurons in the incubated hippocampi.

In order to establish equilibration of the slices with regard to total calcium concentration during the first hour of



incubation, total slice calcium was measured by atomic absorption spectrophotometry (AAS) according to the method described earlier, except for the formaldehyde fixation (Section 3.1.2.).

### 3.2.2.2. Curve Fitting

To perform the kinetic analysis of  $^{45}\text{Ca}$  uptake curves, it is essential to determine the theoretical function that fits the experimental data points with maximum accuracy. Since previous studies using other preparations have shown that the uptake of labelled calcium is best described by a double exponential equation (Borle, 1969; Borle, 1970; Claret-Berthon et al., 1977; Barritt et. al., 1981) the first approach was to test an uptake function that is the sum of two exponentials, of the form:

$$f(t) = A \cdot [1 - \exp(-\lambda_1 \cdot t)] + B \cdot [1 - \exp(-\lambda_2 \cdot t)] \quad (1)$$

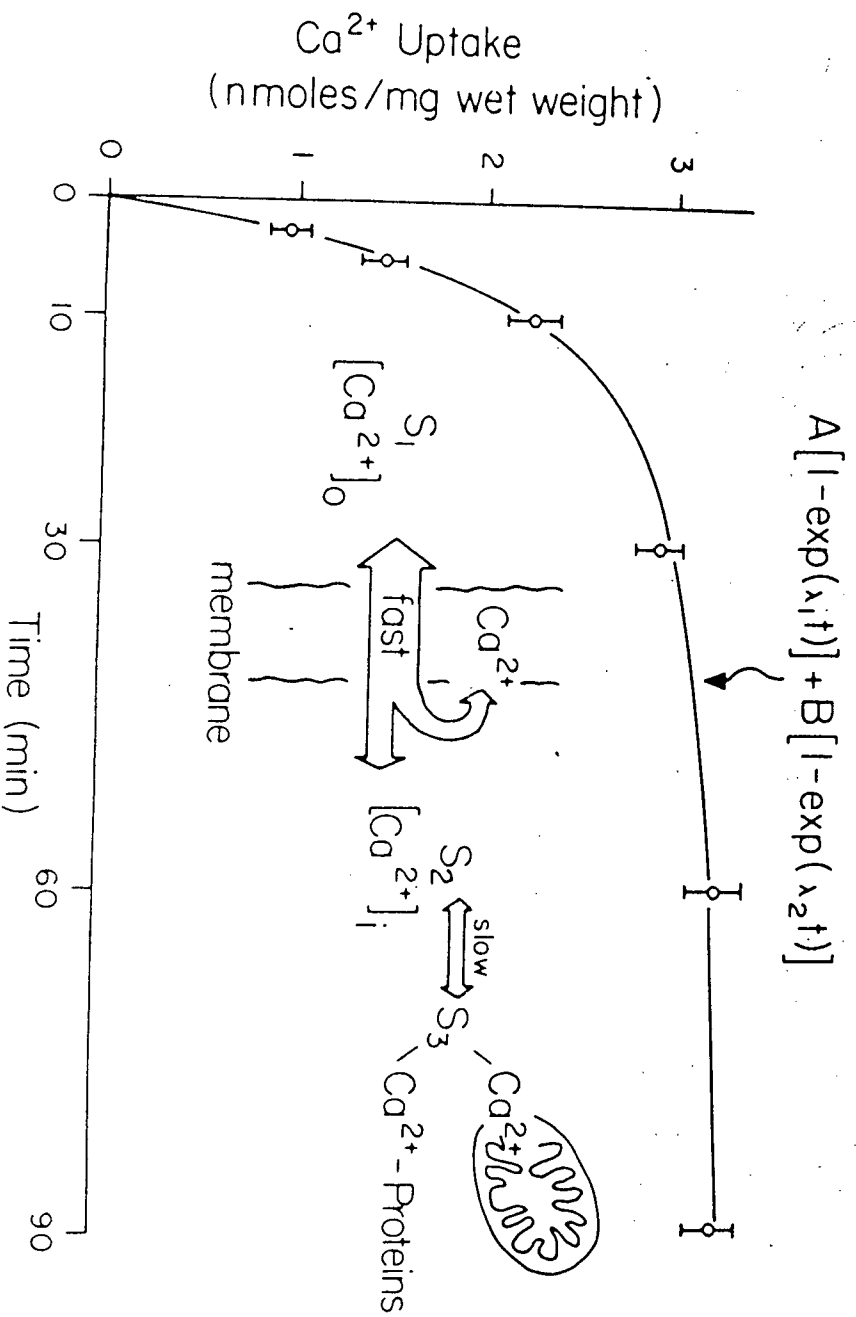
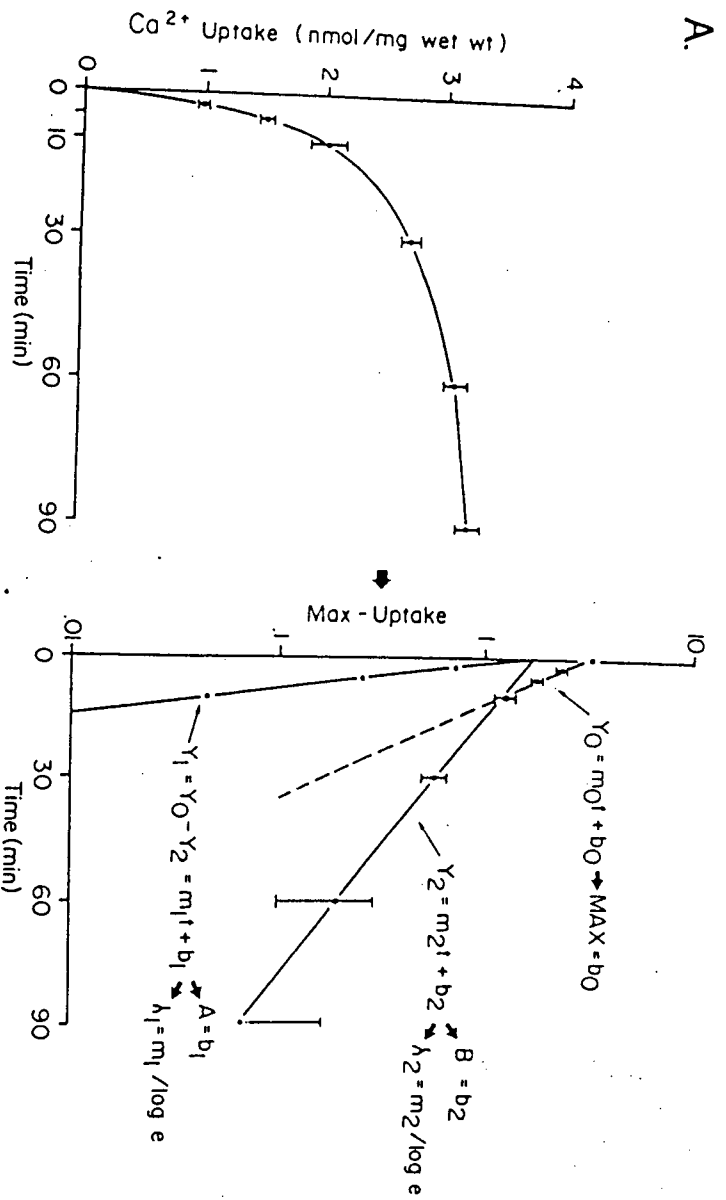
where  $t$  is time;  $A$  and  $B$  are two exponential constants and  $\lambda_1, \lambda_2$  are the reciprocals of the two time constants respectively.

Each uptake curve consisted of 3-5 data points (individual slice calcium uptake expressed per mg of slice wet weight) at every time interval (2.5, 5, 10, 30, 60 and 90 min). The maximum uptake (MAX) was calculated from the mean uptake value at 90 min + 5% and was used for the initial graphical analysis of the curve. The calculation of the maximum uptake using this formula assumes that 95.5% of the asymptote has been reached at 90 min although this may not have been the case in every experiment

especially those having a slow first exponential. However, the use of multiple iterations and the Simplex method (see below) as the final curve fitting algorithm have overridden any errors due to graphical analysis. To derive the first estimates for the constants of the double exponential equation "MAX - UPTAKE" (at each time) was plotted on a semilogarithmic scale (Fig.3.2.A.). Since the semilogarithmic plot could not be fitted by a single straight line (indicating a double exponential function), standard exponential peeling techniques (Riggs, 1963; Jacques, 1972) were applied to yield the intercepts (A and B) and the slopes ( $\lambda_1$  and  $\lambda_2$ ) of the two linear regression lines. Each individual data point was assigned equal weight for contribution to the regression line. The seemingly larger standard error bars at 60 and 90 min of Fig.3.2.A. are due to the logarithmic scale of the Y-axis.

The graphical analysis of the uptake curve only provided the initial estimates of the exponential constants. The constants obtained through the graphical method were further adjusted to yield the "best fit" to the experimental data points through the use of an iterative computer program or by the application of the Simplex method for curve fitting. The iterative method consisted of adjusting the four individual parameters of the double exponential uptake function (A, B,  $\lambda_1$  and  $\lambda_2$ ) until the sum of squares of the differences between the theoretical values and the observed experimental values was minimal, i.e. least squares (Berman et al., 1962b). This rather lengthy method is prone to errors depending on the precision of the initial estimates that

Figure 3.2. Graphical analysis and fitting of the  $^{45}\text{Ca}$  uptake curve. A. Representative uptake curve obtained for a control preparation (left) and its semilogarithmic transform (right). On the semilogarithmic plot the MAX value was determined as being 105% of the uptake at 90 min. Linear regression and standard exponential peeling techniques were used to derive the two intercepts (A and B) and the two slopes ( $\lambda_1$  and  $\lambda_2$ ) from lines  $Y_1$  and  $Y_2$  respectively. B. Following iterative or Simplex non-linear least squares curve fitting methods a double exponential equation of the indicated form was adjusted to the experimental data points. From the parameters of this uptake function the exchange rates and compartment sizes for  $\text{Ca}^{2+}$  could be calculated. The inset shows the theoretical model of hippocampal calcium regulation in a system with a serial arrangement. The first term of the double exponential represents exchange between extracellular  $\text{Ca}^{2+}$  and the  $S_2$  pool (sum of membrane-bound and free ionic intracellular calcium). The second exponential term characterizes the exchange between the  $S_2$  compartment and the sum of all intracellular buffered/sequestered  $\text{Ca}^{2+}$  ( $S_3$ ).

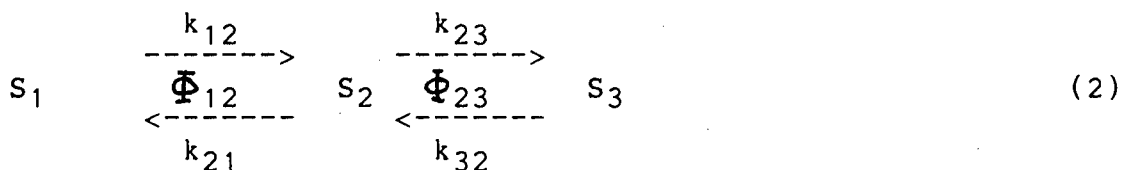


were derived through graphical analysis. However, if sufficient time was allowed (usually 10,000 iterations), the program converged at parameter values that represented the best fit (error level  $< 10^{-4}$ ).

Use of the Simplex algorithm provides an alternative method to overcome difficulties and limitations of the iterative procedure. The "simplexes" (i.e., matrices formed by the parameters to be fitted and the sum of residuals squared) expand and contract during each cycle and automatically converge towards the best fit, i.e., the minimal sum of residuals (Nedler and Mead, 1965). Using a modified computer program of the Simplex algorithm (Caceci and Cacheris, 1984), usually less than 200 cycles were required to obtain the best fit to the experimental data points with an error level less than  $10^{-4}$ . The simplex method provided the further advantage that equations other than a double exponential could easily be tested for the possibility of better fits. In the present experiments single- or triple exponential functions and Michaelis-Menten type kinetics did not yield better approximations to the observed data points. Once the exponential constants were derived through the non-linear least squares analysis the kinetic parameters of the  $^{45}\text{Ca}$  uptake could be calculated.

### 3.2.2.3. Compartmental Analysis

An uptake equation that consists of two exponential terms means that two exchangeable calcium compartments are present in the system under investigation (Berman et al., 1962a; Berman, 1965). The third compartment is the extracellular  $[Ca^{2+}]$  in which the tracer is introduced at time zero. The mathematical derivation of pools, fluxes and rate constants is beyond the scope of the present study and can be found in several reviews (Robertson, 1957; Sheppard, 1962; Berman, 1965; Jacquez, 1972). Since the experiments yielded a three compartment system (with two cellular pools of exchangeable calcium and the calcium of the extracellular medium), the analyses of Robertson et al. (1957) and of Uchikawa and Borle (1981) were adopted to determine the exchange rates in hippocampal slices. A three compartment system may be schematically represented by the following equation according to the notations of Robertson et al. (1957):



Depending whether the investigator has access to the end compartment ( $S_1$ ) or the middle compartment ( $S_2$ ) to introduce the tracer, the system is considered to be "in series" (catenary) or "in parallel" (mammillary) respectively.

If scheme (2) is applied to the experimental conditions, the notations are as follows:

$S_i$  is the amount of calcium in compartment  $i$  (in nmol/mg slice wet weight).

$\Phi_{ij}$  is the flux (or rate of exchange) at steady state in either direction between compartments  $i$  and  $j$  (in nmol/mg slice wet weight/min).

$k_{ij}$  is the rate constant of exchange from compartment  $i$  to  $j$ , i.e., the fraction of  $S_i$  transported to  $S_j$  in unit time ( $\text{min}^{-1}$ ).

Taking into account the assumptions of Uchikawa and Borle (1981) with regard to open or closed systems, the hippocampal slices in the present experiments may be regarded as being part of an "open" system. This requires the extracellular compartment to be infinitely larger than the sum of the intracellular exchangeable calcium compartments. Although this is clearly not the case, since the slices were incubated in a finite amount (300 ml) of artificial CSF, the radioactivity of the extracellular environment during the course of experiments was constant, indicating that the  $\text{Ca}^{2+}$  of the extracellular medium was not significantly affected by uptake into the incubated slices. Therefore, the error introduced by the open-system assumption is in the range of 0.01% (Uchikawa and Borle, 1981).

A typical uptake curve fitted by the double exponential equation is shown on Fig.3.2.B. The insert depicts the serial model system which is considered to be a more accurate reflection

of cellular  $\text{Ca}^{2+}$  distribution in the CNS. In this model, the fast component of the exchange is associated with the rapidly exchangeable  $\text{Ca}^{2+}$  pool (the total of calcium bound to the inside of the plasma membrane and free cytoplasmic  $\text{Ca}^{2+}$ ), i.e., unbuffered pool. The slow component stands for exchange between the unbuffered and the sequestered/buffered pools of calcium. In the parallel model no communication is allowed between the two cellular calcium pools, i.e., both the unbuffered and buffered pools of calcium are in direct connection only with the extracellular environment. The calculations required to obtain the kinetics of the calcium exchange are presented below.

The exponential parameters from equation (1) may be used to derive the calcium pools, fluxes and rate constants for an open system from the time differential of the uptake (Uchikawa and Borle, 1981):

$$dU/dt = a \cdot \exp(-\lambda_1 \cdot t) + b \cdot \exp(-\lambda_2 \cdot t) \quad (3)$$

where U is the uptake, t is time and  $a = A \cdot \lambda_1$  and  $b = B \cdot \lambda_2$ .

From this differential equation the solutions for pools, fluxes and rate constants of the calcium exchange may be calculated for both models as follows:



(a) In series (catenary) system [ $S_1 = \text{extracellular}$ ]

$$\Phi_{21} = a + b \quad (4)$$

$$S_2 + S_3 = a/\lambda_1 + b/\lambda_2 \quad (5)$$

$$S_2 = \frac{(a + b)^2}{a \cdot \lambda_1 + b \cdot \lambda_2} \quad (6)$$

$$S_3 = (S_2 + S_3) - S_2 = \frac{a \cdot b \cdot (\lambda_1 - \lambda_2)^2}{\lambda_1 \cdot \lambda_2 \cdot (a \cdot \lambda_1 + b \cdot \lambda_2)} \quad (7)$$

$$\Phi_{23} = \frac{\lambda_1 \cdot \lambda_2 \cdot S_2 \cdot S_3}{a + b} \quad (8)$$

$$k_{12} = \Phi_{21}/S_1 = 0 \quad (\text{since } S_1 = \infty) \quad (9)$$

$$k_{21} = \Phi_{21}/S_2 \quad (10)$$

$$k_{23} = \Phi_{23}/S_2 \quad (11)$$

$$k_{32} = \Phi_{23}/S_3 \quad (12)$$

(b) In parallel (mamillary) system [ $S_2 = \text{extracellular}$ ]

$$S_1 = a/\lambda_1 \quad (13)$$

$$S_3 = b/\lambda_2 \quad (14)$$

$$\Phi_{12} = a \quad (15)$$

$$\Phi_{23} = b \quad (16)$$

$$k_{21} = \Phi_{21}/S_2 = 0 \quad (\text{since } S_2 = \infty) \quad (17)$$

$$k_{12} = \Phi_{21}/S_1 = \lambda_1 \quad (18)$$

$$k_{23} = \Phi_{23}/S_2 = 0 \quad (\text{since } S_2 = \infty) \quad (19)$$

$$k_{32} = \Phi_{23}/S_3 = \lambda_2 \quad (20)$$

### 3.2.3. Results

The uptake of labelled calcium into hippocampal slices could be best fitted by a double exponential function in every experimental condition examined. This finding indicates that the slices as a whole behave in terms of calcium compartmentalization as having two intracellular exchangeable  $\text{Ca}^{2+}$  pools (Berman et al., 1962b; Uchikawa and Borle, 1981). The uptake curves presented in the figures of this section have been generated by computer from the average values of the exponential constants derived from individual experiments, rather than fitting a single curve to the averages of the individual data points obtained in different experiments. This representation is considered to be mathematically more accurate, since the exponential fitting the averages may not be a true reflection of the average values of the exponential terms (Riggs, 1963).

#### 3.2.3.1. Effect of extracellular calcium ( $[\text{Ca}^{2+}]_0$ )

In this series of experiments hippocampal slices were prepared in artificial CSF containing the standard 1.5 mM  $\text{Ca}^{2+}$ , but were incubated in media with calcium concentrations of 0.1, 2.0 and 4.0 mM. Control slices were always incubated in 1.5 mM  $[\text{Ca}^{2+}]_0$ . The extracellular  $\text{Mg}^{2+}$  concentration was kept constant at 1.5 mM except for the 4.0 mM  $\text{Ca}^{2+}$  containing medium where it

was lowered to 1.0 mM, for this particular ionic composition has been shown to result in long-term alterations in the excitability of hippocampal neurons (Turner et al., 1982; Mody et al., 1984).

Alterations in extracellular calcium concentrations had marked effects on the shape of the  $^{45}\text{Ca}$  uptake curves (Fig. 3.3.A.). Increasing  $[\text{Ca}^{2+}]_o$  caused a significantly faster initial uptake rate than it would be expected from changes in the ionic gradient across the plasma membrane.

The electrophysiological properties of the slices incubated at various calcium concentrations were also affected. The evoked responses of a control slice taken from the  $^{45}\text{Ca}$  incubation chamber with the characteristic population spikes recorded in the CA1 and dentate regions of the hippocampal formation are shown in Fig. 3.3.B. The feed-back inhibition, as measured by activation of inhibitory interneurons by an antidromic conditioning stimulus, was found to be normal. When slices were incubated in medium containing 0.1 mM  $\text{Ca}^{2+}$  subsequent recordings showed the characteristic evoked multiple discharges and later the spontaneous, regular bursting in the CA1 area (Fig 3.3.C.). The  $\text{Ca}^{2+}$  pools, fluxes and rate constants in hippocampal slices at different  $[\text{Ca}^{2+}]_o$  are summarized in Table 3.2. The data have been obtained through kinetic analysis of the uptake curves according to equations (4)-(20) presented in Section 3.2.2.3. The two time constants of the uptake function are the reciprocals of the rate constants ( $k_{12}$  and  $k_{32}$ ) of the parallel model. Regardless whether the serial or the parallel model is used for interpretation, the size of the rapidly

Figure 3.3. Effect of alterations in extracellular  $\text{Ca}^{2+}$  concentrations on the hippocampal  $^{45}\text{Ca}$  uptake curves and electrical activity. A. Computer-fitted  $^{45}\text{Ca}$  uptake curves at four different extracellular  $\text{Ca}^{2+}$  concentrations. The numbers on the curves represent  $[\text{Ca}^{2+}]_o$  and  $[\text{Mg}^{2+}]_o$  in mM respectively. B. Electrophysiological properties of slices transferred from the uptake chamber into a recording chamber. Recordings were taken approx. 5 min following the transfer procedure. Extracellular population spikes (top traces) were recorded from the pyramidal cells of CA1 region (●) evoked by stratum radiatum stimulation (left) and the granule cells of the dentate gyrus (○) subsequent to activation of the perforant path (right). The bottom traces represent inhibition of the population discharge when orthodromic stimulation is preceded by an antidromic stimulus that activates feed-back inhibitory interneurons, indicating good viability of the slices in the uptake chamber (Calibration: 2mV/10ms). C. Left: Synaptically evoked multiple population discharge recorded in the CA1 region during incubation with 0.1 mM  $[\text{Ca}^{2+}]_o$  (Calibration: 2mV/20ms). Right: Spontaneous, regularly occurring field bursts in the absence of synaptic responses following equilibration with the low calcium.  $^{45}\text{Ca}$  was added to the incubation chamber when the slices have presumably reached this stage (Calibration: 2mV/10s). In this and subsequent figures, in all records of electrical activity positive is upwards.

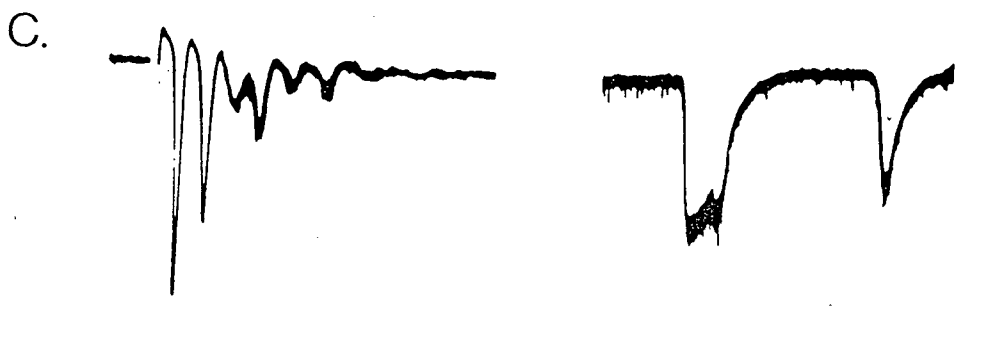
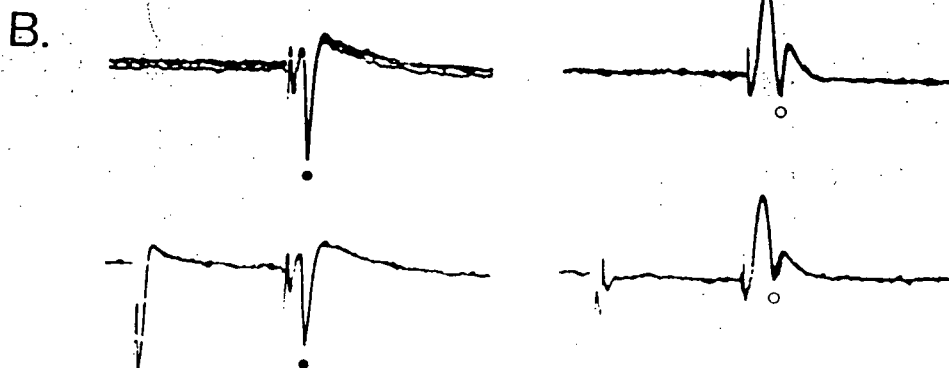
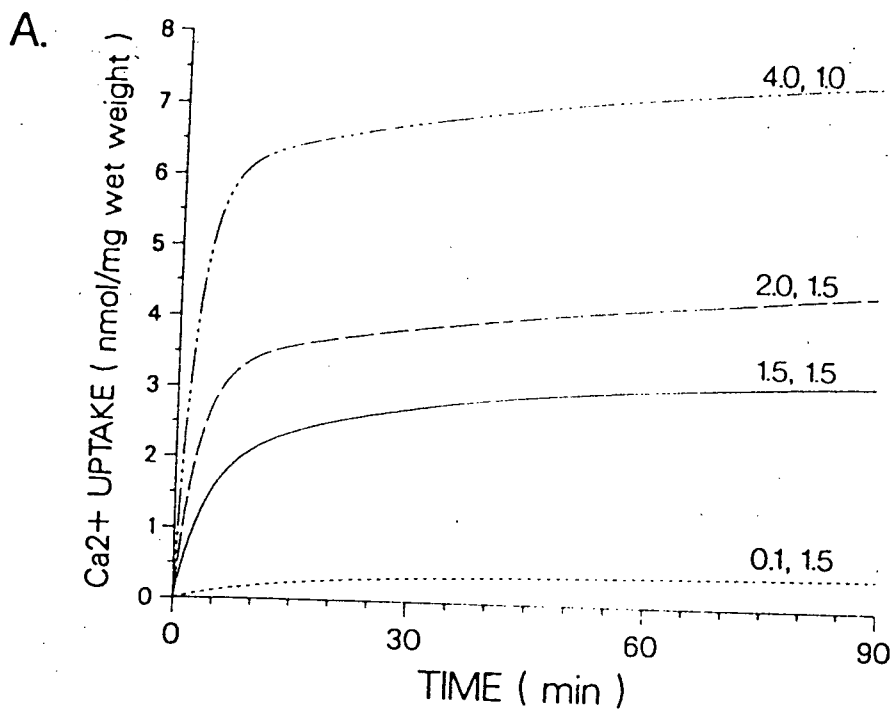


Table 3.2.

Effects of extracellular calcium concentrations on hippocampal  $\text{Ca}^{2+}$  exchange.

The pools, fluxes and rate constants for both the serial model system (extracellular compartment:  $S_1$ ) and the parallel model system (extracellular compartment:  $S_2$ ) of hippocampal cellular  $\text{Ca}^{2+}$  exchange have been calculated according to equations (4)-(20) from the text. Data represented as mean  $\pm$  S.D. derived from the kinetic analysis of 4-8 uptake curves each (no. of slices = 20-27 for every uptake curve).  $[\text{Ca}^{2+}]_o$  is indicated in mmoles/L (mM), while extracellular  $\text{Mg}^{2+}$  was 1.5 mM unless shown otherwise.

	Control [Ca <sup>2+</sup> ] <sub>o</sub> 1.5 mM	[Ca <sup>2+</sup> ] <sub>o</sub> 0.1 mM	[Ca <sup>2+</sup> ] <sub>o</sub> 2 mM	[Ca <sup>2+</sup> ] <sub>o</sub> 4 mM [Mg <sup>2+</sup> ] <sub>o</sub> 1 mM
IN SERIES				
POOL $S_2$	2218 $\pm$ 198	347* $\pm$ 22	3447* $\pm$ 171	6165* $\pm$ 120
POOL $S_3$	1052 $\pm$ 151	160* $\pm$ 17	1603* $\pm$ 128	1495* $\pm$ 30
TOTAL	3270 $\pm$ 50	507* $\pm$ 6	5050* $\pm$ 48	7660* $\pm$ 150
FLUX $S_1$ - $S_2$	489 $\pm$ 49	25* $\pm$ 3	1144* $\pm$ 45	2593* $\pm$ 728
FLUX $S_2$ - $S_3$	36 $\pm$ 9	3* $\pm$ .5	19* $\pm$ 3	30 $\pm$ 4
$k_{21}$	.224 $\pm$ .04	.072* $\pm$ .01	.332* $\pm$ .01	.418* $\pm$ .11
$k_{23}$ [ $\times 10^{-3}$ ]	16.5 $\pm$ 5.3	10.0* $\pm$ 2.3	5.6* $\pm$ 1.1	4.8* $\pm$ .61
$k_{32}$	.034 $\pm$ .006	.021* $\pm$ .001	.012* $\pm$ .001	.020* $\pm$ .002
IN PARALLEL				
POOL $S_1$	1883 $\pm$ 227	236* $\pm$ 14	3330* $\pm$ 186	6010* $\pm$ 140
POOL $S_3$	1387 $\pm$ 190	271* $\pm$ 8	1720* $\pm$ 142	1650* $\pm$ 10
TOTAL	3270 $\pm$ 50	507* $\pm$ 6	5050* $\pm$ 48	7660* $\pm$ 150
FLUX $S_2$ - $S_1$	493 $\pm$ 142	20* $\pm$ 3	1124* $\pm$ 47	2561* $\pm$ 723
FLUX $S_2$ - $S_3$	43 $\pm$ 10	5* $\pm$ .4	20* $\pm$ 3	32* $\pm$ 4
$k_{12}$	.266 $\pm$ .09	.086* $\pm$ .02	.338* $\pm$ .01	.424* $\pm$ .11
$k_{32}$	.030 $\pm$ .005	.018* $\pm$ .001	.012* $\pm$ .001	.019* $\pm$ .003

UNITS: pmoles $\cdot$ mg<sup>-1</sup> slice wet weight for pools, pmoles $\cdot$ mg<sup>-1</sup> slice wet weight $\cdot$ min<sup>-1</sup> for fluxes, min<sup>-1</sup> for rate constants.

\* Denotes significant difference from control (p<0.01 one-way ANOVA).

exchangeable pool ( $S_2$  of the serial model or  $S_1$  of the parallel model) increases linearly 18-25-fold with a 40-fold increase in extracellular  $\text{Ca}^{2+}$  concentration (from 0.1 to 4.0 mM). The calcium flux between this compartment and the extracellular environment shows a comparable linear enhancement. In contrast to the fast component of the uptake, the slowly exchangeable calcium pool of hippocampal slices seems to be saturated at a  $[\text{Ca}^{2+}]_o$  of 2.0 mM while the exchange rate between the slow and fast compartments is maximal at the physiological range of  $[\text{Ca}^{2+}]_o$  of 1.5 mM. Similar data have been obtained by Borle (1970) in isolated kidney cells that have a single intracellular compartment and by Barritt et al. (1981) in liver cells with two intracellular exchangeable calcium compartments.

The total exchangeable  $\text{Ca}^{2+}$  of control preparations, as measured by the kinetic analysis, was found to be 3.27 nmole/mg wet weight. This value is comparable to results of previous studies in slices of brain or other tissues (Stahl and Swanson, 1971; 1972; Barritt et al., 1981; Borle, 1981a). Measured by atomic absorption spectrophotometry (AAS) slices incubated in control conditions have a total calcium of  $4.52 \pm 0.12$  nmole/mg wet weight indicating that about 72% of total slice calcium is exchangeable. Following the preparation of the slices, their equilibration with regard to total calcium was remarkably rapid. The final value of total calcium was attained in less than 5 min of incubation. This finding indicates that during the 60 min of preincubation before addition of the tracer the slices have

surely attained the ionic steady state required for kinetic studies.

### 3.2.3.2. Effect of drugs that alter $\text{Ca}^{2+}$ metabolism

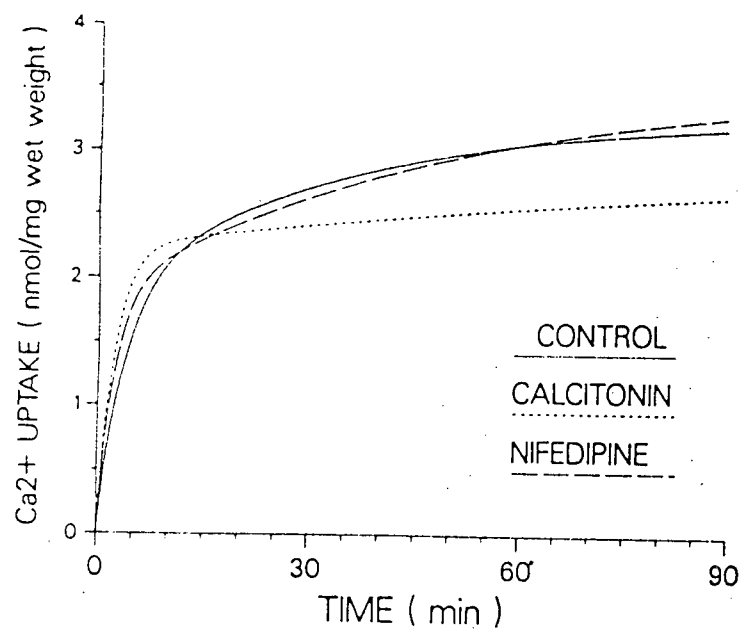
This series of experiments involved testing the effect of drugs that may alter the  $\text{Ca}^{2+}$  homeostasis of hippocampal slices. The dihydropyridine calcium channel antagonist nifedipine in a concentration of  $10^{-6}$  M was used to block  $\text{Ca}^{2+}$  entry but had no marked effect on the shape of the  $^{45}\text{Ca}$  uptake curves (Fig. 3.4.A.). However, kinetic analysis revealed that the drug enhanced the slowly exchangeable pool of  $\text{Ca}^{2+}$  resulting in a larger than normal exchange between intra- and extracellular compartments (Table 3.3.). In contrast, calcitonin (4U/300 ml) enhanced the fast component of the uptake while depressing the slow phase (Fig. 3.4.A.). The net effect of the hormone was to reduce total hippocampal exchangeable  $\text{Ca}^{2+}$  by mobilizing  $\text{Ca}^{2+}$  from the slowly exchangeable  $S_3$  pool (Table 3.3.).

The mitochondrial inhibitor 2,4,-dinitrophenol (DNP) in a concentration of  $10^{-4}$  M had an effect similar to that observed by Borle (1981b) in the kidney. The fast component of the uptake became more rapid while the slow exchange phase was reduced (Fig. 3.4.B.). Kinetic analysis of  $^{45}\text{Ca}$  uptake in the presence of DNP indicates an enhancement (about 38%) of the rapidly exchangeable compartment with a concomitant increase in calcium flux and a significant reduction (about 57%) of the sequestered/buffered pool of  $\text{Ca}^{2+}$  (Table 3.3.). These alterations were reflected in



Figure 3.4. Effects of drugs and hormones on  $^{45}\text{Ca}$  uptake and electrophysiological properties of hippocampal slices. A.  $^{45}\text{Ca}$  uptake curves in the presence of  $10^{-6}$  M nifedipine and 4U/300ml of salmon calcitonin. B. Effects of  $10^{-4}$  M 2,4-dinitrophenol (DNP) and 3-isobutyl-1-methylxanthine (IBMX) on the shape of the  $^{45}\text{Ca}$  uptake curves. C. Left: Control CA1 population spike in a slice removed from the uptake chamber. Right: Enhancement of the evoked response with induction of a second population spike (arrow) following incubation with  $10^{-4}$  M DNP. (Calibration: 4mV/10ms). D: Left: Population spike recorded in the pyramidal cell layer of the CA1 region under control conditions. Right: Potentiation of the evoked response in the presence of  $10^{-4}$  M IBMX. (Calibration: 2mV/10ms).

A.



B.

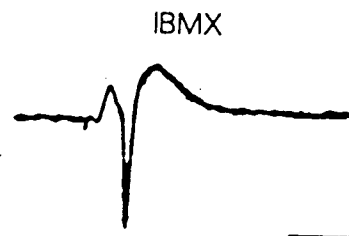
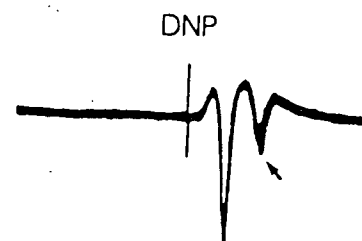
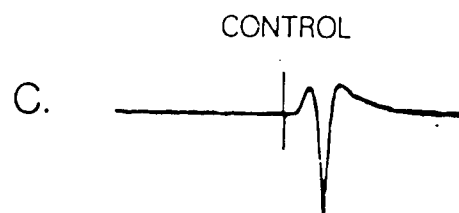
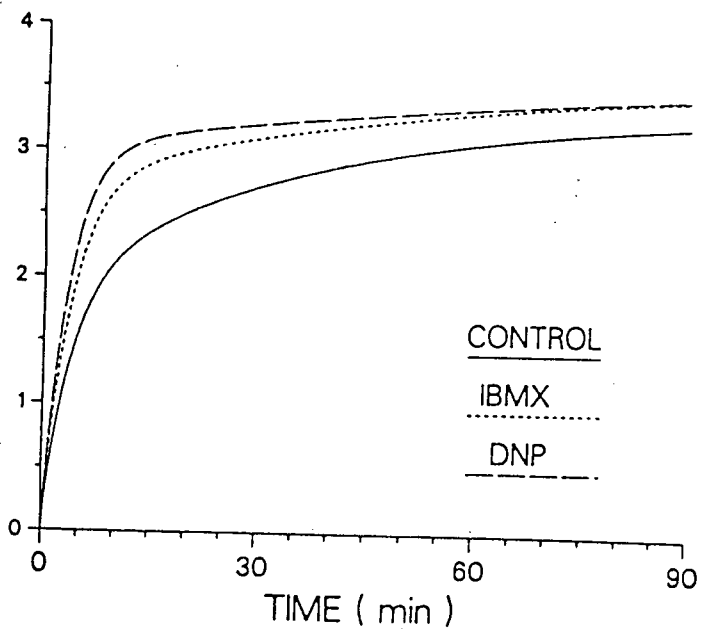


Table 3.3.Effects of drugs on hippocampal  $\text{Ca}^{2+}$  exchange.

Data represented as mean  $\pm$  S.D. derived from the kinetic analysis of 4-8 uptake curves each (number of slices = 19-29 for each uptake curve). For explanation of pools, fluxes, rate constants, and their respective units see text and the the legend for Table 3.2. Drug concentrations are indicated in moles/L (M) except for calcitonin (international units/300 ml).

	Control	Nifedipine [ $10^{-6}$ M]	Calcitonin [4U/300ml]	DNP <sup>a</sup> [ $10^{-4}$ M]	IBMX <sup>b</sup> [ $10^{-4}$ M]
=====					
IN SERIES					
POOL S <sub>2</sub>	2218 $\pm$ 198	2022* $\pm$ 86	2272* $\pm$ 24	3056* $\pm$ 78	2837* $\pm$ 60
POOL S <sub>3</sub>	1052 $\pm$ 151	1513* $\pm$ 109	703* $\pm$ 59	476* $\pm$ 115	658* $\pm$ 15
TOTAL	3270 $\pm$ 50	3305* $\pm$ 35	2975* $\pm$ 35	3532* $\pm$ 106	3495* $\pm$ 75
FLUX S <sub>1</sub> -S <sub>2</sub>	489 $\pm$ 49	827* $\pm$ 20	948* $\pm$ 18	878* $\pm$ 137	735* $\pm$ 21
FLUX S <sub>2</sub> -S <sub>3</sub>	36 $\pm$ 9	32 $\pm$ 8	6* $\pm$ 1	7* $\pm$ 2	15* $\pm$ .4
k <sub>21</sub>	.224 $\pm$ .04	.409* $\pm$ .08	.417* $\pm$ .01	.287 $\pm$ .04	.259 $\pm$ .01
k <sub>23</sub> [ $\times 10^{-3}$ ]	16.5 $\pm$ 5	15.5 $\pm$ 5	2.8* $\pm$ .6	2.3* $\pm$ .9	5.2* $\pm$ .02
k <sub>32</sub> [ $\times 10^{-3}$ ]	34 $\pm$ 6	21* $\pm$ 7	9* $\pm$ 1	16* $\pm$ 7	23* $\pm$ .1
=====					
IN PARALLEL					
POOL S <sub>2</sub>	1883 $\pm$ 227	1865 $\pm$ 125	2240 $\pm$ 30	3003* $\pm$ 100	2710* $\pm$ 50
POOL S <sub>3</sub>	1387 $\pm$ 190	1670* $\pm$ 70	735* $\pm$ 65	528* $\pm$ 117	785* $\pm$ 25
TOTAL	3270 $\pm$ 50	3305* $\pm$ 35	2975* $\pm$ 35	3532* $\pm$ 106	3495* $\pm$ 75
FLUX S <sub>2</sub> -S <sub>1</sub>	493 $\pm$ 142	793* $\pm$ 29	941* $\pm$ 19	870* $\pm$ 137	718* $\pm$ 22
FLUX S <sub>2</sub> -S <sub>3</sub>	43 $\pm$ 10	34 $\pm$ 9	7* $\pm$ 1	8* $\pm$ 3	17* $\pm$ .6
k <sub>12</sub>	.266 $\pm$ .09	.426* $\pm$ .01	.420* $\pm$ .01	.289* $\pm$ .04	.265* $\pm$ .01
k <sub>32</sub> [ $\times 10^{-3}$ ]	30 $\pm$ 5	21* $\pm$ 7	9* $\pm$ 1	15* $\pm$ 6	22* $\pm$ .1
=====					

<sup>a</sup> DNP -- 2,4-dinitrophenol

<sup>b</sup> IBMX -- 3-isobutyl-1-methylxanthine

\* Denotes significant difference from control (p<0.01 one-way ANOVA).

the abnormal electrophysiological properties of hippocampal neurons consisting in an increase of the amplitude of orthodromically evoked responses and occurrence of multiple spike discharges (Fig. 3.4.C.) analogous to the results of Godfraind et al. (1972) obtained in vivo.

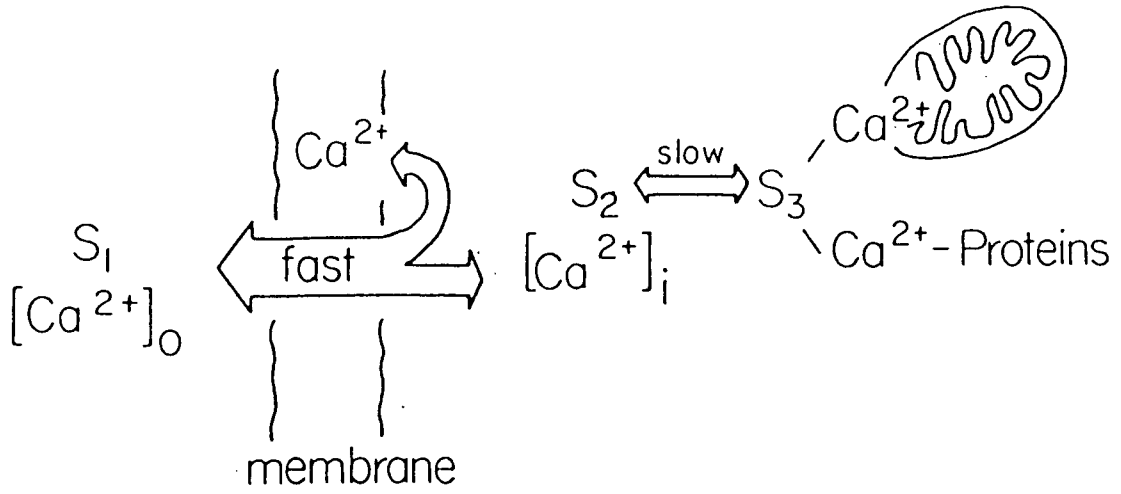
The effect of IBMX (3-isobutyl-1-methylxanthine) on the  $^{45}\text{Ca}$  uptake curves was much like that of DNP but of a lesser magnitude (Fig. 3.4.B. and Table 3.3.). The drug is a potent inhibitor of the cyclic nucleotide phosphodiesterase (Chasin and Harris, 1972) and it has been shown to cause an increase in the levels of cAMP in brain slices (Smellie et al., 1979). This data is consistent with the results of Borle and Uchikawa (1979) who showed that cAMP and its dibutyryl derivative enhanced calcium uptake in cell cultures. The evoked potentials of the CA1 region were also affected by the drug showing a marked potentiation of both the population spikes (Fig. 3.4.D.) and the extracellularly recorded EPSPs.

### 3.2.3.3. Theoretical manipulations of the $S_3$ pool

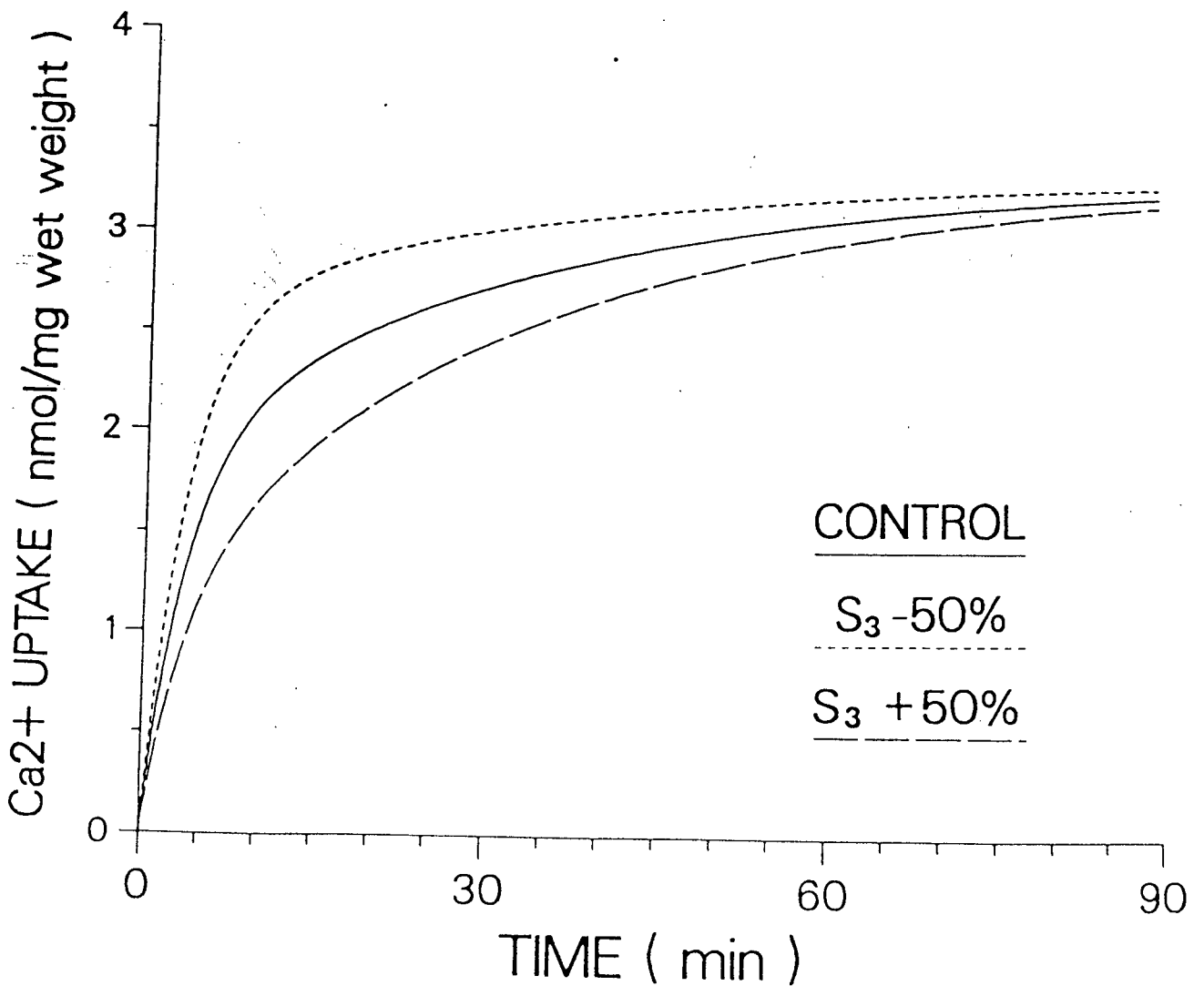
The derivation of  $\text{Ca}^{2+}$  pools, fluxes and exchange rates through a double exponential equation allows for experimental modelling of the system under investigation. Each individual term of the exponential equation may be changed as desired to yield compartments of different sizes and to affect the exchange between various compartments of the model. Fig. 3.5.A. shows the serial model system in which the size of the buffered pool may be

Figure 3.5. Effects of theoretical manipulations of the  $S_3$  (buffered)  $Ca^{2+}$  pool. A. Schematic representation of the serial model of hippocampal intracellular calcium regulation. The  $S_3$  compartment consists of  $Ca^{2+}$  sequestered/buffered by the mitochondria and endoplasmic reticulum as well as  $Ca^{2+}$  bound to intracellular proteins. B. By changing the exponential terms of the fitted uptake equation the size of the  $S_3$  compartment may easily be manipulated. The theoretical uptake curves are shown as they would result from a 50% reduction or alternatively, from a 50% enhancement of the  $S_3$  pool. The control curve was generated from the experimental data obtained from hippocampal slices incubated under normal conditions.

A.



B.



altered by changing the value of the second exponential term of the uptake equation.

The computer-generated curves following a 50% enhancement of the buffered  $S_3$  pool or its reduction to half of the control value are shown in Fig. 3.5.B. These curves are only of a theoretical significance since no experimental condition will result in a pure and isolated effect on the  $S_3$  pool alone. Examination of their shape is however useful for comparisons to various experimental situations.

#### 3.2.4. Discussion

Kinetic analysis of  $^{45}\text{Ca}$  uptake curves revealed the existence of two separate, kinetically distinct pools of exchangeable intracellular calcium in the hippocampal slice preparation. In a model of this system, based on the principles of compartmental analysis (Robertson, 1957; Sheppard, 1962; Jacques, 1972), these two pools may be considered to have either a serial (catenary) or a parallel (mammillary) arrangement (Robertson et al., 1957; Uchikawa and Borle, 1981). The present results do not show any significant differences between these two; however, the serial model more closely resembles the physiological schema of intracellular calcium homeostasis (Brinley, 1978; Blaustein et al., 1980; McGraw et al., 1982). Notations applicable to this model are therefore used in subsequent references to exchangeable  $\text{Ca}^{2+}$  pools.

Several essential criteria must be met before application of kinetic analysis may be considered valid for physiological systems. Most importantly the preparation has to be viable, and in the present study this was demonstrated by the routine electrophysiological recordings in slices removed from the uptake chamber. Also of importance is the assumption regarding the system's steady state for both the total ionic concentration of  $\text{Ca}^{2+}$  and flux of the tracer (Sheppard, 1962; Borle, 1975; Uchikawa and Borle, 1981). This was ensured by a long pre-incubation period of the slices in the presence of drugs or the altered extracellular ionic environment as well as the fact that slices equilibrated quite rapidly in terms of their total calcium content. Furthermore, during the tracer experiments, the uptake of calcium reached an asymptotic value without a subsequent decline indicating that the system was at isotopic equilibrium (Borle, 1981b). These factors together with the similarity with other studies (Borle, 1981a) in terms of the levels of hippocampal exchangeable calcium (3.33 nmoles/mg wet weight) and the exchangeable fraction of total  $\text{Ca}^{2+}$  (about 72%) provide strong evidence for the applicability of  $^{45}\text{Ca}$  uptake kinetics to the in vitro hippocampus.

One difficulty however with using this particular preparation is the fact that the hippocampal formation consists of a large variety of heterogeneous neurons and glial cells, all of which may participate in  $\text{Ca}^{2+}$  regulation (Brostrom et al., 1982; MacVicar, 1984). While the calcium compartments derived through kinetic analysis cannot be attributed to any one of



these populations in particular, they are most likely localized within the cells because the bulk of extracellular  $\text{Ca}^{2+}$  has been washed off by  $\text{LaCl}_3$  following termination of the uptake (Van Breemen and McNaughton, 1970; Hellman et al., 1976; Hellman, 1978; Baimbridge and Miller, 1981). In view of these restrictions, the present experiments do not provide a way of distinguishing between the different elements of the slice preparation but rather characterize the system as a whole with regard to its calcium homeostasis.

The two exponential terms of hippocampal  $^{45}\text{Ca}$  uptake reflect two distinct components of  $\text{Ca}^{2+}$  regulation in this system. The fast component represents exchange between extracellular  $\text{Ca}^{2+}$  and that located within the plasma membrane and/or in its immediate vicinity. The rapidly exchangeable compartment ( $S_2$ ) may thus consist of calcium tightly bound to the glycocalyx (inaccessible to  $\text{LaCl}_3$ ),  $\text{Ca}^{2+}$  bound to the inside of the membrane and free ionic intracellular  $\text{Ca}^{2+}$ . Identification of  $S_2$  as the sum of these  $\text{Ca}^{2+}$  pools is supported by the findings that changes in extracellular calcium concentrations have a significant effect on the magnitude of the fluxes between  $S_2$  and the artificial CSF that bathes the slices. The driving force resulting from an increase in the  $\text{Ca}^{2+}$  gradient across the cell membrane results in an enhancement of the rapid phase of the exchange with a concomitant increase in the size of the  $S_2$  compartment.

In an attempt to further characterize the fast component of hippocampal calcium uptake, the effect of the putative calcium channel blocker nifedipine was tested on the kinetics of  $^{45}\text{Ca}$

exchange. This drug failed to produce the expected antagonism, which is not surprising in light of previous observations that have shown its ineffectiveness on depolarization-induced calcium uptake into synaptosomes (Daniell et al., 1983). The enhancement of the  $S_3$  pool produced by nifedipine may reflect a novel action of this drug in the CNS.

The hormone calcitonin is a potent regulator of  $Ca^{2+}$  homeostasis in several systems (Borle, 1975b; 1981a) and calcitonin receptors are widely distributed in the rat CNS (Rizzo and Goltzman, 1981; Henke et al., 1983). In the present study calcitonin reduced the level of total exchangeable  $Ca^{2+}$  by enhancing the efflux rate of  $Ca^{2+}$  from the elements of the hippocampal slice. Since the size of the unbuffered compartment ( $S_2$ ) was not significantly affected, it might be suggested that the  $Ca^{2+}$  normally present in the buffered compartment ( $S_3$ ) was mobilized by calcitonin. This finding does not resemble calcitonin's action in isolated kidney cells (Borle, 1975b), but it is possible that CNS receptors mediate a different effect than that observed in the periphery.

While the fast calcium compartment is readily altered by changes in extracellular calcium concentrations, the identity of the slowly exchangeable compartment ( $S_3$ ) is less obvious. The application of the mitochondrial inhibitor DNP ( $10^{-4}$  M) resulted in a marked reduction of the slowly exchangeable  $Ca^{2+}$  compartment indicating that mitochondrial calcium is a significant part of the  $S_3$  pool. These data are similar to those observed by Borle (1981b) in isolated kidney cells.

In addition to mitochondria, neuronal tissue is known to have several  $\text{Ca}^{2+}$  buffering/sequestering systems, particularly the endoplasmic reticulum and various calcium-binding proteins (Brinley, 1978; Duce and Keen, 1978; Blaustein et al., 1980; McGraw et al., 1982). The contribution of these calcium-regulatory mechanisms to the slowly exchangeable  $\text{Ca}^{2+}$  compartment is difficult to assess for the lack of specifically acting drugs and blocking agents. Alternative factors regulating the slow compartment may involve cyclic AMP as has been shown in kidney cells (Borle and Uchikawa, 1979). The methylxanthine derivative IBMX is a potent phosphodiesterase inhibitor (Chasin and Harris, 1976) and also releases  $\text{Ca}^{2+}$  from intracellular storage sites such as the sarcoplasmic reticulum in the case of muscle fibers (Miller and Thieleczek, 1977). Its effect on hippocampal  $\text{Ca}^{2+}$ -uptake kinetics is similar to that of DNP in reducing the slowly exchangeable pool of calcium and simultaneously increasing the fast compartment ( $S_2$ ). This would suggest that in the hippocampus cyclic nucleotides participate in the regulation of the slow compartment. Alternatively, it would appear that the endoplasmic reticulum of neuronal elements may play a significant role in hippocampal  $\text{Ca}^{2+}$ -buffering.

At this point no conclusions may be reached with regard to the contribution of various intracellular proteins to the slowly exchangeable  $S_3$  compartment. However, it should be emphasized that one of these proteins, calcium-binding protein (CaBP), has been shown to be confined to nerve cells of the hippocampal formation and has been postulated to buffer intraneuronal calcium

(Jande et al., 1981; Baimbridge and Miller, 1982; Garcia-Segura et al., 1984). The specific loss of this protein from the granule cells of the dentate gyrus during and following kindling-induced epilepsy (Miller and Baimbridge, 1983; Baimbridge and Miller, 1984) may provide an approach to study its role in hippocampal calcium homeostasis (also see Section 3.3.).

Since  $\text{Ca}^{2+}$  participates in many events that involve neuronal excitability, changes in its regulation should be readily reflected in altered electrophysiological characteristics. When a shift of  $\text{Ca}^{2+}$  from the buffered into the unbuffered pool was produced with little change in total exchangeable calcium (the effects of DNP and IBMX), significant alterations were observed in the electrophysiological properties of hippocampal neurons. Both drugs had a marked potentiating effect on the evoked responses and in the presence of DNP aberrant discharge patterns were induced. Similarly, when the buffering capacity of the system is severely challenged by the high extracellular calcium concentration ( $4.0 \text{ mM Ca}^{2+}/1.0 \text{ mM Mg}^{2+}$ ), long-lasting alterations in neuronal function may occur (Turner et al., 1982; Mody et al., 1984). The reduction of hippocampal exchangeable  $\text{Ca}^{2+}$  during incubation of the slices with low  $[\text{Ca}^{2+}]_o$  is reflected in the spontaneous bursting of hippocampal CA1 pyramidal cells (Taylor and Dudek, 1982; Yaari et al., 1983; Haas and Jefferys, 1984). In addition, the steady state  $\text{Ca}^{2+}$  influx into the cells under control conditions may be the underlying mechanism for the slow, persistent inward  $\text{Ca}^{2+}$ -current of hippocampal pyramidal cells (Brown and Griffith, 1983).

The correlation between these alterations in neuronal activity and calcium regulation is not likely to be coincidental, indicating that the  $^{45}\text{Ca}$  uptake measurements provide a valid assesement of neuronal  $\text{Ca}^{2+}$  homeostasis. The method would appear to be valuable for studying the action of hormones and various pharmacological agents on calcium related phenomena. Further characterization of the system should involve separation of the neuronal from glial elements and determination of  $\text{Ca}^{2+}$  regulatory characteristics of certain neuronal populations possibly through the use of cultured cells.

### 3.3. Measurement of $\text{Ca}^{2+}$ -regulation during kindling using the kinetic analysis of $^{45}\text{Ca}$ uptake curves

#### 3.3.1. Introduction

Epileptogenic phenomena may result, in part, from long-term changes in the excitability of nerve cells. Of the several ions within the milieu of the CNS, special interest is attached to calcium because of its important role in neuronal excitability (see Sections 1.2 and 1.3). In the hippocampal formation this cation has been suggested to be involved in somatic and dendritic spike generation (Wong and Prince, 1978; Traub and Llinas, 1979; Brown and Griffith, 1983b), activation of hyperpolarizing conductances (Alger and Nicoll, 1980; Hotson and Prince, 1980; Schwartzkroin and Stafstrom, 1980; Brown and Griffith, 1983a) and participation in aberrant forms of pyramidal cell discharge (Wong and Prince, 1978; Traub and Llinas, 1979; Hotson and Prince, 1981). Furthermore, calcium regulates long-lasting changes in CNS activity as is the case for potentiation phenomena characteristic of the hippocampal formation (Dunwiddie and Lynch, 1979; Baimbridge and Miller, 1981; Turner et al., 1981; Eccles, 1983; Mody et al., 1984; also see Section 1.3.).

Recent studies have also suggested the involvement of  $\text{Ca}^{2+}$  in the predisposition of neuronal tissue to epileptiform activity. Using the experimental model of kindling-induced epilepsy, Miller and Baimbridge (1983) demonstrated a selective

loss of calcium-binding protein (CaBP) from the granule cells of the dentate gyrus. The protein, which binds  $\text{Ca}^{2+}$  with high affinity, is normally localized in particular neuron types of the mammalian CNS (Jande et al., 1981; Baimbridge and Miller, 1982; Garcia-Segura et al., 1984) and is considered to function as an important buffer for intraneuronal  $\text{Ca}^{2+}$  (Baimbridge et al., 1982; Miller and Baimbridge, 1983). Inasmuch as the decrease in hippocampal CaBP is not correlated with seizure activity *per se* but rather to the progression of kindling (Baimbridge and Miller, 1984), it has been suggested that this change represents a functional alteration of calcium homeostasis in neurons of this region predisposing them to aberrant epileptiform activity (Miller et al., 1985). If calcium regulation is altered following kindling-induced epilepsy, then it is important to determine what changes have occurred in the concentration of intracellular  $\text{Ca}^{2+}$  as well as in its compartmentalization and the extent of intracellular buffering. The kinetic analysis of the uptake of radioactive  $\text{Ca}^{2+}$  is a widely used method for the determination of  $\text{Ca}^{2+}$ -compartmentalization and buffering in several non-neuronal preparations (Borle, 1975; 1981a,b; Uchikawa and Borle, 1981). In view of the successful application of  $^{45}\text{Ca}$  uptake kinetics to determine calcium homeostasis in the hippocampal formation (see Section 3.2.), the technique was used to investigate possible alterations in  $\text{Ca}^{2+}$ -regulation of amygdala- and commissural-kindled preparations.

### 3.3.2. Methods

Adult male Wistar rats (200 - 300 g) were divided into three groups: a) controls (n=8); b) commissural-kindled (n=6) and c) amygdala-kindled (n=6). The kindling group and two of the control animals were anesthetized with Nembutal (70 mg/kg i.p.) and were stereotaxically implanted with bipolar stimulating electrodes positioned either in the midline commissural pathway (AP: -1.8 mm from bregma; L: 0; V: 4.2 mm below surface of cortex) or the right amygdala (AP: -2.5 mm; L: 3.6 mm; V: 7.8 mm). Following recovery from surgery the animals, except for controls, were stimulated once a day (150  $\mu$ A, 60 Hz, for 1 sec) until a minimum of five consecutive motor seizures were induced (stage 5 - according to Racine, 1972b).

Hippocampal slices, 450  $\mu$ m in thickness, were prepared on the day following the last seizure according to the methods described previously (see Section 3.2.2.1.). The placements of stimulating electrodes in the hippocampal commissures and the amygdala were verified macroscopically by visual examination during dissection. Usually 24-30 slices were obtained from both hippocampi of one animal and were randomly distributed into six porous uptake vials (4-5 slices/vial). This procedure was necessary to obtain an adequate number of data points at each time interval for the uptake curve fitting routine. Experiments involved determining the  $^{45}\text{Ca}$  uptake in slices obtained from one animal. Double-blind experiments were also performed in which



control and kindled slices were incubated in the same uptake chamber although in separate holding vials. To test neuronal viability, some of the slices were routinely removed from the incubation chamber 1-2 hrs following incubation, and transferred to a superfusion type recording chamber for electrophysiological examination.

The procedures for determination of  $^{45}\text{Ca}$  uptake, curve fitting and compartmental kinetic analysis were similar to those described earlier (see Section 3.2.2.). In twenty slices obtained from control and kindled animals extracellular space was also determined using the [ $^3\text{H}$ ]inulin method (Kleizeller et al., 1964).

### 3.3.3. Results

Animals kindled by stimulation of the hippocampal commissures required substantially more daily stimulations (range: 26-31) than their amygdala-kindled counterparts (range: 13-16). No attempt was made to record afterdischarges during the process of kindling, but the typical behavioral signs described by Racine (1972b) were observed in both groups.

Hippocampal slices prepared from control and kindled animals exhibited normal viability during incubation in the  $^{45}\text{Ca}$  uptake chamber. Electrophysiological recordings in these slices indicated that the characteristic synaptic activity could be evoked from different cell types of the hippocampal formation. Although a detailed electrophysiological analysis was beyond the

scope of the present study, changes in inhibitory mechanisms were noted in kindled slices, similar to those described by Oliver and Miller (1985).

In both control and kindled preparations the uptake of radioactive calcium could be best fitted by a double exponential equation of the form:

$$A \cdot [1 - \exp(-\lambda_1 \cdot t)] + B \cdot [1 - \exp(-\lambda_2 \cdot t)];$$

where A and B are two exponential constants,  $\lambda_1$  and  $\lambda_2$  are the reciprocals of the time constants, and t is time. The asymptote of this function at time  $t = \infty$  represents total exchangeable calcium of hippocampal slices and the two exponential terms indicate the presence of two kinetically distinct intracellular  $\text{Ca}^{2+}$  pools (see Section 3.2.4.). The computer fitted uptake curves for control and kindled hippocampal slices are shown in Fig. 3.6. Each uptake curve was drawn using the average values of the exponential parameters obtained in individual experiments. This representation is justified since the average of the exponentials is a more accurate mathematical representation than the exponential equation that would fit the cumulated data points (Riggs, 1963).

The results obtained through kinetic analysis of the  $^{45}\text{Ca}$  uptake curves for two models of intracellular  $\text{Ca}^{2+}$  compartmentalization are summarized in Table 3.4.. The serial (catenary) organization assumes that transfer between the extracellular pool ( $S_1$ ) and the slowly exchangeable intracellular compartment ( $S_3$ ) has to occur via a rapidly displaceable pool ( $S_2$ ). In the

parallel model extracellular  $\text{Ca}^{2+}$  ( $S_2$ ) is allowed to exchange simultaneously with the two intracellular compartments ( $S_1$  and  $S_3$ ) while no communication between  $S_1$  and  $S_3$  is assumed. In either preparation (control or kindled) significant differences regarding  $\text{Ca}^{2+}$  fluxes were not present between these two models, although the parallel model consistently indicated a larger slowly exchangeable  $\text{Ca}^{2+}$  pool ( $S_3$ ).

Both kindled preparations showed marked alterations in the shape of the uptake curves (Fig. 3.6.) reflected by the pool sizes and exchange rates of  $\text{Ca}^{2+}$  (Table 3.4.). Significant changes in  $\text{Ca}^{2+}$  compartment sizes were only detected in slices obtained from commissural-kindled animals. A 38% enhancement of the  $S_2$  and a marked 55% reduction of the  $S_3$  pool was observed. The amygdala-kindled preparation exhibited a slight but not significant decrease of the  $S_3$  compartment. In both kindled preparations the total of exchangeable intracellular calcium remained fairly constant and was not significantly different from control slices (Fig. 3.7.). The  $3.33 \pm .12$  (mean  $\pm$  S.D.) nmol/mg wet weight of total exchangeable  $\text{Ca}^{2+}$  found in control hippocampal slices is in good agreement with previous studies on slices of brain and other tissues (Stahl and Swanson, 1971; 1972; Barritt et al., 1981; Borle, 1981; also see Section 3.2.3. and Table 3.2.).

The changes in compartment sizes observed in commissural-kindled preparations were paralleled by concomitant alterations in  $\text{Ca}^{2+}$  fluxes and rate constants. Due to the significant decrease of the  $S_3$  pool, the exchange rate ( $\text{FLUX } S_2 \leftrightarrow S_3$ )

Figure 3.6.  $^{45}\text{Ca}$  uptake curves in control, commissural- (HPC) and amygdala-kindled (AMY) hippocampal slices. The double exponential curves have been generated by computer from the average values for the kinetic parameters presented in Table 3.4. (n=6-8). Time zero represents addition of  $^{45}\text{Ca}$  and it is at least 1 hr following preincubation. Note the significant change in the shape of the kindled uptake curves, particularly that of the fast exponential components.

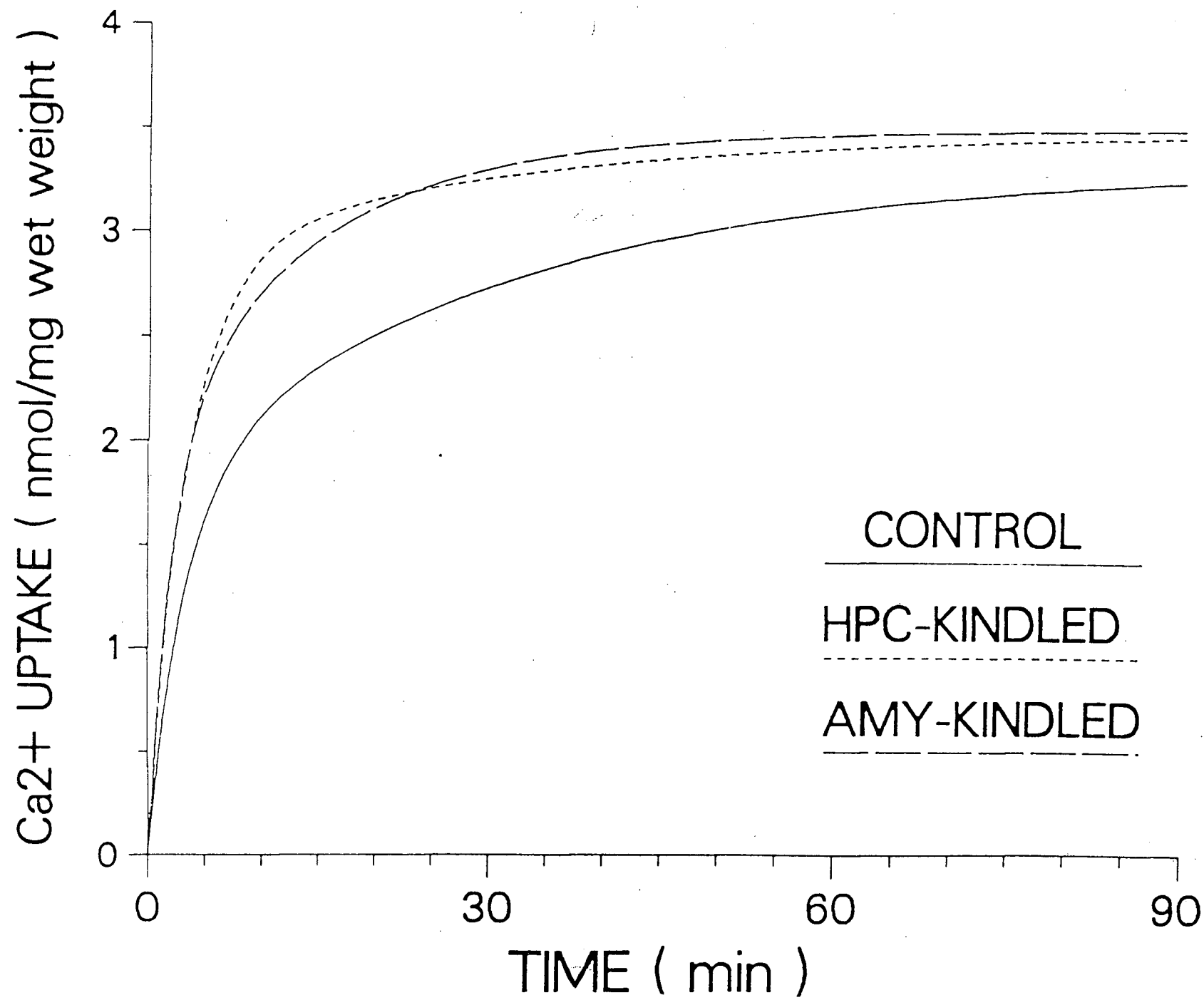


Table 3.4.

Effect of kindling-induced epilepsy on  $\text{Ca}^{2+}$  exchange rates and compartment sizes of hippocampal slices.

The pools, fluxes and rate constants for both the serial model system (extracellular compartment:  $S_1$ ) and the parallel model system (extracellular compartment:  $S_2$ ) of hippocampal cellular  $\text{Ca}^{2+}$  exchange have been calculated according to Section 3.2.2.3. POOLS ( $S_1, S_2, S_3$ ) represent the amount of exchangeable  $\text{Ca}^{2+}$ , FLUX is the rate of  $\text{Ca}^{2+}$  exchange at steady state between any compartment, and  $k$  is the rate constant for exchange between the respective compartments. Data expressed as mean  $\pm$  S.D. derived from the kinetic analysis of 6-8 uptake curves each (number of slices = 24-27 for each uptake curve), units are as indicated in Table 3.2.

	Control	Commissural-Kindled	Amygdala-Kindled
=====			
IN SERIES			
POOL $S_2$	2148 $\pm$ 204	2954* $\pm$ 222	2403 $\pm$ 539
POOL $S_3$	1179 $\pm$ 227	530* $\pm$ 189	1097 $\pm$ 504
TOTAL [ $S_2+S_3$ ]	3327 $\pm$ 115	3484* $\pm$ 216	3500* $\pm$ 175
FLUX $S_1-S_2$	585 $\pm$ 171	868* $\pm$ 101	947* $\pm$ 82
FLUX $S_2-S_3$	41 $\pm$ 15	19* $\pm$ 7	91* $\pm$ 50
$k_{21}$	.280 $\pm$ .1	.294* $\pm$ .03	.421* $\pm$ .12
$k_{23}$ [ $\times 10^{-3}$ ]	19.0 $\pm$ 6.6	6.3* $\pm$ 2.4	44.1 $\pm$ 29.7
$k_{32}$	.037 $\pm$ .017	.039 $\pm$ .015	.056 $\pm$ .028
=====			
IN PARALLEL			
POOL $S_1$	1758 $\pm$ 188	2792* $\pm$ 214	1956 $\pm$ 669
POOL $S_3$	1569 $\pm$ 194	692* $\pm$ 204	1544 $\pm$ 644
TOTAL [ $S_1+S_3$ ]	3327 $\pm$ 115	3484* $\pm$ 216	3500* $\pm$ 75
FLUX $S_2-S_1$	532 $\pm$ 185	842* $\pm$ 107	834* $\pm$ 90
FLUX $S_2-S_3$	53 $\pm$ 25	25* $\pm$ 13	113* $\pm$ 62
$k_{12}$	.303 $\pm$ .1	.301 $\pm$ .03	.474* $\pm$ .15
$k_{32}$	.033 $\pm$ .01	.038 $\pm$ .01	.069* $\pm$ .02
=====			

\* Denotes significant difference from control ( $p < 0.01$  one-way ANOVA).

between the respective compartments of the serial model was diminished, as was the fraction of  $S_2$  transported to  $S_3$  per unit time ( $k_{23}$ ). In the parallel model the rate constants were unaffected but the flux between the extracellular compartment and the slowly exchangeable intracellular  $Ca^{2+}$  pool ( $S_3$ ) was reduced about 50%.

Amygdala-kindled slices, although not characterized by marked alterations in pool sizes, showed a significant facilitation of  $Ca^{2+}$  transport and exchange between all compartments.

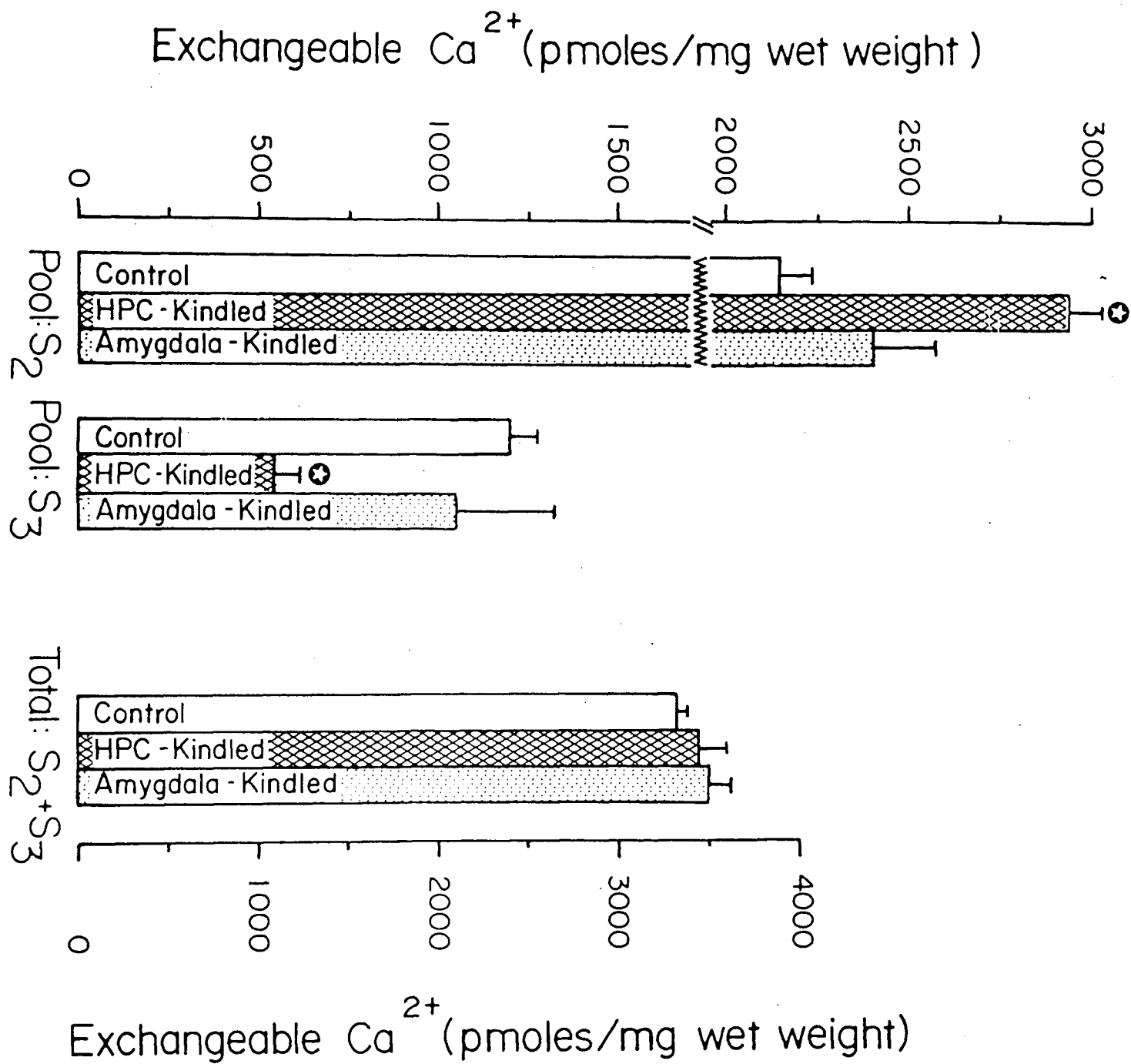
No discrepancies were found between the experiments in which separate incubations of control and kindled hippocampi were made and those in which the two preparations were simultaneously incubated. Results obtained using both procedures are combined and included in Table 3.4. Moreover, the two animals that had implanted stimulating electrodes but received no kindling stimuli exhibited similar hippocampal  $Ca^{2+}$  compartmentalization and exchange rates to that of controls.

The differences in  $^{45}Ca$  uptake kinetics of kindled hippocampi did not seem to be correlated to the number of full motor seizures. No tendency for further alterations was noted in animals with 10 motor seizures when compared with those exhibiting only 5 convulsions. Therefore the data has been pooled for all the kindled preparations regardless of the number of evoked stage 5 seizures.

The extracellular space fraction derived through [ $^3H$ ]inulin measurements in control ( $n=10$ ) and kindled ( $n=10$ ) hippocampal slices yielded similar results, in the range of .29-.31. In

Figure 3.7. Histograms showing exchangeable calcium pools in hippocampal slices obtained from control, commissural- (HPC) and amygdala-kindled animals. Note that the total exchangeable  $\text{Ca}^{2+}$  ( $S_2 + S_3$ ) is similar in all three preparations. (\* - denotes: significantly different from 'CONTROL';  $p < 0.01$  - one-way ANOVA).





addition the wet weight of hippocampal slices was found to be highly consistent: control (n=116) =  $2.69 \pm .06$  mg; commissural-kindled (n=111) =  $2.65 \pm .06$  mg; and amygdala-kindled (n=109) =  $2.68 \pm .06$  mg.

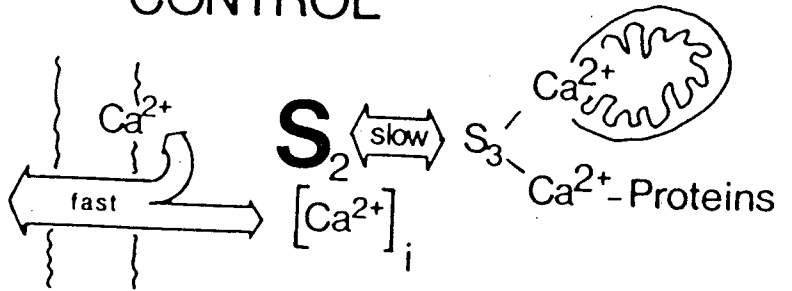
#### 3.3.4. Discussion

Hippocampal slices maintained at a steady state may be characterized in terms of calcium compartmentalization as having two kinetically distinct  $\text{Ca}^{2+}$  pools (See Section 3.2.3.1.). The rapidly exchangeable pool has been shown to be linearly related to extracellular  $[\text{Ca}^{2+}]$  and represents the amount bound to the plasma membrane and in a free ionic state. The more slowly exchangeable compartment is readily modified by the mitochondrial uncoupler 2,4-dinitrophenol (DNP) and by the alkylxanthine derivative 3-isobutyl-1-methylxanthine (IBMX) and is therefore considered to reflect  $\text{Ca}^{2+}$  bound by intracellular sequestering and buffering systems (See Section 3.2.3.2.).

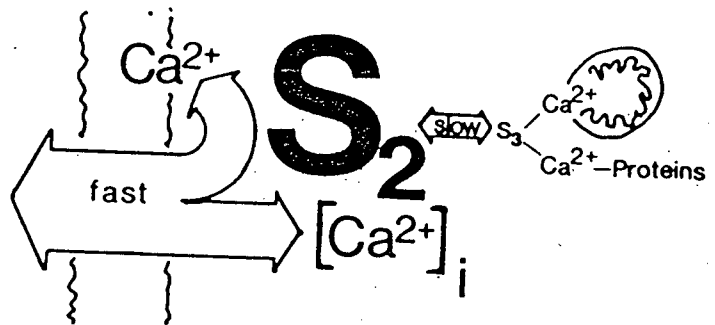
Slices obtained from the hippocampi of commissural- and amygdala-kindled animals showed marked alterations in the kinetics of  $^{45}\text{Ca}$  uptake indicating an abnormal cellular  $\text{Ca}^{2+}$  regulation. These changes are diagrammatically summarized in Fig. 3.8. The size of the buffered  $\text{Ca}^{2+}$  compartment is dramatically reduced in commissural kindling and it is paralleled by a significant increase in the rapid calcium flux as reflected by the faster initial component of the uptake curve.

Figure 3.8. Schematic illustration of alterations observed in calcium exchange kinetics of kindled hippocampi. In all three cases the diagrams refer to the serial arrangement of the exchangeable  $\text{Ca}^{2+}$  pools. The relative size of the letters (representing calcium pools) and arrows (indicating  $\text{Ca}^{2+}$  fluxes) reflect proportional changes in these parameters of cellular calcium regulation. Extracellular calcium ( $S_1$ ) was constant in all three conditions. Note the significant enhancement of pool  $S_2$  and reduction of compartment  $S_3$  in commissural-kindled slices and the large calcium fluxes in amygdala-kindled preparations.

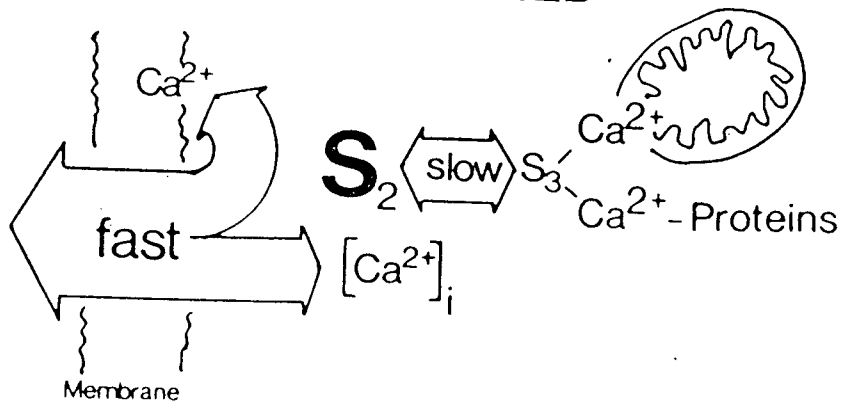
## CONTROL



## COMMISSURAL-KINDLED



## AMYGDALA-KINDLED



**S<sub>1</sub>**  
 $[\text{Ca}^{2+}]_o$

It appears that during commissural kindling,  $\text{Ca}^{2+}$  is transferred from the buffered  $\text{S}_3$  pool into the unbuffered  $\text{S}_2$  compartment. The lack of changes in  $\text{Ca}^{2+}$  compartment sizes during amygdala-kindling is more difficult to interpret. The results show a large degree of variability that is probably due to pooling of ipsi- and contralateral hippocampal slices with regard to the site of stimulation. This however, was necessary to obtain four or more data points for every uptake curve at each time interval to satisfy the statistical accuracy of the curve fitting algorithm. Nevertheless,  $\text{Ca}^{2+}$  homeostasis is likely to be altered in this preparation as well, since there is a significant enhancement of  $\text{Ca}^{2+}$  fluxes and their rate constants.

The data does not distinguish which of the variety of factors involved in the control and regulation of intracellular  $\text{Ca}^{2+}$  are altered during kindling. The shapes of the  $^{45}\text{Ca}$  uptake curves presented in Fig. 3.6. resemble those produced by the application of pharmacological agents that interfere with mitochondrial calcium regulation (Borle, 1981b; also see Section 3.2.3.2.). On the basis of this observation, it may be suggested that mitochondrial  $\text{Ca}^{2+}$  uptake is impaired in kindled hippocampi. Although changes in mitochondrial calcium transport are known to parallel neuronal plasticity in the hippocampus (Baudry et al., 1983), there is no evidence as yet to indicate that alterations in mitochondrial function occur during kindling-induced epileptogenesis (McNamara et al., 1980; Kalichman, 1982; Peterson and Albertson, 1982; McNamara, 1984). The endoplasmic reticulum may also play an important role in  $\text{Ca}^{2+}$  sequestration and long-term

changes in its function may effectively alter neuronal  $\text{Ca}^{2+}$  homeostasis (Duce and Keen, 1978). One recently identified biochemical factor involved in intracellular  $\text{Ca}^{2+}$  regulation which is correlated with kindling is the neuron-specific calcium-binding protein (CaBP) (Miller and Baimbridge, 1983). The fact that there is a selective decrease in the hippocampal levels of this protein during the process of kindling raises the possibility that the alterations seen in the  $^{45}\text{Ca}$  uptake kinetics of kindled hippocampal slices may be due to the loss of this putative intraneuronal  $\text{Ca}^{2+}$ -buffer (Miller and Baimbridge, 1983; Baimbridge and Miller, 1984). If  $\text{Ca}^{2+}$  bound to this protein is indeed part of the buffered ( $S_3$ )  $\text{Ca}^{2+}$  pool then the marked reduction of this compartment following commissural kindling may be explained by the depletion of hippocampal CaBP. Assuming this to be the case, the small change in the size of the  $S_3$  pool observed in amygdala-kindled slices could be attributed to the relatively small decrease in hippocampal CaBP produced by amygdala-kindling (Baimbridge et al., 1985). Further evidence in favor of the relationship between the  $S_3$  compartment and CaBP was obtained from experiments using microdissections of hippocampal slices. These studies, although preliminary, indicate that the change in  $^{45}\text{Ca}$  uptake kinetics during commissural kindling is mainly localized to the dentate gyrus, where the decline of CaBP is observed, with little alteration in the CA2/CA1 regions of the hippocampal formation (Miller and Baimbridge, 1983).

The fact that the number of evoked full motor seizures was not correlated to the magnitude of alterations in  $\text{Ca}^{2+}$  homeo-

stasis indicates that convulsions themselves are not the primary cause of these changes. Preliminary findings (n=2) in partially kindled animals with no motor seizures show alterations similar to those of the fully kindled preparations after 20 commissural stimulations. These data again suggest a correlation between the altered  $^{45}\text{Ca}$  kinetics and the loss of hippocampal CaBP since it has been shown that seizures do not produce a further drop in the levels of the protein that reach a half-maximal decline after only 10 commissural stimulations (Baimbridge and Miller, 1984).

It should be noted that total exchangeable  $\text{Ca}^{2+}$  (the sum of the two cellular exchangeable pools) was not altered in either of the kindled preparations. This result is in good agreement with other findings in which measurements of total hippocampal calcium by atomic absorption spectrophotometry show no significant differences between control and kindled hippocampi (see Section 3.1.3.). Therefore, it is concluded that kindling results in a redistribution rather than an absolute change of the total hippocampal intracellular  $\text{Ca}^{2+}$ . This process involves the mobilization of  $\text{Ca}^{2+}$  from a pool that appears to be the sum of sequestered/buffered cellular  $\text{Ca}^{2+}$ . Although many intracellular organelles and systems may be part of this  $\text{Ca}^{2+}$  compartment (Blaustein et al., 1978; 1980; McGraw et al., 1982), until evidence is available to the contrary, the most likely possibility for the cause of  $\text{Ca}^{2+}$  redistribution during kindling is the loss of hippocampal CaBP.

The observations of this study are valid regardless of whether the two exchangeable cellular compartments are assumed

to be connected in series or in parallel with the extracellular  $\text{Ca}^{2+}$ . The reason for the similarity of the two models is the small fraction (0.019) of the unbuffered pool that is normally exchanged per unit time with the  $\text{Ca}^{2+}$  of the buffered compartment in the serial model. The parallel model does not assume such exchange, i.e., both compartments are only connected to the extracellular space without any reciprocal communication.

Based on the method of compartmental analysis developed in this study, it is evident that kindling results in significant changes in calcium homeostasis in the hippocampal formation. Although this method does not distinguish which cellular elements of this heterogeneous structure are involved, it is reasonable to suggest that if the alteration is associated with neurons, then their discharge properties would also be altered. In this regard, it is notable that following kindling, the granule cells of the dentate gyrus exhibit significantly modified passive membrane properties (Oliver et al., 1983) as well as an enhancement of long-duration inhibitory processes (Tuff et al., 1983; Oliver and Miller, 1985). Recently Wadman et al. (1985) have also been able to demonstrate an increase in the stimulus- or amino acid-induced loss in  $[\text{Ca}^{2+}]_o$  in the dendritic region of CA1 neurons following kindling, indicating a chronic alteration in  $\text{Ca}^{2+}$ -regulation. The manner in which the change in  $\text{Ca}^{2+}$  homeostasis described in the present study may account for the observed electrophysiological changes, or alternatively for some other modifications in biochemical and neurotransmitter functions (McNamara et al., 1980; Kalichman, 1982; Peterson and Albertson,



1982; McNamara, 1984) remains to be determined. Further studies are needed to establish the precise timing of the altered  $\text{Ca}^{2+}$  regulation during development of kindling and to establish a direct link to the loss of hippocampal CaBP and the number of recorded afterdischarges.

## CHAPTER IV.

EFFECT OF IBMX ON HIPPOCAMPAL EXCITABILITY

In contrast to some damaging long-term alterations in nerve cell activity, as is the case during epileptogenesis, other plastic neuronal changes may subserve more vital functions, for example learning and memory. Although the exact molecular mechanisms subserving these important functions have not yet been elucidated, neurophysiological evidence indicates that the hippocampal formation is a major site of plastic alterations. The first accounts for the involvement of the hippocampus in learning and memory in humans come from the studies of B. Milner, W. Penfield and W.B. Scoville on a patient ("H.M.") with bilateral hippocampal lesions (Milner and Penfield, 1955; for review see Milner et al., 1968). The syndromes of H.M. and those of several other similar patients could be replicated only later on animals with bilateral lesions of the hippocampus and the amygdala (Mishkin, 1978). Meanwhile Bliss and colleagues (Bliss and Lomo, 1973; Bliss and Gardner-Medwin, 1973) described the phenomenon of long-term potentiation (LTP) in the hippocampal formation of the rabbit, an event that may represent the

underlying plastic changes necessary for memory formation and learning. It consists of an enhancement of the input/output function of the system that may last for several weeks, or even months in an in vivo preparation following short periods of tetanic stimulation of the perforant pathway. This form of LTP was readily reproducible in rats (Douglas and Goddard, 1975) and it was subsequently shown that the phenomenon may also be induced in the isolated hippocampal slice preparation (Schwartzkroin and Wester, 1975; Alger and Teyler, 1976; Andersen et al., 1977). Naturally, due to the limitations of the in vitro preparation, the LTP of the hippocampal slice is not as long-lasting as in chronic experiments but the isolated hippocampus provides the advantage of more direct experimental manipulations (Teyler et al., 1977). It was however with the hippocampal slice that investigators were able to demonstrate that LTP is not restricted to the dentate gyrus but occurs at essentially every synaptic relay within the hippocampal formation.

Although LTP has since been shown to exist in several other areas of the mammalian CNS such as the superior cervical ganglion (Brown and McAfee, 1982; Briggs et al., 1985), the medial geniculate nucleus (Gerren and Weinberger, 1983), cortical (Lee, 1982) and limbic forebrain structures (Racine et al., 1983), the hippocampal formation remains the most extensively studied region with regard to this plastic alteration in neuronal function. In spite of several comprehensive review articles, all dealing with possible mechanisms underlying LTP (Bliss, 1977; Bliss and Dolphin, 1982; Swanson et al., 1982; Eccles, 1983; Voronin, 1983;

Lynch and Baudry, 1984; Teyler and Discenna, 1984), the exact events responsible for the phenomenon are far from being well understood.

The enhanced efficacy of hippocampal synapses following LTP may be achieved in a multitude of manners. A presynaptic change may lead to a long-term alteration in neurotransmitter release (Skrede and Malthé-Sorensen, 1981; Dolphin et al., 1982) or alternatively, there could be a change in the sensitivity or absolute number of active postsynaptic receptors (Baudry et al., 1980; Lynch and Baudry, 1984). A further complexity is introduced by norepinephrine, which under certain circumstances may modulate the induction of LTP (Bliss et al., 1983; Neuman and Harley, 1983; Hopkins and Johnston, 1984).

The picture is not much clearer when one examines the intracellular correlates of LTP in the CA1 region (Andersen et al., 1977; 1980; Lynch et al., 1983) or in the CA3 region of the hippocampus (Yamamoto and Chujo, 1978; Yamamoto et al., 1980). The major finding of these studies is the enhancement of the intracellular excitatory postsynaptic potential (EPSP) during LTP while other cellular parameters do not seem to be altered.

#### 4.1. Introduction

Regardless of the exact mechanism(s) involved, the induction of LTP is strictly dependent upon the presence of  $\text{Ca}^{2+}$ , indicating an important role for the cation in this form of neuronal plasticity (for review see Eccles, 1983). Although strontium may support LTP in the hippocampus (Wigstrom and Swann, 1980), extracellular  $\text{Ca}^{2+}$  appears to be an essential requirement (Dunwiddie and Lynch, 1979; Wigstrom et al., 1979). It has also been established that intraneuronal  $\text{Ca}^{2+}$  participates in the process of LTP since injection of EGTA into hippocampal pyramidal cells blocks the occurrence of the phenomenon (Lynch et al., 1983). Furthermore, LTP was found to be associated with a significant uptake and a transient retention of calcium (Baimbridge and Miller, 1981) and could be produced either in vitro (Turner et al., 1981; Mody et al., 1984) or in vivo (Bliss et al., 1984) by a brief elevation of the extracellular  $\text{Ca}^{2+}$  concentration ('calcium-induced LTP').

Several lines of evidence suggest however, that calcium is not directly involved in the mechanism of LTP but rather through an intracellular messenger system that triggers some long-lasting biochemical alterations (for reviews see Eccles, 1983; Lynch and Baudry, 1984). One of the prime candidates as the mediator of  $\text{Ca}^{2+}$ -effects is the intracellular calcium receptor protein calmodulin (Cheung, 1980). Its involvement in LTP is likely, since calmodulin blocking agents such as neuroleptic drugs were shown

to inhibit tetanic- and calcium-induced LTP in the hippocampus (Finn et al., 1980; Bliss et al., 1984; Mody et al., 1984). Calmodulin may participate at virtually every level of control of neuronal excitability (Cheung, 1980; Means and Dedman, 1980), but in view of the role of cyclic nucleotides in the CNS (Rasmussen and Goodman, 1977; Rasmussen and Barrett, 1984), calmodulin's influence on cyclic nucleotide metabolisms seems of primary importance. Facilitation of LTP induction by norepinephrine (Bliss et al., 1983; Neuman and Harley, 1983; Hopkins and Johnston, 1984) may occur via the cAMP system which is known to enhance the excitability of hippocampal neurons (Segal, 1981; Madison and Nicoll, 1982). Therefore, activation of calmodulin by  $\text{Ca}^{2+}$  is probably only the first step in a chain of biochemical events involving cyclic nucleotide metabolism and/or protein phosphorylation that ultimately lead to LTP.

The source of  $\text{Ca}^{2+}$  for activation of LTP is not known. Although enhanced uptake and retention of the cation have been shown to be correlates of LTP (Baimbridge and Miller, 1981), the release of  $\text{Ca}^{2+}$  from intraneuronal storage sites cannot be excluded from the process. The aim of the present study has therefore been to elucidate some of the steps and mechanisms subserving LTP by the use of drugs that interfere with intracellular calcium homeostasis and the catabolism of cyclic nucleotides. While a large variety of compounds are available that block calcium entry into nerve cells, agents that interfere with the regulation of intraneuronal calcium are less common. For the present experiments, methylxanthine derivatives were the

drugs of choice, since they are believed to have two properties that may interfere at two different steps in the process of LTP induction. Firstly, these compounds have been shown to release  $\text{Ca}^{2+}$ , at least in the case of skeletal muscle, from intracellular storage sites (Endo, 1977; Miller and Thieleczek, 1977; Martonosi, 1984). Secondly, they are effective inhibitors of the enzyme phosphodiesterase (PDE) responsible for the breakdown of cyclic nucleotides (Chasin and Harris, 1976). Hence if the  $\text{Ca}^{2+}$ -calmodulin-cyclic nucleotide step-by-step activation subserves the mechanism of LTP, it would be expected that methylxanthines could act as long-lasting potentiators of neuronal activity. The augmentation of neuronal excitability could be quite large, since the compounds act at two possible synergistic steps of LTP activation: the increase in cytosolic calcium and the elevation of cyclic nucleotide levels by inhibition of the enzyme responsible for their breakdown.

The present study was carried out using the methylxanthine compounds theophylline (1,3-dimethylxanthine) and 3-isobutyl-1-methylxanthine (IBMX) primarily because of their potent inhibitory effects on the enzyme phosphodiesterase (Chasin and Harris, 1976; Smellie et al., 1979). In addition, IBMX has been shown to release  $\text{Ca}^{2+}$  from intracellular storage sites, in the sarcoplasmic reticulum of skeletal muscle (Miller and Thieleczek, 1979) and the hippocampal slice preparation (see Section 3.2.3.2). Papaverine, a non-methylxanthine compound which has some relatively specific PDE-inhibitory action, was also used in

order to distinguish between possible  $\text{Ca}^{2+}$  and cyclic nucleotide effects on LTP.

#### 4.2. Methods

##### 4.2.1. Extracellular recordings and analysis

Slices (450  $\mu\text{m}$  in thickness) were prepared from the hippocampi of male Wistar rats (200-250 g) using a Sorvall tissue chopper. They were transferred with the aid of a pipette to a chamber that allowed long-term storage as well as experimental manipulation and electrophysiological recordings to be undertaken. The artificial cerebrospinal fluid (CSF) was perfused at a rate of 2 ml/min in the recording chamber, 0.5 ml/min in the storage chamber and contained 124 mM NaCl, 3.75 mM KCl, 1.25 mM  $\text{KH}_2\text{PO}_4$ , 24 mM  $\text{NaHCO}_3$ , 1.5 mM  $\text{CaCl}_2$ , 1.5 mM  $\text{MgSO}_4$  and 10 mM glucose dissolved in bi-distilled water. The ' $\text{Ca}^{2+}$ -free' solution was prepared by omitting  $\text{CaCl}_2$ . When 3 mM  $\text{CoCl}_2$  was added,  $\text{MgSO}_4$  and  $\text{KH}_2\text{PO}_4$  were replaced by equimolar amounts of  $\text{MgCl}_2$  and KCl respectively. The medium was continuously warmed ( $35 \pm 0.5$  °C) and oxygenated with a 95%  $\text{O}_2$ , 5%  $\text{CO}_2$  gas mixture. In addition to the oxygenation of the medium, warmed and humidified gas mixture was allowed to flow on the top of the slices. The artificial CSF used during preparation of the tissue also contained .003%  $\text{H}_2\text{O}_2$  to maintain a better oxygen uptake (Llinas et al., 1981).



Electrophysiological recordings were started following one hour of equilibration of the slices at a constant temperature of  $35 \pm 0.5$  °C. Recording electrodes (resistances 4-10 Mohms) were pulled (using a Narashige or a Frederick Haer microelectrode puller) from glass capillaries (outer diameter of 1.5 mm with Omega Dot, Frederick Haer) and were backfilled with 2 M NaCl solution using a 31 gauge hypodermic needle. The electrodes, mounted on micro-manipulators, were positioned under visual guidance with the aid of a 4x dissecting microscope in the stratum pyramidale and stratum radiatum to record the extracellular population spikes and EPSPs respectively.

Stimulating electrodes, also on micromanipulators, consisted of twin nichrome wires (62  $\mu$ m in diameter) and were used to deliver 0.1 ms square wave pulses of 0.5 - 50 V intensity from isolation units (Medical Systems Corp., Model DS2) with a baseline frequency of 0.133 Hz. These electrodes were positioned in the Schaffer collateral/commissural fiber system of the stratum radiatum for orthodromic activation of the CA1 pyramidal cells. In some experiments an additional stimulating electrode was placed in the alveus to evoke antidromic responses. To test the degree of recurrent inhibition on the pyramidal neurons, an antidromic (conditioning - C) stimulus was delivered followed by orthodromic (test - T) stimulation (C-T interval: 20 ms). Input/output curves for the EPSP and population spike responses were obtained in each experiment by setting the orthodromic stimulus intensity to evoke an initial EPSP response of 1 mV

amplitude in the stratum radiatum and subsequently incrementing the stimulation intensity in 15-20 equal steps.

Potentials, referenced to a silver-silver chloride bath ground, were recorded with a precision electrometer (M-707 WP Instruments) and displayed on a storage oscilloscope (Tektronix) after being filtered at 0.1-10 KHz. The amplified signals were led to a PDP 11/23 computer for on-line averaging, data storage and analysis. Usually four consecutive sweeps were averaged over a period of one minute. The amplitude of the characteristic positive-negative-positive CA1 population spike was measured peak to peak from the first positivity ( $P_1$ ) to peak negativity ( $N_1$ ) (Fig. 4.1.A.). The amplitude of the antidromic population spike recorded in the stratum pyramidale and that of the fiber volley and EPSP recorded in the stratum radiatum was measured as peak negativity compared to baseline (Fig. 4.1.B.). The rate of rise of the EPSP response was taken as the peak of the first order voltage differential:  $dV/dt$  (Fig. 4.1.C.).

Drugs were dissolved in the artificial CSF to yield the final concentration (usually 100  $\mu M$ ) and were applied by perfusion. A three-way valve system allowed switching between perfusates. The design of the recording/incubation chamber made it possible to have the experimental slices exposed only once to a drug and then another slice from the storage part of the chamber could be transferred into the recording compartment. Addition of the drugs to the medium did not change its pH, which remained constant at  $7.4 \pm 0.03$ . Theophylline, papaverine-hydrochloride and 3-isobutyl-1-methylxanthine (IBMX) were

Figure 4.1. Measurement of extracellular potentials in the CA1 region of the hippocampal slice preparation.

A. Stratum radiatum evoked population spike recorded at the level of pyramidal cells. Its amplitude was measured as the voltage difference between the first positivity ( $P_1$ ) and the negative deflection ( $N_1$ ). B. Extracellular EPSP response recorded in the stratum radiatum at the level of the apical dendrites. Stimulation was delivered to the Schaffer collateral/commissural fiber system. The amplitude of the response was measured as peak negativity (marked with a cross) calculated from baseline (BL). The negative deflection which precedes the EPSP marked 'fv' represents the activation of presynaptic fibers and is termed fiber volley. C. First order voltage differential ( $dV/dt$ ) of the EPSP potential. Its peak amplitude (as measured from baseline) corresponds to the fastest rate of rise of the EPSP (left arrow) while its value becomes zero during the peak of the EPSP (right arrow). Calibration bars: horizontal: 5 ms; vertical: 2 mV (for A. and B.) and 5 mV/ms (for C.)

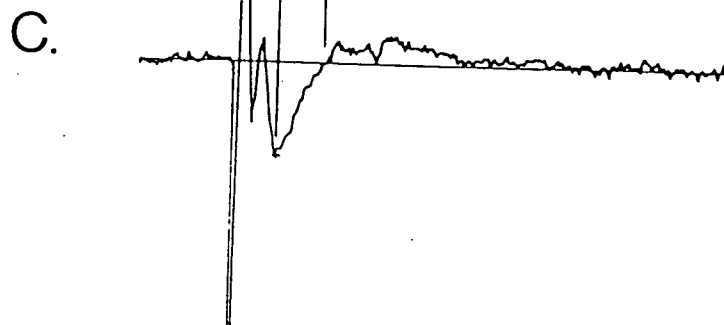
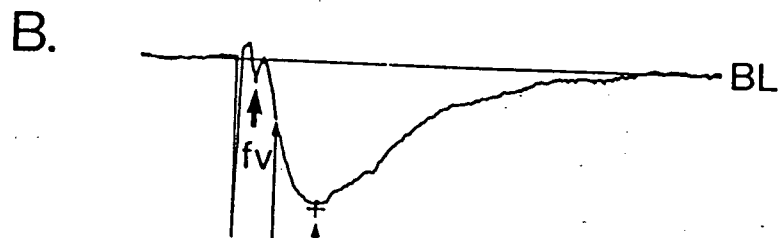
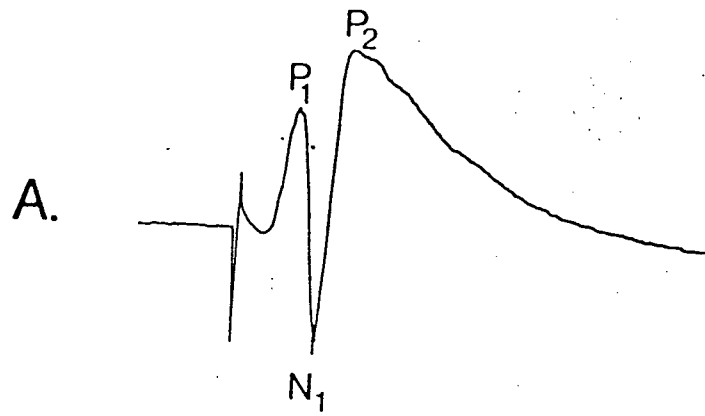
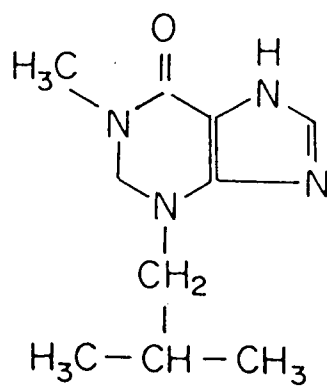


Figure 4.2. Chemical formulae of the drugs used in the present study. Note the similarity in structure between IBMX and theophylline (1,3-dimethylxanthine). Papaverine is an isoquinoline derivative and a potent phosphodiesterase inhibitor.

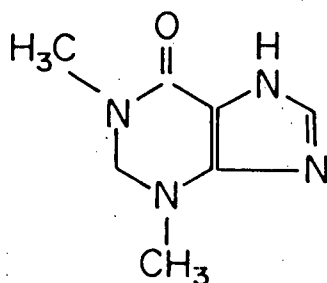
3-Isobutyl-1-methylxanthine  
(IBMX)

---



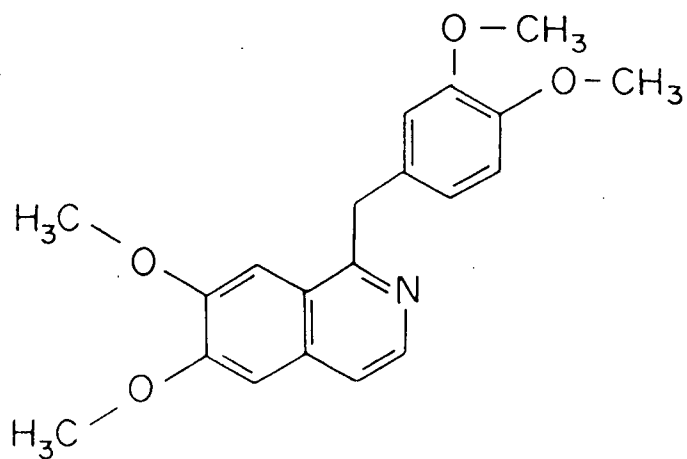
Theophylline

---



Papaverine

---



obtained from Sigma Chemical Company. Their respective chemical formulae are presented in Fig. 4.2.

#### 4.2.2. Intracellular recording and data analysis

The method for preparation and maintenance of hippocampal slices was the same as described in the previous section. Intracellular recording electrodes were pulled from glass capillary tubing (outer diameter of 1.50 mm with Omega Dot, Frederick Haer) and were filled with 2 M potassium acetate (MCB) or in some cases with 2 M potassium methylsulphate (ICN Pharmaceuticals). The electrolyte solutions were carefully filtered through millipore filters to eliminate particles and impurities. Electrode impedances ranged from 30 to 75 Mohms as measured with the aid of an electrometer in the medium of the recording chamber. The electrodes were mounted on a variable speed piezoelectric advance manipulator (Burleigh Inchworm PZ 550) and were lowered into the stratum radiatum under visual guidance with the aid of a dissecting microscope. The characteristics of the recording electrodes were examined before penetration of the cells was attempted. While in the artificial CSF, the electrodes were balanced through a Wheatstone bridge circuit and were considered adequate for intracellular analysis if passing .75-1.0 nA of inward or outward current produced a minimal voltage deflection ( $<2$  mV).

Impalements of hippocampal CA1 pyramidal cells were obtained by a brief activation of capacitive feedback through the

electrode. Following penetration of the cell the voltage response dropped -40 to -60 mV and action potentials caused by membrane-injury were also noted. A variable DC source was used for hyperpolarizing current injections ( $\sim 1.0$  nA) into the cells immediately following their penetration as well as for variable amplitude command pulses.

Potentials, referenced to the bath Ag-AgCl<sub>2</sub> ground, were recorded with a precision electrometer (M 707, WP Instruments). The signals were led to a storage oscilloscope, filtered 10 kHz (DC), displayed for photography and further led to a PDP 11/23 computer for on-line averaging, data storage and analysis. The passive membrane characteristics of hippocampal pyramidal cells were determined as follows: (i) resting membrane potential (RMP) was taken as the potential difference between intra- and extracellular environment following removal of the electrode from the cell. (ii) Input resistance ( $R_n$ ) was calculated by the computer as the slope of the regression line between current injected through the microelectrode and membrane voltage at 6-9 different values of injected current up to 1.0 nA. The current pulses were of 100-150 ms duration and the resulting membrane voltage perturbation was measured after it has reached a steady value (usually after 40-50 ms). When injection of multiple current pulses was not undertaken,  $R_n$  was estimated from the voltage deflection caused by a single inward current injection of 0.5 or 1.0 nA. (iii) The membrane time constant ( $T_c$ ) was also derived by computer from the slope of the regression line drawn to the plot of time vs. the natural logarithm of the changes in



membrane charging profile. The changes in membrane voltage were sampled every 32  $\mu$ s ensuring high accuracy of the measurements. The fitting of the regression line was repeated at different levels of hyperpolarizing current injections and an average time constant was calculated from several determinations.

To study the accommodation properties of hippocampal pyramidal cells during a long-duration (600 ms) depolarizing current pulse, the signals were led to the PDP 11/23 computer through a peak detector. This ensured accurate counting of the evoked spikes as well as their continuous raster-type display. Since there is a reasonable variability in the current-evoked discharge patterns of pyramidal cells, trends of discharge and minor changes with time are difficult to observe through visual examination of oscilloscope photographs or chart-recordings. The continuous raster procedure however, allowed for complete elimination of bias in the estimation of the number of spikes evoked during a given current pulse. In addition, post-stimulus time histograms (PSTs) were also constructed by the computer to check for the significance in changes of pyramidal cell firing patterns.

### 4.3. Results

#### 4.3.1. Effect of drugs on stratum radiatum evoked potentials

Within 5 min of its perfusion 100  $\mu$ M IBMX caused a marked increase in the size of the population spike responses recorded in the pyramidal cell layer. This extracellular potential represents the synchronous discharge of pyramidal neurons after their synaptic activation (Andersen et al., 1971). The potentiation was further enhanced during the perfusion and reached a maximum of 300-900% of the initial response at the end of the 10 min administration period. Following return to the normal artificial CSF the population spike failed to decline or showed only a slight recovery after 2-3 hours of wash (Fig. 4.3.). This effect was maximal with IBMX concentrations of 100  $\mu$ M. At lower drug concentrations (e.g., 50  $\mu$ M) this effect was not as dramatic but was as long-lasting (n=3). At a concentration of 10  $\mu$ M only a slight potentiation of the stratum radiatum evoked response was observed which following the wash period returned to pre-drug levels (n=5). Invariably, no effect of IBMX was recorded on the antidromically evoked synchronous discharges of pyramidal neurons, suggesting that a change in pyramidal cell excitability did not occur in the presence of the drug (Fig. 4.4.).

The effect of IBMX on the extracellular EPSP response recorded at the level of the apical dendrites was similar to that

Figure 4.3. Effect of various drugs on the amplitude of population spikes evoked in the CA1 region of the hippocampal formation. Each response represents the average of four consecutive sweeps as displayed by the computer. Left column: control responses taken prior to the drug perfusions. Middle column: changes in the amplitude of the responses at the end of a 10 min perfusion period. Right column: population spikes recorded at indicated times following washout of the drugs. Note that IBMX and theophylline both caused a marked potentiation of the evoked responses, but only the effect of IBMX was long-lasting. Papaverine produced a non-significant potentiation during its perfusion and caused a slight depression of the population spikes during the washout period.

Control



10 min. Drug

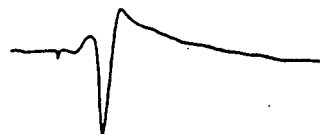
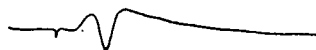


IBMX  
100  $\mu$ M

Wash

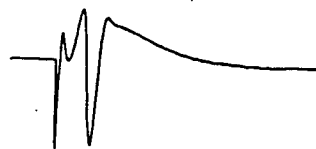
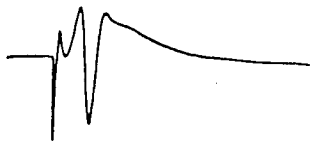


150 min

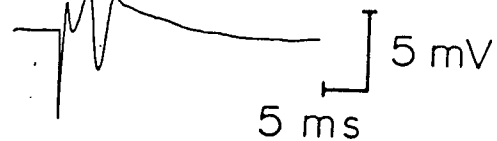


Theophylline  
100  $\mu$ M

15 min



Papaverine  
100  $\mu$ M



10 min

observed for the population spike, but of lesser magnitude (50-400 %). Concurrent with the increase in EPSP amplitude there was a characteristic reduction in the latency to peak amplitude (Andersen et al., 1980). Following stimulation of afferent fibers of the stratum radiatum a small negative field potential may be recorded in the region of the apical dendrites of CA1 pyramidal cells. This potential precedes the EPSP and has been termed 'fiber volley' since it is thought to represent impulse propagation through presynaptic fibers (Andersen et al., 1978). The amplitude and latency of the fiber volley was unchanged by perfusion of IBMX and no long-lasting effects were detected.

As shown in Fig. 4.3., the effect of IBMX on the CA1 population spike responses was to induce a long-lasting potentiation. This action was observed in more than 40 slices and in some cases, where long and stable recordings could be obtained, the evoked responses failed to return to control levels even after 3-3.5 hours of washout. Therefore, it may be stated that analogous to the tetanic stimulation- or calcium-induced LTP, IBMX has caused long-lasting enhancement of the stratum radiatum evoked responses in the CA1 region of the hippocampal formation.

The potent LTP-inducing effect of IBMX was not mimicked by the other methylxanthine derivative theophylline. Theophylline (at 100  $\mu$ M), also an effective adenosine antagonist (Dunwiddie and Hoffer, 1980; Dunwiddie et al., 1981) and a cyclic nucleotide phosphodiesterase inhibitor (Chasin and Harris, 1976), caused a reversible increase in the size of the population spikes and

EPSPs. In all slices examined (n=8) the potentiation induced by theophylline was approximately half of that caused by IBMX at a similar concentration and the recorded potentials returned to pre-drug levels within 10-15 min of the wash period (Fig. 4.3.). These results are similar to data reported by Dunwiddie and Hoffer (1980) who attributed the changes to blockade of adenosine receptors.

Perfusion of papaverine in seven slices (100  $\mu$ M) caused an initial potentiation then a slight inhibition of stratum radiatum evoked responses (Fig. 4.3.). Since papaverine has been shown to be a potent inhibitor of [ $^3$ H]adenosine uptake into cortical synaptosomes (Bender et al., 1980) its effect may be related to enhancement of adenosine responses in addition to inhibition of phosphodiesterase.

The unique LTP-inducing effect of IBMX was not shared by compounds that have presumably similar actions on adenosine receptors and the enzyme phosphodiesterase, indicating that some other property of IBMX may be responsible for the LTP. To further examine the LTP induced by IBMX, the drug's effect was tested on some parameters of neuronal excitability known to be altered by other forms of LTP.

#### 4.3.2. Effect of IBMX on paired-pulse inhibition

Haas and Rose (1982) concluded that changes in inhibitory events are not responsible for LTP in the CA1 area of the hippocampus. However, when inhibition is blocked in the presence

of GABA antagonists, the induction of LTP is facilitated (Wigstrom and Gustafsson, 1983). If the LTP-inducing effect of IBMX is partially due to a decrease of GABA-mediated responses, then the drug should reduce paired-pulse inhibition of hippocampal pyramidal cells.

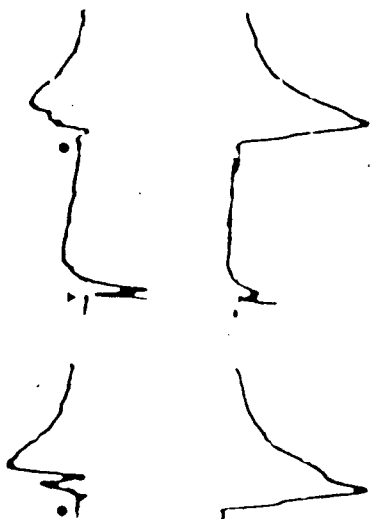
The paired-pulse paradigm consists of delivering two stimuli, usually separated by 20-40 ms, to hippocampal fiber systems that will activate the pyramidal neurons. A conditioning ortho- or antidromic stimulation of CA1 pyramidal cells results in subsequent activation of basket cells which in turn have inhibitory actions on pyramidal cells. If inhibition is present, the next orthodromic test stimulation will evoke a population spike of smaller magnitude (Fig. 4.4.A.). The duration of the inhibition following the conditioning pulse is dependent upon the stimulation paradigm, but it has been shown to last in excess of 40 ms (Haas and Rose, 1982).

Perfusion of IBMX did not alter synaptic events responsible for paired-pulse inhibition of CA1 pyramidal neurons (n=5). In spite of the characteristic potentiation of the population spike responses in the presence of IBMX, the test (T) stimulus delivered 20 ms following antidromic conditioning (C) invariably evoked an inhibited population spike (Fig. 4.4.B.). When the intensity of orthodromic stimulation was reduced to evoke a response comparable to pre-drug values the potency of inhibition was found to be unaltered (Fig. 4.4.C.).

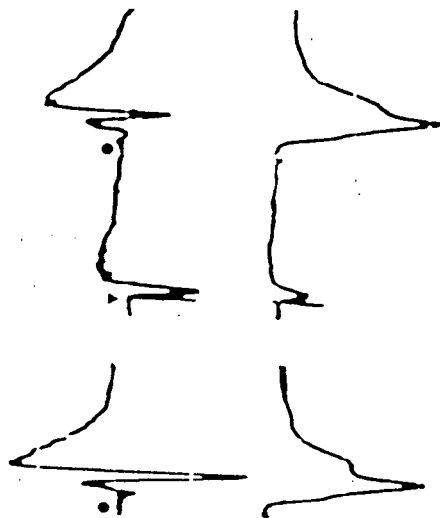
Figure 4.4. Effect of IBMX on paired-pulse inhibition recorded extracellularly. The traces were photographed from a storage oscilloscope and represent population spikes (top) and EPSPs (bottom) following stimulation of the Schaffer collateral-commissural afferent fibers (●) or antidromic activation (▼) of the pyramidal cells. A. Control population spike and EPSP (right) and their paired-pulse inhibition when an antidromic conditioning stimulus (C) precedes the orthodromic activation (T) of pyramidal cells (C-T interval = 20 ms). B. Same as in A. but following IBMX-induced LTP. Note the large potentiation of the orthodromic population spike (~400%) with no significant change in the antidromic response. Inhibition was still present as indicated by the smaller amplitude of the test response. Stimulus intensities for ortho- and antidromic activation were the same as in A. C. To test whether the potency of paired-pulse inhibition was the same as under control conditions, the orthodromic stimulation intensity was reduced (about 50%) while keeping the antidromic stimulation constant. No significant change in the magnitude of the inhibition can be detected following IBMX-induced LTP.



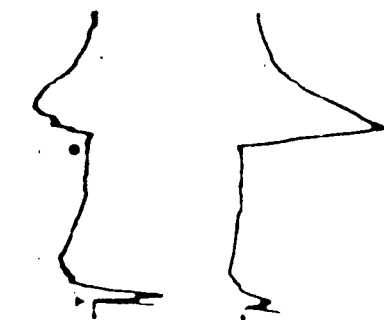
A.



B.



C.



2mV  
10ms

#### 4.3.3. Effect of IBMX on input/output (I/O) curves

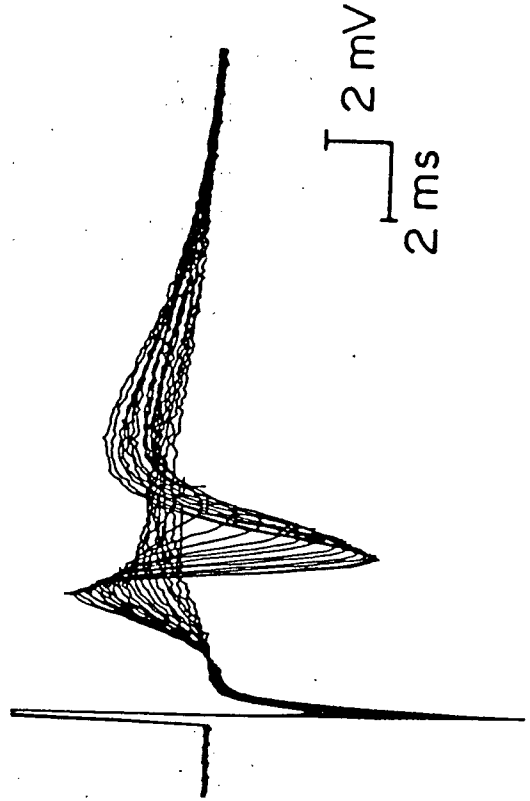
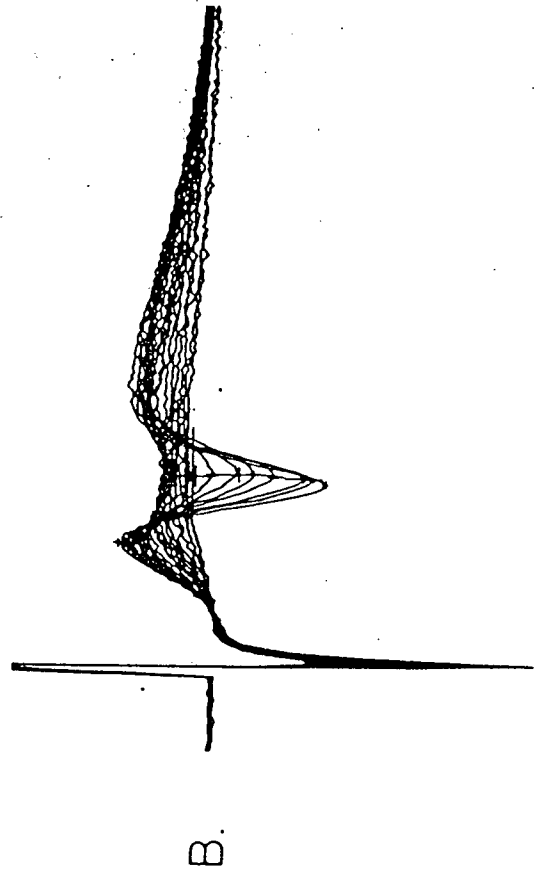
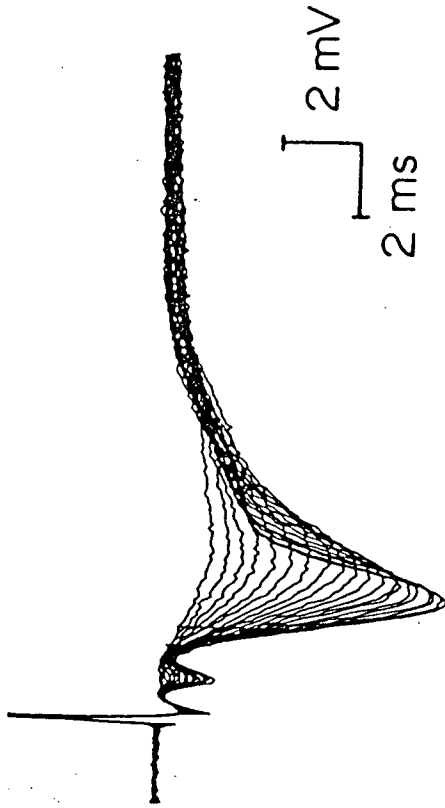
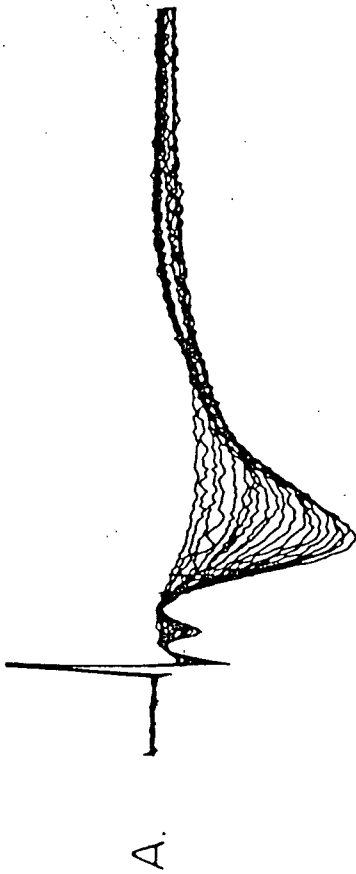
LTP is characterized by specific alterations in the relationship of input/output curves (Schwartzkroin and Wester, 1975; Alger and Teyler, 1976; Andersen et al., 1977; Andersen et al., 1980). By monitoring individual parameters such as stimulus intensity, fiber volley amplitude, rate of rise of the EPSP or the amplitude and latency of EPSP and population spike it is possible to treat each variable as 'independent' and to express the changes in their relationships accordingly. To use the short notations somewhat similar to those of Andersen et al. (1980) the curves will be referred to as SI-S, SI-V, V-E, V-D, D-E and D-S relations, where SI = stimulus intensity, S = population spike amplitude, V = fiber volley amplitude, E = EPSP amplitude and D = rate of rise of the EPSP ( $dV/dt$ ). As pointed out by Andersen et al. (1980) some of these relations may be indicative of pre-synaptic changes (e.g., SI-V, V-E and V-D), while others may reflect postsynaptic events (e.g., D-E and D-S) that occur during LTP.

The I/O curves shown on Figs. 4.6.-4.8. represent plots as measured from the potentials shown in Fig. 4.5. Input/output relationships using 15-20 different stimulation intensities were examined in 15 slices. Twenty averaged and superimposed EPSPs (Fig. 4.5.A.) and population spikes (Fig. 4.5.B.) are displayed, as part of a typical I/O experiment. The net effect of IBMX was to reduce the threshold for evoking a population spike.

Figure 4.5. Potentials recorded in the dendritic and somatic region of area CA1 during input/output curves. Each trace is an average of four sweeps superimposed by the computer and represents the EPSPs (A.) and populations spikes (B.) evoked following 20 successive stimulations of the Schaffer collateral-commissural fibers (from 2.0 to 5.8 V in increments of 0.2 V). Control responses are shown on the left panel while the responses on the right have been obtained after 40 min of washout following a 10 min IBMX perfusion of 100  $\mu$ M concentration. Note the increase in the amplitude of the evoked responses at every stimulation intensity and the lack of change in the fiber volley potential which precedes the EPSP.

Pre - IBMX 100  $\mu$ M

40 min Wash



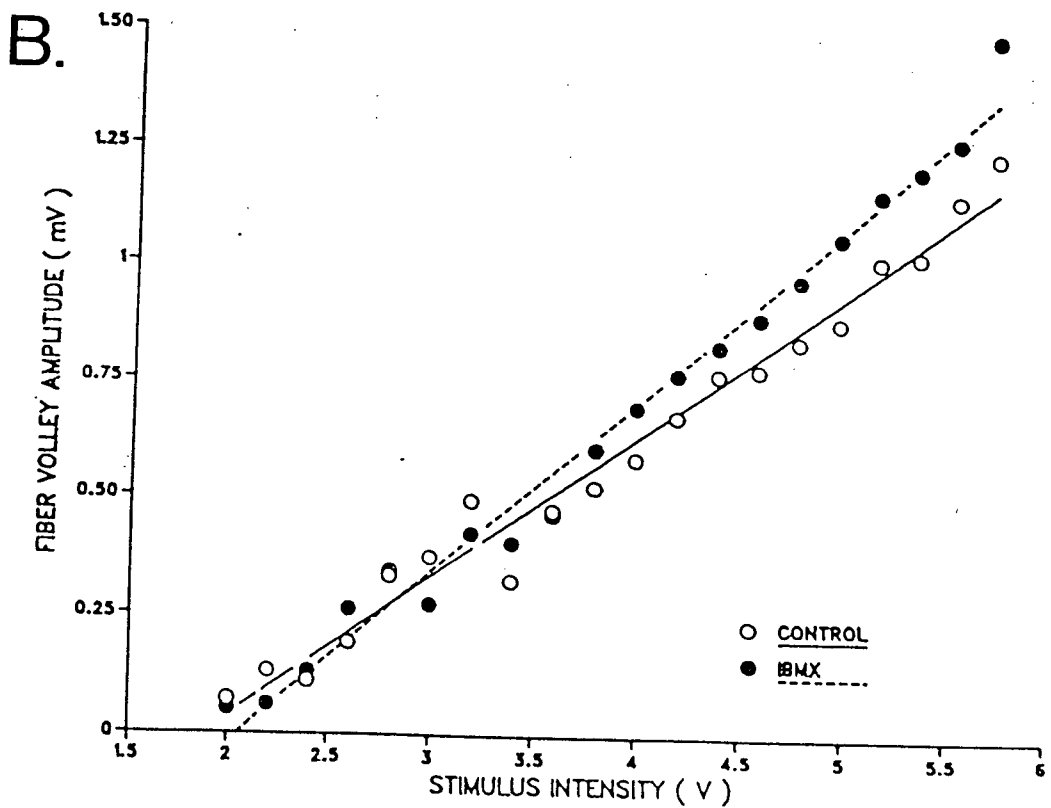
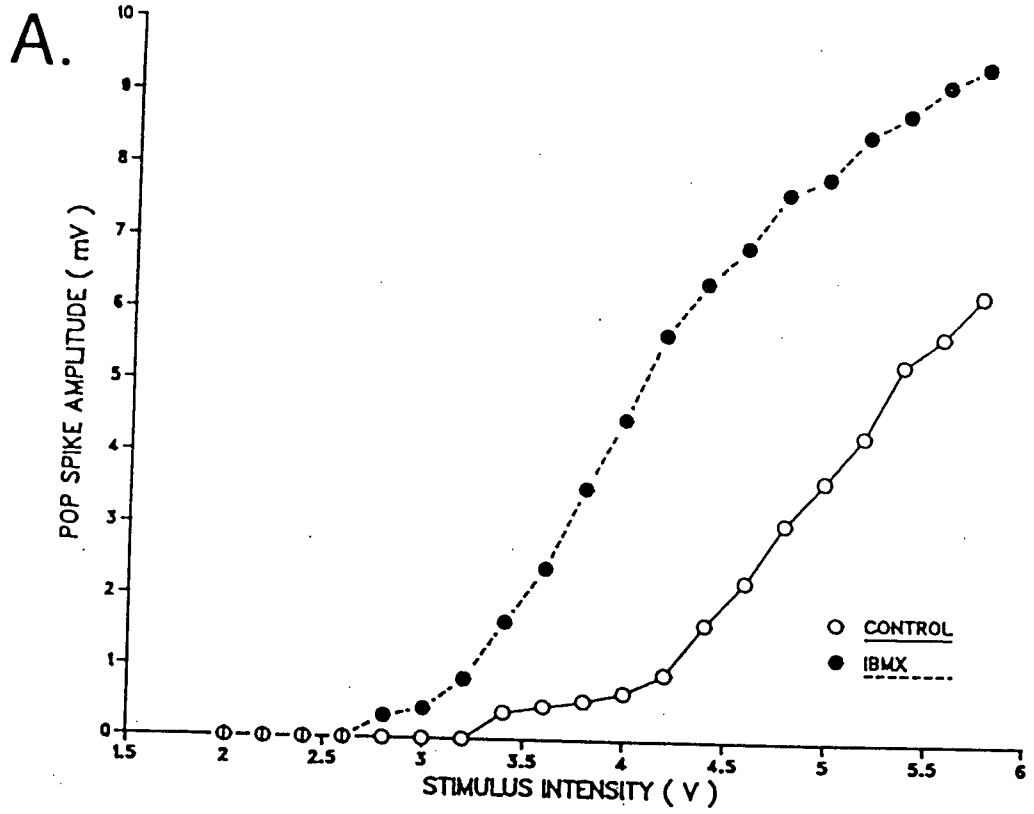
Therefore, at every stimulus intensity, larger population spikes were recorded in the pyramidal cell layer after exposure to the drug. The SI-S relationship shown in Fig. 4.6.A. indicates that during IBMX-induced LTP, maximum potentiation (800-900%) occurs at intermediate stimulus intensities of about 1.5x threshold for evoking a population spike. The change in threshold after IBMX-induced LTP represents a shift to the left of the SI-S curve, similar to that obtained by Andersen et al. (1980) following LTP produced by tetanic stimulation.

A given stimulus intensity (SI) evoked comparable fiber volley (V) potentials both before and after perfusion of IBMX (Fig. 4.6.B.) indicated by the fact that no significant shift was observed in the SI-V relationship. Since the fiber volley represents impulse propagation through presynaptic fibers (Andersen et al., 1978), there was probably no change in the number of presynaptic fibers activated by a given intensity of stimulation following perfusion of IBMX. This finding, observed in all preparations examined, is analogous to the SI-V relationship following tetanus-induced LTP (Andersen et al., 1980), which also does not seem to change presynaptic excitability.

The I/O curves most sensitive to synaptic changes are the V-E and V-D relationships. The amplitude (E) and the rate of rise or  $dV/dt$  (D) of the extracellular EPSP represent current flow during synaptic activation of pyramidal neurons. When these parameters are plotted against the amplitude of the fiber volley (V), they usually show a linear relationship. As shown on Fig.

Figure 4.6. I/O curves having stimulus intensity (SI) on the abscissa. A. Plot of stimulus intensity (SI) vs. population spike amplitude (S), called the 'SI-S' curve. Note the change in threshold stimulus intensity for evoking a population spike following perfusion of IBMX. The maximal potentiation was observed between stimulation intensities of 4-4.5 V, which were approximately 1.5x the original threshold value. B. Plot of stimulus intensity (SI) vs. the amplitude of the fiber volley response (V), i.e., the 'SI-V' curve. Both regression lines were fitted by computer and no significant changes were detected in either correlation coefficient or slope of the relationship after LTP induced by IBMX.

In the present and the following I/O curves 'IBMX' refers to potentials recorded after 40 min of washout, i.e., following LTP induced by a 10 min perfusion of 100  $\mu$ M IBMX.



4.7.A and B.), the linearity was not changed during LTP induced by IBMX but the slopes of the regression lines were significantly enhanced (40-60%). This increase in slope occurred concomitant with a shift of the lines to the left, i.e., a comparable fiber volley response (V) invariably evoked a larger amplitude EPSP (E) and a greater  $dV/dt$  (D) after IBMX-induced LTP. The change in slope and the shift to the left of the V-E and V-D relationships, found in all slices examined (15/15), indicates that a similar presynaptic activation (V) results in a significantly larger synaptic drive and efficacy (characterized by E and D) following perfusion of IBMX.

As shown by the overlapping data points of Fig. 4.8.A. and B. taken before and after IBMX perfusion, no significant differences were found between the curves representing D-E and D-S relationships. Following IBMX-induced LTP both D-E and D-S curves showed some overlap with their control counterparts appeared as extensions of the control curves. This however was only due to the greater  $dV/dt$  (D) of the EPSPs evoked after LTP. While the D-E curves did not appear shifted in every preparation examined, the D-S curves exhibited alterations in 6/15 slices. In these remaining slices the D-S curves were shifted to the right (4/15) or to the left (2/15), but these shifts were found not to be statistically significant. The lack of significant changes in the D-E and D-S curves indicate that similar synaptic activation (reflected by D) evokes a comparable amplitude EPSP (E) or population spike (S) even after LTP has been induced by IBMX.



Figure 4.7. I/O curves having fiber volley amplitude (V) on the abscissa. A. The V-E relationship, or the plot of fiber volley amplitude (V) vs. the the amplitude of the extracellularly recorded EPSP (E). B. Plot of the fiber volley amplitude (V) vs. the rate of rise of the EPSP ( $dV/dt$  or D), i.e., the V-D relationship. In both graphs the regression lines were fitted by computer. Note the shift to the left of both lines after IBMX-induced LTP as well as the significant difference in slopes ( $p < 0.1$  for A. and  $p < 0.005$  for B. as measured by two tailed t-test).

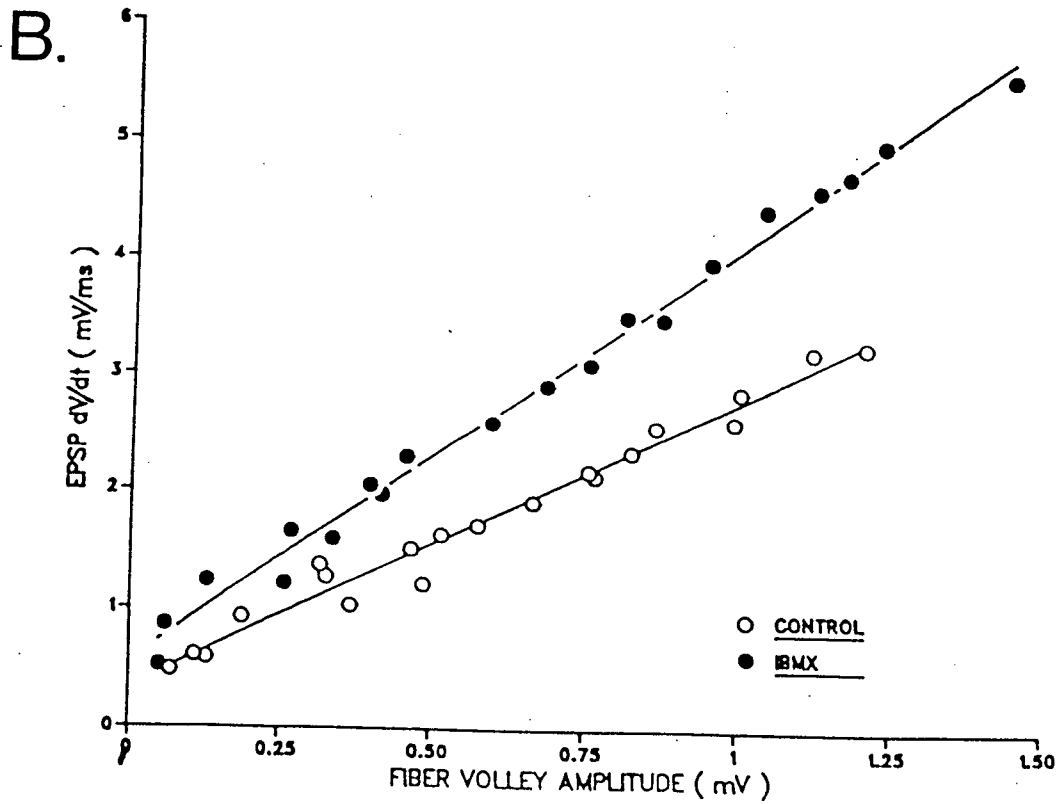
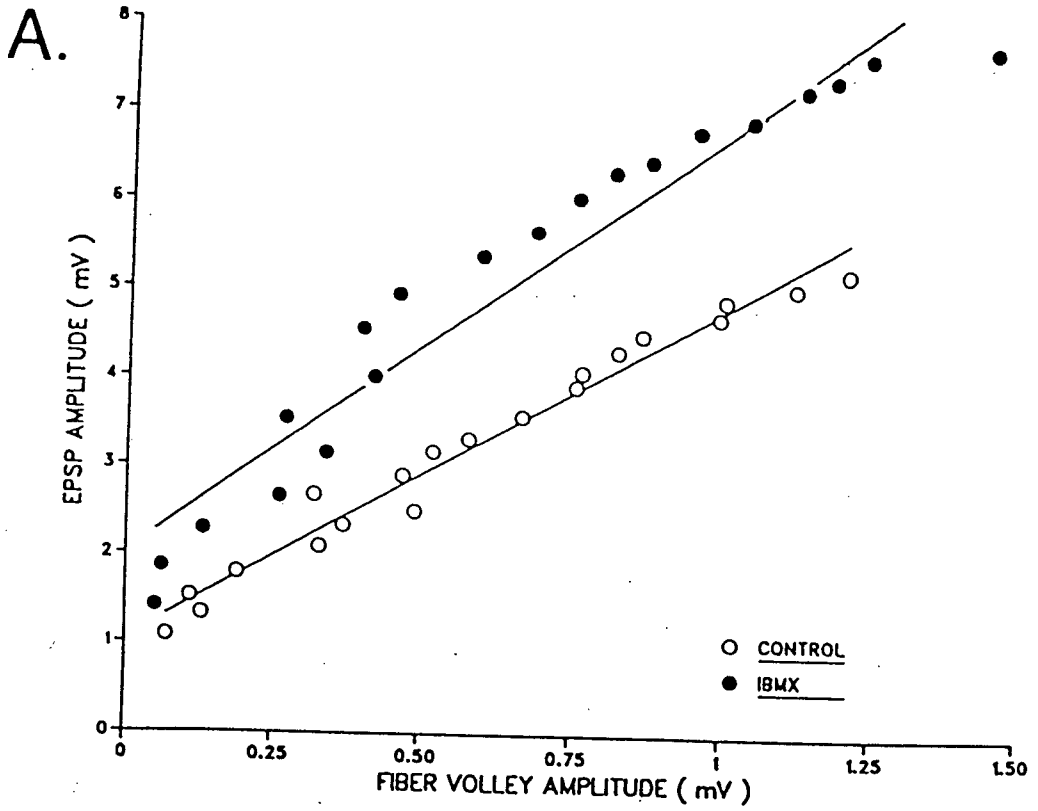
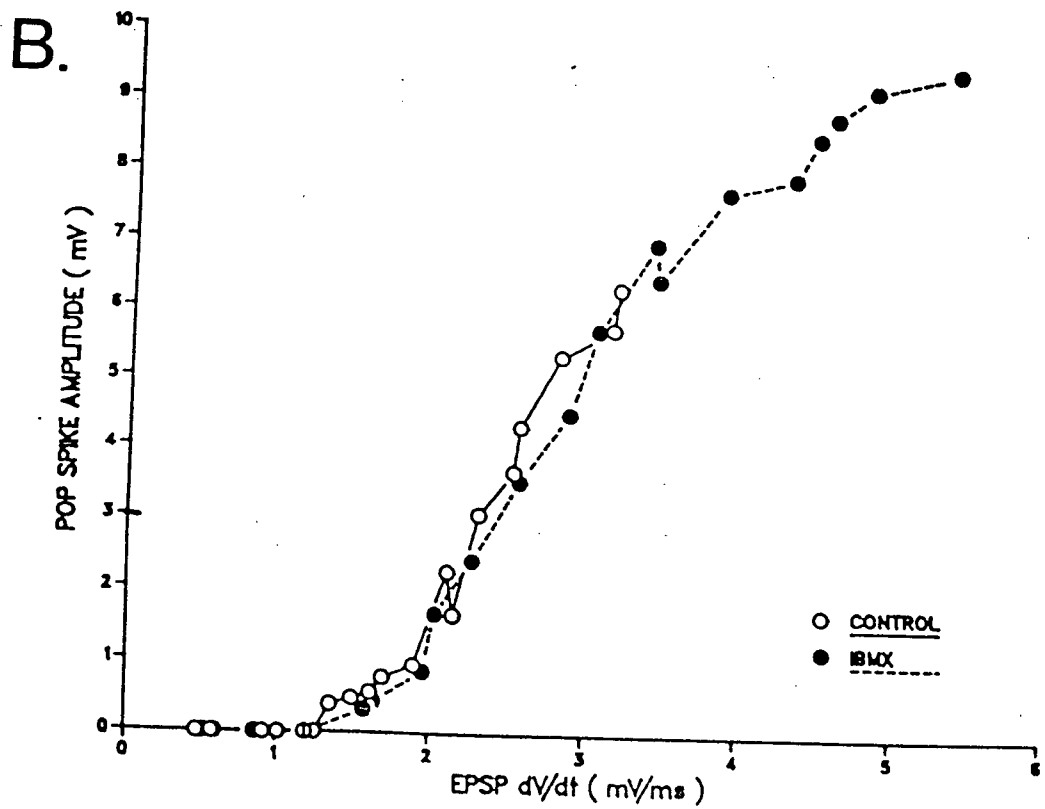
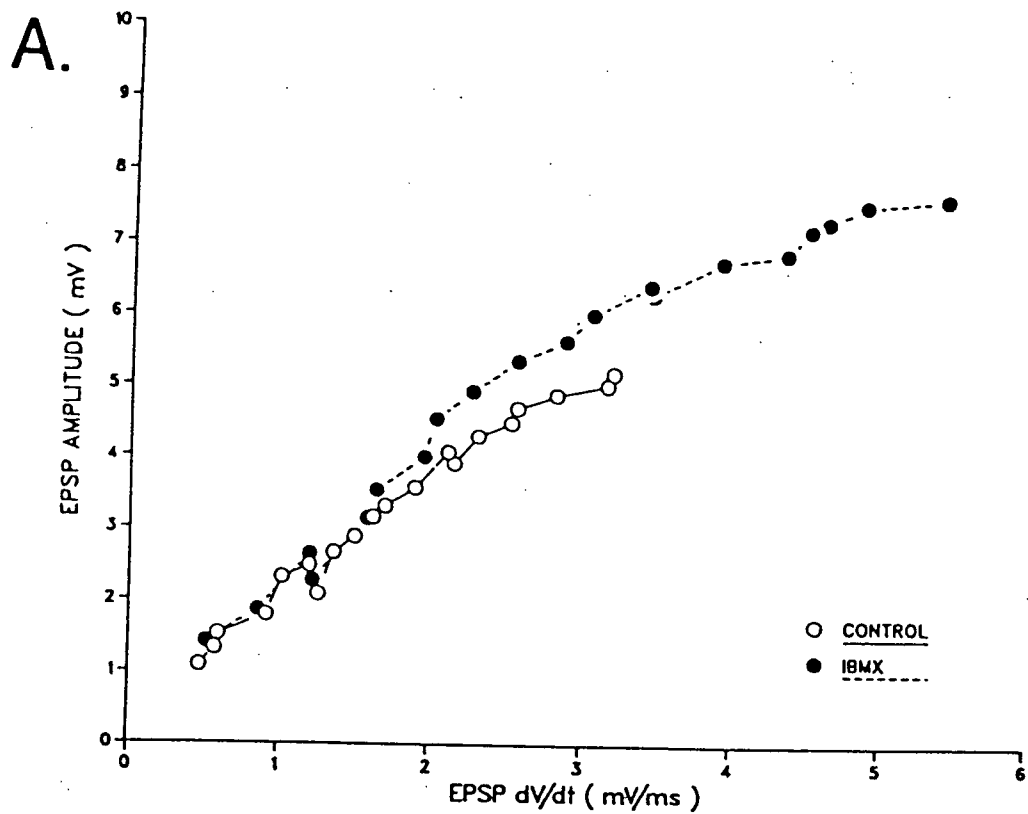


Figure 4.8. I/O curves with the rate of rise of the EPSP (D) on the abscissa. A. Plot of the rate of rise of the EPSP (D) vs. its own amplitude (E), or the D-E curve. B. The D-S relationship, i.e., the EPSP's  $dV/dt$  vs. the amplitude of the population spike before and after IBMX-induced LTP. In either plot no significant differences were detected in the region of overlap of the 'control' and 'IBMX' curves. This is to show that after LTP induced by IBMX a comparable size  $dV/dt$  evokes a similar EPSP or population spike response. The reason for the apparent extension of the 'IBMX' curves beyond the 'controls' is the significant enhancement of the EPSP's rate of rise following IBMX-induced LTP.



#### 4.3.4. Calcium and IBMX-induced LTP

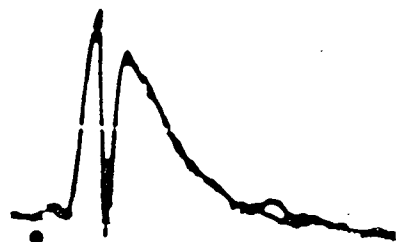
The presence of extracellular  $\text{Ca}^{2+}$  is required for tetanus-induced LTP in the hippocampal slice preparation (Dunwiddie et al., 1978; Dunwiddie and Lynch, 1979) and slices retain significantly larger amounts of calcium when challenged with a high frequency stimulus (Baimbridge and Miller, 1981). In addition, Turner et al. (1982) have shown that the increase in total intracellular  $\text{Ca}^{2+}$  resulting from brief exposure to a higher than normal extracellular calcium concentration may by itself cause LTP.

To examine the contribution of calcium entry to the LTP induced by IBMX, the effect of the  $\text{Ca}^{2+}$ -channel blocker  $\text{Co}^{2+}$  was tested. Within 30-35 min, perfusion of 3 mM  $\text{CoCl}_2$  in 6 hippocampal slices gradually decreased the amplitude of the CA1 evoked responses, indicating that synaptic transmission was impaired (Fig. 4.9.A. and B.). When 100  $\mu\text{M}$  IBMX was perfused for 10 min in the presence of  $\text{Co}^{2+}$ , the responses became potentiated to levels 200-300% larger than pre-cobalt values. Upon return to normal CSF both the population spike (6/6) and EPSP (3/6) remained potentiated, i.e., LTP had occurred (Fig. 4.9.C.) indicating that  $\text{Ca}^{2+}$  entry per se was not a prerequisite of IBMX-induced LTP.

In order to determine whether synaptic events were required to produce the IBMX-induced LTP, synaptic potentials were reduced or abolished by perfusing ' $\text{Ca}^{2+}$ -free' medium for a variable time.

Figure 4.9. Effect of  $\text{Co}^{2+}$  on IBMX-induced LTP. The potentials are photographs of oscilloscope traces following stimulation of the Schaffer collateral/commissural fiber system and represent population spikes recorded at the level of CA1 pyramidal cells (top panel) or EPSPs recorded near the apical dendrites (bottom panel). A. Control evoked potentials. B. Reduction of the evoked responses following a 30 min perfusion of 3 mM  $\text{Co}^{2+}$ -containing artificial CSF. C. In spite of the presence of the calcium entry blocking agent  $\text{Co}^{2+}$ , IBMX caused a potentiation of the evoked responses, particularly evident for the population spikes, since the EPSP response contains an interfering reflection of the large population spike. These potentials were recorded at 20 min of washout following a 10 min IBMX perfusion.

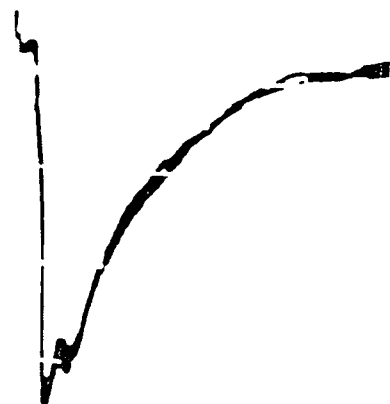
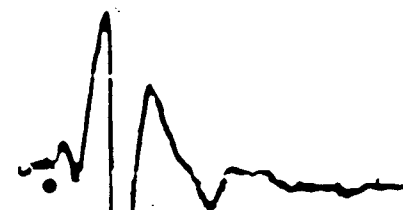
A.



B.



C.



1mV  
10ms

(Note: omission of  $\text{CaCl}_2$  from the artificial CSF does not ensure total loss of the cation since the glassware used for preparation of solutions is a considerable source for  $\text{Ca}^{2+}$ . It is therefore reasonable to assume that the ' $\text{Ca}^{2+}$ -free' medium contains at least 10-50  $\mu\text{M}$   $\text{Ca}^{2+}$ , as measured by Yaari et al., 1983). The concentration of  $\text{Mg}^{2+}$  was raised in this medium (from 1.5 mM to 9 mM) to reduce synaptic transmission and to avoid spontaneous bursting (Richards and Sercombe, 1970; Haas and Jefferys, 1982).

In the presence of the above perfusate, synaptic responses were greatly diminished and decreased to non-detectable levels within 35-45 min ( $n=6$ ). When IBMX was perfused prior to the complete loss of synaptic transmission at a point when a reasonable size ( $>1$  mV) EPSP (but no population spike) could still be evoked, the drug caused the characteristic potentiation (Fig. 4.10.A. and B.). However, the potentiation lasted only as long as IBMX was present in the medium. Following return to normal perfusate the responses returned to control values showing no LTP. When sufficient time ( $\sim 60$  min) was allowed for the preparation to reach the state of zero synaptic transmission in the absence of extracellular  $\text{Ca}^{2+}$  (Fig. 4.11.A. and B.), IBMX-induced potentiation was not observed.

The antidromic population spike and the fiber volley were only slightly affected during the 30-60 min of '0 mM  $\text{Ca}^{2+}$ ' perfusion (Figs. 4.10.C. and 4.11.C.). It was only during the perfusion of IBMX (Figs. 4.10.C. and 4.11.C.) under these conditions that the amplitude of the antidromic population spike reversibly decreased. This finding is somewhat surprising since



Figure 4.10. Effect of a short duration (<30 min) perfusion of 0 mM  $\text{Ca}^{2+}$ /9 mM  $\text{Mg}^{2+}$  solution on the action of IBMX in the CA1 region of the hippocampus. When potentials were still evokable (after about an 18 min perfusion of the low  $\text{Ca}^{2+}$  medium) 100  $\mu\text{M}$  IBMX caused only a reversible potentiation of the EPSP (A.) and population spike (B.) responses. The amplitude of the fiber volley (C.  $\times$ ) declined slightly during the perfusion of the '0 mM  $\text{Ca}^{2+}$  medium but returned to control levels during IBMX perfusion. The changes in the amplitude of the antidromically evoked population spike (C.  $\Delta$ ) were not significant in the lack of extracellular  $\text{Ca}^{2+}$ . However, perfusion of IBMX during the low  $\text{Ca}^{2+}$  medium produced a transient reduction of the antidromic spike. The bars above panel A. indicate the respective perfusion durations and refer to all of the panels.

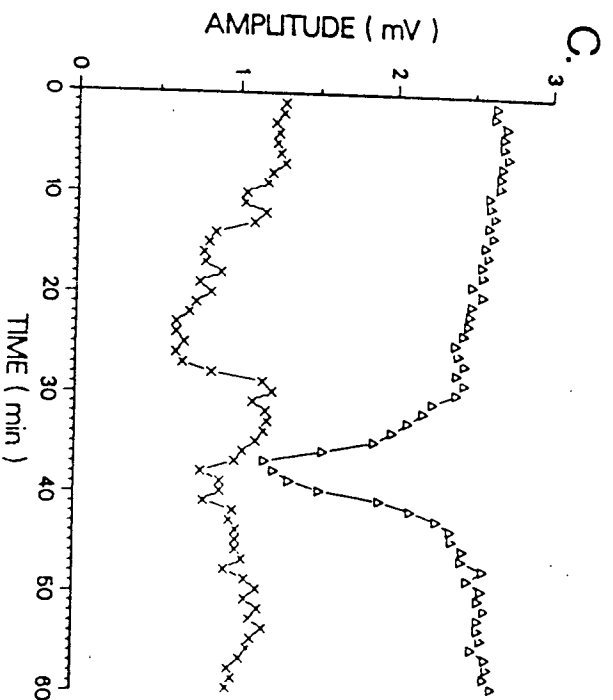
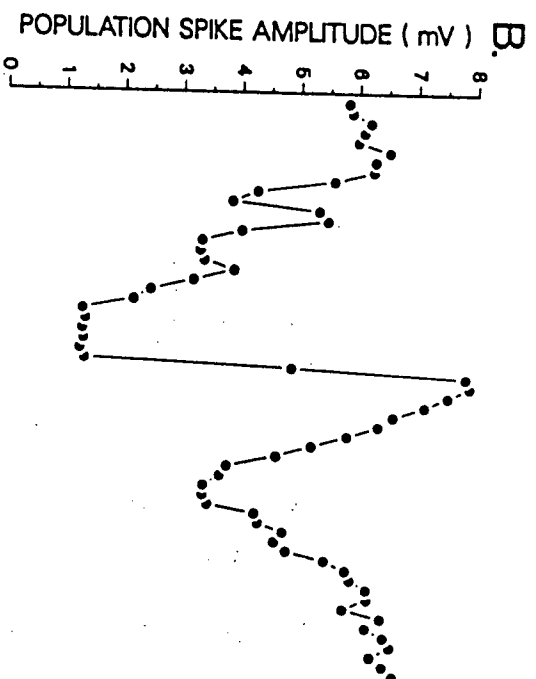
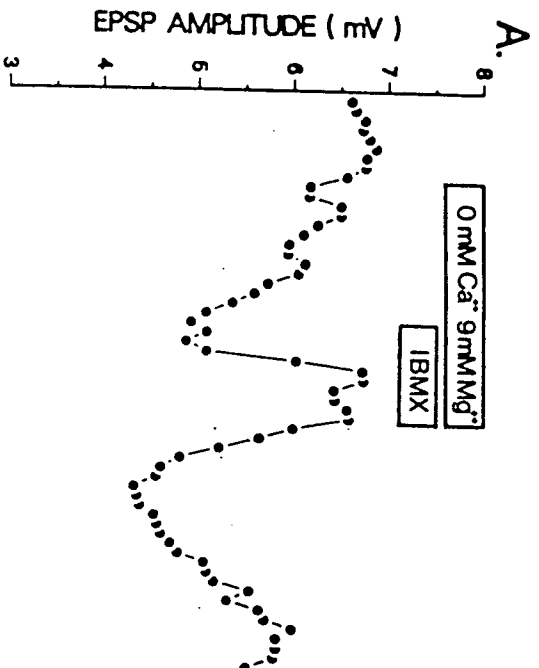
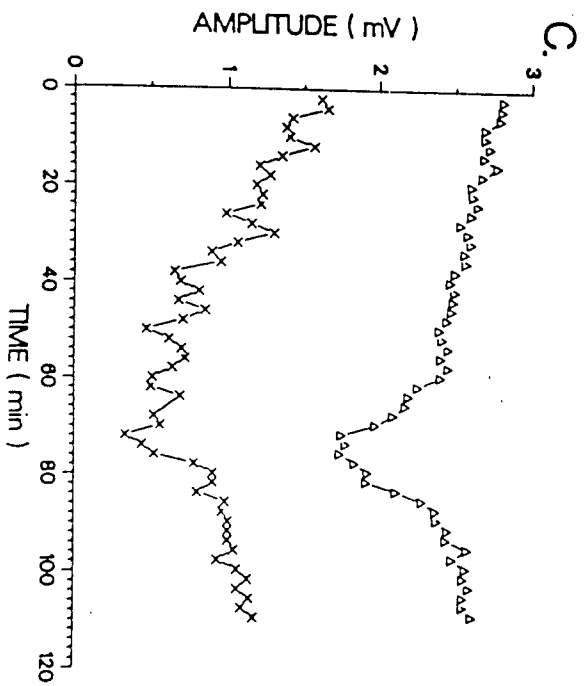
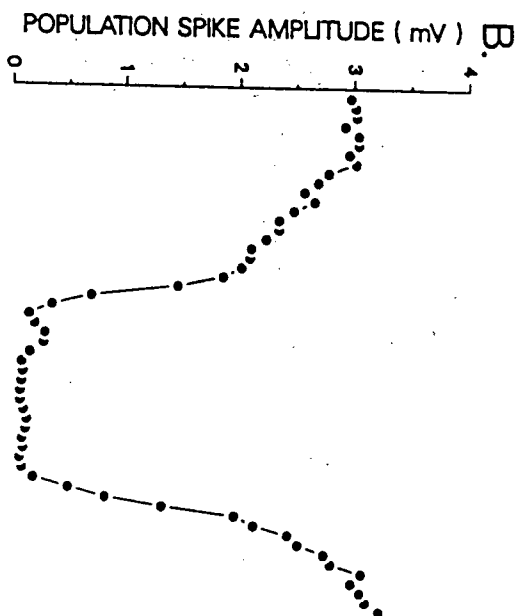
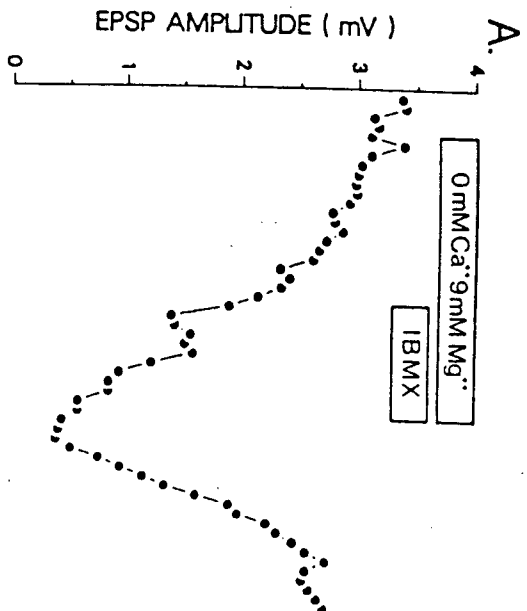


Figure 4.11. Effect of a long duration perfusion (60 min) of 0 mM  $\text{Ca}^{2+}$ /9 mM  $\text{Mg}^{2+}$  solution on the action of IBMX in the CA1 region of the hippocampus. When the duration of the perfusion of low  $\text{Ca}^{2+}$  medium was prolonged, within approximately 40 min a significant impairment of synaptic transmission was observed as indicated by the very small amplitude EPSP (A.) and no detectable population spike (B.) . Perfusion of IBMX under these circumstances produced only non-significant changes in the amplitude of the evoked responses. No long-lasting change was detected, since the evoked potentials returned to control values following perfusion of normal artificial CSF. The fiber volley response (C. X) declined steadily during perfusion of the low  $\text{Ca}^{2+}$  and was little affected by IBMX. In contrast, the antidromically evoked population spike (C.  $\Delta$ ) exhibited little change in the absence of extracellular  $\text{Ca}^{2+}$ , but perfusion of 100  $\mu\text{M}$  IBMX caused its transient decline. The bars above panel A. indicate the respective perfusion durations and refer to all of the panels.



IBMX did not influence the antidromic responses in control conditions.

Input/output curves ( $n=4$ ) were also examined during perfusion of '0 mM  $\text{Ca}^{2+}$ '. Again, if the responses were allowed to reach maximal depression in the ' $\text{Ca}^{2+}$ -free' medium, IBMX did not result in potentiation.

#### 4.3.5. Effect of IBMX on bursting induced by low calcium

The ratio of  $\text{Ca}^{2+}/\text{Mg}^{2+}$  in the extracellular fluid is an effective regulator of neuronal excitability (Frankenhaeuser and Hodgkin, 1957; Richards and Sercombe, 1970). The hippocampus is particularly prone to periodic bursting in the absence of synaptic transmission induced by lower than normal  $\text{Ca}^{2+}$  concentrations (Jefferys and Haas, 1982; Taylor and Dudek, 1982; Yaari et al., 1983). The postsynaptic effect of drugs may be examined in this preparation since no synaptic activity is present (Haas et al., 1984).

Bursting of hippocampal CA1 neurons was induced in 9 slices by perfusion of CSF containing '0 mM'  $\text{Ca}^{2+}$  and 1.5 mM (normal)  $\text{Mg}^{2+}$ . Following exposure to this medium regular bursts consisting of negative DC shifts and superimposed spiking were recorded in the CA1 pyramidal cell layer. The bursts, which occurred with a characteristic frequency of about 0.05 Hz, were not changed by addition of 100  $\mu\text{M}$  IBMX to the perfusate in 5/9 slices examined. In the remaining cases IBMX tended to accelerate the frequency of the bursts while having no marked effects on

their magnitude or duration. Following return to normal  $\text{Ca}^{2+}$  the bursts were abolished and the evoked responses returned to normal. No long-lasting effect of IBMX was recorded under these conditions.

#### 4.3.6. Effect of IBMX on passive membrane characteristics of hippocampal pyramidal cells

Perfusion of 100  $\mu\text{M}$  IBMX did not cause significant changes in the resting membrane potential (RMP) of CA1 pyramidal neurons, which is similar to the finding of Segal (1981). A slight (2-3 mV) depolarization was sometimes noted, but this effect was not consistent. The average ( $\pm$  S.D.) RMP of 41 CA1 pyramidal cells was  $-61.3 \pm 2.9$  mV and their input resistances ( $R_{\text{in}}$ ) ranged from 25 to 37 Mohms (note however, that only cells with input resistances higher than 25 Mohms were included in the study). The membrane time constant ( $T_{\text{c}}$ ) of pyramidal neurons was found to be in the range of 11-14.7 ms. The two passive membrane parameters ( $R_{\text{in}}$  and  $T_{\text{c}}$ ) were unaltered by IBMX (Fig. 4.12.A. and B.) and therefore changes in their values are unlikely to be responsible for the long-lasting effects of the drug.

In four cells, spontaneously occurring fast prepotentials (FPPs) of 2-5 mV amplitude were recorded but their frequency or magnitude was not affected by IBMX treatment.

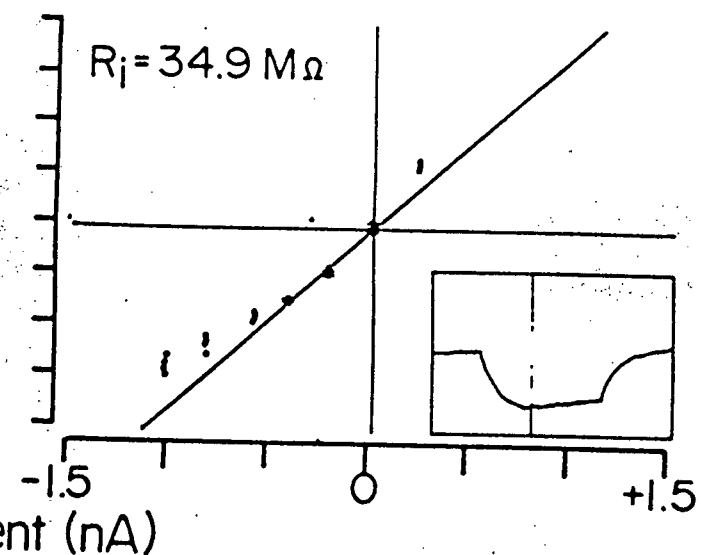
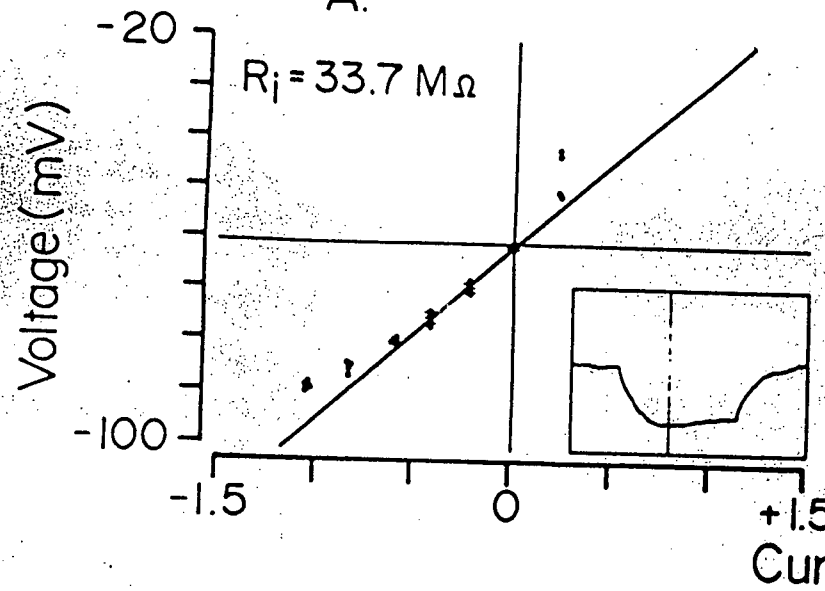
Figure 4.12. Effect of 100  $\mu\text{M}$  IBMX on the passive membrane characteristics of CA1 pyramidal neurons. Panels A. and B. represent current-voltage plots of a typical pyramidal cell before and during IBMX perfusion respectively. The membrane input resistances are indicated as derived through the fitting of a regression line to the linear part of the I-V relationship. Insets show the change in membrane voltage upon injection of one of the 7 steps of current pulses. The vertical line of the inset denotes the membrane potential at which measurements were taken. Panels C. and D. represent the calculation of the membrane time constant ( $\tau$ ) for the same cell through the fitting of a regression line to the natural logarithm of the voltage changes ( $\Delta V$ ). The slope of the relationship taken during the linear portion (indicated by vertical lines) reflects the time constant of the membrane and its value is shown both before (C.) and during (D.) a 100  $\mu\text{M}$  IBMX perfusion. No significant effects of IBMX were noted on either RMP, input resistance or time constant of CA1 pyramidal neurons.

Control

IBMX (100  $\mu$ M)

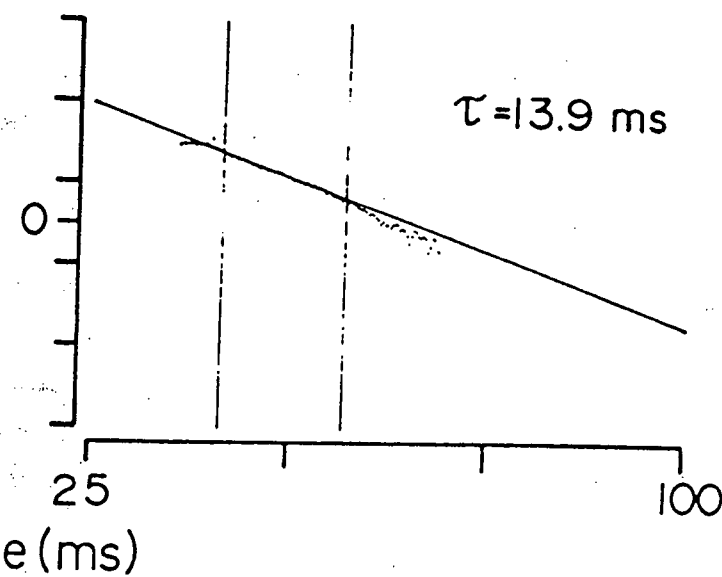
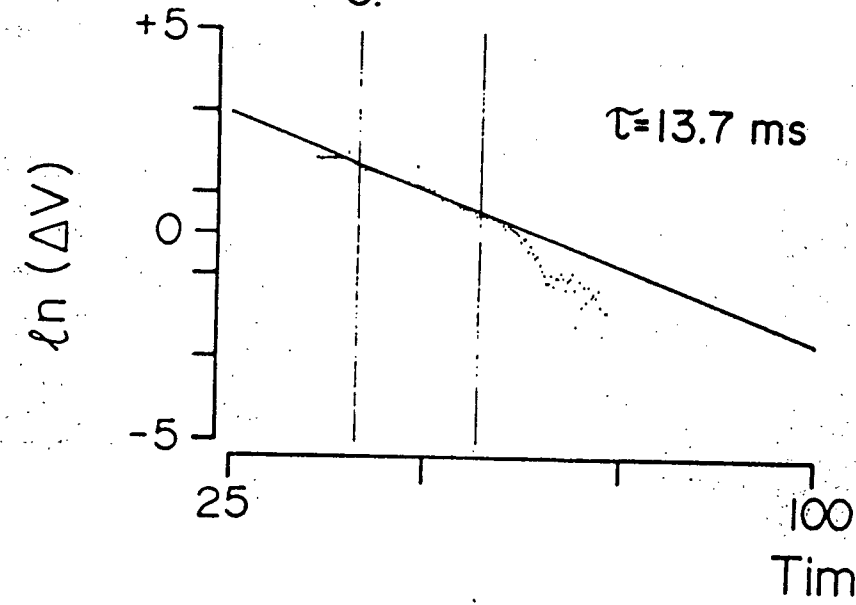
A.

B.



C.

D.

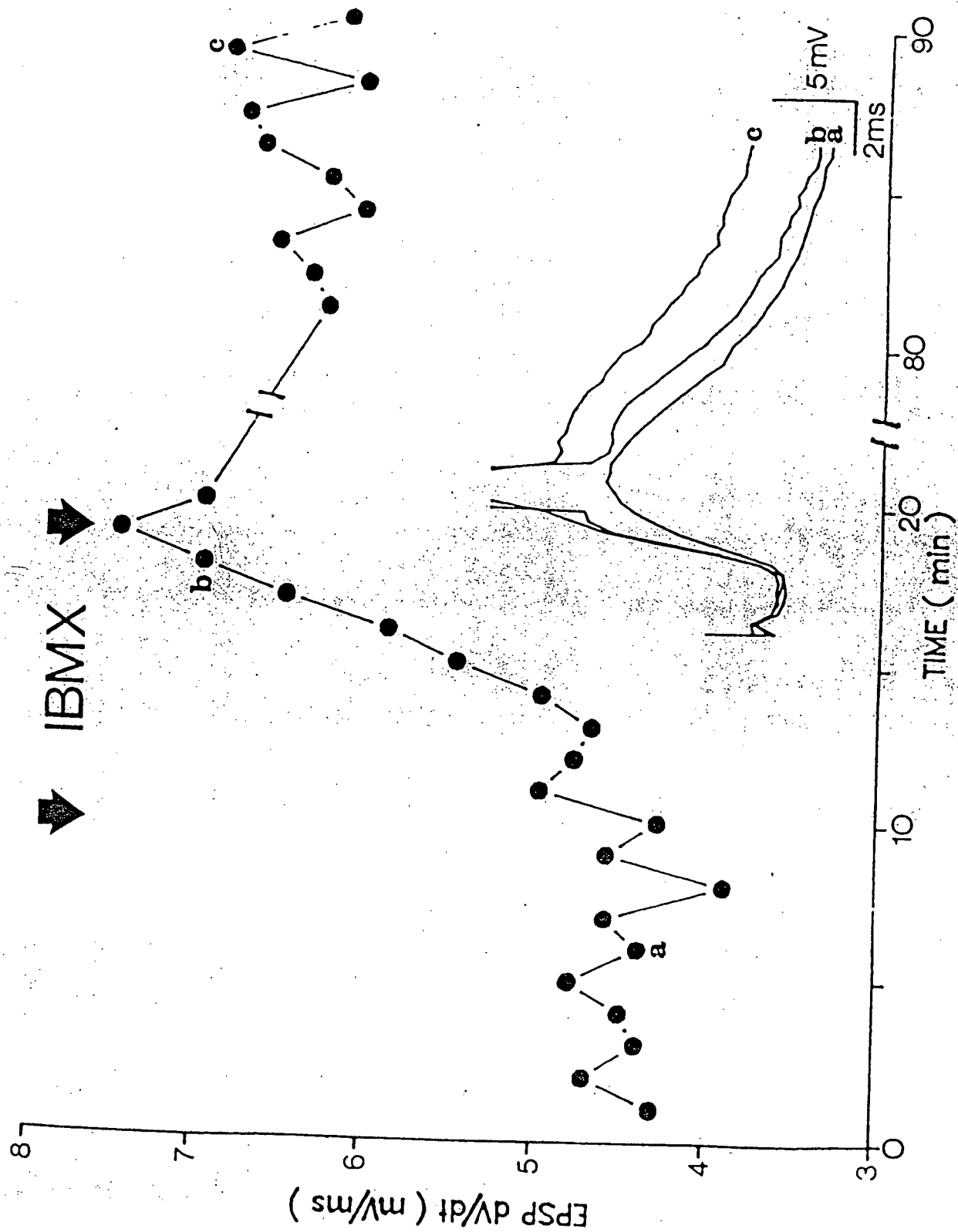




#### 4.3.7. Long-term effect of IBMX on the rate of rise of intracellularly recorded EPSPs

The first order voltage differential ( $dV/dt$ ) of the intracellularly recorded EPSP following stimulation of the stratum radiatum represents current flow across the synaptic membrane of CA1 pyramidal cells if membrane capacitance remains constant. At just below threshold stimulation its value typically ranges between 3 and 6  $mV \cdot ms^{-1}$ . In the presence of IBMX (Fig. 4.13.) the rate of rise of the EPSP gradually increased and failed to return to control values even after 1 hour of washout period. The rapid rate of rise and the enhanced amplitude of the EPSP during and following IBMX resulted in spike-activation of pyramidal neurons as shown in insets b. and c. of Fig. 4.13. This long-lasting effect of IBMX was observed in all 14 cells where stable recordings could be maintained in excess of 45 min of post-drug washout. These findings also agree with the potentiation of extracellularly recorded population spikes since neurons brought to firing threshold by the action of IBMX will add to the size of the negative field potential. Therefore, analogous to tetanic stimulation (Andersen et al., 1980; Lynch et al., 1983), it is reasonable to suggest that IBMX produced LTP at the single cell level in the hippocampal CA1 region.

Figure 4.13. Effect of IBMX on the rate of rise ( $dV/dt$ ) of intracellularly recorded EPSPs. Perfusion of 100  $\mu$ M IBMX (between arrows) caused a long-lasting enhancement of the rate of rise of the intracellularly recorded EPSP in a representative CA1 pyramidal neuron. The inset shows the synaptic potentials recorded following stratum radiatum stimulation corresponding to the times marked by small letters. Note that an initially subthreshold EPSP (a) became suprathreshold during (b) and following (c) perfusion of IBMX.

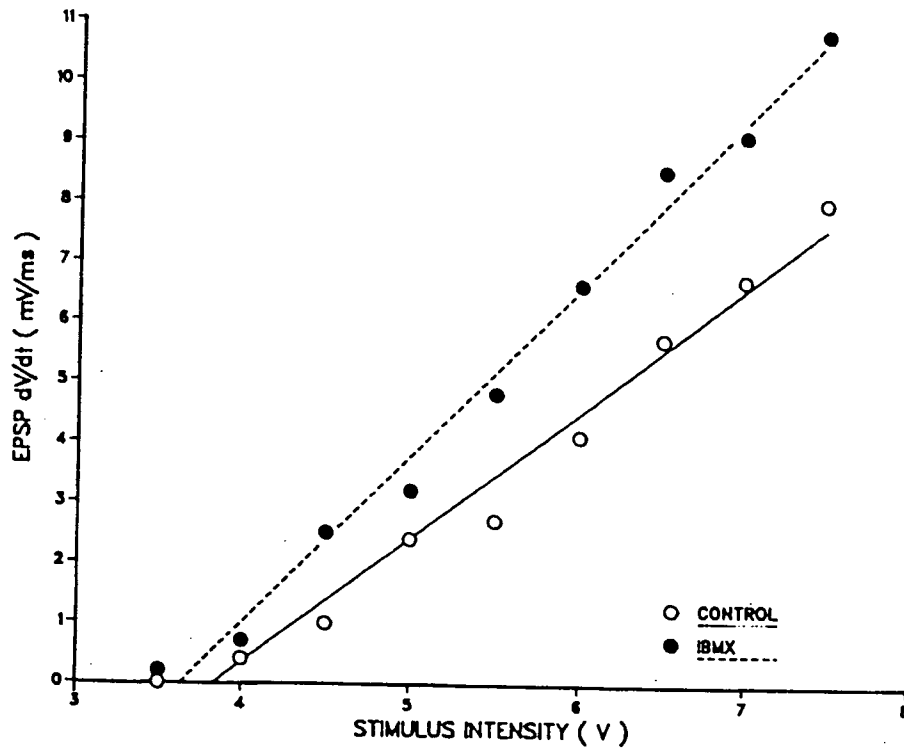


#### 4.3.8. Intracellular input/output relationships following IBMX perfusion

Analogous to extracellular potentials, single cell LTP should alter the input/output (I/O) relationship of individual pyramidal cells. To test this hypothesis varying intensities of stimulation were delivered to the stratum radiatum during intracellular injection of a 70 ms hyperpolarizing current pulse. This allowed for simultaneous measurement of membrane properties, such as input resistance and time constant, and characteristics of the EPSP. In addition, several stimulus intensities could be applied before the cell reached spike threshold (Fig. 4.14.B.). The I/O curves were obtained by plotting the stimulus intensity vs. the rate of rise ( $dV/dt$ ) of the EPSP (Fig. 4.14.A.) before and at least 40 min after perfusion of IBMX. In all cells examined ( $n=5$ ) the slope of the I/O relationship was significantly enhanced following the drug but its linearity was unaltered. The rate of rise and the amplitude of the EPSP were potentiated at every stimulus intensity. In the absence of changes in time-constant and input resistance of the cells, this finding indicates that a larger synaptic current flow has been induced by stimuli of equal magnitude. In addition, EPSPs that were initially subthreshold for firing the pyramidal cells became suprathreshold after perfusion of IBMX. The stimulus intensities that were most effective in potentiating the responses were of intermediate strength (Fig. 4.14.A.), a finding similar to that

Figure 4.14. Intracellular I/O relationship following perfusion of IBMX in a CA1 pyramidal cell. A. The rate of rise ( $dV/dt$ ) of the intracellularly recorded EPSP plotted against the intensity of stimulation. Values were obtained from the traces in B. and C. and represent  $dV/dt$ s at 9 different stimulus intensities (range: 3.5-7.5 V in 0.5 V increments) delivered to the Schaffer collateral/commissural fiber system before ('CONTROL') and following 45 min of washout of 100  $\mu$ M IBMX. The regression lines were fitted by computer and their slopes are significantly different from each other ( $p < 0.01$ : two tailed t-test). B. and C. represent the computer-averaged EPSPs superimposed on a 0.25 nA hyperpolarizing current pulse. Note that membrane resistance as it can be deducted from the voltage deflection before the stimulus artefact did not change during IBMX-induced LTP. Also note that while none of the control EPSPs produced cell discharge, the two potentials evoked at the last two steps of stimulation intensities (7 and 7.5 V) both brought the neuron to firing threshold after LTP has been induced.

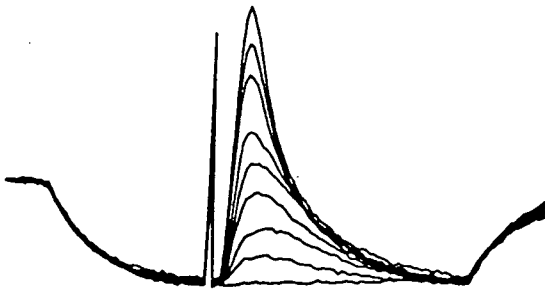
A.



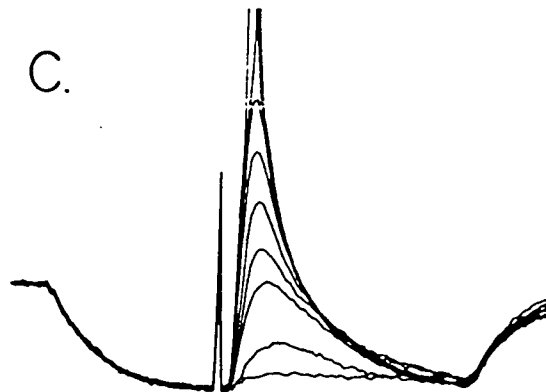
Control

IBMX

B.



C.



5 mV  
10 ms

observed with potentiation of extracellular responses (see Sections 4.3.1. and 4.3.3.).

#### 4.3.9. Effect of IBMX on inhibitory mechanisms of CA1 pyramidal cells recorded intracellularly

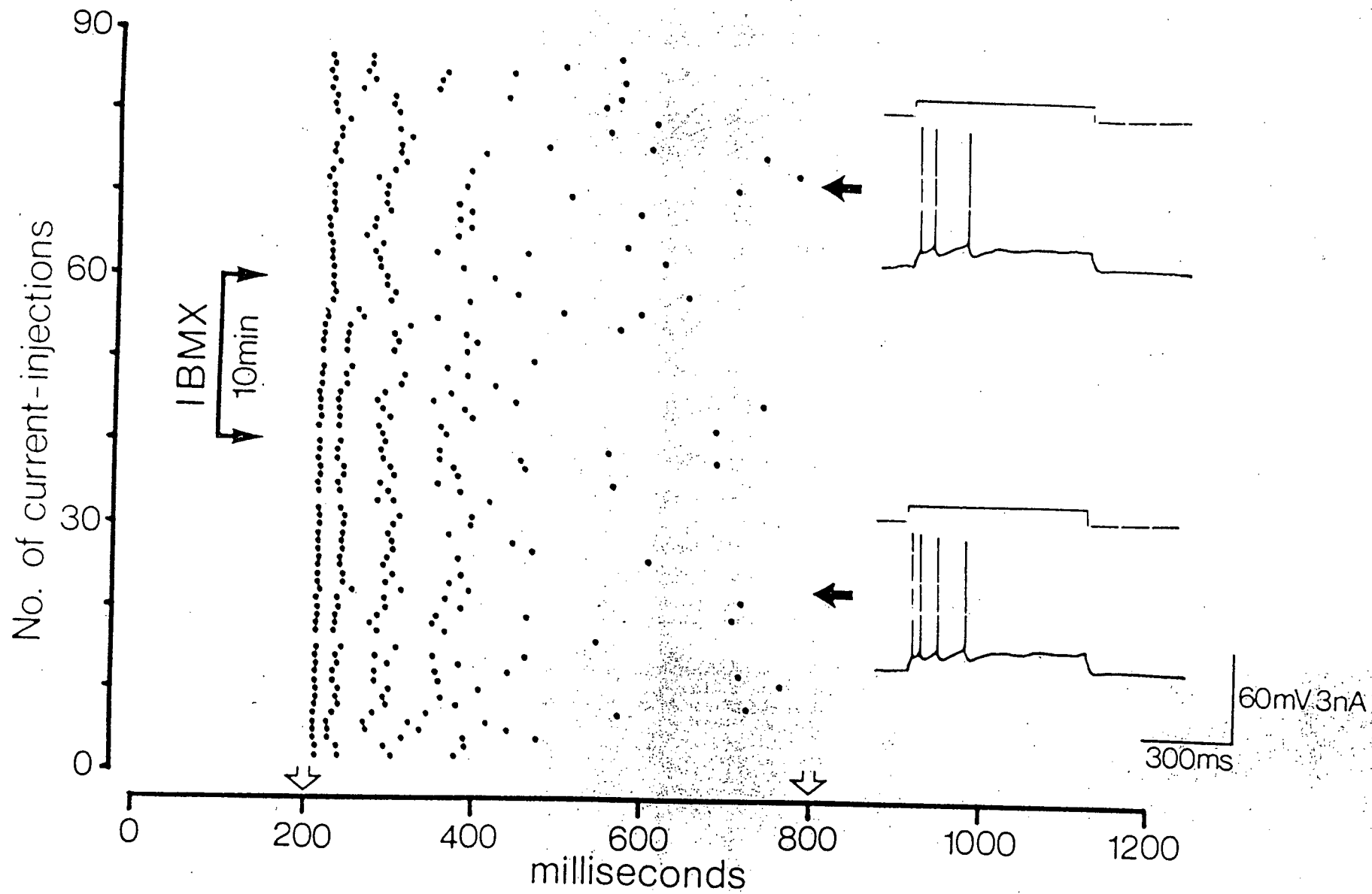
Potentiation of intracellular potentials may result if the pyramidal cells were to be released from the influence of an intrinsic or extrinsic inhibitory process. To account for this possibility the effect of IBMX was tested on some inhibitory events of CA1 neurons.

##### (i) Accommodation

When challenged with a long duration (600-700 ms) depolarizing current pulse, hippocampal pyramidal cells fire several action potentials but the initial high frequency discharge declines significantly towards the end of the current pulse. The underlying mechanism is the activation of a  $\text{Ca}^{2+}$ -dependent  $\text{K}^+$  conductance ( $\text{gK}_{\text{Ca}}$ ) with a contribution from the M-current (Madison and Nicoll, 1984). In addition, Madison and Nicoll (1980) have shown that cyclic nucleotides and their derivatives are effective regulators of accommodation. If elevated in the tissue, these compounds reduce the  $\text{gK}_{\text{Ca}}$  thus diminishing the accommodation properties of CA1 pyramidal cells. The effect of 100  $\mu\text{M}$  IBMX was tested on the accommodation properties of 8 hippocampal pyramidal neurons. Depolarizing

Figure 4.15. Effect of IBMX on the accommodation of pyramidal cell discharge. Raster display of the number of spikes during 600 ms depolarizing current injections (between open arrows on the abscissa) delivered every 30 sec. Note the slight decrease in accommodation produced during and following a 10 min IBMX perfusion as reflected by the two insets. These represent oscilloscope traces at the times indicated by closed arrowheads. The continuous raster display itself, which is considered to be a more accurate measurement of accommodation, shows a slight decrease in accommodation during and following perfusion of IBMX.



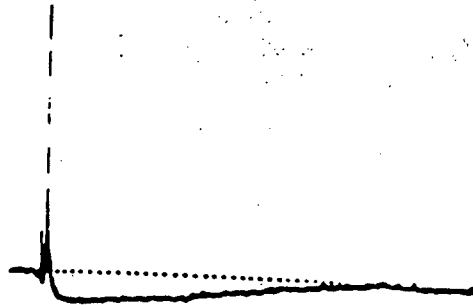
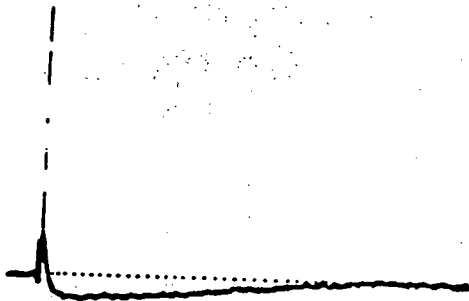
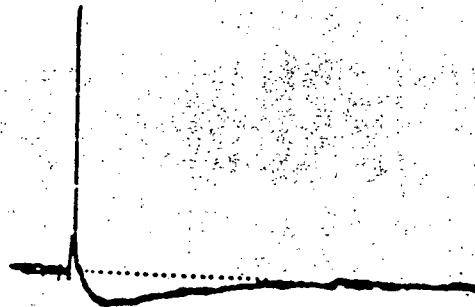
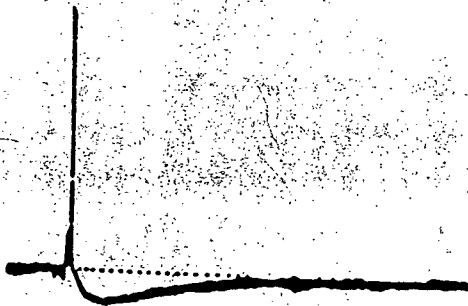
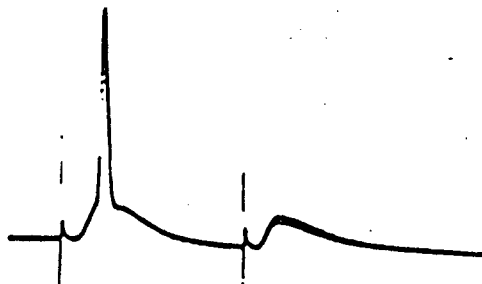
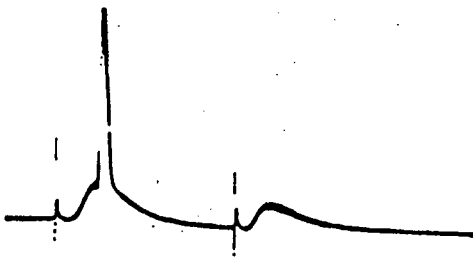


current pulses (600 ms in duration) were delivered every 30 s and the number of evoked spikes was continuously monitored as described in Section 4.2.2. A typical example of a raster display is shown on Fig. 4.15. A slight enhancement of the accommodation was noted in 5/8 cells, the remainder showing no alteration. This finding is rather inconsistent with the inhibitory action of IBMX on the enzyme phosphodiesterase, since elevation of cyclic nucleotide levels should have decreased the accommodation.

(ii) Long-lasting hyperpolarization (LHP)

Following their synaptic activation, hippocampal pyramidal neurons usually display a hyperpolarizing potential lasting in excess of 200 ms, that is termed LHP (Alger, 1984; Lancaster and Wheal, 1984). Lancaster and Wheal (1984) using intracellular injections of the  $\text{Ca}^{2+}$  chelator EGTA provided evidence that  $\text{gK}_{\text{Ca}}$  activation may have little contribution to the LHP. According to the recent study of Alger (1984) the underlying mechanism appears to be a synaptically activated  $\text{K}^{+}$  conductance. As shown on Fig. 4.16.A. the amplitude and duration of the LHP was in most cases slightly but not significantly increased by IBMX.

Figure 4.16. Effect of IBMX on inhibitory events acting on CA1 pyramidal neurons. A. Slight enhancement of the long lasting afterhyperpolarization (AHP) that follows synaptic activation of CA1 pyramidal cells in the presence of 100  $\mu$ M IBMX. B. No significant change was produced by IBMX in a typical IPSP evoked following orthodromic stimulation of pyramidal neurons. C. Intracellular paired-pulse inhibition was also unaltered by IBMX as reflected by the failure of the second orthodromic pulse to evoke cell discharge. The dotted lines indicate the resting membrane potentials (RMP) of the respective cells. RMPs were not changed by addition of IBMX to the perfusate.

**Control****IBMX****A. AHP** $\perp 10\text{ mV}$   
50 ms**B. IPSP** $\perp 10\text{ mV}$   
20 ms**C. Paired Pulse** $\perp 20\text{ mV}$   
5 ms

(iii) Inhibitory post-synaptic potentials (IPSPs) and intracellular paired-pulse inhibition

A decrease in the feed-back inhibition of hippocampal pyramidal cells mediated through GABA-releasing basket cells is not of primary importance for the induction of LTP, but changes in the levels of inhibition may modulate the degree of potentiation (Haas and Rose, 1982). IPSPs of pyramidal neurons can be triggered by their ortho- or antidromic activation. Fig. 4.16.B. depicts the lack of effect of 100  $\mu$ M IBMX on an IPSP evoked through orthodromic stimulation of the Schaffer collateral-commissural fibers; similar results were obtained for the antidromic stimulation-evoked IPSPs (not shown).

To estimate the effectiveness of the inhibition, a supra-threshold conditioning stimulus was delivered to the afferent fiber system followed, 20 ms later, by a test stimulus of equal intensity (Fig. 4.16.C.). As a result of the activated inhibition, the second stimulus evoked a smaller EPSP that failed to trigger an action potential. The paired-pulse paradigm was then repeated in the presence of 100  $\mu$ M IBMX but no changes were detected in the potency of inhibition confirming the results obtained under similar circumstances in the study of extracellular potentials.

#### 4.3.10. Long-term effect of IBMX on stimulus threshold

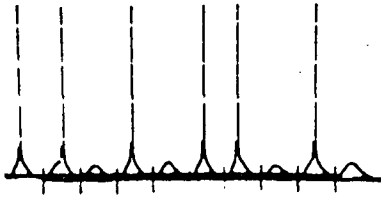
By definition, when the stimulation intensity of afferent fibers is adjusted to 'threshold' only 50% of the stimuli will evoke an action potential in the neurons under study. In Fig. 4.17.A. an experiment is shown where the intensity of stimulation delivered to the Schaffer collateral/commissural fibers was adjusted to this threshold value. Before perfusion of the drug 6 out of 10 successive stimuli evoked an action potential in the CA1 pyramidal neurons. In the presence of IBMX (Fig. 4.17.B.) all stimuli delivered (10/10) caused a spike discharge. A reduction of stimulus intensity to approximately half of its original value (Fig. 4.17.C.) could now evoke spikes with 6 out of 10 pulses thus indicating that a new threshold for synaptic activation was established following IBMX-induced LTP. A characteristic 22-50% reduction in threshold stimulation intensity was observed in all cells examined (n=7) and persisted after washout as long as steady recordings could be obtained.

To clarify whether the lowering of stimulation threshold was due to a general somatic alteration of firing level, a short (20 ms) depolarizing current pulse was used to evoke spiking of pyramidal cells (Fig. 4.17.E.). The firing level and the amount of current needed to evoke spiking were not affected by IBMX (Fig. 4.17.F.), indicating that the CA1 cell soma is an unlikely site of drug action.

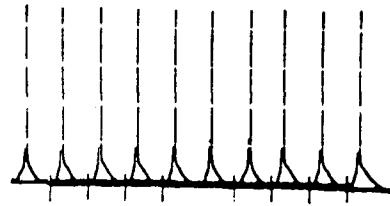
Figure 4.17. Effect of IBMX on stimulus- and firing threshold of CA1 pyramidal neurons. Panels A.-D. represent a typical experiment in which the change in synaptic stimulus threshold (T) was determined. On each trace, 10 successive synaptic activations of a pyramidal cell are shown, which have been manually shifted for clarity by 20 ms on the oscilloscope. The threshold stimulus intensity evoked firing of the cell in 6/10 cases (A.) while the same stimulus intensity produced discharge of the cell in 10/10 cases during perfusion of 100  $\mu$ M IBMX (B.). When stimulus intensity was reduced to approximately half of its original value ( $1/2$  T) in the presence of IBMX (C.), the initial 6/10 spikes could be evoked, indicating a lowering of the synaptic threshold. This phenomenon persisted for a long time following washout of the drug (D.), indicating that LTP was produced. Panels E. and F. represent the firing level of a pyramidal neuron as measured by a short duration (20 ms) depolarizing current injection. Since the resting membrane potential was not changed by IBMX, it is reasonable to say that voltage at which spiking of the pyramidal cell was observed (firing level), indicated by the two arrowheads, was not altered by the drug. Therefore, the observed changes in synaptic threshold are not due to a decreased firing level caused by IBMX.

**STIMULUS THRESHOLD ( T )**

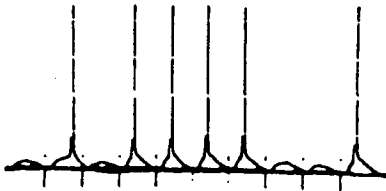
A.



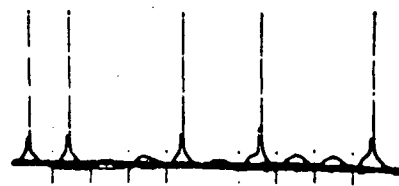
B.



C.



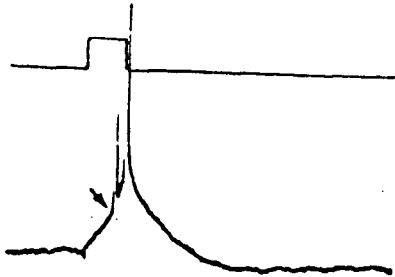
D.



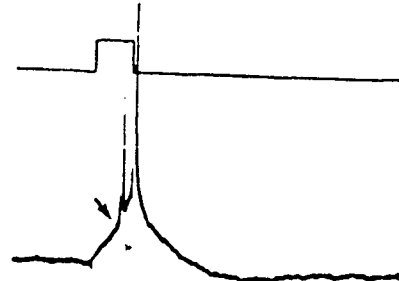
┘ 20mV  
20 ms

**Spike/Current Threshold**

E.

**Control**

F.

**IBMX**

┘ 5mV/.5nA  
20 ms



#### 4.4. Discussion

Despite considerable research the exact mechanism of the long-lasting potentiation (LTP) in the hippocampal formation has not yet been elucidated. Several pharmacological agents have been successfully employed in blocking the long-term enhancement of synaptic responses and thus have provided useful information about the possible molecular events involved in the process (Finn et al., 1980; Mody et al., 1984; Stringer et al., 1984). While certain drugs are effective in hindering the induction of LTP, only a limited number of agents other than tetanic stimulation and a brief elevation in extracellular  $\text{Ca}^{2+}$  were shown to trigger its occurrence. Neuman and Harley (1983) have found that iontophoretic application of norepinephrine in the dentate gyrus results in a long-lasting enhancement of the extracellular field responses evoked by perforant path stimulation. The present findings indicate that synaptic plasticity in the CA1 region of the in vitro hippocampus may also be induced by the methylxanthine derivative IBMX. Several mechanisms of action may subserve this LTP-inducing effect of IBMX. The drug may block adenosine receptors or inhibit the enzyme phosphodiesterase and finally, could cause release of  $\text{Ca}^{2+}$  from intraneuronal storage sites.

Methylxanthine compounds are known for their double antagonism of adenosine responses in the central nervous system by inhibiting purine release and by blocking postsynaptic

adenosine receptors (Stone, 1981). Previous studies on these substances in the hippocampus have focused on their properties to antagonize adenosine receptors (Schubert and Mitzdorf, 1979; Dunwiddie and Hoffer, 1980; Okada and Ozawa, 1980; Dunwiddie et al., 1981). These investigators have demonstrated that adenosine is an effective inhibitor of hippocampal evoked responses and suggested the possibility for its tonic release since applications of adenosine receptor antagonists lead to enhanced synaptic activity. Dunwiddie and Hoffer (1980) reported that evoked potentials were potentiated only as long as theophylline was present in the bathing medium. These investigators also noted that although it antagonized adenosine responses in a concentration of 400  $\mu$ M, IBMX failed to have any effect on the EPSP responses. In another region of the hippocampus, the CA3, Okada and Ozawa (1980) observed epileptiform activity upon exposure of the slices to high (500  $\mu$ M) levels of IBMX.

In the present study drug concentrations were considerably lower, resulting in comparable findings regarding the effect of theophylline but significant differences with regard to IBMX's action. The reason for the discrepancy is not known since potentiation of the Schaffer collateral/commissural evoked responses recorded at the pyramidal cell layer as well as at the level of apical dendrites was observed in all of the slices examined (n=48). In addition, in 44/48 preparations the effect of IBMX was long-lasting, i.e. the responses failed to return to pre-drug levels until the experiment was discontinued (usually in excess of 2 hours). Only one other methylxanthine derivative

(8-phenyl-theophylline) has been reported to cause somewhat analogous long-term enhancing effects in the rat hippocampus when the stimulation frequency was 2 Hz (Corradetti et al., 1984). However, such a frequency of stimulation may by itself cause potentiation of the evoked responses and therefore a valid conclusion regarding the drug's action cannot be reached.

If the actions of IBMX on adenosine receptors are considered as being responsible for its LTP-inducing effect, then a long-term blocking action has to be postulated, or alternatively a very slow washout time of the drug has to be present. These alternatives seem unlikely, however, in light of the short retention times and fast recoveries for IBMX as measured by Snyder et al. (1981) using radioactively labelled methylxanthine compounds. An effect of IBMX on adenosine receptors alone is also not probable in view of its differential effect from that of theophylline. Theophylline has a two-fold lower  $IC_{50}$  for adenosine receptors than IBMX (Snyder et al., 1981) and yet the magnitude of potentiation produced during perfusion of IBMX was invariably larger than that caused by theophylline. Furthermore, while the washout times of the two drugs are similar (Snyder et al., 1981), theophylline failed to produce any long-lasting enhancement of the hippocampal evoked responses. The deviant properties of IBMX which distinguish this drug from a variety of other methylxanthines were also noted in several behavioural studies (e.g., Snyder et al., 1981; Yarbrough and McGuffin-Clineschmidt, 1981). In view of these observations and the results of the present study it is concluded that antagonism of

adenosine receptors may be partially responsible for the potentiation of the evoked responses during IBMX perfusion, but cannot play a role in the LTP-producing effect of IBMX.

As a second possible mechanism of action, inhibition of the enzyme phosphodiesterase (PDE) would result in elevated intracellular concentrations of cyclic nucleotides. According to Chasin and Harris (1976) the relative potencie of theophylline on PDE inhibition is considered to be 1, then IBMX's and papaverine's potencies are 15 and 10-1,000 respectively (see also Smellie et al., 1979). In addition to its inhibitory action on PDE, papaverine has been shown to activate the adenylate cyclase of the cerebral cortex thus causing added elevations of cyclic AMP levels (Iwangoff and Enz, 1971). The results of the present study show that papaverine had an opposite effect to that of IBMX (slightly depressed the population spike and EPSP responses) suggesting that elevations in cyclic nucleotide levels are not responsible for the action of IBMX. Bursting induced by low  $Ca^{2+}$  is also modulated by drugs that interfere with cyclic nucleotides (Haas et al., 1984) whereas IBMX had no major effect on this type of epileptiform activity. The lack of effect on cyclic nucleotide metabolism is further underscored by the slight enhancement of pyramidal cell discharge accommodation caused by IBMX. Drugs that elevate cAMP of hippocampal slices and cyclic nucleotides themselves have an opposite effect on the accomodation of CA1 pyramidal neurons (Madison and Nicoll, 1980).

Since the contributions of adenosine receptor antagonism and phosphodiesterase inhibition to the IBMX-induced LTP have been

ruled out, a third possible mechanism, namely the effect of the drug on intracellular  $\text{Ca}^{2+}$ -regulation has to be considered. The observations that IBMX retained its LTP inducing potency even in the presence of the  $\text{Ca}^{2+}$  channel antagonist  $\text{Co}^{2+}$  and caused potentiation of field responses while extracellular  $\text{Ca}^{2+}$  was significantly lowered indicate that the action of IBMX does not occur through augmentation of  $\text{Ca}^{2+}$  entry into neurons. An enhanced  $\text{Ca}^{2+}$  influx would have also manifested itself during depolarizing current pulses in the form of a long-duration depolarizing potential as is clearly visible in CA1 pyramidal cells when the  $\text{Ca}^{2+}$  gradient is increased by intracellular application of the  $\text{Ca}^{2+}$  chelator EGTA (see Fig. 2. of Madison and Nicoll, 1984). No such effect was observed in this study during IBMX perfusion.

The fact that the dependency of IBMX-induced LTP on extracellular  $\text{Ca}^{2+}$  was not critical correlates well with the results of  $^{45}\text{Ca}$  uptake experiments presented in Section 3.2.3.2. As shown by the kinetic analysis of  $^{45}\text{Ca}$  uptake curves in the presence of IBMX, the drug was able to mobilize  $\text{Ca}^{2+}$  from an intracellular buffered/sequestered pool. Total exchangeable intraneuronal  $\text{Ca}^{2+}$  was not affected by IBMX suggesting that calcium entry per se did not play a significant role. Therefore, it is likely that the end result of drug action consists of a redistribution of intracellular  $\text{Ca}^{2+}$  from a slowly exchangeable (buffered/sequestered) compartment into a more rapidly exchangeable pool that includes free cytoplasmic  $\text{Ca}^{2+}$ . Similar shifts in calcium homeostasis have been observed in the kindling

model of epilepsy possibly due to the loss of an intraneuronal  $\text{Ca}^{2+}$ -buffer, i.e., the calcium-binding protein, CaBP (Section 3.3.3.). In the case of the IBMX-induced LTP there is no evidence for a decrease in the levels of an intraneuronal calcium binding- and buffering system but rather an activation of release from intraneuronal storage sites.

The neuronal equivalent of sarcoplasmic reticulum, is the endoplasmic reticulum. One of the several functions associated with this cellular element has been shown to be a major  $\text{Ca}^{2+}$ -buffering system in nerve cells whereas the mitochondria seem to play a less significant role (Duce and Keen, 1978; Blaustein et al., 1980; Brinley, 1980; McGraw et al., 1982). A calcium-dependent  $\text{Ca}^{2+}$  release from the endoplasmic reticulum of neurons is therefore feasible, similar to the process described for the sarcoplasmic reticulum of skeletal muscle (for reviews see Endo, 1977; Martonosi, 1984). Thus the  $\text{Ca}^{2+}$  sequestering pool shown to be affected by IBMX in the analysis of  $^{45}\text{Ca}$  uptake kinetics may be the neuronal endoplasmic reticulum rather than the lower affinity mitochondrial compartment. If this is the case, IBMX may reset the sensitivity of the endoplasmic reticulum for  $\text{Ca}^{2+}$ , analogous to its effect in skeletal muscle (Miller and Thieleczek, 1978) or to that of caffeine in bullfrog sympathetic neurons (Akaike et al., 1983), resulting in a larger  $\text{Ca}^{2+}$ -induced  $\text{Ca}^{2+}$  release. Alternatively, IBMX may elevate the levels of inositol triphosphate ( $\text{InsP}_3$ ) and enhance the release of endoplasmic reticular  $\text{Ca}^{2+}$  through the pathway described by Berridge and Irvine (1984). Although there is no evidence yet

whether IBMX has any effect on phosphatidylinositol metabolism, this alternate route of drug action seems plausible since tetanus-induced LTP has recently been shown to enhance the levels of  $\text{InsP}_3$  in the hippocampal formation (Bar et al., 1984).

If release of intracellular calcium is indeed responsible for the neuronal plasticity caused by IBMX, several molecular mechanisms, at either pre- or postsynaptic sites, may in turn be activated by the excess of available  $\text{Ca}^{2+}$ . The synaptic localization of the changes following perfusion of IBMX is demonstrated by the alterations of the I/O curves observed in the present study. The efficacy of the synapses became enhanced without any considerable increase in cellular excitability as shown by the little change detected in the relationship between the rate of rise of the EPSP and population spike amplitude (D-S curves). Consequently, when post-synaptic current was the same (as reflected by the rate of rise of the EPSP) it produced the synchronous firing of approximately the same number of CA1 pyramidal neurons (since a comparable size population spike was evoked) both before and after administration of the drug. However, synaptic transmission had to be enhanced since under equivalent input conditions (stimulus intensity or fiber volley amplitude) a larger output function (synaptic current flow or EPSP amplitude) was generated following IBMX-induced LTP.

The synaptic changes which occur during any form of LTP may be localized at the levels of the postsynaptic cell or could be caused by alterations in the presynaptic terminal (Bliss and Dolphin, 1982; Swanson et al., 1982; Eccles, 1983; Voronin,

1983). There may be a selective postsynaptic change responsible for the mechanism of LTP (Dunwiddie et al., 1978; Baudry et al., 1980). The release of  $\text{Ca}^{2+}$  from intraneuronal storage sites as a result of IBMX in the post-synaptic cell may increase the number of postsynaptic glutamate receptors as proposed by Lynch and Baudry (1984) and thus cause a lasting change in synaptic efficacy. The increase in the size of the intracellular EPSP and its rate of rise would be explained by this phenomenon. As shown for a computer-derived model of a motoneuron when synaptic input is held constant, the voltage change during an EPSP is most sensitive to the density of active synapses on the postsynaptic membrane (Lev-Tov et al., 1983). In this model, changes in passive membrane characteristics of the cell seem to be parameters of lesser significance. In the present experiments however, there is no reason to assume that the synaptic input was not altered by IBMX, although the number of activated presynaptic fibers, as shown by the constancy of the fiber volley potential, is probably unaffected. As in the model of Lev-Tov et al. (1983) no changes were detected in the passive membrane characteristics (RMP,  $R_n$  and  $T_c$ ) of hippocampal pyramidal cells during perfusion of IBMX. But somatic recordings cannot reflect changes in the electrophysiological properties of distant dendrites and dendritic spines. If these spines are assumed to have active channels, then small changes in their diameter which either increase or decrease spine shaft resistance produce considerable amplifications of the EPSP (Miller et al., 1985; Perkel and Perkel, 1985). If IBMX causes a long-lasting alteration in the



morphology of the spine apparatus, the final result may well be a persistent enhancement of the synaptic responses.

As an alternate mechanism, the excess free calcium in the presynaptic terminals may trigger the biochemical substrate for a long-lasting increase in neurotransmitter release. Such an enhanced release has been shown to be a correlate of tetanus-induced LTP in the hippocampus (Skrede and Malthe-Sorensen, 1981; Dolphin et al., 1982) and presynaptic mechanisms have thus been implicated (Sastry, 1982; Dolphin, 1983). The long-term alterations reflected by the intracellular input/output curves may also be accounted for by a presynaptic action of IBMX if induction of a larger neurotransmitter release is assumed. The excess  $\text{Ca}^{2+}$  in the presynaptic terminal, particularly originating from intraneuronal storage sites, may produce an enhanced resting neurotransmitter release as demonstrated for the neuromuscular junction (Rahamimoff, 1976; Rahamimoff et al., 1980). This phenomenon would only last while the drug is present in the perfusate and responses should return to control values following washout. This however, is clearly not the case since reduction of synaptic threshold and enhancement of evoked intracellular EPSPs were observed as long as recordings were maintained from the CA1 pyramidal cells. Since the retention of  $\text{Ca}^{2+}$  after tetanic stimulation is only transient (Baimbridge and Miller, 1981), a long-lasting biochemical change of the presynaptic terminal would have to be postulated for the chronic increase in transmitter release.

The resulting enhancement of EPSP amplitude and its rate of rise, recorded inside the pyramidal cells, was sustained for a longer period of time than in the case of LTP induced by conventional high frequency stimulation techniques thus stressing the potency of IBMX. However, as found by other investigators for the LTP induced by tetanic stimulation (Yamamoto and Chujo, 1978; Andersen et al., 1980; Yamamoto et al., 1980; Lynch et al., 1983) the event took place without any observable long-term changes in the passive membrane properties ( $RMP$ ,  $R_n$  and  $T_c$ ) of CA1 pyramidal neurons suggesting that the major factors responsible for the phenomenon are localized to the synaptic junction.

The present study does not distinguish between the two possible sites of the LTP-inducing effect of IBMX. However, the results show a novel form of LTP in the mammalian CNS whereby release of intraneuronal  $Ca^{2+}$ , possibly from the endoplasmic reticulum, is responsible for the sustained potentiation of synaptic responses. This hypothesis awaits further testing especially since it may be applicable to the tetanus- and calcium-induced forms of LTP.

## CHAPTER V.

### CONCLUSIONS

The important role of calcium in the control of nerve cell function is well established. Extracellular calcium exerts profound actions on the excitability of neuronal membranes while cytosolic  $\text{Ca}^{2+}$  can by itself, or through the activation of second messengers, regulate the activity of neurons. It is therefore of no surprise that its concentration both intra- and extracellularly is under rigorous control. Inside the cell, several mechanisms, including buffering by intracellular organelles and proteins, participate in the maintenance of a steady  $\text{Ca}^{2+}$  concentration at an optimal level. Changes in the capacity of neurons to cope with a  $\text{Ca}^{2+}$  challenge may result in their altered discharge patterns which, if they occur on a large enough scale, may influence the activity of the whole CNS. Therefore, any durable change in neuronal  $\text{Ca}^{2+}$ -regulatory mechanisms could result in severe consequences with regard to the normal functioning of the nervous system. The present study examined some aspects of the intraneuronal  $\text{Ca}^{2+}$ -homeostasis during long-term alterations in neuronal excitability.

Kindling-induced epilepsy, whereby status epilepticus is induced by daily electrical stimulation, is a prime example of such a gradual but persistent change in nerve cell excitability. It is characterized by the early occurrence of repetitive, synchronous firings of groups of neurons (afterdischarges or AD's), which culminate with time in full tonic-clonic seizures analogous to the human disease. As presented in Section 2.3., the development of AD's was correlated to the loss of an intraneuronal calcium-binding protein (CaBP) in the hippocampal formation. Although the role of this protein is not fully established, one of its main functions may be the buffering of excess intraneuronal  $\text{Ca}^{2+}$ . The exact causal link between CaBP and AD's could not be established, but changes in the levels of the protein paralleled the progressive lengthening of the AD's in the hippocampus.

An impaired calcium regulation, as reflected by diminished levels of CaBP in certain cortical areas, was found in yet another model of experimental epilepsy. The genetically epileptic strain of mice (El), in which seizures are induced by successive vestibular stimulations, had significantly lower cortical levels of the protein than a control strain. This finding is relevant, since one of the CaBP-deficient cortical areas, the hippocampus, is also thought to be the focus of the paroxysms. It is therefore possible that the enhanced susceptibility to seizures in this strain is due to a genetically altered intraneuronal  $\text{Ca}^{2+}$  regulation.

Measurement of intraneuronal  $\text{Ca}^{2+}$  is a difficult task and can only be achieved with high accuracy in the large nerve cells of molluscs. With the presently available techniques it is only possible to estimate calcium activities in elements of the mammalian CNS. In the more accessible non-neuronal preparations, the kinetic analysis of  $^{45}\text{Ca}$  uptake curves has long been used to reliably determine exchangeable  $\text{Ca}^{2+}$  levels. In the present study this technique was successfully applied to the in vitro hippocampus. The validity of the method was assured by comparing the hippocampal  $\text{Ca}^{2+}$  measurements to the data of other studies that used the same procedure in non-neuronal preparations as well as to available  $\text{Ca}^{2+}$  determinations in the mammalian CNS. Although a distinction could not be made between glial and neuronal elements using the current technique, due to the heterogeneity of the hippocampal slice preparation, it was established that exchangeable  $\text{Ca}^{2+}$  is distributed, as in other systems, into two kinetically separate pools. The first rapidly exchangeable compartment includes among other entities free ionic intracellular  $\text{Ca}^{2+}$ , while the second more slowly exchangeable compartment consists of the sum of buffered cellular  $\text{Ca}^{2+}$ . Once the reliability of the  $^{45}\text{Ca}$  uptake kinetics was established, the method was used to detect possible alterations in  $\text{Ca}^{2+}$  homeostasis following the chronic predisposition of neuronal tissue to epileptiform activity.

Significant alterations in exchangeable  $\text{Ca}^{2+}$  were observed in hippocampal slices obtained from amygdala and commissural kindled animals. Although there was no change in the absolute

levels of intracellular calcium, there was a significant redistribution of calcium from a buffered compartment into an unsequestered pool. If the calcium-binding protein CaBP is considered to be part of the intraneuronal  $\text{Ca}^{2+}$  buffering system, it is evident that following its loss during kindling-induced epilepsy  $\text{Ca}^{2+}$  would be transferred to other intracellular exchangeable compartments. The finding that total exchangeable  $\text{Ca}^{2+}$  of kindled hippocampi was unaltered, an observation confirmed by atomic absorption spectrophotometry measurements, adds important conceptual consequences to our present understanding of neuronal  $\text{Ca}^{2+}$  regulation. It indicates that persistent changes in neuronal excitability do not necessarily depend upon the amount of total  $\text{Ca}^{2+}$  in the system but rather on the quantity of the cation freely available for regulatory processes. This finding stresses the importance of intraneuronal  $\text{Ca}^{2+}$  stores which may release or take up  $\text{Ca}^{2+}$  according to the physiological (or pathophysiological) needs and stimuli.

It is this calcium release mechanism that most likely underlies the action of 3-isobutyl-1-methylxanthine (IBMX) in the hippocampal slice preparation, although the exact site of release could not be determined by  $^{45}\text{Ca}$  kinetics. Analogous to the effects of tetanic stimulation and brief exposure to elevated extracellular  $\text{Ca}^{2+}$ , IBMX was shown in the present study to produce long-term potentiation (LTP) of the stratum radiatum evoked field potentials in the CA1 region of the hippocampal slice. Regardless whether the  $\text{Ca}^{2+}$  release occurs at a pre- or postsynaptic site or both, the IBMX-induced LTP is the first

available evidence indicating that an agent which translocates intraneuronal  $\text{Ca}^{2+}$  causes a lasting change in neuronal excitability.

The present study has only dealt with some aspects of the contribution of intraneuronal  $\text{Ca}^{2+}$ -regulatory systems to long-duration changes in neuronal function. Naturally, many alternate pathways of research will be available in the future to establish the precise roles of the several mechanisms that participate in the control of  $\text{Ca}^{2+}$  within nerve cells. In this context, particular emphasis should be placed on the various neuronal calcium-binding proteins and the endoplasmic reticulum which has received little attention so far. Finally, the method of kinetic analysis of  $^{45}\text{Ca}$  uptake curves, extended to the CNS by the present study, should prove to be a valuable tool in determining differences in calcium homeostasis among homogeneous, possibly cultured, populations of neurons. This could lead to a better understanding of the functional characteristics of different types of nerve cells within the CNS.

## REFERENCES

- Akaike, N., Brown, A.M., Dahl, G., Higashi, H., Isenberg, G., Tsuda, Y. and Yatani, A. [1983] Voltage-dependent activation of potassium current in *Helix* neurones by endogenous cellular calcium. *J. Physiol.*, 334: 309-324.
- Akerman, K.E.O. and Nicholls, D.G. [1983] Physiological and bioenergetic aspect of mitochondrial calcium transport. *Rev. Physiol. Biochem. Pharmacol.*, 95: 149-201.
- Aldenhoff, J.B., Groul, D.L., Rivier, J., Vale, W. and Siggins, G.R. [1983] Corticotropin releasing factor decreases postburst hyperpolarizations and excites hippocampal neurons. *Science*, 221: 875-877.
- Alger, B.E. [1984] Characteristics of a slow hyperpolarizing synaptic potential in rat hippocampal pyramidal cells *in vitro*. *J. Neurophys.*, 52: 892-910.
- Alger, B.E. and Nicoll, R.A. [1980] Epileptiform burst after-hyperpolarization: calcium-dependent potassium potential in hippocampal CA1 pyramidal cells. *Science*, 210: 1122-1124.
- Alger, B.E. and Teyler, T.J. [1976] Long-term and short-term plasticity in the CA1, CA3 and dentate regions in the rat hippocampal slice. *Brain Res.*, 110: 463-480.
- Alvarez-Leefmans, F.J., Rink, T.J. and Tsien, R.Y. [1981] Free calcium ions in neurones of *Helix Aspersa* measured with ion-selective microelectrodes. *J. Physiol.*, 315: 531-548.
- Andersen, P., Bliss, T.V.P. and Skrede, K.K. [1971] Unit analysis of hippocampal population spikes. *Exp. Brain Res.*, 13: 208-221.
- Andersen, P., Silfvenius, H., Sundberg, S.H., Sveen, O. and Wigstrom, H. [1978] Functional characteristics of unmyelinated fibres in the hippocampal cortex. *Brain Res.*, 144: 11-18.
- Andersen, P., Sundberg, S.H., Sveen, O., Swann, J.W. and Wigstrom, H. [1980] Possible mechanism for long-lasting potentiation of synaptic transmission in hippocampal slices from guinea-pigs. *J. Physiol.*, 302: 463-482.



- Andersen, P., Sundberg, S.H., Sveen, O. and Wigstrom, H. [1977] Specific long-lasting potentiation of synaptic transmission in hippocampal slices. *Nature*, 266: 736-737.
- Assaf, S.Y. and Chung, S.H. [1984] Release of endogenous  $Zn^{2+}$  from brain tissue during activity. *Nature*, 308: 734-736.
- Baimbridge, K.G. and Miller, J.J. [1981] Calcium uptake and retention during long-term potentiation of neuronal activity in the rat hippocampal slice preparation. *Brain Res.*, 221: 299-305.
- Baimbridge, K.G. and Miller, J.J. [1982] Immunohistochemical localization of calcium-binding protein in the cerebellum, hippocampal formation and olfactory bulb of the rat. *Brain Res.*, 245: 223-229.
- Baimbridge, K.G. and Miller, J.J. [1984] Hippocampal calcium-binding protein during commissural kindling-induced epileptogenesis: progressive decline and effects of anti-convulsants. *Brain Res.*, 324: 85-90.
- Baimbridge, K.G., Miller, J.J. and Parkes, C.O. [1982] Calcium-binding protein distribution in the rat brain. *Brain Res.*, 239: 519-525.
- Baimbridge, K.G., Mody, I. and Miller, J.J. [1985] Reduction of rat hippocampal calcium-binding protein following commissural, amygdala, septal, perforant path and olfactory bulb kindling. *Epilepsia*, in press.
- Baimbridge, K.G. and Parkes, C.O. [1980] Vitamin D-dependent calcium-binding protein in the chick brain. *Cell Calcium*, 2: 65-76.
- Baimbridge, K.G., Selke, P.A., Ferguson, N. and Parkes, C.O. [1980] Human calcium-binding protein. In: *Calcium-Binding Proteins: Structure and Function* (F.L. Siegel, E. Carafoli, R.H. Kretsinger, D.H. MacLennan and R.H. Wasserman, Eds.), Elsevier North Holland, pp: 401-404.
- Baldissera, F. and Parmiggiani, F. [1979] After hyperpolarization conductance time-course and repetitive firing in a motoneurone model with early inactivation of the slow potassium conductance system. *Biol. Cybernetics*, 34: 233-240.
- Baraldi, M., Caselgrandi, E., Borella, P. and Zeneroli, M.L. [1983] Decrease of brain zinc in experimental hepatic encephalopathy. *Brain Res.*, 258: 170-172.
- Barish, M.E. and Thompson, S.H. [1983] Calcium buffering and slow recovery kinetics of calcium-dependent outward current in molluscan neurones. *J. Physiol.*, 337: 201-219.

- Barritt, G.J., Parker, J.C. and Wadsworth, J.C. [1981] A kinetic analysis of the effects of adrenaline on calcium distribution in isolated rat liver parenchymal cells. *J. Physiol.*, 312: 29-55.
- Baudry, M., Fuchs, J., Kessler, M. Arst, D. and Lynch, G. [1982] Entorhinal cortex lesions induce a decreased calcium transport in hippocampal mitochondria. *Science*, 216: 411-413.
- Baudry, M. and Lynch, G. [1981] Hippocampal glutamate receptors. *Mol. Cell. Biochem.*, 38: 5-18.
- Baudry, M., Oliver, M., Creager, R., Wieraszko, A. and Lynch, G. [1980] Increase in glutamate receptors following repetitive electrical stimulation in hippocampal slices. *Life Sci.*, 27: 325-330.
- Bar, P.R., Wiegant, F., Lopes da Silva, I.H. and Gispen, W.H. [1984] Tetanic stimulation affects the metabolism of phosphoinositides in hippocampal slices. *Brain Res.*, 321: 381-385.
- Benardo, L.S. and Prince, D.A. [1982] Dopamine action on hippocampal pyramidal cells. *J. Neurosci.*, 2: 415-423.
- Bender, A.S., Wu, P.H. and Phillis, J.W. [1980] The characterization of [<sup>3</sup>H]adenosine uptake into rat cerebral cortical synaptosomes. *J. Neurochem.*, 35: 629-640.
- Berman, M. [1965] Compartmental analysis in kinetics. In: *Computers in Biomedical Research* (Stacy, R. and Waxman, B. Eds.) Vol. 2., Academic Press, New York, pp: 173-201.
- Berman, M., Shan, E. and Weiss, M.F. [1962a] The routine fitting of kinetic data to models: A mathematical formalism for digital computers. *Biophys. J.*, 2: 275-287.
- Berman, M., Weiss, M.F. and Shan, E. [1962b] Some formal approaches to the analysis of kinetic data in terms of linear compartment systems. *Biophys. J.*, 2: 289-316.
- Berridge, M.J. and Irvine, R.F. [1984] Inositol triphosphate, a novel second messenger in cellular signal transduction. *Nature*, 312: 315-321.
- Blaustein, M.P., Ratzlaff, R.W. Kendrick, N.C. and Schweitzer, E.S. [1978] Calcium buffering in presynaptic nerve terminals. I. Evidence for involvement of a nonmitochondrial ATP-dependent sequestration mechanism. *J. Gen. Physiol.*, 72: 15-41.

- Blaustein, M.P., Ratzlaff, R.W. and Schweitzer, E.S. [1980] Control of intracellular calcium in presynaptic nerve terminals. *Federation Proc.*, 39: 2790-2795.
- Blinks, J.R., Wier, W.G., Hess, P. and Prendergast, F.G. [1982] Measurement of  $\text{Ca}^{2+}$  concentrations in living cells. *Prog. Biophys. Molec. Biol.*, 40: 1-114.
- Bliss, T.V.P. and Dolphin, A.C. [1982] What is the mechanism of LTP in the hippocampus? *Trends in Neurosci.*, 5: 289-290.
- Bliss, T.V.P., Dolphin, A.C. and Feasey, K.J. [1984] Elevated calcium induces a long-lasting potentiation of commissural responses in hippocampal CA3 cells of the rat *in vivo*. *J. Physiol.*, 350: 65P (Abstr.).
- Bliss, T.V.P. and Gardner-Medwin, A.R. [1973] Long-lasting potentiation of synaptic transmission in the dentate area of the unanaesthetized rabbit following stimulation of the perforant path. *J. Physiol.*, 232: 357-374.
- Bliss, T.V.P., Goddard, G.V. and Riives, M. [1983] Reduction of long-term potentiation in the dentate gyrus of the rat following selective depletion of monoamines. *J. Physiol.*, 334: 475-491.
- Bliss, T.V.P. and Lomo, T. [1973] Long-lasting potentiation of synaptic transmission in the dentate area of the anaesthetized rabbit following stimulation of the perforant path. *J. Physiol.*, 232: 334-356.
- Borle, A.B. [1969] Kinetic analyses of calcium movements in HeLa cell cultures. I. Calcium influx. *J. Gen. Physiol.*, 53: 43-56.
- Borle, A.B. [1970] Kinetic analyses of calcium movements in HeLa cell cultures. III. Effect of calcium and parathyroid hormone in kidney cells. *J. Gen. Physiol.*, 55: 163-186.
- Borle, A.B. [1975a] Methods for assessing hormone effects on calcium fluxes *in vitro*. *Methods in Enzymology*, 39: 513-573.
- Borle, A.B. [1975b] Regulation of cellular calcium metabolism and calcium transport by calcitonin. *J. Membr. Biol.*, 21: 125-146.
- Borle, A.B. [1981a] Control, modulation, and regulation of cell calcium. *Rev. Physiol. Biochem. Pharmacol.*, 90: 13-153.
- Borle, A.B. [1981b] Pitfalls of the  $^{45}\text{Ca}$  uptake method. *Cell Calcium*, 2: 187-196.

- Borle, A.B. and Uchikawa, T. [1979] Effects of adenosine 3',5'-monophosphate, dibutyryl adenosine 3',5'-monophosphate, aminophylline, and imidazole on renal cellular calcium metabolism. *Endocrinology*, 104: 122-129.
- Brinley, F.J. Jr. [1978] Calcium buffering in squid axons. *Ann. Rev. Biophys. Bioeng.*, 7: 363-392.
- Brostrom, M.A., Brostrom, C.O., Brotman, L.A., Lee, C., Wolff, D.J. and Geller, H.M. [1982] Alterations of glial tumor cell  $\text{Ca}^{2+}$  metabolism and  $\text{Ca}^{2+}$ -dependent cAMP accumulation by phorbol myristate acetate. *J. Biol. Chem.*, 257: 6758-6765.
- Brown, D.A. and Griffith, W.H. [1983a] Calcium-activated outward current in voltage-clamped hippocampal neurones of the guinea-pig. *J. Physiol.*, 337: 287-301.
- Brown, D.A. and Griffith, W.H. [1983b] Persistent slow inward calcium current in voltage-clamped hippocampal neurones of the guinea-pig. *J. Physiol.*, 337: 303-320.
- Brown, T.H. and McAffe, D.A. [1982] Long-term synaptic potentiation in the superior cervical ganglion. *Science*, 215: 1411-1413.
- Burnham, W.M. [1975] Primary and 'transfer' seizure development in the kindled rat. *Can. J. Neurol. Sci.*, 2: 417-428.
- Caceci, M.S. and Cacheris, W.P. [1984] Fitting curves to data. The Simplex algorithm is the answer. *Byte*, 9(May): 340-362.
- Campbell, A.K. [1983] *Intracellular Calcium: Its Universal Role as Regulator*. John Wiley & Sons.
- Celio, M.R. and Heizmann, C.W. [1981] Calcium-binding protein parvalbumin as a neuronal marker. *Nature*, 293: 300-302.
- Celio, M.R. and Heizmann, C.W. [1982] Calcium-binding protein parvalbumin is associated with fast contracting muscle fibres. *Nature*, 297: 504-506.
- Chad, J., Eckert, R. and Ewald, D. [1984] Kinetics of calcium-dependent inactivation of calcium current in voltage-clamped neurones of *Aplysia californica*. *J. Physiol.*, 347: 279-300.
- Chasin, M. and Harris, D.N. [1976] Inhibitors and activators of cyclic nucleotide phosphodiesterase. *Adv. Cyclic Nucl. Res.*, 7: 225-264.
- Cheung, W.Y. [1970] Cyclic 3',5'-phosphodiesterase: demonstration of an activator. *Biochem Biophys. Res. Commun.*, 38: 533-538.

- Cheung, W.Y. [1980] Calmodulin plays a pivotal role in cellular regulation. *Science*, 207: 19-27.
- Christakos, S., Friedlander, E.J., Frandsen, B.R. and Norman, A.W. [1979] Studies on the mode of action of calciferol XIII. Development of a radioimmunoassay for vitamin D-dependent chick intestinal calcium-binding protein and tissue distribution. *Endocrinology*, 104: 1495-1503.
- Christakos, S. and Norman, A.W. [1980] Vitamin D-dependent calcium-binding protein and its relation to 1,25-dihydroxy-vitamin D receptor localization and concentration. In: *Calcium Binding Proteins: Structure and Function* (F.L. Siegel, E. Carafoli, R.H. Kretsinger, D.H. MacLennan and R.H. Wasserman, Eds.), Elsevier North Holland, pp: 371-378.
- Chung, S.-H. and Johnson, M.S. [1983] Divalent transition-metal ions ( $\text{Cu}^{2+}$  and  $\text{Zn}^{2+}$ ) in the brains of epileptogenic and normal mice. *Brain Res.*, 280: 323-334.
- Claret-Berthon, B., Claret, M. and Mazet, J.L. [1977] Fluxes and distribution of calcium in rat liver cells: kinetic analysis and identification of pools. *J. Physiol.*, 272: 529-552.
- Corradetti, R., Moroni, F., Passani, M.B. and Pepeu, G. [1984] 8-Phenyltheophylline potentiates the electrical activity evoked in hippocampal slices. *Eur. J. Pharmacol.*, 103: 177-180.
- Corradino, R.A. and Fullmer, C.S. [1980] Stimulation of a Cd-binding protein, and inhibition of the vitamin D-dependent calcium-binding protein, by zinc or cadmium in organ-cultured embryonic chick duodenum. *Arch. Biochem. Biophys.*, 199: 43-50.
- Crawford, I.L [1983] Zinc and the hippocampus. In: *Neurobiology of Trace Elements* (I.E. Dreosti and R.M. Smith, Eds.) Humana Press, Clifton, pp: 163-211.
- Crawford, I.L. and Connor, J.D. [1972] Zinc in maturing rat brain: hippocampal concentration and localization. *J. Neurochem.*, 19: 1451-1458.
- Dalgrano, D., Klevit, R.E., Levine, B.A. and Williams, R.J.P. [1984] The calcium receptor and trigger. *Trends in Pharmacol. Sci.*, 5: 266-271.
- Daniell, L.C., Barr, E.M. and Leslie, S.W. [1983]  $^{45}\text{Ca}^{2+}$  uptake into rat whole brain synaptosomes unaltered by dihydropyridine calcium antagonists. *J. Neurochem.*, 41: 1455-1459.

- Danscher, G. [1981] Histochemical demonstration of heavy metals. A revised version of the sulphide silver method suitable for both light and electronmicroscopy. *Histochemistry*, 71: 1-16.
- Danscher, G., Shipley, M.T. and Andersen, P. [1975] Persistent function of mossy fibre synapses after metal chelation with DEDTC (Antabuse). *Brain Res.*, 85: 522-526.
- DeLorenzo, R.J. [1982] Calmodulin in synaptic function and neurosecretion. In: *Calcium and Cell Function*. Vol III. (W.Y. Cheung, Ed.), Academic Press, New York, pp: 271-309.
- DeLorenzo, R.J., Freedman, S.D., Yohe, W.B. and Maurer, S.C. [1979] Stimulation of  $\text{Ca}^{2+}$ -dependent neurotransmitter release and presynaptic nerve terminal protein phosphorylation by calmodulin and a calmodulin-like protein isolated from synaptic vesicles. *Proc. Natl. Acad. Sci. U.S.A.*, 76: 1838-1842.
- Demaille, J.G. [1982] Calmodulin and calcium-binding proteins: evolutionary diversification of structure and function. In: *Calcium and Cell Function*. Vol. II. (W.Y. Cheung, Ed.) Academic Press, New York, pp: 111-144.
- Dodge, F.A. and Rahamimoff, R. [1967] Cooperative action of calcium ions in transmitter release at the neuromuscular junction. *J. Physiol.*, 193: 419-432.
- Dolphin, A.C. [1983] The excitatory amino-acid antagonist gamma-d-glutamylglycine masks rather than prevents long term potentiation of the perforant path. *Neuroscience*, 10: 377-383.
- Dolphin, A.C., Errington, M.L. and Bliss, T.V.P. [1982] Long-term potentiation of the perforant path *in vivo* is associated with increased glutamate release. *Nature*, 297: 496-498.
- Douglas, R.M. and Goddard, G.V. [1975] Long-term potentiation of the perforant path -- granule cell synapse in the rat hippocampus. *Brain Res.*, 86: 205-215.
- Duce, I.R. and Keen, P. [1978] Can neuronal smooth endoplasmic reticulum function as a calcium reservoir? *Neuroscience*, 3: 837-848.
- Dunwiddie, T.V. and Hoffer, B.J. [1980] Adenine nucleotides and synaptic transmission in the *in vitro* rat hippocampus. *Br. J. Pharmacol.*, 69: 59-68.
- Dunwiddie, T.V., Hoffer, B.J. and Fredholm, B.B. [1981] Alkylxanthines elevate hippocampal excitability. Evidence for a role of endogenous adenosine. *Naunyn-Schmiedeberg's Arch. Pharmacol.*, 316: 326-330.

- Dunwiddie, T.V. and Lynch, G. [1979] The relationship between extracellular calcium concentrations and the induction of hippocampal long-term potentiation. *Brain Res.*, 169: 103-110.
- Dunwiddie, T.V., Madison, D. and Lynch, G. [1978] Synaptic transmission is required for the initiation of long-term potentiation. *Brain Res.*, 150: 413-417.
- Ebadi, M., Itoh, M., Bifano, J., Wendt, K. and Earle, A. [1981] The role of  $Zn^{2+}$  in pyridoxal phosphate mediated regulation of glutamic acid decarboxylase in brain. *Int. J. Biochem.*, 13: 1107-1112.
- Eccles, J.C. [1983] Calcium in long-term potentiation as a model for memory. *Neuroscience*, 10: 1071-1081.
- Eckert, R. and Tillotson, D. [1981] Calcium-mediated inactivation of the calcium conductance in caesium-loaded giant neurones of *Aplysia californica*. *J. Physiol.*, 314: 265-280.
- Emdin, S.O., Dodson, G.G., Cutfield, J.M. and Cutfield, S.M. [1980] Role of zinc in insulin biosynthesis. Some possible zinc-insulin interactions in the pancreatic B-cell. *Diabetologia*, 19: 174-182.
- Endo, M. [1977] Calcium release from the sarcoplasmic reticulum. *Physiol. Rev.*, 57: 71-108.
- Engel, J., Jr. and Ackerman, R.F. [1980] Interictal EEG spikes correlate with decreased rather than increased epileptogenicity in amygdaloid kindled rats. *Brain Res.*, 190: 543-548.
- Erulkar, S.D. and Fine, A. [1979] Calcium in the nervous system. *Rev. Neurosci.*, 4: 179-232.
- Euler, C. von [1962] On the significance of the high zinc content in the hippocampal formation. In: *Physiologie de l'Hippocampe*. (P. Passonaut, Ed.) Editions du CNRS, Paris, pp: 135-145.
- Finn, R.C., Browning, M. and Lynch, G. [1980] Trifluoperazine inhibits long-term potentiation and the phosphorylation of a 40,000 dalton protein. *Neurosci. Lett.*, 19: 103-108.
- Fjeringstad, E., Danscher, G. and Fjeringstad, E.J. [1974] Zinc content in hippocampus and whole brain of normal rats. *Brain Res.*, 79: 338-342.
- Frankenhaeuser, B. and Hodgkin, A.L. [1957] The action of calcium on the electrical properties of squid axons. *J. Physiol.*, 137: 218-244.

- Fricke, R.A. and Prince, D.A. [1984] Electrophysiology of dentate gyrus granule cells. *J. Neurophys.*, 51: 195-209.
- Frederickson, C.J., Manton, W.I., Frederickson, M.H., Howell, G.A. and Mallory, M.A. [1982] Stable-isotope dilution measurement of zinc and lead in rat hippocampus and spinal cord. *Brain Res.*, 246: 338-341.
- Fujita, Y., Harada, H., Takeuchi, T., Sato, H. and Minami, S. [1983] Enhancement of EEG spikes and hyperpolarizations of pyramidal cells in the kindled hippocampus of the rabbit. *Jap. J. Physiol.*, 33: 227-238.
- Garcia-Segura, L.M., Baetens, D., Roth, J., Norman, A.W. and Orci, L. [1984] Immunohistochemical mapping of calcium-binding protein immunoreactivity in the rat central nervous system. *Brain Res.*, 296: 75-86.
- Gerren, R.A. and Weinberger, N.M. [1983] Long term potentiation in the magnocellular medial geniculate nucleus of the anesthetized cat. *Brain Res.*, 265: 138-142.
- Goddard, G.V. [1967] Development of epileptic seizures through brain stimulation at low intensity. *Nature*, 214: 1020-1021.
- Goddard, G.V., McIntyre, D.C. and Leech, C.K. [1969] A permanent change in brain function resulting from daily electrical stimulation. *Exp. Neurol.*, 25: 295-330.
- Godfraind, J.M., Kawamura, H., Krnjevic, K. and Pumain, R. [1971] Actions of dinitrophenol and some other metabolic inhibitors on cortical neurones. *J. Physiol.*, 215: 199-222.
- Gorman, A.L.F. and Hermann, A. [1979] Internal effects of divalent cations on potassium permeability in molluscan neurones. *J. Physiol.*, 296: 393-410.
- Gorman, A.L.F. and Thomas, M.V. [1980] Potassium conductance and internal calcium accumulation in a molluscan neurone. *J. Physiol.*, 308: 287-313.
- Griffiths, T., Evans, M.C. and Meldrum, B.S. [1982] Intracellular sites of early calcium accumulation in the rat hippocampus during status epilepticus. *Neurosci. Lett.*, 30: 329-334.
- Haas, H.L. and Jefferys, J.G.R. [1984] Low-calcium field burst discharges of CA1 pyramidal neurones in rat hippocampal slices. *J. Physiol.*, 354: 185-201.
- Haas, H.L., Jefferys, J.G.R., Slater, N.T. and Carpenter, D.O. [1984] Modulation of low calcium induced field bursts in the hippocampus by monoamines and cholinomimetics. *Pflugers Arch.*, 400: 28-33.



- Haas, H.L. and Konnerth, A. [1983] Histamine and noradrenaline decrease calcium-activated potassium conductance in hippocampal pyramidal cells. *Nature*, 302: 432-434.
- Haas, H.L. and Rose, G. [1982] Long-term potentiation of excitatory synaptic transmission in the rat hippocampus: the role of inhibitory processes. *J. Physiol.*, 329: 541-552.
- Hagiwara, S. and Byerly, L. [1981] Calcium channel. *Ann. Rev. Neurosci.*, 4: 69-125.
- Haug, F.-M. S. [1974] Light microscopical mapping of the hippocampal region, the pyriform cortex and the cortico-medial amygdaloid nuclei of the rat with Timm's sulphide silver method. I. Area dentata, hippocampus and subiculum. *Z. Anat. Entwickl.-Gesch.*, 145: 1-27.
- Heinemann, U., Lux, H.D. and Gutnick, M.J. [1977] Extracellular free calcium and potassium during paroxysmal activity in the cerebral cortex of the cat. *Exp. Brain Res.*, 27: 237-243.
- Heizmann, C.W. [1984] Parvalbumin, an intracellular calcium-binding protein; distribution, properties and possible roles in mammalian cells. *Experientia*, 40: 910-921.
- Hellman, B. [1978] Calcium and pancreatic beta-cell function. 3. Validity of the  $\text{La}^{3+}$ -wash technique for discriminating between superficial and intracellular  $^{45}\text{Ca}$ . *Biochem. Biophys. Acta*, 540: 532-542.
- Hellman, B., Sehlin, J. and Taljedal, I.B. [1976] Calcium uptake by pancreatic islets as studied by the lanthanum method. *J. Physiol.*, 254: 639-656.
- Henke, H., Tobler, P.H. and Fischer, J.A. [1983] Localization of salmon calcitonin binding sites in rat brain by autoradiography. *Brain Res.*, 272: 373-377.
- Hesse, G.W. [1979] Chronic zinc deficiency alters neuronal function of hippocampal mossy fibers. *Science*, 205: 1005-1007.
- Hiramatsu, M. and Mori, A. [1977] Brain catecholamine concentrations and convulsions in El mice. *Folia Psychiat. Neurol. Jap.*, 31: 491-495.
- Hopkins, W.F. and Johnston, D. [1984] Frequency-dependent noradrenergic modulation of long-term potentiation in the hippocampus. *Science*, 226: 350-352.
- Hotson, J.R. and Prince, D.A. [1980] A calcium-activated hyperpolarization follows repetitive firing in hippocampal neurons. *J. Neurophys.*, 43: 409-419.

- Hotson, J.R. and Prince, D.A. [1981] Penicillin- and barium-induced epileptiform bursting in hippocampal neurons: actions on  $\text{Ca}^{++}$  and  $\text{K}^+$  potentials. *Ann. Neurol.*, 10: 11-17.
- Howell, G.A., Welch, M.G. and Frederickson, C.J. [1984] Stimulation-induced uptake and release of zinc in hippocampal slices. *Nature*, 308: 736-738.
- Hyden, H. and Lange, P.W. [1973] Do specific biochemical correlates to learning processes exist in brain cells? In: *Biology of Memory* (G. Adam, Ed.), Plenum Press, New York, pp. 69-86.
- Imaizumi, K., Ito, S., Kutsukake, G., Takizawa, T., Fujiwara, K. and Tsuchikawa, K. [1959] Epilepsy-like anomaly of mice. *Exp. Anim. (Jap.)*, 8: 6-10.
- Imaizumi, K. and Nakano, T. [1964] Mutant stocks, strain: El. *Mouse News Lett.*, 31: 57.
- Iwangoff, P. and Enz, A. [1971] The effect of dihydroergotamine on the phosphodiesterase activity of cat grey matter. *Experientia*, 27: 1258-1259.
- Iwata, H., Yamagami, S., Lee, E., Matsuda, T. and Baba, A. [1979] Increase of brain taurine contents of El mice by physiological stimulation. *Japan. J. Pharmacol.*, 29: 503-507.
- Jack, J.J.B., Noble, D. and Tsien, R.W. [1975] *Electric Current Flow in Excitable Cells*. Clarendon Press. Oxford.
- Jande, S.S., Maler, L. and Lawson, D.E.M. [1981] Immunohistochemical mapping of vitamin D-dependent calcium-binding protein in brain. *Nature*, 294: 765-767.
- Jaques, J.A. [1972] *Compartmental Analysis in Biology and Medicine*. Elsevier, Amsterdam.
- Jefferys, J.G.R. and Haas, H.L. [1982] Synchronized bursting of CA1 hippocampal pyramidal cells in the absence of synaptic transmission. *Nature*, 300: 448-450.
- Jobe, P.C. and Laird, H.E. [1981] Neurotransmitter abnormalities as determinants of seizure susceptibility and intensity in the genetic models of epilepsy. *Biochem. Pharmacol.*, 30: 3137-3144.
- Johnson, J.D., Wittenauer, L.A. and Nathan, R.D. [1983] Calmodulin,  $\text{Ca}^{2+}$ -antagonists and  $\text{Ca}^{2+}$ -transporters in nerve and muscle. *J. Neural Transm., Suppl.* 18: 97-111.

- Kakiuchi, S. and Yamazaki, R. [1970] Calcium-dependent phosphodiesterase activity and its activating factor (PAF) from brain. Studies on 3',5'-nucleotide phosphodiesterase (III). *Biochem. Biophys. Res. Commun.*, 41: 1104-1110.
- Kalichman, M.W. [1982] Neurochemical correlates of the kindling model of epilepsy. *Neurosci. Biobehav. Rev.*, 6: 161-181.
- Kandel, E.R. [1981] Calcium and the control of synaptic strength by learning. *Nature*, 293: 697-700.
- Kato, G. and Somjen, G.G. [1969] Effects of micro-ionophoretic administration of magnesium and calcium on neurones in the central nervous system of cats. *J. Neurobiol.*, 2: 181-195.
- Katz, B. and Miledi, R. [1965] The effect of calcium on acetylcholine release from motor nerve terminals. *Proc. R. Soc. B.*, 161: 495-503.
- Katz, B. and Miledi, R. [1967] The release of acetylcholine from nerve endings by graded electrical pulses. *Proc. R. Soc. B.*, 167: 23-38.
- Kemp, K. and Danscher, G. [1979] Multi-element analysis of the rat hippocampus by proton induced X-ray emission spectroscopy (phosphorus, sulphur, chlorine, potassium, calcium, iron, zinc, copper, lead, bromine, and rubidium). *Histochemistry*, 59: 167-176.
- Klee, C.B., Crouch, T.H. and Richman, P.G. [1980] Calmodulin. *Ann. Rev. Biochem.*, 49: 489-515.
- Klein, M., Shapiro, E. and Kandel, E.R. [1980] Synaptic plasticity and the modulation of the  $\text{Ca}^{2+}$  current. *J. Exp. Biol.*, 89: 117-157.
- Kohsaka, M., Hiramatsu, M. and Mori, A. [1978] Brain catecholamine concentrations and convulsions in El mice. *Adv. Biochem. Psychopharmacol.*, 19: 389-392.
- König, J.F.R. and Klippel, R.A. [1963] *The Rat Brain: A Stereotaxic Atlas of the Forebrain and Lower Parts of the Brain Stem*. Williams & Wilkins, Baltimore.
- Kretsinger, R.H. [1976] Calcium-binding proteins. *Ann. Rev. Biochem.*, 45: 239-266.
- Kretsinger, R.H. (Ed.) [1981] Mechanism of selective signalling by calcium. *Neurosci. Res. Progr. Bull.*, 19: 213-328.
- Krieg, W.J.S. [1946] Connections of the cerebral cortex. I. The albino rat. A. Topography of cortical areas. *J. Comp. Neurol.*, 84: 221-275.

- Krnjevic, K. and Lisiewicz, A. [1972] Injections of calcium ions into spinal motoneurons. *J. Physiol.*, 225: 363-390.
- Kuba, K. [1980] Release of calcium ions linked to the activation of potassium conductance in a caffeine-treated sympathetic neurone. *J. Physiol.*, 298: 251-269.
- Kurokawa, M., Naruse, H. and Kato, M. [1966] Metabolic studies on ep mouse, a special strain with convulsive pre-disposition. *Progr. Brain Res.*, 21A: 112-130.
- Laird, H.E., Dailey, J.W. and Jobe, P.C. [1984] Neurotransmitter abnormalities in genetically epileptic rodents. *Federation Proc.*, 43: 2505-2509.
- Lancaster, B. and Wheal, H.V. [1984] The synaptically evoked late hyperpolarisation in hippocampal CA1 pyramidal cells is resistant to intracellular EGTA. *Neuroscience*, 12: 267-275.
- Lee, K.S. [1982] Sustained enhancement of evoked potentials following brief, high-frequency stimulation of the cerebral cortex *in vitro*. *Brain Res.*, 239: 617-623.
- Lehninger, A.L., Carafoli, E. and Rossi, C.S. [1977] Energy-linked ion movements in mitochondrial systems. *Adv. Enzymol.*, 29: 259-319.
- Levine, B.A. and Williams, R.J.P. [1982] Calcium binding to proteins and other large biological anion centers. In: *Calcium and Cell Function*. Vol. II. (W.Y. Cheung, Ed.) Academic Press, New York, pp: 1-38.
- Lev-Tov, A., Miller, J.P., Burke, R.E. and Rall, W. [1983] Factors that control amplitude of EPSPs in dendritic neurons. *J. Neurophysiol.*, 50: 399-412.
- Lin, C., Dedman, J.R., Brinkley, B.R. and Means, A.R. [1980] Localization of calmodulin in rat cerebellum by immunoelectron microscopy. *J. Cell Biol.*, 85: 473-480.
- Llinas, R.R. [1977] Calcium and transmitter release in squid synapse. In: *Society for Neuroscience Symposia* Vol. II. *Approaches to the Cell Biology of Neurons* (W.M. Cowan and J.A. Ferrendelli, Eds.), Bethesda, pp: 139-160.
- Llinas, R.R. and Heuser, J.E. (Eds.) [1977] Depolarization-release coupling in neurons. *Neurosci. Res. Progr. Bull.*, 15: 556-687.
- Llinas, R. and Sugimori, M. [1980a] Electrophysiological properties of *in vitro* cell somata in mammalian cerebellar slices. *J. Physiol.*, 305: 171-195.

- Llinas, R. and Sugimori, M. [1980b] Electrophysiological properties of *in vitro* Purkinje cell dendrites in mammalian cerebellar slices. *J. Physiol.*, 305: 197-213.
- Llinas, R. and Yarom, Y. [1981a] Properties and distribution of ionic conductances generating electroresponsiveness of mammalian inferior olivary neurones *in vitro*. *J. Physiol.*, 315: 569-584.
- Llinas, R. and Yarom, Y. [1981b] Electrophysiology of mammalian inferior olivary neurones *in vitro*. Different types of voltage-dependent ionic conductances. *J. Physiol.*, 315: 549-567.
- Llinas, R., Yarom, Y. and Sugimori, M. [1981] Isolated mammalian brain *in vitro*: new technique for analysis of electrical activity of neuronal circuit function. *Fed. Proc.*, 40: 2240-2245.
- Locke, F.S. [1894] Notiz uber den Einfluss physiologischer Kochsalzlosung auf die elektrische Erregbarkeit von Muskel und Nerv. *Zentralbl. Physiol.*, 8: 166-167.
- Lynch, G. and Baudry, M. [1984] The biochemistry of memory: a new and specific hypothesis. *Science*, 224: 1057-1063.
- Lynch, G., Larson, J., Kelso, S., Barrionuevo, G. and Schottler, F. [1983] Intracellular injections of EGTA block induction of hippocampal long-term potentiation. *Nature*, 305: 719-721.
- MacVicar, B.A. [1984] Voltage-dependent calcium channels in glial cells. *Science*, 226: 1345-1347.
- Madison, D.V. and Nicoll, R.A. [1982] Noradrenaline blocks accommodation of pyramidal cell discharge in the hippocampus. *Nature*, 299: 636-638.
- Madison, D.V. and Nicoll, R.A. [1984] Control of the repetitive discharge of rat CA1 pyramidal neurones *in vitro*. *J. Physiol.*, 354: 319-331.
- Madryga, F.J., Goddard, G.V. and Rasmusson, D.D. [1975] The kindling of motor seizures from hippocampal commissure in the rat. *Physiol. Psychol.*, 3: 369-373.
- Martonosi, A.N. [1984] Mechanism of  $\text{Ca}^{2+}$  release from sarcoplasmic reticulum of skeletal muscle. *Physiol. Rev.*, 64: 1240-1320.
- McGraw, C.F., Nachsen, D.A. and Blaustein, M.P. [1982] Calcium movement and regulation in presynaptic nerve terminals. In: *Calcium and Cell Function*. Vol. II. (W.Y. Cheung, Ed.) Academic Press, New York, pp: 81-110.

- McNamara, J.O. [1984] Role of neurotransmitters in seizure mechanisms in the kindling model of epilepsy. *Fed-Proc.*, 43: 2516-2520.
- McNamara, J.O., Byrne, M.C., Dasheiff, R.M. and Fitz, J.G. [1980] The kindling model of epilepsy: a review. *Progr. Neurobiol.*, 15: 139-159.
- Means, A.R. and Dedman, J.R. [1980] Calmodulin - an intracellular calcium receptor. *Nature*, 285: 73-77.
- Meech, R.W. [1972] Intracellular calcium injection causes increased potassium conductance in *Aplysia* nerve cells. *Comp. Biochem. Physiol.*, 42A: 493-499.
- Miller, D.J. and Thieleczek, R. [1977] Calcium release by caffeine and other methylxanthines in skinned skeletal muscle fibres. *J. Physiol.*, 273: 67P-68P.
- Miller, J.J. and Baimbridge, K.G. [1983] Biochemical and immunohistochemical correlates of kindling-induced epilepsy: role of calcium-binding protein. *Brain Res.*, 278: 322-326.
- Miller, J.P., Rall, W. and Rinzel, J. [1985] Synaptic amplification by active membrane in dendritic spines. *Brain Res.*, 325: 325-330.
- Millichap, J.G. [1969] Systemic electrolyte and neuroendocrine mechanisms. In: *Basic Mechanisms of the Epilepsies*. (H.H. Jasper, A.A. Ward and A. Pope, Eds.) Little, Brown & Co., pp: 709-726.
- Milner, B., Corkin, S. and Teuber, H.L. [1968] Further analysis of the hippocampal amnesic syndrome: 14-year follow-up study of H.M. *Neuropsychologia*, 6: 215-234.
- Milner, P.M. and Penfield, W. [1955] The effect of hippocampal lesions on recent memory. *Trans. Am. Neurol. Assoc.*, 80: 42-48.
- Mishkin, M. [1978] Memory in monkeys severely impaired by combined but not by separate removal of amygdala and hippocampus. *Nature*, 273: 297-298.
- Mody, I., Baimbridge, K.G. and Miller, J.J. [1984] Blockade of tetanic- and calcium-induced long-term potentiation in the hippocampal slice preparation by neuroleptics. *Neuropharmacology*, 23: 625-631.
- Moore, B.W. [1982] Chemistry and biology of the S-100 protein. *Scand. J. Immunol.*, 15[Suppl.9]: 53-74.

- Moriarty, C.M. [1980] Kinetic analysis of calcium distribution in rat anterior pituitary slices. *Am. J. Physiol.*, 238: E167-E173.
- Morris, M.E., Krnjevic, K. and Ropert, N. [1983] Changes in free  $\text{Ca}^{2+}$  recorded inside hippocampal pyramidal neurons in response to fimbrial stimulation. *Soc. Neurosci. Abstr.*, 9: 395. (Abstr.).
- Naruse, H., Kato, M., Kurokawa, M., Haba, R. and Yabe, T. [1960] Metabolic defects in a convulsive strain of mouse. *J. Neurochem.*, 5: 359-369.
- Nedler, J.A. and Mead, R. [1965] A simplex method for function minimization. *Computer J.*, 7: 308-313.
- Neuman, R.S. and Harley, C.W. [1983] Long-lasting potentiation of the dentate gyrus population spike by norepinephrine. *Brain Res.*, 273: 162-165.
- Newmark, M.E. and Penry, J.K. [1980] *Genetics of Epilepsy: A Review*. Raven Press, New York.
- Okada, Y. and Ozawa, S. [1980] Inhibitory action of adenosine on synaptic transmission in the hippocampus of guinea pig *in vitro*. *Eur. J. Pharmacol.*, 68: 483-492.
- Oliver, M.W. and Miller, J.J. [1985] Alterations of inhibitory processes in the dentate gyrus following kindling-induced epilepsy. *Exp. Brain Res.*, 57: 443-447.
- Oliver, M.W., Richardson, T.L. and Miller, J.J. [1983] Electrophysiological properties of hippocampal pyramidal and dentate granule cells following kindling-induced epilepsy. *Can. J. Physiol. Pharmacol.*, 61: Axx. (Abstr.).
- Owen, D.G., Segal, M. and Barker, J.L. [1984] A Ca-dependent  $\text{Cl}^-$  conductance in cultured mouse spinal cord neurones. *Nature*, 311: 567-570.
- Pei, Y., Zhao, D., Huang, J. and Cao, L. [1983] Zinc-induced seizures: a new experimental model of epilepsy. *Epilepsia*, 24: 169-176.
- Pellegrino, L.J., Pellegrino, A.S. and Cushman, A.J. [1979] *A Stereotaxic Atlas of the Rat Brain*. Plenum Press, New York.
- Perkel, D.H. and Perkel, D.J. [1985] Dendritic spines: role of active membrane in modulating synaptic efficacy. *Brain Res.*, 325: 331-335.
- Peterson, S.L. and Albertson, T.E. [1982] Neurotransmitter and neuromodulator function in the kindled seizure and state. *Progr. Neurobiol.*, 19: 237-270.

- Prasad, A.S. [1979] Clinical, biochemical, and pharmacological role of zinc. *Ann. Rev. Pharmacol. Toxicol.*, 20: 393-426.
- Pybus, J., Feldman, F.J. and Bowers, G.N. Jr. [1970] Measurement of total calcium in serum by atomic absorption spectrophotometry, with use of a strontium internal reference. *Clin. Chem.*, 16: 998-1007.
- Racine, R.J. [1972a] Modification of seizure activity by electrical stimulation: I. After-discharge threshold. *Electroenceph. Clin. Neurophysiol.*, 32: 269-279.
- Racine, R.J. [1972b] Modification of seizure activity by electrical stimulation: II. Motor seizure. *Electroenceph. Clin. Neurophysiol.*, 32: 281-294.
- Racine, R.J. [1978] Kindling: the first decade. *Neurosurgery*, 3: 234-252.
- Rahamimoff, R. [1976] The role of calcium in transmitter release at the neuromuscular junction. In: *Motor Innervation of Muscle*. (S. Thesleff, Ed.), Academic Press, New York, pp: 117-150.
- Rahamimoff, R., Lev-Tov, A. and Meiri, H. [1980] Primary and secondary regulation of quantal transmitter release: calcium and sodium. *J. Exp. Biol.*, 89: 5-18.
- Rasmussen, H. and Barrett, P.Q. [1984] Calcium messenger system: an integrated view. *Physiol. Rev.*, 64: 938-984.
- Rasmussen, H. and Goodman, D.B.P. [1977] Relationship between calcium and cyclic nucleotides in cell activation. *Physiol. Rev.*, 57: 421-509.
- Reuter, H. [1983] Calcium channel modulation by neurotransmitters, enzymes and drugs. *Nature*, 301: 569-574.
- Richards, C.D. and Sercombe, R. [1970] Calcium, magnesium and the electrical activity of guinea-pig olfactory cortex *in vitro*. *J. Physiol.*, 211: 571-584.
- Riggs, D.S. [1963] *The Mathematical Approach to Physiological Problems*. Williams & Wilkins, Baltimore.
- Rizzi, A.J. and Goltzman, D. [1981] Calcitonin receptors in the central nervous system of the rat. *Endocrinology*, 108: 1672-1677.
- Robertson, J.S. [1957] Theory and use of tracers in determining transfer rates in biological systems. *Physiol Rev.*, 37: 133-154.



- Robertson, J.S., Tosteson, D.C. and Gamble Jr., J.L. [1957] The determination of exchange rates in three-compartment steady state closed systems through the use of tracers. *J. Lab. Clin. Med.*, 49: 497-503.
- Robertson, S.P., Johnson, J.D. and Potter, J.D. [1981] The time course of  $\text{Ca}^{2+}$  exchange with calmodulin, troponin, parvalbumin, and myosin in response to transient increases in  $\text{Ca}^{2+}$ . *Biophys. J.*, 34: 559-569.
- Rosenblatt, D.E., Lauter, C.J. and Trams, E.G. [1976] Deficiency of a  $\text{Ca}^{2+}$ -ATPase in brains of seizure prone mice. *J. Neurochem.*, 27: 1299-1304.
- Roth, J., Baetens, D., Norman, A.W. and Garcia-Segura, L.-M. [1981] Specific neurons in chick central nervous system stain with an antibody against chick intestinal vitamin D-dependent calcium-binding protein. *Brain Res.*, 222: 452-457.
- Rubiales de Barioglio, S. and Orrego, F. [1982] A study of calcium compartments in rat brain cortex thin slices: effects of veratridine, lithium and of a mitochondrial uncoupler. *Neurochem-Res.*, 7: 1427-1435.
- Sastry, B.R. [1982] Presynaptic change associated with long-term potentiation in hippocampus. *Life Sci.*, 30: 2003-2008.
- Sato, S.M., Frazier, J.M. and Goldberg, A.M. [1984] The distribution and binding of zinc in the hippocampus. *J. Neurosci.*, 4: 1662-1670.
- Schanne, F.A.X., Kane, A.B., Young, E.E. and Farber, J.L. [1979] Calcium-dependence of toxic cell death: a final common pathway. *Science*, 206: 700-702.
- Schubert, P. and Mitzdorf, U. [1979] Analysis and quantitative evaluation of the depressive effect of adenosine on evoked potentials in hippocampal slices. *Brain Res.*, 172: 186-190.
- Schwartzkroin, P.A. and Stafstrom, C.E. [1980] Effects of EGTA on the calcium-activated afterhyperpolarization in hippocampal CA3 pyramidal cells. *Science*, 210: 1125-1126.
- Schwartzkroin, P.A. and Wester, K. [1975] Long-lasting facilitation of a synaptic potential following tetanization in the *in vitro* hippocampal slice. *Brain Res.*, 89: 107-119.
- Schwarz, W. and Passow, H. [1983]  $\text{Ca}^{2+}$ -activated  $\text{K}^{+}$  channels in erythrocytes and excitable cells. *Ann. Rev. Physiol.*, 45: 359-374.

- Segal, M. [1981] The action of norepinephrine in the rat hippocampus: intracellular studies in the slice preparation. *Brain Res.*, 206: 107-128.
- Sheppard, C.W. [1962] *Basic Principles of the Tracer Method*. John Wiley & Sons.
- Skrede, K.K. and Malthe-Sorensen, D. [1981] Increased resting and evoked release of transmitter following repetitive electrical tetanization in hippocampus: a biochemical correlate to long-lasting synaptic potentiation. *Brain Res.*, 208: 436-441.
- Skrede, K.K., Teyler, T.J. and Thompson, R.F. (Eds.) [1982] Hippocampal long-term potentiation: Mechanisms and implications for memory. *Neurosci. Res. Prog. Bull.*, 20: 613-769.
- Slotnick, B.M. and Leonard, C.M. [1975] *A Stereotaxic Atlas of the Albino Mouse Forebrain*. U.S. Department of Health, Education and Welfare, Rockville.
- Smellie, F.W., Davis, C.W., Daly, J.W. and Wells, J.N. [1979] Alkylxanthines: inhibition of adenosine-elicited accumulation of cyclic AMP in brain slices and of brain phosphodiesterase activity. *Life Sci.*, 24: 2475-2482.
- Snyder, S.H., Katims, J.J., Annau, Z., Bruns, R.F. and Daly, J.W. [1981] Adenosine receptors and behavioral actions of methylxanthines. *Proc. Nat. Acad. Sci. U.S.A.*, 78: 3260-3264.
- Somlyo, A.P., Bond, M. and Somlyo, A.V. [1985] Calcium content of mitochondria and endoplasmic reticulum in liver frozen rapidly *in vivo*. *Nature*, 314: 622-625.
- Stahl, W.L. and Swanson, P.D. [1971] Movements of calcium and other cations in isolated cerebral tissues. *J. Neurochem.*, 18: 415-427.
- Stahl, W.L. and Swanson, P.D. [1972] Calcium movements in brain slices in low sodium or calcium media. *J. Neurochem.*, 19: 2395-2407.
- Stein, R.B. [1967] The information capacity of nerve cells using a frequency code. *Biophys. J.*, 7: 797-826.
- Stengaard-Pedersen, K., Fredens, K. and Larsson, L.-I. [1983] Comparative localization of enkephalin and cholecystokinin immunoreactivities and heavy metals in the hippocampus. *Brain Res.*, 273: 81-96.
- Stone, T.W. [1981] Physiological roles for adenosine and adenosine 5'-triphosphate in the nervous system. *Neuroscience*, 6: 523-555.

- Stringer, J.L., Hackett, J.T. and Guyenet, P.G. [1984] Long-term potentiation blocked by phencyclidine and cyclazocine *in vitro*. Eur. J. Pharmacol., 98: 381-388.
- Stumpf, W.E., Sar, M., Clark, S.A. and DeLuca, H.F. [1982] Brain target sites for 1,25-dihydroxyvitamin D<sub>3</sub>. Science, 215: 1403-1405.
- Su, J.Y. and Hasselbach, W. [1984] Caffeine-induced calcium release from isolated sarcoplasmic reticulum of rabbit skeletal muscle. Pflugers Arch., 400: 14-21.
- Suzuki, J. [1976] Paroxysmal discharges in the electroencephalogram of the El mouse. Experientia, 32: 336-338.
- Suzuki, J. and Nakamoto, Y. [1977] Seizure patterns and electroencephalograms of El mouse. Electroenceph. Clin. Neurophysiol., 43: 299-311.
- Suzuki, J., Nakamoto, Y. and Shinkawa, Y. [1983] Local cerebral glucose utilization in epileptic seizures of the mutant El mouse. Brain Res., 266: 359-363.
- Swanson, L.W., Teyler, T.J. and Thompson, R.F. (Eds.) [1982] Hippocampal long-term potentiation: mechanisms and implications for memory. Neurosci.Res.Progr.Bull., 20: 611-769.
- Szebenyi, D.M.E., Obendorf, S.K. and Moffat, K. [1981] Structure of vitamin D-dependent calcium-binding protein from bovine intestine. Nature, 294: 327-331.
- Taylor, A.N. [1974] Chick brain calcium-binding protein. Comparison with intestinal vitamin D-induced calcium-binding protein. Arch. Biochem. Biophys., 161: 100-108.
- Taylor, C.P. and Dudek, F.E. [1982] Synchronous neural after-discharges in rat hippocampal slices without active chemical synapses. Science, 218: 810-812.
- Tillotson, D. [1979] Inactivation of calcium conductance dependent on entry of calcium ions in molluscan neurons. Proc.Natl.Acad.Sci.USA, 77: 1497-1500.
- Timm, F. [1958] Zur Histochemie des Ammonshorngebietes. Z. Zellforsch., 48: 548-555.
- Traub, R.D. and Llinas, R. [1979] Hippocampal pyramidal cells: significance of dendritic ionic conductances for neuronal function and epileptogenesis. J. Neurophysiol., 42: 476-496.
- Tsien, R.W. [1983a] Calcium channels in excitable cell membranes. Ann. Rev. Physiol., 43: 341-358.

- Tsien, R.W. [1983b] Intracellular measurement of ion activities. *Ann. Rev. Biophys. Bioeng.*, 12: 91-116.
- Tuff, L.P., Racine, R.J. and Adamec, R. [1983] The effects of kindling on GABA-mediated inhibition in the dentate gyrus of the rat. I. Paired-pulse depression. *Brain Res.*, 277: 79-90.
- Turner, R.W., Baimbridge, K.G. and Miller, J.J. [1982] Calcium-induced long-term potentiation in the hippocampus. *Neuroscience*, 7: 1411-1416.
- Uchikawa, T. and Borle, A.B. [1978a] Kinetic analysis of calcium desaturation curves from isolated kidney cells. *Am. J. Physiol.*, 234: R29-R33.
- Uchikawa, T. and Borle, A.B. [1978b] Studies of calcium-45 desaturation from kidney slices in flow-through chambers. *Am. J. Physiol.*, 234: R34-R38.
- Uchikawa, T. and Borle, A.B. [1981] Solutions for the kinetic analysis of  $^{45}\text{Ca}$  uptake curves. *Cell Calcium*, 2: 173-186.
- Van Breemen, C. and McNaughton, E. [1970] The separation of cell membrane calcium transport from extracellular calcium exchange in vascular smooth muscle. *Biochem. Biophys. Res. Commun.*, 39: 567-574.
- Voronin, L.L. [1983] Long-term potentiation in the hippocampus. *Neuroscience*, 10: 1051-1069.
- Wadman, W.J., Heinemann, U., Konnerth, A. and Neuhaus, S. [1985] Hippocampal slices of kindled rats reveal calcium involvement in epileptogenesis. *Exp. Brain Res.*, 57: 404-407.
- Wakabayashi, S. and Goshima, K. [1981] Kinetic studies on sodium-dependent calcium uptake by myocardial cells and neuroblastoma cells in culture. *Biochim. Biophys. Acta*, 642: 158-172.
- Ward, A.A. [1969] The epileptic neuron: chronic foci in animals and man. In: *Basic Mechanisms of the Epilepsies*. (H.H. Jasper, A.A. Ward and A. Pope, Eds.) Little, Brown & Co., pp: 263-288.
- Wasserman, R.H. [1980] Vitamin D-induced calcium-binding protein - an overview. In: *Calcium-Binding Proteins: Structure and Function* (F.L. Siegel, E. Carafoli, R.H. Kretsinger, D.H. MacLennan and R.H. Wasserman Eds.), Elsevier North Holland, pp: 357-361.
- Wasserman, R.H. and Fullmer, C.S. [1983] Calcium transport proteins, calcium absorption, and vitamin D. *Ann. Rev. Physiol.*, 45: 375-390.

- Wasserman, R.H. and Taylor, A.N. [1966] Vitamin D<sub>3</sub> induced calcium-binding protein in chick intestinal mucosa. *Science*, 152: 791-793.
- Wasserman, R.H., Shimura, F., Meyer, S.A., and Fullmer, C.S. [1983] Possible roles of the vitamin D-induced calcium-binding protein in intestinal calcium transport. In: *Calcium Binding Proteins* (B. de Bernard, G.L. Sottocasa, G. Sandri, E. Carafoli, A.N. Taylor, T.C. Vanaman and R.J.P. Williams Eds.), Elsevier Science Publishers, pp: 183-188.
- Weber, A. and Herz, R. [1968] The relationship between caffeine contracture of intact muscle and the effect of caffeine on reticulum. *J. Gen. Physiol.*, 52: 750-759.
- Weiss, B. and Levin, R.M. [1978] Mechanism for selectively inhibiting the activation of cyclic nucleotide phosphodiesterase and adenylate cyclase by antipsychotic agents. *Adv. Cyclic Nucl. Res.*, 9: 285-303.
- Wigstrom, H. and Gustafsson, B. [1983] Facilitated induction of hippocampal long-lasting potentiation during blockade of inhibition. *Nature*, 301: 603-604.
- Wigstrom, H., Swann, J.W. and Andersen, P. [1979] Calcium dependency of synaptic long-lasting potentiation in the hippocampal slice. *Acta Physiol. Scand.*, 105: 126-128.
- Willis, J.B. [1963] Analysis of biological materials by atomic absorption spectroscopy. *Methods Biochem. Anal.*, 11: 1-67.
- Wolf, G. and Schmidt, W. [1982] Zinc (II) as a putative regulatory factor of glutamate dehydrogenase activity in glutamatergic systems. In: *Neuronal Plasticity and Memory Formation*. (C. Ajmone Marsan and H. Matthies, Eds.) Raven Press, New York, pp: 437-440.
- Wong, R.K.S. and Prince, D.A. [1978] Participation of calcium spikes during intrinsic burst firing in hippocampal neurons. *Brain Res.*, 159: 385-390.
- Wright, D.M. [1984] Zinc: effect and interaction with other cations in the cortex of the rat. *Brain Res.*, 311: 343-347.
- Yaari, Y., Konnerth, A. and Heinemann, U. [1983] Spontaneous epileptiform activity of CA1 hippocampal neurons in low extracellular calcium solutions. *Exp. Brain Res.*, 51: 153-156.
- Yamamoto, C. and Chujo, T. [1978] Long-term potentiation in thin hippocampal sections studied by intracellular and extracellular recordings. *Exp. Neurol.*, 58: 242-250.

Yamamoto, C., Matsumoto, K. and Takagi, M. [1980] Potentiation of excitatory postsynaptic potentials during and after repetitive stimulation in thin hippocampal slices. Exp. Brain Res., 38: 469-477.

Yarbrough, G.G. and McGuffin-Clineschmidt, J.C. [1981] *in vivo* behavioral assessment of central nervous system purinergic receptors. Eur. J. Pharmacol., 76: 137-144.